

**Dottorato di Ricerca in Scienze Biochimiche e Biotecnologiche**

**Ciclo XXVII**

Settore Concorsuale 03/D1

Settore Scientifico Disciplinare CHIM/11

**MICROBIAL ECOLOGY OF  
BIOTECHNOLOGICAL PROCESSES**

**Presentata da:**

Dott.ssa Serena Fraraccio

**Coordinatore Dottorato**

Chiar.mo Prof.  
Santi Mario Spampinato

**Relatore**

Chiar.mo Prof. Fabio Fava

**Correlatori**

Giulio Zanaroli, Ph.D.

Assoc. Prof. Ondřej Uhlík, Ph.D.

---

**Esame finale anno 2015**

## Abstract

The investigation of phylogenetic diversity and functionality of complex microbial communities in relation to changes in the environmental conditions represents a major challenge of microbial ecology research. Nowadays, particular attention is paid to microbial communities occurring at environmental sites contaminated by recalcitrant and toxic organic compounds. Extended research has evidenced that such communities evolve some metabolic abilities leading to the partial degradation or complete mineralization of the contaminants. Determination of such biodegradation potential can be the starting point for the development of cost effective biotechnological processes for the bioremediation of contaminated matrices. This work showed how metagenomics-based microbial ecology investigations supported the choice or the development of three different bioremediation strategies. First, PCR-DGGE and PCR-cloning approaches served the molecular characterization of microbial communities enriched through sequential development stages of an aerobic cometabolic process for the treatment of groundwater contaminated by chlorinated aliphatic hydrocarbons inside an immobilized-biomass packed bed bioreactor (PBR). In this case the analyses revealed homogeneous growth and structure of immobilized communities throughout the PBR and the occurrence of dominant microbial phylotypes of the genera *Rhodococcus*, *Comamonas* and *Acidovorax*, which probably drive the biodegradation process. The same molecular approaches were employed to characterize sludge microbial communities selected and enriched during the treatment of municipal wastewater coupled with the production of polyhydroxyalkanoates (PHA). Known PHA-accumulating microorganisms identified were affiliated with the genera *Zooglea*, *Acidovorax* and *Hydrogenophaga*. Finally, the molecular investigation concerned communities of polycyclic aromatic hydrocarbon (PAH) contaminated soil subjected to rhizoremediation with willow roots or fertilization-based treatments. The metabolic ability to biodegrade naphthalene, as a representative model for PAH, was assessed by means of stable isotope probing in combination with high-throughput sequencing analysis. The phylogenetic diversity of microbial populations able to derive carbon from naphthalene was evaluated as a function of the type of treatment.

## Keywords

Microbial ecology; metagenomics; biotechnological process; bioremediation; aerobic cometabolism; chlorinated aliphatic hydrocarbons (CAHs); polycyclic aromatic hydrocarbons (PAHs); polyhydroxyalkanoates (PHA); denaturing gradient gel electrophoresis (DGGE); stable isotope probing (SIP).

*A mia madre...*

## Acknowledgements

The first thanks is for my parents and my sister. Thank you for your unconditional support, no matter how distant, no matter how tired...you have always been next to me, as emblem of honesty, simplicity and what really love is.

Thank you zia Pina and zio Franco for all your teachings, patience and hilarity! I thank my other uncles and cousins and of course I thank my grandmother, she is almost a century of thoughts, joys, sorrows, wars...so many stories to hear!

A very thankful hug to my closest friends Melania, Aurora, Martina, Luca and to all of the people that make my life special. I thank Lucie and her family for the warm welcome they gave to me everytime I needed and for the great time spent together in Prague.

I am endlessly grateful, for the opportunities afforded to me, to Ondřej Uhlík, Professor Tomáš Macek and all of the great people around the Lab 209 at the Department of Biochemistry and Microbiology, University of Chemistry and Technology of Prague. A special thought is for Lucka, Jachym, Michal, Jitka, Terka, and Blanka. I also wish to thank all of the other people who allowed me to work at the research project in Prague and the Dr. Mary Beth Leigh of University of Alaska Fairbanks.

The research activity conducted at the University of Bologna, Department of Civil, Chemical, Environmental and Material Engineering (DICAM), was supported by the European Commission under Grant Agreement No. 265946 (MINOTAURUS Project, 7<sup>th</sup> FP). I thank Professor Davide Pinelli and Dario Frascari, Ph.D, for their kindness and all of the things they taught me.

Chapter Five of my dissertation was realized in the framework of a cooperation with the “Sapienza” University of Rome and the work was supported by the EU ROUTES project (Contract No 265156, FP7 2007–2013, THEME [ENV.2010.3.1.1-2] Innovative system solutions for municipal sludge treatment and management).

## Table of Contents

<b>Chapter 1. Introduction.....</b>	<b>1</b>
<b>1.1. General introduction.....</b>	<b>1</b>
<b>1.2. Research objectives and rationale .....</b>	<b>3</b>
<b>1.3. Dissertation organization .....</b>	<b>4</b>
<b>Chapter 2. Literature review .....</b>	<b>5</b>
<b>2.1. Bioremediation of aquifers contaminated by chlorinated aliphatic hydrocarbons (CAHs).....</b>	<b>5</b>
2.1.1. CAHs: distribution in the environment, chemical and physical properties, toxicity .....	5
2.1.2. Biodegradation of CAHs.....	7
2.1.2.1. Anaerobic microbial dehalogenation .....	8
2.1.2.2. Microbial aerobic oxidation of CAHs.....	10
2.1.2.3. Aerobic cometabolic degradation of CAHs .....	11
2.1.2.4. Key enzymes in the aerobic cometabolism of CAHs .....	14
2.1.2.4.1. Soluble di-iron monooxygenases (SDIMO) .....	14
2.1.2.4.2. Methane monooxygenase (MMO) .....	14
2.1.2.4.3. Butane and propane monooxygenases .....	15
2.1.2.4.4. AlkB super-family.....	16
2.1.2.4.5. Bacterial cytochrome P450 .....	17
2.1.3. <i>In situ</i> aerobic cometabolic bioremediation of CAH-contaminated aquifers .....	18
2.1.3.1. Main technologies for the <i>in situ</i> bio-treatment of contaminated aquifers .....	19
2.1.3.2. On-site treatment with immobilized-biomass systems .....	20
<b>2.2. Bioremediation of polycyclic aromatic hydrocarbon (PAH)-contaminated soils .....</b>	<b>21</b>
2.2.1. PAHs: distribution, chemical and physical properties, toxicity .....	21
2.2.2. PAH biodegradation.....	22
2.2.3. Bacterial aerobic biodegradation .....	23
2.2.4. Phytoremediation and rhizoremediation of PAH-contaminated soil .....	25
<b>2.3. Production of polyhydroxyalkanoates (PHAs).....</b>	<b>27</b>
2.3.1. PHAs: main characteristics and applications .....	27
2.3.2. PHA production by pure microbial cultures and process implementation at industrial scale.....	28
2.3.3. Other PHA production strategies: employment of mixed microbial cultures.....	30

2.3.4. “Sludge minimization in municipal wastewater treatment by polyhydroxyalkanoates (PHA) production” (Valentino et al. 2014b) .....	31
<b>2.4. Molecular advances in biotechnology to characterize microbial communities.....</b>	<b>33</b>
2.4.1. Introduction to metagenomics and sequence analysis as powerful tools in microbial ecology .....	33
2.4.2. Describing environmental microbial communities’ biodiversity.....	34
2.4.3. Molecular fingerprinting of microbial communities.....	35
2.4.3.1. PCR-based techniques.....	35
2.4.3.2. Semi quantitative analysis of DGGE patterns.....	37
2.4.3.3. Nucleic acids hybridization-based techniques .....	38
2.4.4. Linking microbial phylogeny and functionality: stable isotope probing .....	39
2.4.5. Next generation sequencing (NGS) technologies .....	42
2.4.6. Evaluation of NGS data and statistics .....	43
<b>Chapter 3. Aerobic cometabolic bioremediation of CAH-contaminated groundwater in packed bed bioreactors: support of community characterization to the process development and optimization.....</b>	<b>45</b>
<b>3.1. Objectives and rationale of the research.....</b>	<b>45</b>
<b>3.2. Materials and methods .....</b>	<b>47</b>
3.2.1. Environmental contaminated matrix, cultivation media and biomass immobilization support materials .....	47
3.2.2. Experimental set up.....	50
3.2.2.1. Batch microcosms .....	50
3.2.2.1.1. Set up of batch microcosms .....	50
3.2.2.1.2. Selection of the best growth substrate, microbial consortium and immobilization support material in batch microcosms at 30 and 15°C .....	50
3.2.2.1.3. Maintenance of the enriched microbial consortia .....	52
3.2.2.2. Process development in 1 L PBR.....	52
3.2.2.2.1. Set up of 1 L PBR systems.....	52
3.2.2.2.2. Operative conditions adopted in 1 L PBRs.....	53
3.2.2.3. Scale up of the processes: 31 L pilot plant.....	54
3.2.2.3.1. Set up of a 31 L PBR system .....	54
3.2.2.3.2. Operative conditions adopted in 31 L PBR system .....	55
3.2.3. Analytical techniques .....	57
3.2.3.1. Gas chromatography for the measurement of growth substrates, oxygen and chlorinated organic compounds .....	57

3.2.3.2. Microbial biomass quantification via protein concentration determination .....	57
3.2.4. Molecular analyses of microbial communities .....	59
3.2.4.1. Metagenomic DNA extraction and purification.....	59
3.2.4.2. PCR-DGGE approach for the microbial community characterization .....	59
3.2.4.2.1. Amplicons preparation and quantification for DGGE .....	59
3.2.4.2.2. DGGE analysis.....	60
3.2.4.3. PCR-cloning approach for the microbial community characterization .....	62
3.2.4.3.1. Amplicons preparation for the cloning reaction .....	62
3.2.4.3.2. Clone libraries construction and screening .....	63
3.2.4.4. Sequencing analysis result evaluations .....	64
<b>3.3. Results and discussion .....</b>	<b>65</b>
3.3.1. Selection of the best growth substrate and the best microbial consortium under batch conditions at 30°C.....	65
3.3.2. Selection of the best immobilization support material and evaluation of the microbial community immobilization under batch conditions at 30 and 15°C.....	67
3.3.3. Process development in 1 L PBR.....	74
3.3.3.1. Kinetic aspects of the microbial biomass enriched in 1 L PBRs .....	74
3.3.3.2. Molecular characterization of the enriched microbial communities.....	75
3.3.3.3. Identification of monooxygenase encoding genes .....	80
3.3.4. Scale up of the process: 31 L pilot plant .....	82
3.3.4.1. Kinetic aspects and discussion of the 31 L PBR.....	84
3.3.4.2. Molecular characterization of the enriched microbial communities.....	87
<b>3.4. Conclusions.....</b>	<b>92</b>
<b>Chapter 4. Microbial communities in the bioremediation of PAH-contaminated soil.....</b>	<b>95</b>
<b>4.1. Objectives and rationale of the research.....</b>	<b>95</b>
<b>4.2. Materials and Methods .....</b>	<b>96</b>
4.2.1. SIP-microcosms experimental design .....	96
4.2.1.1. Soil samples .....	96
4.2.1.2. SIP microcosms setup .....	96
4.2.2. Experimental workflow to characterize the microbial communities .....	96
4.2.2.1. Metagenomic DNA extraction .....	96
4.2.2.2. Isopycnic Centrifugation and Gradient Fractionation.....	97
4.2.2.3. Heavy-DNA containing-region identification by quantitative PCR (qPCR).....	97
4.2.2.4. Tag-encoded amplicons preparation for 454 pyrosequencing .....	97

4.2.2.5. Pyrosequencing Data Processing .....	98
<b>4.3. Results and discussion .....</b>	<b>99</b>
4.3.1. Evaluation of the heavy-DNA enrichment among SIP-communities .....	99
4.3.2. Investigation of the total community structure .....	100
4.3.3. Taxonomic identity of naphthalene-degrading communities.....	103
<b>4.4. Conclusions .....</b>	<b>106</b>
<b>Chapter 5. Production of PHA by sludge communities: community composition and evolution among selective and enriching processes. ....</b>	<b>107</b>
<b>5.1. Objectives of the work .....</b>	<b>107</b>
<b>5.2. Materials and methods .....</b>	<b>108</b>
<b>5.3. Results and discussion .....</b>	<b>108</b>
<b>5.4. Conclusions .....</b>	<b>111</b>
<b>Appendix – Phylogenetic classification of detected microbial phlotypes.....</b>	<b>113</b>
<b>Literature cited.....</b>	<b>127</b>

## List of Abbreviations

AC	Aerobic cometabolism
bp	Base pair
CAHs	Chlorinated aliphatic hydrocarbons
CCA	Correspondence analysis
cDCE	<i>cis</i> -1,2-Dichloroethene
°C	Degree Celsius
CF	Chloroform
CM	Methyl chloride
COD	Chemical oxygen demand
DCM	Dichloromethane
DGGE	Denaturing gradient gel electrophoresis
DNA	Deoxyribonucleic acid
DNAPLs	Dense non-aqueous phase liquids
dNTP	Deoxy nucleoside triphosphate
DRO	Diesel range organics
e.g.	For example (Latin: <i>exempli gratia</i> )
<i>et al.</i>	And others (Latin: <i>et alteri</i> )
FAD	Flavin adenine dinucleotide
FISH	Fluorescent <i>in situ</i> hybridization
GW	Groundwater
HD	High density
HMW	High molecular weight
HRT	Hydraulic retention time
LD	Low density
LMW	Low molecular weight
NAD(P)	Nicotinamide adenine dinucleotide (phosphate)
NGS	Next generation sequencing
NMDS	Non-metric multidimensional scaling
OLR	Organic loading rate
OTU	Operational taxonomic unit
PAHs	Polycyclic aromatic hydrocarbons
PBR	Packed bed bioreactor
PCA	Principal component analysis
PCE	Tetrachloroethylene
PCR	Polymerase chain reaction
PHA	Polyhydroxyalkanoates
P(3HB) or PHB	Poly(3-hydroxybutyrate)
PLFA	Phospholipid-derived fatty acids
pMMO	Particulate methane monooxygenase
prMO	Propane monooxygenase
RBCOD	Readily biodegradable COD
RD	Reductive dechlorination
RDA	Redundancy analysis
RDP	Ribosomal database project
RISA	Ribosomal intergenic spacer analysis
rRNA	Ribosomal ribonucleic acid
SBR	Sequencing batch reactor
SDIMO	Soluble di-iron monooxygenase
SIP	Stable isotope probing

sBMO	Soluble butane monooxygenase
sMMO	Soluble methane monooxygenase
SRT	Sludge retention time
TCE	Trichloroethylene
TeCA	1,1,2,3-Tetrachloroethane
TGGE	Temperature gradient gel electrophoresis
T-RFLP	Terminal-restriction fragment length polymorphism
UPGAMA	Unweighted pair group arithmetic averages
VC	Vinyl chloride
VFA	Volatile fatty acids
VOC	Volatile organic compound
v/v	Volume per volume
w/v	Weight per volume

# Chapter 1. Introduction

## 1.1. General introduction

The presented research work is at the interface between the field of environmental pollution science and progress in the exploration of diversity and activity of environmentally relevant microbial communities. Such interface is represented by the field of study of environmental biotechnology, dealing with the employment of biological systems to develop sustainable processes for the bioremediation of contaminated environments. These concepts are better explained in this introductory section.

Anthropogenic activities are source of organic compounds intentionally or accidentally released into the environment. Such compounds include heavy metals, pesticides, polychlorinated biphenyls (PCBs), chloroethenes (CE), or polycyclic aromatic hydrocarbons (PAHs), as well as the so-called “emerging pollutants”, including human pharmaceuticals, veterinary medicines, nanomaterials and other products (Boxall 2010). Many of these compounds have proven to be toxic to humans and the seepage of these contaminants into the environment, due to improper disposal, involuntary spillage, or airborne diffusion, resulted in an altered functioning of several natural ecosystems. On the other hand, the persistence of these xenobiotics in the environment can result in the adaptation of microorganisms to the contamination. Under such circumstances, a variety of microorganisms is able to evolve new metabolic pathways leading to the partial transformation, or mineralization, of the pollutant, a phenomenon known as natural attenuation (Daubaras *et al.* 1992; Bento *et al.* 2005; Diaz 2008; Kolvenbach *et al.* 2014). The wide metabolic potential possessed by complex microbial communities occurring in the environment represents a precious resource of viable degradation capabilities potentially capable of driving the removal of hazardous contaminants.

The utilization of natural microbial communities in order to treat contaminated environmental matrices is the challenge for many studies of environmental biotechnology. The branch of this discipline addressing the development of processes for the treatment of contaminated matrices is usually based on the utilization of complex microbial consortia enriched from the same contaminated site, taking advantage of their acclimation to the higher level of contaminants and probable involvement in natural remediation processes. In addition, during the biotechnological treatment of the matrix, a proper addition of specific nutrients, or substrates, is used to biostimulate the microbial degradation activity; in some cases, an exogenous microbial consortium, with proved ability to degrade the contaminants, can be introduced as inoculum (bioaugmentation) (Joutey *et al.* 2013). Furthermore, different approaches can be utilized for the stimulation of specific microbial activities

other than the utilization of organic contaminants. Such activities can involve the microbial production of commercially relevant compounds, with particular regard to biotechnological processes for the treatment and valorization of agro-industrial or urban waste matrices (Scoma *et al.* 2011; Valentino *et al.* 2014b).

The establishment of biotechnological processes is preferentially performed within contained and/or controlled systems, where operational parameters, such as temperature, pH, or, oxygen and substrate concentrations, are adjusted to enhance the desired microbial activities (e.g. pollutants abatement). During the development and optimization of the process, physical and chemical parameters need to be monitored constantly and properly modified, yet even that is not sufficient.

The choice, the development and the optimization of an appropriate and cost-effective process for the treatment of contaminated matrices strictly rely on the comprehensive investigation of the microbial ecology within the contaminated environment. This implies studying the extent of the microbial diversity and how it is affected by environmental and/or operational factors, such as temperature, pH, salinity, pressure, nutrients availability. In addition, it is important to obtain information about microbial activities and their role in the net of synergic microbial interactions. Investigating the microbial ecology of the community gives an idea of its metabolic potential and how it can be exploited to drive a biological process. Thus, it appears essential to keep under monitoring the complexity of microbial communities enriched during the conduction of a biotechnological process. The knowledge gained about the community structure, composition and functional organization over time complements the information obtained by monitoring process parameters, and the pollutants removal efficiency. Such a pool of information suggests the best way of modifying operational parameters, gradually, towards the optimization of the process, in terms of stability and robustness.

In this framework, a relevant role is represented by the techniques utilized for the microbial ecology investigation of complex environmental communities. This aspect attracts even more attention, when an exhaustive and relatively fast analysis of the community structure and composition needs to be performed during the monitoring of progressive operative phases of a process.

The requirement to deeply understand the diversity and functionality of complex microbial communities cannot be accomplished by means of traditional microbiology culturing techniques, limiting the analysis to culturable microorganisms (Rappe *et al.* 2003). Instead, the microbial ecology investigations can rely on culture-independent methods, accessing to the majority of uncultured microorganisms. Thanks to the progress in the molecular analysis of genomes, metagenomic techniques can serve microbial ecology studies, by analysing pools of genomes retrieved from the total microorganisms contained within environmental samples (Handelsman 2007; Thomas *et al.*

2012). Metagenomics is a viable way of accurately monitoring microbial communities which reside in environmental sites and are relevant to biotechnological processes.

## **1.2. Research objectives and rationale**

The main objective of the presented work was the utilization of molecular biology tools to characterize complex microbial communities involved in three different biotechnological processes. The characterization analysis was based on analysing metagenomes to determine the communities diversity and functional organization, aiming at the identification of the dominant phylotypes and how they relate to the efficiency of the process. Different culture-independent molecular techniques were employed according to different requirements and types of information necessary to each specific case of the study. The following points briefly describe the different tasks for each process of interest.

1. Molecular characterization of different microbial consortia, enriched through progressive development phases of an immobilized-biomass process, aimed to bioremediate chlorinated aliphatic hydrocarbons (CAHs) contaminated groundwater. The employed molecular tools for the analysis were mainly denaturing gradient gel electrophoresis (DGGE), and Sanger-based sequencing. Such tools are particularly suitable to obtain fast and clear fingerprinting profiles of the analysed communities. This is necessary to evaluate the extent of changes in the community structure occurring as a response to the variation of process factors, such as temperature, type of substrate, cells immobilization, or type of cell-growth-supporting material. This information supports the kinetic analysis of the process and permits its efficient development.
2. Comprehensive determination of the microbial diversity and functionality of communities enriched in a diesel-contaminated soil, subjected to rhizoremediation- or fertilization-based treatments. The microbial metabolic activity was assessed for the biodegradation of naphthalene, a representative model for polycyclic aromatic hydrocarbons (PAHs), a class of contaminants occurring in the diesel-contaminated soil. Such an investigation was performed by combining stable isotope probing (SIP) experiments and high-throughput sequencing analysis based on the pyrosequencing chemistry. This comprehensive study of the soil community composition, and identification of the microbes metabolically active in the degradation of the PAHs, helped to evaluate the most successful strategy of treatment of the contaminated soil.

3. Identification of microbial species with a key role in the production of polyhydroxyalkanoates (PHA) enriched during biotechnological processes for the treatment and sludge minimization of municipal wastewater. The construction of clone libraries in association with a denaturing gradient gel electrophoresis (DGGE) analysis was utilized to identify dominant microbial phylotypes enriched through specific phases of conduction and clarify how they related to the PHA-production process.

### **1.3. Dissertation organization**

This dissertation consists of three studies, each one conducted in the framework of different research projects in collaboration with different partners. My contribution to these studies was the investigation of the microbial ecology of biotechnological processes.

The Chapter 2 of the dissertation consists of a literature review, encompassing the main environmental issues and possible solutions, related to the three projects mentioned above. In the section 2.4., the scientific approaches and the molecular techniques used to characterize diversity and functionality of microbial communities are reviewed. Chapters 3,4 and 5 are specifically dedicated to discuss the research performed and the data obtained during the research performed in order to achieve the objectives 1 2 and 3, respectively.

## Chapter 2. Literature review

### 2.1. Bioremediation of aquifers contaminated by chlorinated aliphatic hydrocarbons (CAHs)

#### 2.1.1. CAHs: distribution in the environment, chemical and physical properties, toxicity

Chlorinated aliphatic hydrocarbons (CAHs) constitute one of the major class of environmental contaminants, mainly persistent in soil and groundwater. Anthropogenic activities and, to a minor extent, natural sources determine the widespread occurrence of CAHs in the biosphere. These compounds found massive applications as solvents in the dry-cleaning (metal and plastic), as refrigerants in manufacturing, in the production of polymeric materials, rubbers, cosmetics, drugs, and in the textile industry, the latter producing high volumes of highly contaminated wastewater (Bhatt *et al.* 2007; Frascari *et al.* 2015). Such activities often result in the accidental or intentional release of these compounds into the environment. At the same time, some natural processes, like the oxidation of soil humus (Keppler *et al.* 2000; Ballschmiter 2003), as well as some plants, algae, or fungi can be sources of CAHs (Hoekstra *et al.* 1998; Harper 2000; Öberg 2003).

Typically, CAHs derive from hydrocarbons by substitution of hydrogen atoms with chlorine. According to the molecular structure, they are mainly classified into chloromethanes, chloroethanes, and chloroethenes. Within each category, it is possible to distinguish between lower- or higher-chlorinated compounds. The number of chlorine substitutions strongly affects chemical and physical properties of CAHs; therefore, higher chlorinated CAHs are less soluble in water, have low interfacial tension between liquid CAH and water and are more recalcitrant to biodegradation. With only few exceptions, such as vinyl chloride (VC), CAHs have higher density than water and tendency to exist as dense non-aqueous phase liquids (DNAPLs), able to seep through the soil and contaminate aquifers. The main CAHs frequently occurring in the environment are shown in Figure 1 and can be considered the most popular due to their extensive industrial usage. The chemical and physical properties of CAHs are listed in Table 1.

Many of the CAHs, such as TCE or PCE, are volatile – they are referred to as volatile organic compounds (VOCs). This is important with particular regard to air contamination of the urbanized areas (US EPA). As in the case of TCE, CAHs persistence in the air is limited (half-life of 7 days) by moderate degradation process consisting of the reaction with photochemically produced hydroxyl radicals (Scarano 2012). Despite this, properties like volatility, hydrophobicity and low viscosity favour a quick transport of these compounds far away from the source, ending with contamination of soil and shallow or deep water systems (Zogorski *et al.* 2006). In such systems, they show higher

mobility into the aqueous phase rather than adsorption onto the soil particles. The persistence of contaminants, such as TCE or PCE, in groundwater can be a matter of years (ATSDR 1997).

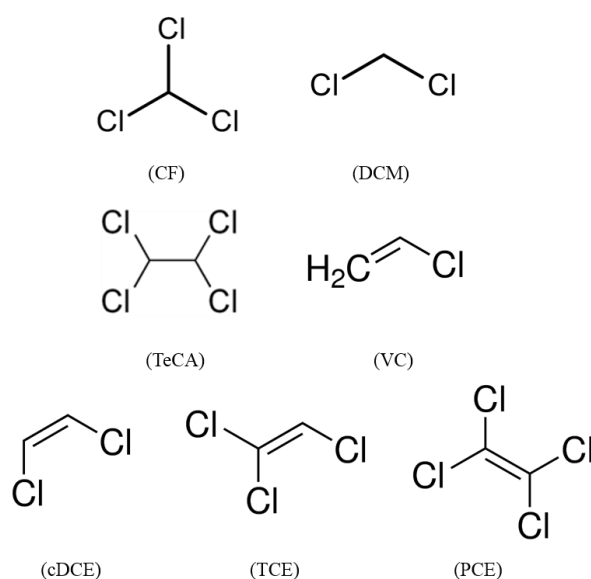


**Figure 1.** Molecular structure of the CAHs frequently detected in the environment.

**Table 1.** Salient features of the main CAHs of concern.

CAH	Density (g·cm <sup>-3</sup> ); 25°C	Boiling point (°C)	Solubility in water (g·L <sup>-1</sup> ); 25°C	MCL <sup>a</sup> (mg·L <sup>-1</sup> )	Toxicity and Carcinogenicity <sup>b</sup>
Chloroform (CF)	1.49	61.7	8.2	0.080	Cardiovascular; hepatic; neurological; reproductive; increased risk of cancer.
Dichloromethane (DCM)	1.33	39.7	17.5	0.005	Hepatic; cardiovascular; neurological; increased risk of cancer.
1,1,2,2-Tetrachloroethane (TeCA)	1.59	145.2	2.97	0	Hepatic; respiratory.
Vinyl chloride (VC)	0.91	-13.9	2.7	0.002	Cardiovascular; hepatic; developmental; immunological; carcinogenic to humans.
cis-1,2-Dichloroethene (cDCE)	1.28	60.1	3.5	0.07	Hepatic; cardiovascular; haematological.
Trichloroethylene (TCE)	1.46	88	1.10	0.005	Hepatic; developmental; neurological; carcinogenic to humans.
Tetrachloroethene (PCE)	1.62	121	0.15	0.005	Hepatic; developmental; neurological; respiratory; increased risk of cancer.

a) Maximum contaminant level (MCL) allowed in drinking water. US EPA, 816-F-09-0004, National Primary Drinking Water Regulations, 2009; US EPA 2011 Edition of the Drinking Water Standards and Health Advisories.

b) Reported by the Agency for Toxic Substances and Disease Registry (ATSDR); accessed on 11<sup>th</sup> February 2015.

With regard to the chemical-physical complexity of the natural systems, it should be mentioned that several environmental factors, such as pH and temperature of aqueous systems, might determine abiotic transformations of CAHs. In aqueous systems, CAHs may undergo abiotic hydrolytic dehalogenation, consisting of substitution or elimination reactions. The former consists of the water-mediated hydrolysis of the C-Cl bond, substituting the chlorine with the hydroxyl group. The latter is more frequent and the elimination of chlorine as hydrochloric acid occurs after the formation of a double bond between the chlorine bearing carbon and the adjacent carbon. The elimination reaction was demonstrated for the abiotic transformation of TeCA into TCE, in the subsurface (Cooper *et al.* 1987; Joens *et al.* 1995). However, abiotic transformations are slow and not efficient for the removal of high amounts of CAHs.

The wide diffusion of CAHs is of public concern due to their highly adverse effects to the human health, a toxicity often associated with the presence of chlorine (Table 1). Ingestion, inhalation and dermal exposure are the main ways by which CAHs, such as CF and TCE, access the human body (Weisel *et al.* 1996). The exposure to the majority of CAHs usually cause headaches, dizziness and confusion, but a prolonged exposure can provoke chronic problems to liver, kidney, endocrine and respiratory systems (ATSDR 1997; US EPA 2010). DCM, TCE and PCE are particularly dangerous to the central nervous system of humans and animals (Bushnell *et al.* 2005; Bale *et al.* 2011). Furthermore, VC is a proven carcinogen, mainly affecting the liver, where the oxidative metabolism of VC by cytochrome P450 produces a chlorooxirane epoxide, whose high reactivity gives rise to DNA-damaging (Gennaro *et al.* 2008; Cave *et al.* 2010). Medical research evidence suggests that TCE exposure increases the risk of cancer to lymphatic or endocrinal systems (Scott *et al.* 2011; Chow *et al.* 2010). Cases of PCE-contaminated drinking waters have been associated with the occurrence of breast cancer (Gallagher *et al.* 2011). In addition, several higher chlorinated CAHs, not associated with such a high toxicity, are considered hazardous as well, since their reactivity is likely to produce lower chlorinated compounds, such as VC, with proven carcinogenicity.

All of the discussed environmental and health CAHs-related issues explain the great efforts of the last decades to find sustainable strategies to clean-up CAHs-contaminated environmental sites.

### **2.1.2. Biodegradation of CAHs**

The CAHs release from anthropogenic or natural sources, often resulting in the long-term contamination of several environmental sites, have suggested the existence of microorganisms acclimated to the contamination and, probably, able to utilize CAHs as carbon and energy source. A large number of research studies demonstrated that several microbial metabolic pathways drive the partial degradation or the complete mineralization of chlorinated compounds in the environment,

resulting in the natural attenuation of the contamination (Tiehm *et al.* 2007). Such evidence incredibly broadened the range of natural, thus more sustainable, processes potentially exploitable to bioremediate CAH-contaminated matrices. In order to develop effective bioremediation processes, a comprehensive determination of the site characteristics is necessary, including physical and chemical properties of the matrix and its microbial ecology. The following paragraphs present the main catabolic mechanisms that microorganisms utilize to degrade CAHs, either through anaerobic reductive dechlorination, or through aerobic oxidation and aerobic cometabolism, focusing on the latter, while briefly overviewing the first two processes.

### **2.1.2.1. Anaerobic microbial dehalogenation**

Several anaerobic CAH-degradation mechanisms are well documented (Bradley 2003; Field *et al.* 2004; Smidt *et al.* 2004; Futagami *et al.* 2008). The most investigated anaerobic process is the reductive dechlorination (RD), taking place when microbial cells utilize CAHs, especially the higher chlorinated ones, as terminal electron acceptors. Of course, the reaction requires the presence of suitable electron donors, such as butyrate, propionate, ethanol and formate, easily fermentable to acetate and hydrogen by hydrogen-producing microbes of the community (Drzyzga *et al.* 2002; Villemur *et al.* 2006). Microbial RD can be a cometabolic process or a direct metabolic process, referring to the latter as halo-respiration. The anaerobic cometabolic RD of CAHs occurs under denitrifying or sulphate reducing conditions, mainly due to anaerobic microbes possessing metal-porphyrin-containing cofactors mediating an incomplete RD of PCE or TCE (Gossett *et al.* 1997). The process is very slow and random, without any energy profit for microbial cells. Much more interesting is CAH-dehalogenation driven by halo-respiring bacteria. Such a reaction occurs mainly via hydrogenolysis, when two moles of hydrogen are used for the sequential substitution of chlorines (Holliger *et al.* 2003), or via dichloroelimination, utilizing one mole of hydrogen to remove chlorines bound to two adjacent carbons, forming a double bond (de Wildelman *et al.* 2003). Halo-respiration seems to be a widespread strategy among several anaerobic microorganisms, mainly affiliated with Deltaproteobacteria (genera *Desulfovibrio*, *Anaeromyxobacter*, *Trichlorobacter*, *Geobacter*, *Desulfuromonas*), Epsilonproteobacteria (*Sulfurospirillum* spp.), Firmicutes (genera *Dehalobacter*, *Desulfitobacterium*) and Chloroflexi (*Dehalococcoides* spp.). Members of these phylogenetic groups possess a great metabolic potential to degrade higher chlorinated CAHs to lower chlorinated compounds, or utilize the latter ones as primary growth substrates. For instance, the strains *Desulfuromonas michiganensis* BB1 and BRS1 can transform PCE to cDCE using lactate, acetate, pyruvate, succinate, fumarate or malate as electron donors (Sung *et al.* 2003). Another isolate related to *Desulfitobacterium* spp. (strain Y51) is able to degrade PCE, along with some chloroethanes such

as TeCA, into dichloroethenes (Suyama *et al.* 2001). Furthermore, *Desulfitobacterium dichloroeliminans* strain DCA1 is capable of degrading haloalkanes via dichloroelimination (de Wildelman *et al.* 2003). In most of the cases, RD is a more effective process rather for the degradation of the higher chlorinated CAHs than for the lower ones (Smidt *et al.* 2004). The only exception to this trend is represented by *Dehalococcoides* spp.; to date, *Dehalococcoides mccarty* strain 195 is the only bacterial isolate that completely reduces PCE to ethene (Figure 2) through four reaction steps, where the first three are energy yielding and growth-supporting steps, while the last one is a cometabolic transformation from VC to ethene (Maymó-Gatell *et al.* 1997). In addition, several other *Dehalococcoides* spp. drive the RD of cDCE to VC (Maymó-Gatell *et al.* 2001), TCE to ethene (He *et al.* 2005), or, VC to ethene utilizing hydrogen, acetate or pyruvate as electron donors (He *et al.* 2003). Despite these capabilities, the conversion of lower chlorinated CAHs into ethene is rather slow, and often limited by unfavourable environmental conditions, such as an insufficient microbial metabolic potential or absence of key microorganisms. As an example, *Dehalococcoides* spp. require strictly anaerobic conditions of the contaminated environment, where these microbes also need to compete with other hydrogen-consuming bacteria. For these reasons, the accumulation of lower chlorinated CAHs is still one of the main drawbacks of RD (Tiehm *et al.* 2007).

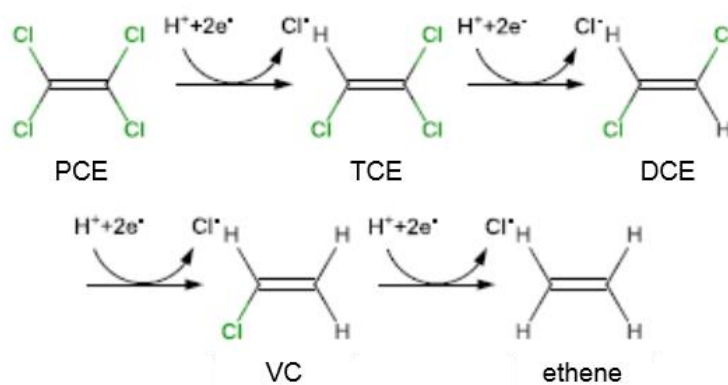


**Figure 2.** Anaerobic transformation of PCE into ethene.

In addition to the RD, other biological processes can contribute to the degradation of CAHs, although they are far less understood. For instance, some studies demonstrated that cDCE and VC can undergo anaerobic oxidation in the presence of terminal electron acceptors, such as nitrate (denitrifying conditions), sulphate ( $SO_4^{2-}$  reducing conditions),  $CO_2$  (methanogenic conditions), or some metals, like Fe(III) and Mn(IV) (Bradley *et al.* 1998; Bradley *et al.* 2005).

### 2.1.2.2. Microbial aerobic oxidation of CAHs

A direct oxidation of CAHs under aerobic conditions takes place when microbial cells utilize the chlorinated compounds as electron donors. Typically, the oxidation of CAHs can occur via alpha-hydroxylation reaction or via epoxide formation. On one hand, the hydroxylation is common for saturated CAHs obtained by the hydrolytic removal of chlorine, which is substituted by a hydroxyl group. On the other hand, CAHs containing a double bond undergo the formation of an epoxide stage, a quite instable compound, thus are rapidly degraded to non-halogenated compounds like organic acids or alcohols. The aerobic oxidation of CAHs is better understood than the anaerobic mechanisms, even though to date it is known to occur mostly for few lower-chlorinated CAHs, and a low number of microorganisms have been identified to possess such metabolic pathways.

Microorganisms belonging to the genera *Methylobacterium*, *Hyphomicrobium* and *Aminobacter*, *Nocardioides*, or *Rhizobium* are able to utilize methyl chloride (CM) as a sole carbon and energy source, while employing methyltransferase enzyme (CmuA) (McAnulla *et al.* 2001; McDonald *et al.* 2002). Such an enzyme has been identified in several seawater-living microbes, mainly Alphaproteobacteria, where genes encoding for the methyltransferase/corrinoid-binding protein CmuA have been characterized (Schäfer *et al.* 2005). Microorganisms strictly related to the above mentioned genera in addition to others belonging to the genera *Paracoccus*, *Albibacter* and *Methylopila* have been isolated and confirmed as DCM-utilizers (Doronina *et al.* 2001). Further studies demonstrated that VC can support the growth of several microbes, including *Mycobacterium* spp. (Hartmans *et al.* 1992; Chu *et al.* 2004), *Nocardioides* spp. (Coleman *et al.* 2002a), *Pseudomonas* spp. (Verge *et al.* 2000). A less frequent utilization of cDCE as sole carbon source has been associated only with *Polaromonas* spp. (Coleman *et al.* 2002b). However, the aerobic utilization of cDCE as a growth-supporting substrate has been demonstrated for complex microbial cultures enriched from chloroethene-contaminated groundwater (Schmidt *et al.* 2010). Other studies assess direct oxidation of cDCE by microbial communities occurring into freshwater stream sediments, subsurface aquifer sediments or organic-rich soils, though without demonstrating microbial growth (Mattes *et al.* 2010). For both VC and cDCE, the first oxidation degradative step is catalysed by a monooxygenase with the formation of an epoxide intermediate.

### 2.1.2.3. Aerobic cometabolic degradation of CAHs

The terminology ‘aerobic cometabolism’ (AC) is conventionally intended as the fortuitous oxidation of a non-growth substrate stimulated by the obligate presence of a cells’ growth substrate (Semprini 1997; Arp *et al.* 2001). Only the latter enhances cellular growth and metabolism, providing reducing power (NADH) to promote the activity of the enzymes involved in the substrate catabolic pathway. The oxidation of the former compound, also sometimes referred to as co-substrate, does not provide any benefit to microbial cells and takes advantage of the cellular enzymatic activity in the absence of the contemporary metabolism of the primary substrate.

The AC is an effective process to mineralize several lower and higher chlorinated CAHs. Since CAHs have hydrocarbon-like molecular structure, the most suitable primary substrates are saturated or unsaturated hydrocarbons, but also some aromatic compounds. Typical substrates are methane (Frascari *et al.* 2012b), propane (Wackett *et al.* 1989; Phelps *et al.* 1990), butane (Kim *et al.* 2000; Frascari *et al.* 2006b, 2013b), propene (Ensign *et al.* 1992), phenol (Folsom *et al.* 1990; Harker *et al.* 1990), toluene (Landa *et al.* 1994; Leahy *et al.* 1996) and ammonia (Vannelli *et al.* 1990; Hyman *et al.* 1995). Furthermore, some lower chlorinated CAHs, such as cDCE, can be cometabolized in the presence of other chloroethenes, such as VC (Hartmans *et al.* 1992; Le *et al.* 2011). Gaseous alkanes, such as methane and butane, are widespread in the environment and a large number of microbes can degrade them by means of several different metabolic pathways. Thus, gaseous alkanes could be considered as efficient growth-supporting substrates for microbial cultivation.

Extended research showed that complex microbial communities enriched in the presence of the above-mentioned substrates and could serve the degradation of a wide range of chlorinated hydrocarbons (Anderson *et al.* 1997; Frascari *et al.* 2006a). In addition, several microorganisms have been identified and characterized for their versatile capability to aerobically cometabolize CAHs. For instance, *Methylosinus trichosporium* and *Nitrosomonas europaea* efficiently cometabolize lower chlorinated methanes and ethanes, as well as CF, in the presence of methane and ammonia, respectively (Oldenhuis *et al.* 1989; Vannelli *et al.* 1990). *Rhodococcus* spp. were found to be involved in the CF cometabolism (Frascari *et al.* 2006b). Some microbial species belonging to the genera *Mycobacterium* and *Methylosinus* grow on VC and cometabolize all of the DCE isomers (Hartmans *et al.* 1992; Fox *et al.* 1990). TCE aerobic cometabolic degradation has been widely investigated either by mixed microbial cultures, mostly grown on methane, phenol and butane, or by pure cultures. Microbial species relevant to the AC of TCE are *Pseudomonas* spp., *Ralstonia* spp., *Burkholderia* spp., *Mycobacterium* spp., *Methylosinus* spp. and *Rhodococcus* spp. (Leahy *et al.* 1996; Folsom *et al.* 1990; Harker *et al.* 1990; Oldenhuis *et al.* 1989; Suttinun *et al.* 2009).

Aerobic microorganisms require molecular oxygen to modify the molecular structure of aliphatic or aromatic hydrocarbons, producing reactive degradation intermediates that are further converted into fatty acids and finally undergo the  $\beta$ -oxidation catabolic pathway to generate acetyl-CoA. The latter enters the tricarboxylic acids cycle to yield carbon dioxide and energy (Watkinson *et al.* 1990). Microbial biodegradation of different types of hydrocarbons starts with the activity of cellular mono- or di-oxygenase enzymes that introduce, respectively, one or two oxygen atoms to their substrate utilizing reductants provided by cofactors such as NAD(P)H. Oxygenases constitute an extended group of enzymes, assisting a large variety of biochemical processes both in prokaryotic and eukaryotic organisms. The majority of these enzymes have a remarkably relaxed substrate range (Arp *et al.* 2001), which confers them the ability to fortuitously oxygenate chlorinated compounds, when stimulated by the presence of a suitable primary substrate. The oxygenation of CAHs yields highly unstable intermediate compounds, often undergoing abiotic hydrolytic transformations and HCl elimination. In some cases, such intermediates are utilized by microorganisms (Oldenhuis *et al.* 1989; Fox *et al.* 1990). For instance, the aerobic cometabolic transformation of TCE by monooxygenases of *Methylosinus trichosporium* OB3b, proceeds via TCE-epoxide formation (Fox *et al.* 1990). The epoxide rapidly breaks down, giving rise to the formation of HCl, carbon monoxide, and organic acids such as formic acid or glyoxylic acid (Figure 3) (Wackett *et al.* 1995). In the case of TCE oxidation catalysed by dioxygenase expressed by *Pseudomonas putida*, the oxygenated intermediate could contain two oxygen atoms stabilized with an iron-bridge (Field *et al.* 2004).

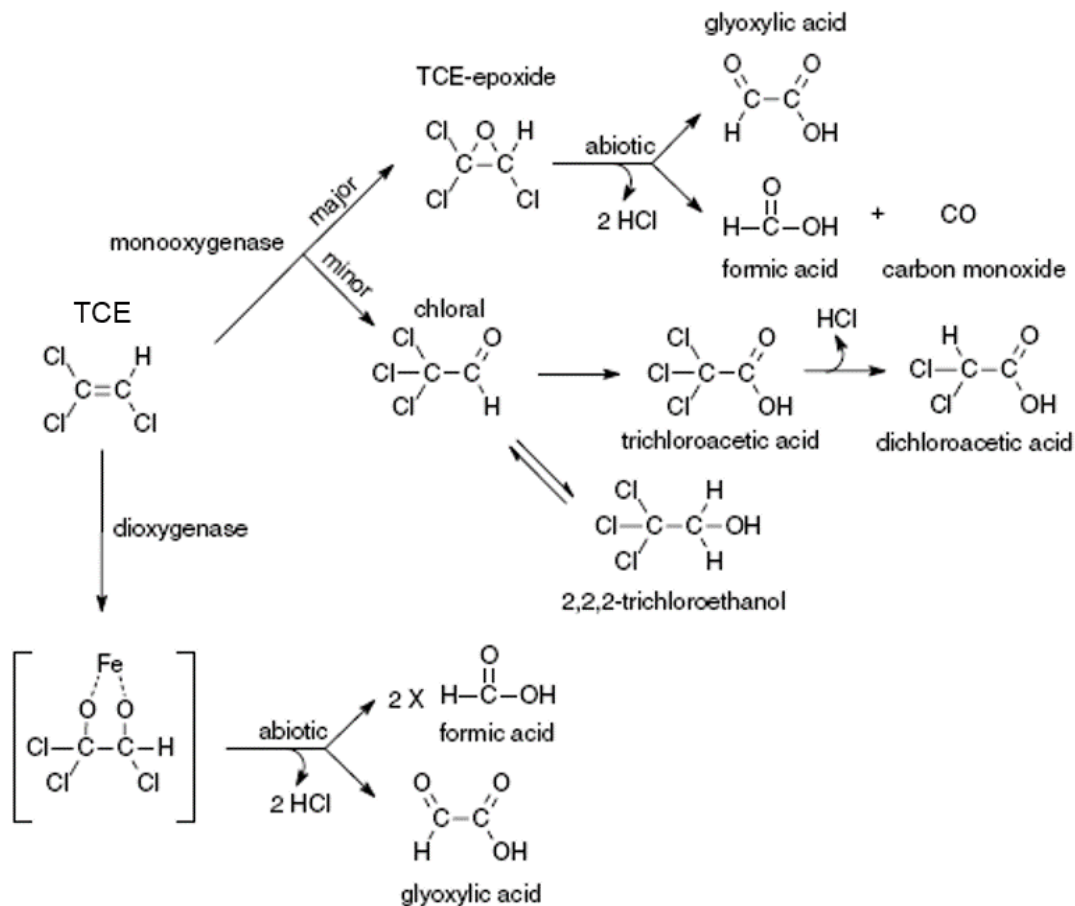


**Figure 3.** Proposed TCE aerobic cometabolic degradation pathways. (Reproduced from: Field *et al.* 2004).

An important limiting aspect of the AC is represented by intracellular toxicity of a variety of CAHs-oxygenation intermediates produced. These unstable intermediates give rises to general or specific toxicity by reacting with several cellular macromolecules (Alvarez-Cohen *et al.* 2001). In particular, a specific cellular damage was demonstrated to the oxygenase catalyser (Figure 4).

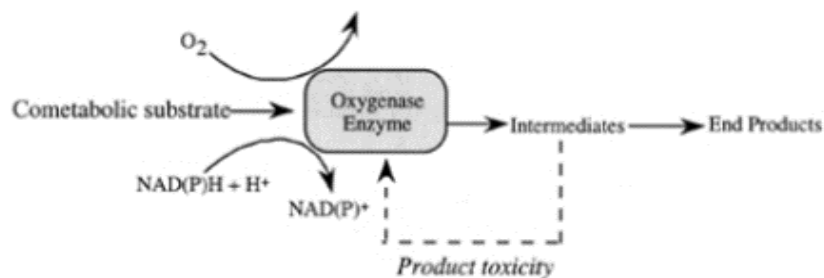


**Figure 4.** Product toxicity on the oxygenase activity (Reproduced from: Alvarez-Cohen *et al.* 2001).

#### **2.1.2.4. Key enzymes in the aerobic cometabolism of CAHs**

Oxygenases belong to the major class of oxidoreductase enzymes. As previously mentioned, mono- and di-oxygenases are utilized in nature to drive a wide variety of metabolic functions, introducing oxygen atoms into a large range of substrates and releasing more reactive compounds, such as alcohols, aldehydes, carboxylic acids, or epoxides. The activation and utilization of molecular oxygen is facilitated by the presence of prosthetic groups, which mediate the electron transfer from the reduced coenzyme NAD(P)H to oxygen (Arp *et al.* 2001). Varieties of prosthetic groups have been characterized, including binuclear and mononuclear iron clusters, iron sulphur clusters, flavin, heme, and Cu (Arp *et al.* 2001). The following paragraphs briefly discuss some molecular details of the main classes of oxygenases having crucial role in the AC of CAHs.

##### **2.1.2.4.1. Soluble di-iron monooxygenases (SDIMO)**

Soluble di-iron monooxygenases (SDIMO) are multi-component enzyme systems (Coleman *et al.* 2006). This enzymatic family derive its name from a conserved non-heme di-iron active site contained in the hydroxylase subunit of the enzymatic system. The latter consists of three or four main components: a dimeric hydroxylase protein; an NADH oxidoreductase subunit, transferring electrons from the NAD(P)H to the hydroxylase; a small coupling protein reducing the O<sub>2</sub> to H<sub>2</sub>O<sub>2</sub>. In some cases, a Rieske-type ferredoxin protein is a part of the enzyme (Leahy *et al.* 2003). Several oxygenases are included in the SDIMO group, such as the soluble methane monooxygenases (sMMO), toluene monooxygenases, alkene monooxygenases, and phenol hydroxylases (Leahy *et al.* 2003). Enzymes belonging to SDIMO class are capable of cometabolically degrade TCE and VC (Fox *et al.* 1990; Saeki *et al.* 1999), when expressed by microorganisms growing on methane, butane, propane or phenol (Coleman *et al.* 2006). The ability to grow on gaseous and short alkanes has been proven in some microbes belonging to the genera *Pseudomonas* (Sluis *et al.* 2002), *Nocardia* (Hamamura *et al.* 2001), *Methylosinus* (Oldenhuis *et al.* 1989), *Mycobacterium* (Wackett *et al.* 1989), or *Rhodococcus* (Larkin *et al.* 2005; Frascari *et al.* 2006b). Some of the SDIMO-enzymes are described below.

##### **2.1.2.4.2. Methane monooxygenase (MMO)**

Methanotrophs are Gram-negative bacteria, including members affiliated with Alphaproteobacteria and Gammaproteobacteria, which aerobically utilize methane as an energy source. Their ability to oxidize methane into methanol is conferred by methane monooxygenase (MMO) (Dumont *et al.* 2005). Two forms of MMO occur in nature: soluble (sMMO), a cytoplasmic system, and particulate (pMMO), associated with cellular membranes.

The sMMO are expressed under copper-limiting conditions (Stanley *et al.* 1983; Hakemian *et al.* 2007) in certain Type I, Type II and Type X methanotrophs (Arp *et al.* 2001). The substrate range for sMMO includes C<sub>1</sub>-C<sub>7</sub> alkanes, alkenes and aromatic compounds, oxidized into the corresponding alcohols, epoxides, or enols (Green *et al.* 1989). sMMO belong to the SDIMO group and the reductase subunit transfers electrons from NADH to the hydroxylase subunit via FAD and an iron-sulfur cluster (Arp *et al.* 2001; Leahy *et al.* 2003). The expression of sMMO occurs, for instance, in *Methylosinus trichosporium* OB3b (Oldenhuis *et al.* 1989), *Methylococcus capsulatus* Bath (Green *et al.* 1989) and *Methylomonas* spp. (Shigematsu *et al.* 1999), all of which are associated with the degradation of TCE.

A larger number of methanotrophs, which in many cases are not able to produce the sMMO, express particulate pMMO. The molecular structure of pMMO is not well determined yet due to difficulties to obtain a purified membrane protein. However, some pMMO have been purified, for instance the one from *Methylococcus capsulatus* Bath (Nguyen *et al.* 1998), and it is known that the enzyme is composed of three subunits, namely, PmoA, PmoB and PmoC (Lieberman *et al.* 2004). Furthermore, it seems that the active site of the enzyme contains copper (Hakemian *et al.* 2007). Several studies showed the higher pMMO substrate selectivity toward C<sub>1</sub>-C<sub>5</sub> alkanes and alkenes, along with the capability to oxidize TCE in *Methylosinus trichosporium* OB3b (Lontoh *et al.* 2000).

#### **2.1.2.4.3. Butane and propane monooxygenases**

Some enzymes involved in the microbial degradation of short C<sub>2</sub>-C<sub>4</sub> gaseous alkanes are closely related to sMMO, yet without being able to oxidize methane (Hamamura *et al.* 1999). Among them is a soluble butane monooxygenase (sBMO), partially isolated from *Pseudomonas butanovora*, which can hydroxylate C<sub>2</sub>-C<sub>9</sub> alkanes by sequential oxidation of the alkane terminal methyl group (Sluis *et al.* 2002). Similarly to sMMO, sBMO is a NADH-dependent SDIMO enzyme; on the other hand, sBMO transforms butane exclusively into 1-butanol, while 2-butanol is the main product of sMMO. The molecule of 1-butanol is subsequently transformed into the respective aldehyde and finally into butyrate, which probably undergoes  $\beta$ -oxidation. From the molecular point of view, sBMO consists of three components essential to the multicomponent system activity: a hydroxylase component (BMOH), a reductase NADH-utilizing protein (BMOR), and, a small regulatory protein (BMOB) that does not possess any redox activity, nor binds any cofactor (Sluis *et al.* 2002). The sBMO enzymatic activity of *P. butanovora* has been associated with TCE AC process (Arp *et al.* 2001). Other BMO-like enzymes have been characterized in *Mycobacterium vaccae* JOB5 and *Nocardioides* sp. CF8, the latter containing copper in the active site, similarly to pMMOs (Hamamura *et al.* 1999).

Another example of SDIMO enzyme is a propane monooxygenase (PrMO), first purified from the Gram-positive microorganism *Gordonia* sp. TY-5 (Shennan 2006). This PrMO has a very narrow substrate range, since it can exclusively oxidize propane. Propane is subjected to sub-terminal oxidation with the production of 2-propanol, which is then sequentially transformed into acetone, methylacetate, acetic acid and methanol (Kotani *et al.* 2003, 2007). As in the cases of sBMO and MMO, PrMO consists of a hydroxylase (large and small subunits), an oxidoreductase (PrmB) and a coupling protein (PrmD) (Kotani *et al.* 2003). Other microorganisms, namely *Mycobacterium* sp. TY-6 and *Pseudonocardia* sp. TY-7, possess similar PrMO to oxidise propane at the terminal or sub-terminal positions, respectively (Kotani *et al.* 2006).

#### **2.1.2.4.4. AlkB super-family**

AlkB oxygenases belong to a super-family of integral-membrane proteins, containing a non-heme diiron cluster, typical of SDIMO enzymatic group. AlkB initiates the alkane hydroxylation by introducing one oxygen atom at the terminal position, while the second oxygen atom, derived from O<sub>2</sub> molecule, it is used to form water.

A wide range of alkanes can be substrates for the AlkB family of hydroxylases, which have been detected in many widespread environmental microbes. For example, microorganisms belonging to the genera *Mycobacterium*, *Acinetobacter*, or the strain *Nocardioides* sp. CF8 possess AlkB-like oxygenases active on alkanes long up to 13 carbons (Hamamura *et al.* 2001; Cole *et al.* 1998; Geissdorfer *et al.* 1995). The most studied AlkB system is the one of *Pseudomonas putida* GPo1, which is considered a model system (van Beilen *et al.* 2001). This strain can oxidize linear alkanes ranging from n-pentane to n-dodecane (van Beilen *et al.* 2005).

Although the crystal structure of the *P. putida* AlkB is not available, it was demonstrated that the AlkB membrane-system works in coordination with two soluble proteins for the electron transfer from the NAD(P)H, namely rubredoxin and rubredoxin reductase (van Beilen *et al.* 2001; Geissdorfer *et al.* 1995). The latter transfers electrons from NAD(P)H via its cofactor FAD to the rubredoxin, which drives the reductant flux to the AlkB active site, facing the cytoplasm (Figure 5).

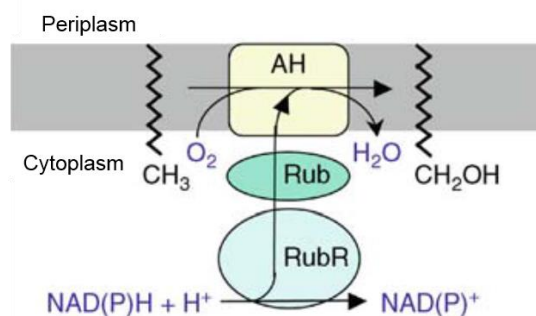


**Figure 5.** *Pseudomonas putida* GPO1 AlkB hydroxylase, electron transfer mechanism. Rub: rubredoxin protein. RubR: rubredoxin reductase protein. (Reproduced from: Rojo 2010).

Several research studies deduced that the AlkB system contains six transmembrane  $\alpha$ -helices forming a hydrophobic pocket through the cytoplasmic membrane and the substrate is properly positioned into this pocket in order to be oxidized at its terminal methyl group. Furthermore, the active site consists of four histidine residues that chelate two iron atoms (Figure 6) (van Beilen *et al.* 2005; Rojo 2010).

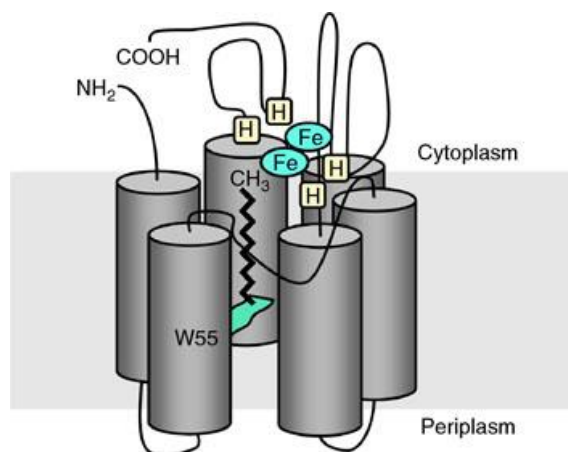


**Figure 6.** *Pseudomonas putida* GPO1 AlkB membrane-hydroxylase, proposed model. (Reproduced from: Rojo 2010).

#### 2.1.2.4.5. Bacterial cytochrome P450

Cytochrome P450 are heme-iron hydroxylases ubiquitous in all phylogenetic kingdoms. To date, about 4000 enzymatic types are known (van Beilen *et al.* 2007). The majority of the prokaryotic P450 are soluble and have a more restricted substrate range in comparison with their eukaryotic counterpart (Karlson *et al.* 1993). Despite few pieces of evidence of the P450 involvement in the n-alkanes degradation, its enzymatic activity is interesting, because it has been detected in several microbial species often involved in the bioremediation of environmental contaminated sites. Several C<sub>5</sub>-C<sub>10</sub> alkane-degrading microbial species express P450 belonging to a new family whose first

member was the cytochrome CYP153A1 derived from *Acinetobacter calcoaceticus* EB104 (Maier *et al.* 2001). CYP153A1 is the only one able to oxidize butane. The electron transfer from NAD(P)H to this protein is mediated by ferredoxin reductase and ferredoxin proteins. Closely related cytochromes were purified from *Mycobacterium* spp. with the ability to degrade C<sub>6</sub>-C<sub>11</sub> alkanes (Fanhoff *et al.* 2006), or identified in other strains affiliated with rhodococci and Proteobacteria. Such enzymes are able to oxidize C<sub>5</sub>-C<sub>10</sub> alkanes (van Beilen *et al.* 2006).

### **2.1.3. *In situ* aerobic cometabolic bioremediation of CAH-contaminated aquifers**

Chemical and physical properties of CAHs confer them the nature of DNAPLs, which easily seep through the permeable subsurface layers reaching and accumulating in shallow aquifers of the non-permeable zone of the Earth, where the DNAPL mass constitutes a risky long-term source of contamination. Such a zone is defined as DNAPL source zone (ITRC 2008). The occurrence of DNAPL source zones in the subsurface aquifers is of current public concern. Numerous efforts for the restoration of contaminated aquifers gave rise to the development of several technologies, with particular regard to the *in situ* treatments.

As discussed in the section 2.1.2., several biological mechanisms of CAH degradation occur among natural ecosystems and might contribute to natural attenuation of contaminated sites. Considering strengths and weaknesses of each process, namely RD, aerobic oxidation and AC, the latter seems to be the most viable strategy to bioremediate contaminated environmental matrices. AC is effective for a larger number of CAHs and can be carried out by a larger number of microbial species in comparison to the other two metabolic processes. Furthermore, it shows higher degradation rates, ensuring at the same time a complete mineralization of the contaminants.

The employment of AC process for *in situ* treatment of contaminated aquifers is a promising bioremediation strategy. The process can be enhanced directly in the contaminated well by addition of suitable cell-growth primary substrate and oxygen supply. The main advantages of this approach over the traditional decontamination technologies is the complete removal of the contaminants. Traditional methods were based on the extraction of the contaminated ground water and its treatment on-site by adsorption of the contaminants onto sorbent materials, hence not actually destroying the contaminants, but just transferring them to a different phase (sorbent). However, an AC *in situ* treatment implies some possible drawbacks. First, the simultaneous presence of the growth-substrate and the contaminants (CAHs) can cause mutual enzymatic inhibition of the process, lowering the CAHs-degradation rates. Second, an excessive microbial growth could take place near the substrate-injection well, clogging the aquifer. Finally, the homogeneousness of the process is not ensured through all the aquifer (Frasconi *et al.* 2015). Such issues could be overcome by injecting oxygen and

cell-growth substrate into the well as alternating pulses, a strategy defined as *pulsed feeding strategy* (Roberts *et al.* 1990; Frascari *et al.* 2015). In this way, the oxygen, indispensable for the activity of the oxygenase enzymes, and the growth substrate (hydrocarbon) will not be simultaneously available to the indigenous microbial biomass except for few narrow zones, called bioreactive zones. Here, both oxygen and growth substrate will occur at a low concentrations because of hydrodynamic dispersion and substrate sorption phenomena. This overlapping zone represents the only opportunity for the *in situ* enrichment of microorganisms able to oxidize CAHs fortuitously, minimizing the issues related to the substrate inhibition. Furthermore, this region will progressively move through the aquifer taking advantage of the water flow and will promote the CAHs degradation throughout the DNAPLs source zone (Figure 7).

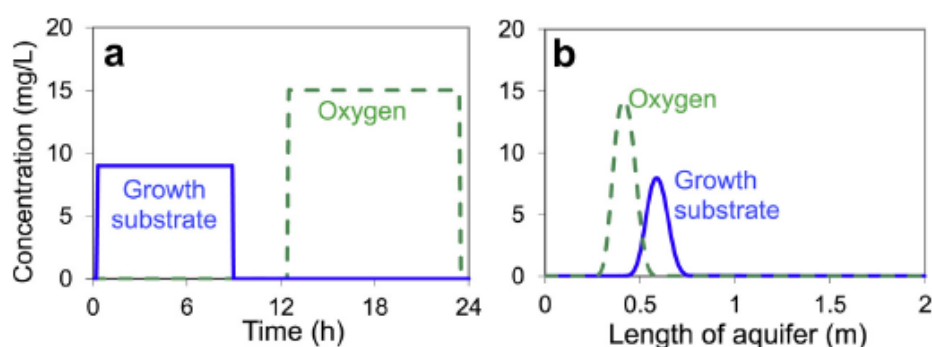


**Figure 7.** Schematization of the pulsed feeding principle: the alternating supply of oxygen and growth substrate over time (a) and the formation of a bioreactive zone along the aquifer length (b). (Reproduced from: Frascari *et al.* 2015).

### 2.1.3.1. Main technologies for the *in situ* bio-treatment of contaminated aquifers

Several technologies have been employed for the *in situ* AC treatment of contaminated aquifers. One of the most used technologies is the air sparging, which rests on the *in situ* supply of gaseous compounds, such as oxygen (Hinchee *et al.* 1995). Air sparging can be integrated with the simultaneous *in situ* introduction of the cell-growth supporting substrate, either as a concentrated solution or as a gas (Blackert *et al.* 2007; Hazen *et al.* 1994; Semprini 1997). In some applications, the oxygen and the substrate were directly released into the lower part of an aquifer by using a submerged pump (Semprini 1997; Frascari *et al.* 2015), while the homogeneous solubilisation and distribution of the two compounds among the entire well was promoted with a recirculation system. The air sparging of both oxygen and gaseous substrates is defined as cometabolic air sparging (U.S. Department of Defense 2001).

Another possible *in situ* treatment of CAHs is the bioaugmentation with resting microbial cells (Duba *et al.* 1996; Semprini 1997). Such a technology relies on the enrichment of pure or mixed

microbial cultures with on-site located bioreactor systems. At this level, the microbial biomass is grown in the presence of a suitable substrate that provides the microorganisms with the reducing power necessary to the subsequent CAH aerobic degradation inside the well.

In many cases, the bioremediation of higher-chlorinated hydrocarbons was accomplished utilizing sequential anaerobic-aerobic processes, by virtue of the RD-based degradation of highly chlorinated CAHs and of the AC-based degradation of lower-chlorinated compounds, accumulated through the previous step (Tiehm *et al.* 2011).

### **2.1.3.2. On-site treatment with immobilized-biomass systems**

Some of the main concerns of *in situ* bioremediation is the need to target the contaminated zone, avoiding the migration of the contaminants elsewhere in the subsurface. Such needs often determine the choice of an on-site *pump and treat* approach, which consists of the physical extraction of the contaminated matrix (ground water), on-site treatment and subsequent re-injection into the subsurface, usually into a well located upstream of the well utilized for the extraction of the matrix.

An interesting option to implement the *pump and treat* approach is the utilization of an immobilized-biomass system for the AC-based remediation of groundwater. This represents a viable solution for a fast and complete mineralization of the contaminants, with the additional advantage that the process is cost-effective, since it is conducted on-site. An innovative aspect of such a bioremediation strategy is the utilization of immobilized biomass, namely microbial cells, onto suitable immobilization supporting material. A properly selected immobilization material promotes the growth of the microbial cells as biofilm, and it can be used to pack the bioreactor system obtaining a packed bed bioreactor (PBR).

The PBR technology operating the AC of CAHs via microbial biofilm offers numerous advantages, such as the possibility of working with higher biomass concentrations and cell retention times, avoiding the biomass-settling step and obtaining a partial protection of cells against toxic substances (Singh *et al.* 2006; Frascari *et al.* 2013b). Other intrinsic advantages of this strategy are the possibility to utilize higher organic loads and the lower risk of clogging, even if the growth substrate is fed continuously (Frascari *et al.* 2013b).

## **2.2. Bioremediation of polycyclic aromatic hydrocarbon (PAH)-contaminated soils**

### **2.2.1. PAHs: distribution, chemical and physical properties, toxicity**

Polycyclic aromatic hydrocarbons (PAHs) constitute a class of widespread environmental contaminants. Their diffusion and accumulation is given by natural phenomena, such as incomplete combustion of organic material, forest fires and volcanic eruptions, but also by several human activities (Chauhan *et al.* 2008; Haritash *et al.* 2009). In fact, PAH anthropogenic sources are accidental petroleum product spillage, coal gasification, engine exhaust, cigarette smoke and other industrial activities.

From the chemical point of view, PAH molecular structure consists of two or more fused benzene rings; according to the ring number, PAHs are classified into lower molecular weight (LMW-PAHs) or higher molecular weight (HMW-PAHs), the latter containing four or more rings. Their aromatic nature along with other physical properties, such as low aqueous solubility and high solid-water distribution ratios (Johnsen *et al.* 2004), make PAHs stable and recalcitrant in the environment. In addition, these hydrophobic characteristics of PAHs become stronger with the increase in the number of aromatic rings, thus PAHs are easily adsorbed on organic particles of soil matrix, accumulate in sediments, or aggregate in non-aqueous phase liquid (NAPL)-film into water systems. PAH persistence in the environment is of public concern, because of the toxic effects on environmental ecosystems (Jaward *et al.* 2012) and human health. PAHs can be inhaled with air particles or otherwise introduced into the body with food and contaminated water. Since they are lipid-soluble, they can be adsorbed at gastrointestinal level and distributed in mammalian fatty tissues (Samanta *et al.* 2002). The human exposure to PAHs can result in toxic or chronic adverse health effects and there are many research studies evidencing that some PAHs, primarily the benzo[*a*]pyrene, are carcinogenic compounds (Lalib *et al.* 2013). The US Environmental Protection Agency (US EPA) classified sixteen PAHs as priority pollutants, and some of them are shown in Figure 8 (Habe *et al.* 2014).

In this scenario, remediation of PAH-contaminated environmental matrices, with particular focus on soil, is crucial for the public health.

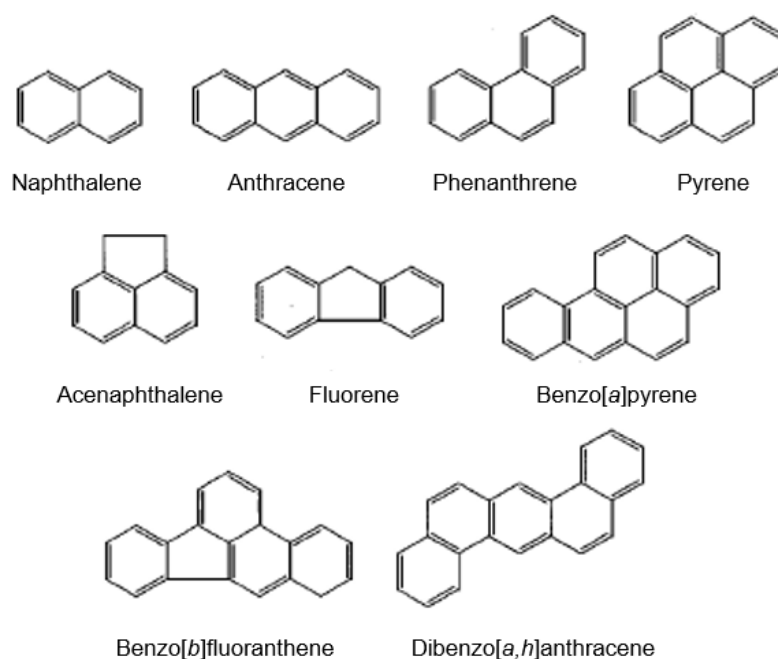


**Figure 8.** Chemical structure of some PAHs, classified as hazardous from the US EPA.

### 2.2.2. PAH biodegradation

Commonly utilized physical and mechanical treatments for the PAH removal in contaminated soil, such as incineration, soil vapour extraction or thermal desorption, are expensive and not much successful, since most of the contaminants are just transferred into a different phase (Haritash *et al.* 2009). On the other end, it is well known that several widespread environmental bacterial species play a role in the total mineralization of PAHs or in their transformation into less hazardous compounds (Juhasz *et al.* 2000; Bamforth *et al.* 2005). The microbial biodegradation of pollutants like PAHs has a potential to be a highly efficient and cost effective treatment, especially considering its *in situ* applicability. For these reasons, it has been deeply investigated and exploited (Johnsen *et al.* 2004; Chauhan *et al.* 2008; Haritash *et al.* 2009). The establishment of such a process takes advantage of the broad range of metabolic capabilities possessed by the indigenous microbial communities in the contaminated matrix. Here, the microbial metabolism can be biostimulated by treatment with the addition of growth-limiting nutrients or some plant biomass (Bamforth *et al.* 2005; Das *et al.* 2011).

The accomplishment of PAH mineralization mediated by microorganisms is a complex process that can be limited by several factors. First, it can be strongly affected by the physical and chemical characteristics of the soil matrix, mainly its pH, temperature, the presence of nutrients such as nitrogen and phosphorus (Bamforth *et al.* 2005). In turn, these characteristics determine a different distribution of LMW- and HMW-PAHs according to the degree of hydrophobicity. The LMW-PAHs

are much more accessible to the soil microbial community than the HMW-PAHs, which have tendency to accumulate in smaller cavities of the soil matrix, limiting their bioavailability (Johnsen *et al.* 2004; Chauhan *et al.* 2008). As a result, much attention has been paid to study the mechanisms of the aerobic biodegradation of LMW PAHs. To date, such mechanisms are well known and widely described for several microbial species (Juhasz *et al.* 2000). Although less investigated, an increasing number of studies has also focused on the anaerobic degradation of PAHs, which can occur under denitrifying or sulphate-reducing conditions taking advantage of nitrate, ferrous iron and sulphate as final electron acceptors other than oxygen (Bamforth *et al.* 2005; Davidova *et al.* 2007).

It is possible that the minor bioavailability of HMW PAHs has become a limiting factor for the evolution of catabolic pathways among the microorganisms; only few microbial species have been identified as HMW-PAHs degraders (Heitkamp *et al.* 1988; Chauhan *et al.* 2008). Unfortunately, these compounds are the most hazardous among PAHs. On the other hand, it has been shown that some aerobic bacteria, able to grow on LMW PAHs as primary carbon and energy sources, are able to co-metabolically degrade HMW-PAHs (Heitkamp *et al.* 1988; Haritash *et al.* 2009). Thus, the addition of proper nutrients and amendments to the soil, used to enhance the growth and to biostimulate the PAHs degraders, represents a possible strategy to degrade complex mixtures of PAHs and overcome the persistence of the most recalcitrant compounds (Haritash *et al.* 2009).

Finally, along with the soil characteristics and the bioavailability of PAHs, the microbial potential of the indigenous communities of the contaminated matrix is a determining factor in the overall efficiency of the biodegradation process. The potential ability of the microbial biomass to drive a biodegradation process is determined by its genetic characteristics and the presence of the catabolic genes required. The knowledge on the microbial diversity of the contaminated matrix and its relation to the degradation activity of specific pollutants is crucial to establish, monitor and control a proper biodegradation process of a mixture of PAHs (Singleton *et al.* 2011).

### **2.2.3. Bacterial aerobic biodegradation**

The aerobic biodegradation of PAHs has been well investigated and it can be performed by numerous Gram negative and positive bacterial species, as well as by algae and fungi (Haritash *et al.* 2009). Focusing on bacteria, some common degradation mechanisms were identified. The typical PAH catabolic pathway starts with the enzymatic activity of a multicomponent dioxygenase system incorporating two adjacent hydroxyl groups (-OH) into an aromatic nucleus to form a *cis*-dihydrodiol. A dehydrogenase enzyme then acts to form dihydroxylated intermediates, which undergo oxidation to ortho- or meta-cleavage of the aromatic ring. Further reactions lead to the production of acetyl-

CoA and other precursors of tricarboxylic acid cycle (TCA) (Juhász *et al.* 2000; Chauhan *et al.* 2008; Habe *et al.* 2014).

Naphthalene is the simplest compound among PAHs, containing only two aromatic rings. For this reason, it is commonly utilized as a representative model to study the mechanisms of biodegradation. In addition, naphthalene represents a growth-supporting substrate for several bacterial species. In particular, the first studies in this field focused on the naphthalene degradation by pseudomonads (Davies *et al.* 1964; Yen *et al.* 1988; Wackett *et al.* 2001). It was shown that in many pseudomonads, the genes encoding for the naphthalene catabolic enzymes are located on a transmissible plasmid, identified as NAH7 and firstly isolated from *Pseudomonas putida* strain G7 (Dunn *et al.* 1973). NAH7 is organized in three operons encoding for the (i) upper pathway, (ii) the lower pathway and (iii) for a regulatory protein, NahR (Habe *et al.* 2014). As depicted in the Figure 9, the upper catabolic pathway of naphthalene leads to the production of salicylate. Salicylate is an intermediate of the naphthalene degradation, which induces both the upper and the lower pathways, acting at transcriptional level of the *nah* operons (Schell *et al.* 1985).

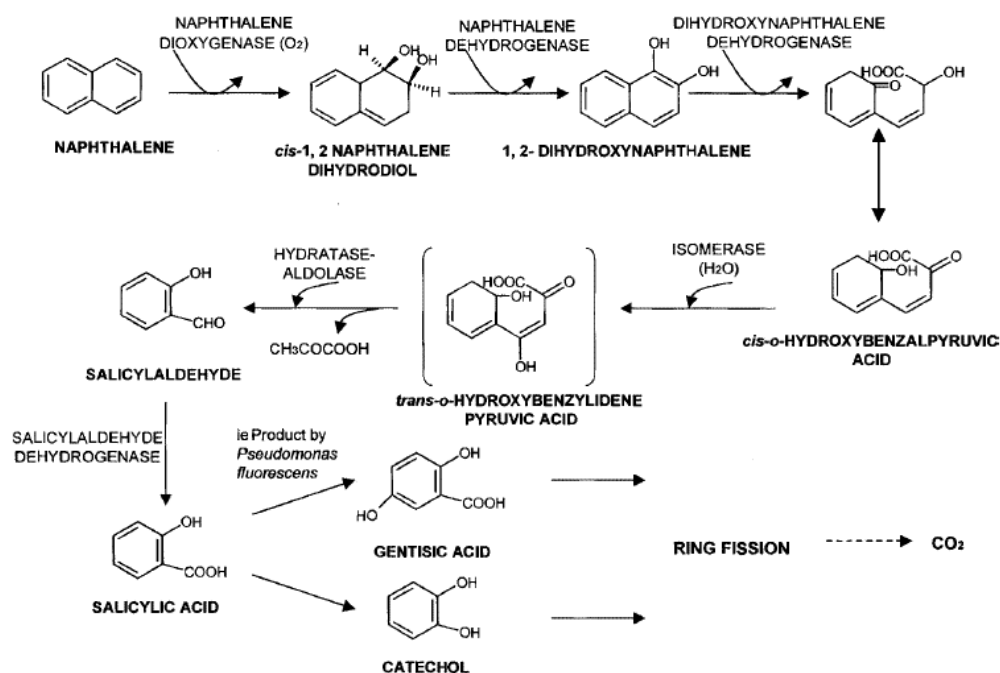


**Figure 9.** Main naphthalene aerobic degradation pathways. (Reproduced from: Bamforth *et al.* 2005).

To date, several other *Pseudomonas* spp. have been found to utilize very similar pathways (*nah*-like genes) for the naphthalene degradation; moreover, a wide variety of catabolic genes utilized by other bacteria for the PAH biodegradation has been described (Habe *et al.* 2014). The genera *Comamonas*, *Ralstonia*, *Burkholderia*, *Alcaligenes*, *Flavobacterium* and *Sphingomonas* are widespread soil Gram-negative microorganisms mostly associated to the degradation of lower-molecular weight PAHs utilizing different types of catabolic pathways (Mueller *et al.* 1996;

Pinyakong *et al.* 2003; Samanta *et al.* 2002; Juhasz *et al.* 1997; Habe *et al.* 2014). In addition, some *Burkholderia* spp. and *Pseudomonas* spp. along with Gram-positive genera, such as *Rhodococcus*, *Mycobacterium* or *Nocardioidea*, have been associated with the degradation of higher-molecular weight PAHs (Juhasz *et al.* 2000; Zang X. *et al.* 2006; Chauhan *et al.* 2008).

#### **2.2.4. Phytoremediation and rhizoremediation of PAH-contaminated soil**

Phytoremediation is a technology based on the utilization of green plants to remove, degrade or accumulate organic pollutants located in soil, water systems, or even in the atmosphere (Karen *et al.* 2009; Susarla *et al.* 2002). Phytoremediation of contaminated soil is a cost-effective treatment and it can be exploited *in situ* to cover large polluted areas. Particular attention is given to a branch of phytoremediation, namely rhizoremediation, defined as the plant-assisted microbial degradation of contaminants in the rhizosphere. The high biodegradation potential of the rhizoremediation strategy relies on synergic plant roots-microorganisms interactions. From this point of view, soil microbes gain nutritional benefit from a continuous release of organic compounds such as amino acid, carbohydrates, primary and secondary plant metabolites into the soil matrix through root exudation, or root turnover (Rovira *et al.* 1976; Siciliano *et al.* 1998). Such compounds are able to support the growth and the metabolic activity of microbes occurring in the rhizosphere (Kuiper *et al.* 2004). For these reasons, the microbial composition of rhizospheric communities is strictly dependent on the type of plant species utilized. Thus, choosing the right plant to treat the contaminated environmental matrix is crucial for the development of a proficient microbial consortium for the biodegradation of organic pollutants.

Another advantage of rhizoremediation is represented by the chemical capabilities of some root exudate compounds, such as organic acids, that increase the PAH solubility, thus their bioavailability to the microbial community in the rhizosphere (Karen *et al.* 2009). This phenomenon is accentuated when root material is present in the soil, since hydrophobic compounds like PAHs tend to adsorb on the roots (Karen *et al.* 2009), coming in strict contact with its exudates and the interacting microorganisms.

Many nutrient compounds released by plants in the rhizosphere, such as flavonoids and coumarins, are structurally similar to several organic contaminants, including PAHs, and can promote the fortuitous degradation of these contaminants by cometabolism or biostimulating their removal by degrader microbes (Qiu *et al.* 2004; Chaudhry *et al.* 2005; Karen *et al.* 2009). Several studies showed that secondary plant metabolites, in particular phenolic compounds, could promote the growth of soil bacteria degrading PAHs (Nichols *et al.* 1997; McFarlin 2010). Between them, salicylate is not only an inducer of the naphthalene degradation, as above mentioned, but it also stimulates the initial

degradation steps of other hydrocarbons including HMW-PAHs. For instance, phenanthrene, fluoranthene, pyrene, benz[*a*]anthracene and benz[*a*]pyrene can be degraded by *Pseudomonas* sp., *Sphingomonas* sp. after induction with salicylate (Chen *et al.* 1999; McCutcheon *et al.* 2003; Rentz *et al.* 2004).

The utilization of willow trees (*Salix* spp.) in phytoremediation of different type of contaminants, including petroleum derivatives, received an increasing attention (Wani *et al.* 2011). The main reasons for its good reputation in the environmental restoration are a fast growth and vegetative propagation, tolerance of flooded or saturated soils, or ability to contain high levels of toxic metals (Wani *et al.* 2011). Willow trees can release a variety of phenolic compounds through the plant tissues, but the most abundant is salicin (Collet 2004), and its transformation product salicylic acid (Lambers *et al.* 2008). Several applications of willow-mediated phytoremediation have been reported.

Case study. A research conducted at the Alaska Fairbanks University (McFarlin 2010) investigated the possibility to rhizoremediate a diesel-contaminated soil by utilizing a willow species *Salix alaxensis*. The authors described the rhizoremediation process of the contaminated soil by evaluating the biodegradation activity of the native soil microbial communities towards diesel range organics (DRO). The microbial activity was biostimulated by (i) amending the contaminated soil with crushed-willow-roots, to simulate the root turnover, (ii) addition of a fertilizer solution, or (iii) combining both of these treatments. The biodegradation efficiency of the diesel range organics (DRO) removal in the three experimental settings was compared against a control – untreated contaminated soil. The efficiency of each treatment was assessed through the monitoring of the DRO concentration and the most probable number of the diesel-degrading microorganisms. The results of the study (McFarlin 2010) showed that only the utilization of *S. alaxensis* biomass strongly promoted the DRO removal, while in combination with the fertilization of the soil a major number of soil microorganisms was observed. Although it was demonstrated that the addition of a fertilizer solution served the microbial growth or/and the increase of the plant biomass, “the addition of *Salix alaxensis* to diesel contaminated soil had a greater impact on the biodegradation of DROs” (McFarlin 2010).

A deep characterization of the microbial communities involved in the different biodegradation processes developed during the research study conducted in Alaska was the subject of the present dissertation. The microbial diversity and its relation to the degradation of naphthalene was investigated by exploiting cultivation-independent molecular techniques and it will be discussed in the Results of this dissertation.

## 2.3. Production of polyhydroxyalkanoates (PHAs)

### 2.3.1. PHAs: main characteristics and applications

Polyhydroxyalkanoates (PHAs) are biobased, completely biodegradable polymers, since they are naturally synthesized and utilized by a wide variety of microorganisms as intracellular reserve of carbon and energy (Braunegg *et al.* 1998). Currently, they represent a promising alternative to the conventional petro-chemically derived plastics (such as polyethylene and propylene). Despite the increasing popularity of PHA-polymeric materials, their usage for the replacement of traditional plastics is hindered by the high costs of production, ranging from 2.5-3.0 €/kg up to 12 €/kg depending on the type of polymer and production process (Castilho *et al.* 2009; Chanprateep 2010). Nowadays, much attention is paid to improve the production process in terms of costs and PHA productivity.

The majority of PHAs are aliphatic polyesters (Figure 10) (Braunegg *et al.* 1998). The type of functional group indicated as *R* and the value of *x*, shown in Figure 10, determine the identity of a monomer unit (Braunegg *et al.* 1998).

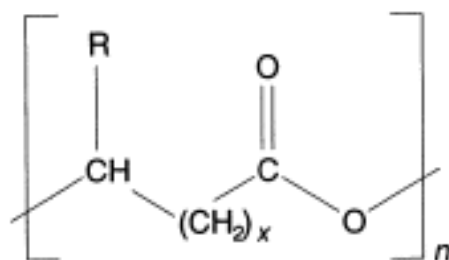


**Figure 10.** General formula for PHAs.

As an example, the most common polymer units have  $x = 1$  and when *R* is represented by hydrogen, methyl, ethyl or propyl, the units bear the name of poly(3-hydroxypropionate), poly(3-hydroxybutyrate), poly(3-hydroxyvalerate), or poly(3-hydroxyhexanoate), respectively (Braunegg *et al.* 1998). Practically, PHAs are polyesters of hydroxyl fatty acids and according to their chain length are classified as short-chain ( $C_3$ - $C_5$ ) and medium-chain ( $C_6$ - $C_{14}$ ). The chemical structure of PHA polymers and co-polymers (combination of different monomer units) confers them general thermoplastic and elastomeric properties, very similar to those of conventional polymeric plastics, with the benefits of biodegradability and biocompatibility (Keshavarz *et al.* 2010). Furthermore, a great variability of other mechanical properties stems from the high number of possible monomeric units forming PHAs. The chemical-physical versatility of such a class of biopolymers broadens their application field. PHAs are very intriguing not only as new bio-polymeric materials, for packaging films, containers utensils or hygiene products, but they gained relevance also in medicine and tissue engineering. For instance, they were utilized for bone plates, osteosynthetic material and surgical

sutures, or as drug carriers, for their ability to slowly release the active principle in the body (Philip *et al.* 2007; Grage *et al.* 2009; Keshavarz *et al.* 2010).

### 2.3.2. PHA production by pure microbial cultures and process implementation at industrial scale

Most of the microorganisms in the environment have the ability to naturally synthesize and store PHAs mostly as a carbon and energy source, when conditions of limiting nutrients, such as nitrogen, phosphate, sulphur, oxygen, magnesium or potassium, occur in the presence of an excess of carbon source (Lee *et al.* 1996). An unbalanced nutrient availability or fluctuations in the nutrient contents “support the population actively involved in PHA accumulation to meet the metabolic energy requirements during starvation period” (Saharan *et al.* 2014). PHAs are accumulated as intracellular insoluble PHA-granules (Figure 11), consisting of a polyester core, surrounded by a boundary layer with embedded or attached proteins that include the PHA, and can be visualized by means of a phase contrast light microscope due to their high refractivity (Khanna *et al.* 2009; Grage *et al.* 2009).

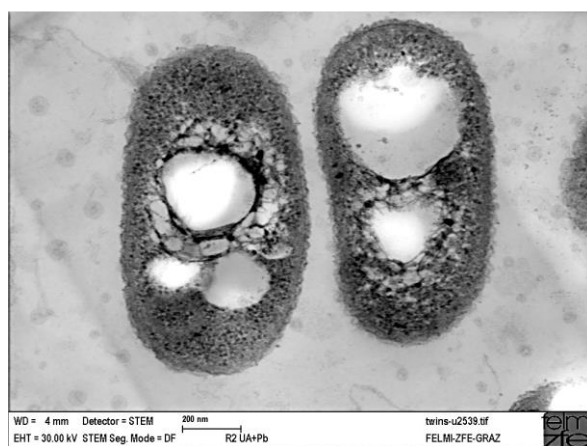


**Figure 11.** PHAs granules in *Cupriavidus necator*. STEM picture (Reproduced from Koller *et al.* 2012).

A first evidence of PHA accumulation inside microbial cells occurred in 1927 thanks to Lemoigne, who found that poly(3-hydroxybutyrate), abbreviated as P(3HB), was used from *Bacillus megaterium* as a reserve material (Braunegg *et al.* 1998). Since then, many other microbial PHAs-producers have been characterized. These include bacteria belonging to the genera *Bacillus*, *Pseudomonas*, *Azotobacter*, *Hydrogenomonas*, *Chromatium* (Braunegg *et al.* 1998; Jossek *et al.* 1998; Gerngross *et al.* 1995; Ramsay *et al.* 1990), and the strains *Ralstonia eutropha*, *Alcaligenes latus*, or *Burkholderia sacchari*, which have been widely exploited for the PHA industrial production (Lenz *et al.* 2005). Moreover, several recombinant strains, for example *Escherichia coli* and *Ralstonia eutropha*, have been used to increase the productivity of PHAs at an industrial scale (Wang *et al.* 2012; Nickel *et al.* 2006; Budde *et al.* 2011; Tsuge *et al.* 2004; Fukui *et al.* 2002). Interestingly, during

the last decade, several studies revealed that microorganisms growing in contaminated environments, hence in the presence of toxic and/or xenobiotic compounds, and involved in the degradation of such organic pollutants, were also able to accumulate PHAs (Saharan *et al.* 2014). For instance, it was the case of microorganisms belonging to genera *Pseudomonas*, *Acinetobacter*, *Sphingobacterium*, *Brochothrix*, *Caulobacter*, *Ralstonia*, *Burkholderia* and *Yokenella*, able to derive carbon from petroleum contaminants, by transformation into aliphatic hydrocarbons, which in turn are precursors of PHA synthesis (Amache *et al.* 2013; Dalal *et al.* 2010).

A crucial factor for the quality and type of PHA produced, the carbon source initially utilized for the PHA production, are glucose, sucrose, methanol or acetic and propionic acids or other volatile fatty acids (VFA) mixtures (Amache *et al.* 2013). In academic research, one of the highest productivity of PHB polymer ever reached was equal to  $5.13 \text{ g}\cdot\text{L}^{-1}\cdot\text{h}^{-1}$  by fed-batch growth of *Alcaligenes latus* DSM1123 on glucose and propionic acid under nitrogen limitation (Wang *et al.* 1997). The drawback was that these growth substrates are very expensive, especially considering the scale up of the production at commercial level. Hence, the need of renewable and cheap or no-cost carbon sources led to the utilization of raw matrices produced from agro-industrial activities. Among them are sugar-, starch- and whey-based matrices, such as tomato cannery wastewater (Liu *et al.* 2008) and sugar cane molasses (Albuquerque *et al.* 2007), municipal and agro-industrial wastewater, for instance olive oil mill effluent (Beccari *et al.* 2009) and paper mill wastewater (Bengtsson *et al.* 2008; Koller *et al.* 2012; Amache *et al.* 2013; Saharan *et al.* 2014). One possible strategy of microbial growth on such carbon sources consists of two steps. The first is a growth-stage conducted in batch mode, where the PHA production might start. Successively, a fed-batch process is established by maintaining an unbalanced presence of nutrients (e.g. nitrogen), while the carbon source is fed, in order to enhance the microbial PHA production (Amache *et al.* 2013). Second, several studies demonstrated that potential higher PHA productivities could be attained by means of cultivation in continuous mode, because of higher possibilities to control the process (Amache *et al.* 2013). Sugarcane and sugar beet molasses are some the most common feeding matrices for the PHA production processes. By utilizing beet molasses, PHB-polymers productivities of  $1 \text{ g}\cdot\text{L}^{-1}\cdot\text{h}^{-1}$  were attained with fed-batch fermentation of engineered *Azotobacter vinelandii* strain or recombinant *E. coli* strain (Chen *et al.* 1997; Liu *et al.* 1998). Another successful PHB-producing strain is represented by *Bacillus megaterium*, able to produce  $1.27 \text{ g}\cdot\text{L}^{-1}\cdot\text{h}^{-1}$  when grown on sugar beet molasses (Kulpreecha *et al.* 2009). *Ralstonia eutropha* NCIMB 11599 was able to produce  $1.47 \text{ g}\cdot\text{L}^{-1}\cdot\text{h}^{-1}$  of PHB by fed-batch growth on saccharified waste potato starch with phosphate limitation (Haas *et al.* 2008).

Nowadays, the industrial production of PHAs relies on fermentation processes of pure microbial cultures, either wild type strains or recombinant strains, with engineered metabolic capabilities (Kahar *et al.* 2004; Chen *et al.* 2001; Van Wegen *et al.* 1998). Some currently commercial trademarks are listed in the Table 2 (Chanprateep 2010; Bugnicourt *et al.* 2014).

**Table 2.** Commercially available PHA-based biopolymers.

<b>Trade</b>	<b>Polymer</b>	<b>Manufacturer/s</b>
Biomer™	homopolymer of (3HB)	Biomer Inc. (D)
Nodax™	copolymer of 3HB and 3-hydroxyhexanoate (3HH)	Procter and Gamble (US); Liany Biotech (China)
Biocycle™	homopolymer of 3HB, copolymer of 3HB and 3HV	PHB Industrial (Brazil)
Mirel™	Several different types of homopolymers, copolymers and terpolymers	Metabolix (US)
Biogreen®	homopolymer of (3HB)	Mitsubishi Gas Chemical Company Inc. (Japan)

In spite of high yields, PHA production with pure microbial cultures presents some drawbacks. Mainly the high costs of synthetic substrate and sterilization have an economically negative impact on PHA production. Other issues can be related to the maintenance of sterile conditions, stability and robustness of the process, or high cost for the downstream PHA cellular extraction and recovery procedures (Dias *et al.*, 2006; Chanprateep 2010).

### **2.3.3. Other PHA production strategies: employment of mixed microbial cultures**

An interesting and cheaper alternative way for the biological production of PHAs is the employment of complex microbial consortia, circumventing the need to maintain sterile conditions during the microbial growth and the need to utilize well-defined nutrient media.

In the last years, extensive research has focused on the PHA accumulation from microbial communities retrieved from activated sludge of wastewater treatment plants (Morgan-Sagastume *et al.* 2010; Valentino *et al.* 2012). Usually, these types of matrices include a wide variety of microbial species, and represent a great source of natural PHA-producers. In order to stimulate and increase the PHA accumulation ability, the microbial communities need to be properly enriched under specific selective pressure conditions, which will allow the microorganisms able to accumulate higher amounts of PHAs, as energy storage material, to prevail over the others. An effective selection and enrichment of the microorganisms producing PHAs is typically accomplished imposing a dynamic feeding condition, referred to as feast-famine regime (Dionisi *et al.* 2007; Valentino *et al.* 2014a).

This strategy consists of alternating the ‘feast’ phase, characterized by abundance of substrate available to the microbial biomass, and the ‘famine’ phase, when the biomass undergoes starvation. In such a regime, the microorganisms have a competitive advantage which are able to quickly store higher amounts of PHAs during the feast stage, and quickly utilize them as energy source during famine stage. Due to the intrinsic nature of the feast-famine feeding regime, the selection and enrichment process of biomass with high PHA-store ability is typically established inside sequencing batch reactors, SBR, under aerobic conditions (Valentino *et al.* 2014a).

The employment of mixed microbial communities can be easily coupled with the usage of carbon sources represented by complex municipal and agro-industrial matrices, as those ones mentioned above (section 2.3.2.). In order to maximise the PHA microbial production inside the SBR, these types of agro-industrial matrices are subjected to an upstream anaerobic acidogenic fermentation, resulting in high enrichment of volatile fatty acids (VFA), and then are conveyed to the SBR. Thus, the PHA production process from organic waste matrices is traditionally conducted through three stages (Reis *et al.* 2011): (i) acidogenic fermentation of the feeding matrix, (ii) SBR for the selection/enrichment of microbial communities, (iii) PHA accumulation stage. The latter is performed inside a different bioreactor, by using the selected biomass enriched in the SBR stage and allowing only the feast phase. Subsequently, the PHAs accumulated in microbial cells are recovered. Several studies showed good potentiality of this approach, with PHAs productivities up to  $6.0 \text{ g}_{\text{PHA}} \cdot \text{L}^{-1} \cdot \text{day}^{-1}$  (Dionisi *et al.* 2006).

#### **2.3.4. “Sludge minimization in municipal wastewater treatment by polyhydroxyalkanoates (PHA) production” (Valentino *et al.* 2014b)**

Valentino *et al.* (2014) investigated the feasibility of utilizing a low-VFA-content municipal wastewater to select and enrich high performant PHA-accumulating microbial communities, during a SBR stage for the wastewater sludge minimization and valorization.

Such an investigation was performed at laboratory scale, where a synthetic “complex mixture of different organic substrates” (COD equal to  $275 \text{ mg} \cdot \text{L}^{-1}$ ) was utilized to simulate a not fermented, thus VFA-poor, soluble fraction of municipal wastewater SBR feeding phase. The process, linking wastewater treatment and PHAs production, was established in six replicated SBRs (each SBR conduction is also referred to as *Run*), conducted under identical operative conditions and strict control of the process parameters, in order to evaluate the process reliability and robustness. The only difference between the SBR runs was their inoculum, consisting of an activated sludge (rich in microbial biomass) collected from the same municipal wastewater treatment plant, located in Italy, at different sampling times. Furthermore, the six SBR processes were carried out for different spans

of time and the feeding strategy was aimed to establish a dynamic feast and famine regime. In particular, the feast phase was defined as the period included between the start of the feeding and the moment when all of the readily biodegradable COD (RBCOD) was exhausted, indicated by an increase of the dissolved oxygen. Some of the main operative conditions applied were: organic loading rate (OLR)  $3.08 \text{ g COD} \cdot \text{L}^{-1} \cdot \text{day}^{-1}$ , hydraulic retention time (HRT) 2.14 h, sludge retention time (SRT) 1.5 day, cycle length 1.5 h, temperature  $22.5^{\circ}\text{C}$ , pH 8.

Experimental evidence showed that after about one week of acclimation, the sludge-microbial biomass response to the imposed process conditions became more stable and the process reproducibility among the six runs was very good. Furthermore, a stable feast-famine regime was established, despite initial low content in VFA of the fed solution, differently from the traditional treatment methods, while up to 89% removal of the initial COD was attained. The authors found that the average values of the feast phase lengths of the six SBR runs, during the steady-state operation, ranged between 7 and 15% of the total length of the aerobic phase of the cycle, namely the phase exploited for the reaction. A short feast phase, lower than 20% of the cycle, was previously reported to enhance the selective enrichment of microbial populations with high PHA-storage abilities. However, the analyses of the PHA accumulation by the microbial biomass (sludge) samples collected at the end of each feast phase showed a remarkable variability of the storage response over time. A further assessment of the SBR-enriched-biomass storage response was evaluated into separated batch accumulation tests, this time fed with a VFA-rich synthetic solution, and readily stopped as soon as the total RBCOD was consumed, thus the PHAs accumulation was subsequently measured. The complex microbial communities were able to accumulate polymer up to 23% grams of PHAs per gram of cell dry weight in 24 h. These PHA accumulation data were lower than those ones obtained by means of typical three stage-process for the PHA accumulation, but still good considering the development of the here-proposed process is still in its infancy. In particular, the SBR runs along with the batch experiments pinpointed the different biomass settling properties of each run as the possible cause of uncontrolled variations of sludge retention times and specific organic loading rates (the ratio between OLR and SBR volatile suspended solids concentration calculated at the end of the feast). Hence, future research efforts are required to optimize and stabilize such a process parameters. In conclusion, the study highlighted the potentialities of unifying the municipal wastewater fermentation stage and the selection of PHA-accumulating microbial communities, resulting into the sludge minimization.

## **2.4. Molecular advances in biotechnology to characterize microbial communities**

### **2.4.1. Introduction to metagenomics and sequence analysis as powerful tools in microbial ecology**

As anticipated in the section 1.1., microbial ecology, among other disciplines, is the study of the diversity and functional relationships of microbial communities (Xu 2006; Konopka 2009). Investigating the microbial ecology can elucidate the dynamics of microbial functions and the biogeochemical cycles occurring in the environment or in a controlled system, such as biotechnological process. In the past, this knowledge was partially eclipsed by the limits of the traditional microbiology unable to detect the microorganisms recalcitrant to cultivation (Leadbetter 2003; Malik *et al.* 2008). It has been reported that cultivation-dependent techniques could detect only about 1% of the microbes occurring in the environment (Zhang *et al.* 2008). In order to overcome this lack of information, since 1980s culture-independent techniques have been extensively used to explore the diversity of environmental communities (Pace *et al.* 1985). Majority of the culture-independent techniques of community characterization are based on the direct analysis of the collective genomic DNAs, called ‘metagenome’, isolated from all of the microorganisms occurring in the environmental community (Xu 2006; Handelsman 2007; Thomas *et al.* 2012). With such approach, the extraction method of genomic DNA from microbial cells is crucial to the success of all the downstream applications (Jones 2010; Delmont *et al.* 2011; Thomas *et al.* 2012). Critical aspects are the isolation of high quality DNA, along with its purification from humic acids and other contaminants occurring in environmental samples (Desai *et al.* 2007).

The initial metagenomics approaches were based on the isolation of the metagenomic DNA from the environmental sample followed by a construction of clone libraries (Rondon *et al.* 2000; Entcheva *et al.* 2001). The further characterization of the cloned genes could be attempted by either function-based or sequence-based screening of the library (Schmeisser *et al.* 2007). The former was based on biochemical studies, where the expression of captured-functional genes of the microbial community was evaluated in a suitable host (Schmeisser *et al.* 2007). This analysis could potentially reveal the existence of new functional genes; however, a big investigation potential was also attributable to the sequence-based screening (Handelsman 2007).

The number of applications of the sequence-based metagenomics has steadily increased over the past ten years. The sequencing of large DNA cloned inserts (Rondon *et al.* 1999) was soon overcome by the “random shotgun sequencing”. The shotgun approach is based on the digestion of the metagenome into few thousand bases-long DNA sequences, which are used to build a clonal

library, followed by sequence analysis and assembling of the sequence data (Fuhrman 2012). Despite the hard work of assembling the sequences, based on the recognition of overlapping regions, this approach served some of the most extensive projects for the investigation of environmental microbial communities, such as the study concerning the Sargasso Sea in the Atlantic Ocean (Venter *et al.* 2004). In addition, other studies demonstrated the complexity of microbial communities in soil, estimating that one gram of soil might contain over ten billion microbial cells (Xu 2006).

The first attempts to characterize environmental metagenomes by means of PCR, in combination with Sanger DNA sequencing technology, relied on PCR to target the DNA regions coding for small subunit ribosomal RNA (SSU rRNA). For instance, the 16S rDNA was utilized as phylogenetic marker for the identification and classification of new microorganisms (Pace *et al.* 1986; Winker *et al.* 1991). Additional potentialities of the “tag-sequencing” approach (Fuhrman 2012) are far more than taxonomically informative; in particular, specific functional genes within the investigated community can be targeted and amplified by PCR, thus further sequenced, providing precious information about the metabolic role of unknown species in the main biogeochemical cycles.

A continuous progress in the sequencing technologies and computational analysis of the data led to the production of gigabases of sequences deposited and available in public databases, such as Genbank, or the US National Center for Biotechnology Information (NCBI).

#### **2.4.2. Describing environmental microbial communities' biodiversity**

The concept of ‘diversity’ in microbial ecology can be expressed through different indices; some of them are phylogenetic diversity, functional diversity, metabolic diversity, or structural diversity. Thus, the term diversity encompasses several aspects of the microbial ecology of a site, even considering their temporal changes, shifting to the concept of ‘dynamics’. The most important parameters utilized to describe a microbial community are its *richness*, the number of species, and *evenness*, the relative abundance of species (Wilsey *et al.* 2000). Information about these two parameters can give a preliminary idea of the community functional stability, in response to environmental stress. High richness could ensure a redundancy of genomic and metabolic resources, meaning that different microorganisms can perform the same metabolic role under different conditions (Konopka 2009). Furthermore, it was demonstrated that an initial community evenness, namely characterized by equivalent species abundances at the beginning of the enrichment process, increases the functional stability of a community (Wittebolle *et al.* 2009).

To date, several nucleic acid-based techniques rely on the PCR amplification of phylogenetic or functional molecular markers in order to assess the biodiversity of environmental samples. PCR

itself is a widely used method to explore microbial communities; with particular regard to multiplex PCR and real-time PCR, it has been possible to detect and/or quantify functional genes, or microbial species, implied in catabolic pathways of organic contaminants (Ginzinger 2002; Ibekwe *et al.* 2002; Baldwin *et al.* 2003; Ritalahti *et al.* 2006). On the other hand, the phylogenetic microbial identification, based on 16S rRNA genes as phylogenetic marker, is the most reliable approach to profile community structure. However, some limitations should be considered when using PCR-based techniques for community profiling. These bottlenecks are mainly caused by the impossibility to establish genome size and rRNA operon copy number of uncultivated microorganisms (Spiegelman *et al.* 2005). As a result, PCR-based 16S community analysis cannot be considered as an accurate quantification of microbial cells (Farrelly *et al.* 1995; Spiegelman *et al.* 2005).

### **2.4.3. Molecular fingerprinting of microbial communities**

Nucleic acid-based molecular fingerprinting is a relatively fast approach to monitor the biodiversity of microbial communities occurring into environmental samples. It is often used to investigate the phylogenetic diversity, and its spatial-temporal changes during biotechnological processes (Bertin *et al.* 2012; Valentino *et al.* 2014a). Despite the limitations associated with each fingerprinting technique, these represent a viable strategy to identify the dominant species taking part in the process. PCR-based fingerprinting techniques are aimed to detect molecular differences between pools of fragments amplified from the metagenomic DNA.

#### **2.4.3.1. PCR-based techniques**

The mainly utilized molecular techniques for community profiling include the ribosomal intergenic spacer analysis (RISA), terminal-restriction length polymorphism (T-RFLP), denaturing/temperature gradient gel electrophoresis (DGGE/TGGE) and cloning. RISA investigates the differences of intergenic spacer regions (IGS) between 16S and 23S rRNA genes, variable both in length and sequence, providing a more detailed taxonomic resolution of the amplicons in comparison with other techniques (Spiegelman *et al.* 2005). However, the fingerprinting characterization potentiality of RISA is affected by the limited amount of sequence databases available. They are far less comprehensive as those of 16S rRNA genes (Spiegelman *et al.* 2005).

T-RFLP is a modification of the ARDRA (amplified ribosomal DNA restriction analysis) and relies on the utilization of a fluorescently labelled forward primer during the PCR amplification of the 16S rRNA genes (Liu *et al.* 1997). Thus, the following restriction digestion produces only single labelled fragments, which are identified and quantified by means of capillary electrophoresis systems.

The resulting T-RFLP profile, consisting of the fragment intensity plotted against the fragment size, is typical for each community, where, in theory, each terminal fragment represents a ribotype (Spiegelman *et al.* 2005). When utilized to investigate relatively simple communities, T-RFLP can have several advantages, for instance the high throughput resolution of the labelled restriction fragments. T-RFLP has been successfully employed to describe microbial communities of polychlorinated biphenyl (PCB) contaminated soils (Uhlík *et al.* 2009; Fedi *et al.* 2005), hydrocarbon polluted marine-environment (Denaro *et al.* 2005), or trichloroethylene-mineralizing communities (Richardson *et al.* 2002).

DGGE is one the most utilized techniques for a rapid survey and comparison of the microbial diversity among different samples. It is an electrophoretic method for the identification of DNA fragments with differences in their nucleotidic sequences (Fischer *et al.* 1983). A metagenomic pool of PCR-amplified 16S rDNA fragments (usually <500 bp-sized) can be resolved during the electrophoretic run through a polyacrylamide gel containing an increasing linear gradient of DNA-denaturing compounds, such as urea and formamide (Muyzer *et al.* 1993). Increasing denaturing conditions, in addition to the fact that the run is conducted at 60°C, determine a gradual melting of the double stranded DNA fragments, reducing their mobility until each molecule stops at a precise point of the gradient (Muyzer *et al.* 1998). The two DNA strands are kept together with an approximately 40 bp long GC-rich clamp, which will not be denatured even at high denaturing concentrations (Myers *et al.* 1985; Sheffield *et al.* 1989). The migration distance on the gel is strictly dependent on the nucleotide sequence; it was demonstrated that co-migrating bands generally correspond to identical sequences (Kowalchuk *et al.* 1997), while even differences of one base pair can result in a different migration (Nübel *et al.* 1996). Anyway, the DGGE band pattern resolution depends on the denaturing compound concentration range utilized, and can be improved by narrowing the gradient (Muyzer *et al.* 1998). Subsequently, the obtained bands can be excised from the gel and the DNA sequence purified. Sometimes, especially when working with complex microbial communities, a further purification step of the excised bands needs to be performed by DGGE, to purify the sequences from a background DNA running throughout the gel. The purified sequences are amplified, sequenced and taxonomically identified. The main limitation of the DGGE is the possibility to detect only the most represented taxa of the community, excluding those species representing the 0.1-1% of the community (Muyzer *et al.* 1998). In addition, it must be considered that more than one DGGE band can be related to the same microbial species, due to multiple copies (up to 14) of the rRNA operon (Nübel *et al.* 1997), overestimating the community richness; in the opposite way, more non related fragments can have the same mobility through the gel (Kowalchuk *et al.* 1997). It is worth mentioning that the same limitations apply for the T-RFLP, which is often

utilized with the same purposes of DGGE. Other minor drawbacks are the short length of the fragments, high amounts of initial sample (about 400-500 ng), or the impossibility to recognize heteroduplex molecules produced during the amplification. Nevertheless, the DGGE is a fast and reliable tool to detect and monitor the occurrence of the dominant species within communities, even though it provides only a qualitative analysis of the bands pattern not usable to determine the actual abundances of the microbial species (Muyzer *et al.* 1998; de Araújo *et al.* 2008).

TGGE (Rosenbaum *et al.* 1987) is a technique very similar to DGGE, bringing the same advantages and limitations (Spiegelman *et al.* 2005); the difference is that TGGE is based on a temperature gradient to denature the DNA fragments instead of chemical denaturants. DGGE and TGGE have been widely used in microbial ecology of soil and rhizosphere (Macnaughton *et al.* 1999; Duineveld *et al.* 2001), water systems (Chang *et al.* 2000; Frascari *et al.* 2013b), or processes for the valorization of agro-industrial wastes (Scoma *et al.* 2011; Valentino *et al.* 2014a).

When a deeper investigation of a microbial community is requested, the construction of clone libraries of the metagenomic 16S amplicons provides major sensitivity. In contrast to DGGE, even less represented taxa can be detected. Another advantage is the possibility to work with longer DNA sequences, even full-length 16S rRNA gene, which allows a more reliable phylogenetic identification. On the other hand, the cloning is a long and laborious procedure, which can become too expensive if the direct sequence analysis of the clones is considered. A viable and cheaper approach to obtain immediate information about the community structure and detailed information about the community composition is the parallel utilization of a fingerprinting technique. The clone library of the full-length 16S rRNA gene amplicons is screened by DGGE and compared to the community DGGE profile. In this way, each cloned fragment can be also recognized in the community profile (Valentino *et al.* 2014b).

#### **2.4.3.2. Semi quantitative analysis of DGGE patterns**

DGGE profiles of environmental microbial communities can appear quite complex and sometimes it is hard to immediately appreciate changes among DGGE band patterns obtained from spatially or temporally different samples. The utilization of software specific for the DGGE image analysis helps the evaluation of the band-pattern diversity for a single DGGE profile, or within profiles embedded on the same gel. Thus, it is possible to establish a semi-quantitative evaluation of DGGE community profiles, but it is important to remember that it is referred to DGGE band patterns, not to real species abundances of the taxa in the environment. A software-assisted analysis of the densitometric curves of each DGGE profile considers the following factors: the number of bands,

their intensities and their position on the gel picture. Basing on these data it is possible to mathematically calculate indexes of the DGGE-profile diversity, such as the Shannon-Wiener index (Gafan *et al.* 2005), or computing a matrix of percentage values of similarity between two profiles, for instance, according to the Dice coefficient, or the Jaccard coefficient (Fromin *et al.* 2002). However, the similarity between DGGE profiles in the same gel is better summarized in the form of dendrograms, obtained by clustering analysis performed by applying algorithms such as unweighted pair group method using arithmetic averages (UPGMA) (Gafan *et al.* 2005). In addition, unconstrained ordination methods, such as non-metric multidimensional scaling (NMDS) and principal component analysis (PCA), represent viable statistical tools to describe the variance of the samples (Fromin *et al.* 2002; Bernhard *et al.* 2005; Gafan *et al.* 2005).

Marzorati *et al.* (2008) described a useful analytical procedure to compare DGGE profiles embedded in different gels at three levels: range-weighted richness (*Rr*), dynamics (*Dy*) and functional organization (*Fo*). The former is calculated by considering both the number of bands occurring along a single DGGE profile and the percentage range of denaturing gradient where all the bands are distributed. Dynamics evaluates how fast changes of the DGGE-band patterns of the same community occur between profiles obtained for consecutive sampling times. In this case, the similarity percentage between two progressive DGGE profiles relies on the Pearson correlation index, and, by difference, it is possible to retrieve the percentage of the difference (or change). In relation to consecutive intervals of time, the percentage of the difference represents the rate of change for a specific sample, graphically plotted against time, in the so-called moving window analysis (Wittebolle *et al.* 2005). Finally, the functional organization of a microbial community refers to the internal proportion of dominant and resilient microorganisms (Marzorati *et al.* 2008). This concept relates the community evenness to the functional stability of the community subjected to a sudden stress exposure. It was demonstrated that an optimal balance of dominant and resilient species results in a major functional stability of the community, although harbouring changes of the community structure (Fernandez *et al.* 2000).

Even though mentioned only in the case of DGGE, these analytical methods can serve the results evaluation of several other fingerprinting techniques, such as TGGE, T-RFLP, etc..

#### **2.4.3.3. Nucleic acids hybridization-based techniques**

Other taxonomic and/or functional analytical techniques rely on DNA or rRNA probes to hybridize with target sequences directly in the environmental sample, assessing the occurrence, quantity and the distribution within the analysed sample. Two of the main exploited taxonomic tools are the fluorescent *in situ* hybridization (FISH) and microarray technology.

FISH relies on the utilization of fluorescently labelled rRNA probes targeting microbial species at the levels of genera, families or phyla (Malik *et al.* 2008). Traditionally, the microbial cells are treated by chemical fixation prior to hybridization, and are further visualized and quantified with epifluorescence or confocal laser microscopy (Malik *et al.* 2008). Despite a great degree of specificity, the utilization of short oligo-probes can limit the potentialities of the technique, for instance because they are designed based on already known sequences available in databases. Several modifications have been introduced to the classical FISH procedure to increase its sensitivity; furthermore, FISH has been also combined with other techniques, such as T-RFLP or DGGE. FISH and its variants (Behnam *et al.* 2012; Wright *et al.* 2014) resulted to be a very powerful technique to correlate identity and functionality of microorganisms. It has been utilized in a large number of microbial ecology studies, such as investigations of river anoxic sediments (García-Moyano *et al.* 2012), hydrocarbon-contaminated aquifer (Schattenhofer *et al.* 2014), or processes in membrane bioreactors for the treatment of landfill leachate (Ziemińska *et al.* 2012).

Microarray technology is a powerful high-throughput technique, mainly because it provides a wide spectrum of information about taxonomy and functionality of microbial communities. The technique consists of a glass system embedding a large set of DNA- or RNA-probes targeting sequences of the environmental metagenome. The number of investigated nucleotide sequences for a single assay can reach a quarter of a million (Spiegelman *et al.* 2005). The employment of microarray to characterize environmental complex communities has some limitations in specificity, sensitivity and quantification (Zhou *et al.* 2002; Spiegelman *et al.* 2005). Nevertheless, three main forms of environmental microarray are used in microbial ecology: functional gene arrays (FGA), community genome arrays (CGA) and phylogenetic oligonucleotide array (POA) (Malik *et al.* 2008). For instance, FGA was utilized to characterize functional genes involved in the main biogeochemical cycles of microbial communities occurring in marine sediments from the Gulf of Mexico (Wu *et al.* 2008). Additional recent improvements of the microarray technique served the characterization of several complex communities (Larsson *et al.* 2011).

#### **2.4.4. Linking microbial phylogeny and functionality: stable isotope probing**

Stable isotope probing (SIP) is a powerful approach revealing a direct correlation between phylogeny and functionality of microorganisms within complex communities. In the last fifteen years, SIP has been widely used to identify microorganisms able to utilize particular substrates (Radajewski *et al.* 2000; Singleton *et al.* 2005; Uhlík *et al.* 2012) and track the utilization of intermediate metabolites from other microbes of the community. The technique relies on the assimilation of a

stable isotope-labelled substrate into microbial cells, thus the incorporation of the heavy isotope into the main informative molecular biomarkers, in particular, nucleic acids (DNA/RNA), phospholipid-derived fatty acids (PLFA) and proteins. Stable isotopes mostly used are  $^{13}\text{C}$  (Neufeld *et al.* 2007; Dumont *et al.* 2011) and  $^{15}\text{N}$  (Roh *et al.* 2009; Bell *et al.* 2011).

Earlier SIP-based community studies evaluated the incorporation of  $^{13}\text{C}$  isotope into PLFA of microorganisms active in some biogeochemical processes (Boschker *et al.* 1998) or toluene degradation (Pelz *et al.* 2001). Despite its great sensitivity, PLFA-SIP of environmental communities is strongly limited by the paucity of information about PLFA composition of unknown microorganisms (Friedric 2006). Exploring the  $^{13}\text{C}$ -enrichment of DNA (Radajewski *et al.* 2000; Neufeld *et al.* 2007) or RNA (Manefield *et al.* 2002; Dumont *et al.* 2011) represents a far more informative way from both a taxonomic and functional points of view. The technical principle of the nucleic acid-based SIP is the difference of density established between the molecules incorporating  $^{13}\text{C}$  (heavier) and the other ones (lighter). After metagenomic DNA isolation from a microbial community exposed to the presence of a labelled substrate, the heavier DNA (or RNA) of the  $^{13}\text{C}$ -labelled substrate assimilating microbes and the lighter DNA (or RNA) can be resolved by density gradient ultracentrifugation (isopycnic centrifugation) in a solution of caesium chloride (CsCl) or caesium trifluoroacetate (CsTFA). Since the first applications of nucleic acid-SIP, many methodological advances have been introduced to achieve a more efficient and precise analysis of the isopycnic gradient formed and the distribution of the DNA/RNA through its increasing density. The best approach is the fractionation (Manefield *et al.* 2002; Neufeld *et al.* 2007) of the gradient and further analysis of the DNA (or RNA) in each fraction. Lueders and co-workers (Lueders *et al.* 2004) introduced the utilization of the real-time PCR to detect and quantify the nucleic acids content of gradient fractions.

The utilization of RNA-based SIP is advantageous from some point of view, because RNA is a more responsive biomarker than DNA, due to its faster turnover and the possibility to obtain higher amounts of labelled RNA, than DNA even in non-growing cells (Manefield *et al.* 2002; Radajewski *et al.* 2003). Some drawbacks of the technique are related to the difficult isolation of high quantities of RNA to be used for SIP (McDonald *et al.* 2005), or the fact that its analysis does not provide access to functional genes encoding the metabolic functionalities of the community (Uhlík *et al.* 2013). Nevertheless, rRNA and even mRNA have been successfully used in several SIP studies (Manefield *et al.* 2002; Lueders *et al.* 2004; Huang *et al.* 2009; Dumont *et al.* 2011).

A very informative biomarker remains to be DNA. Given the high potentialities of working with labelled genomes, DNA-SIP is the most used method to study functional genes of the

microorganisms identified as degraders of certain compounds. A comprehensive biodiversity analysis of the active microbes of the community in relation to specific metabolic pathways can be accomplished by targeting (PCR) and analysing the labelled-metagenome genes of interest with DGGE (Yamasaki *et al.* 2012), T-RFLP (Redmond *et al.* 2010; Dumont *et al.* 2011), constructing clone libraries (Jones 2010), or using high throughput sequencing (as elucidated below). Some critical steps to the establishment of a DNA-SIP experiment are (i) ensure the reproduction of environmental-like conditions inside closed microcosms (Uhlík *et al.* 2013), (ii) estimate optimal substrate concentration (Radajewski *et al.* 2003), (iii) estimate optimal incubation times of the sample in the presence of the labelled compound (Radajewski *et al.* 2002). These aspects are crucial for a microbial community behaviour similarly to the environmental contest, as well as the ability to enrich sufficient amounts of the labelled isotope exclusively in the real degrader microbes, avoiding cross feeding of labelled-intermediate metabolites, thus misunderstanding the carbon flow through the system. In order to satisfy such requirements preliminary tests are usually performed to determine as precisely as possible the better design of the definitive SIP experiment. Other critical steps concern the recovery and analysis of the heavy DNA. For instance, a background of unlabelled DNA can be detected throughout the isopycnic gradient (Lueders *et al.* 2004); to circumvent this problem, it is important to optimize the ultracentrifugation phase, or, if necessary, the retrieved heavy DNA fraction can be purified with a second ultracentrifugation step. Furthermore, it is always a good practice to process an unlabelled metagenomic DNA sample, in order to assess the linearity and distribution of the lighter DNA versus the heavier DNA. SIP approach is suitable for studying assimilatory processes, even though some applications attempted to identify microorganisms driving anaerobic dissimilatory PCE dehalogenation (Yamasaki *et al.* 2012).

Recently, labelled metagenomes retrieved from SIP have been downstream analysed with high throughput microarray technology, shotgun sequencing, or pyrosequencing-based techniques (Uhlík *et al.* 2012, 2013).

#### 2.4.5. Next generation sequencing (NGS) technologies

Technological development and cost reduction of sequence analysis resulted in a widespread adoption of next generation sequencing (NGS) technologies. The general features of the NGS technologies are represented by the possibility of working with the total DNA of the community, randomly producing millions of DNA fragments, immobilizing the fragments on solid materials (e.g. beads, solid surface) and parallel sequencing. To date, few high-throughput sequencing technologies are available on the market; the most extensively utilized to analyse metagenomic samples are 454/Roche/Life Sciences, Illumina/Solexa, SOLID and Ion-Torrent (Thomas *et al.* 2012; Escalante *et al.* 2014; Zhou *et al.* 2015).

The Roche/454 GLS FLX Titanium pyrosequencer is the type of platform utilized in one of the studies presented in this dissertation. This technology is based on the pyrosequencing chemistry, which was firstly introduced in the mid-1990s (Ronaghi *et al.* 1996). Pyrosequencing is based on the synthesis of DNA on a single stranded PCR fragment as template. The sequential incorporation of dNTPs driven by DNA polymerase releases inorganic pyrophosphate (PPi), which is utilized by ATP sulfurylase, contained in the reaction mixture, to produce ATP. A third enzyme, luciferase, utilizes ATP to convert luciferin into oxiluciferin, a reaction generating light. The light emission is the signal detected by a charge-coupled device (CCD) camera and it is translated into a peak of a pyrogram. Each peak intensity indicates the incorporation of one or more nucleosides.

The pyrosequencing instrument applies an emulsion PCR to amplify and attach the fragments to the beads by means of the adaptors complementarity to an oligonucleotide sequence located on the surface of each bead. Only to one type of DNA molecule is associated with one bead, clonally amplified within the micelle. Finally, each bead is deposited into a single well of a picoliter plate and further sequenced (Escalante *et al.* 2014). This technology has been optimized for the utilization of an initial amount of tens nanograms of DNA; furthermore, it can produce read lengths up to 800 bases (Thomas *et al.* 2012).

Pyrosequencing, along with other NGS platforms, have found many applications in diagnostics, for mutation detection or characterization of single-nucleotide polymorphisms (SNPs) in epigenomics and, in metagenomics, for the taxonomic and functional identification of a large number of environmental microbial species (Ronaghi *et al.* 2002; Marsh 2007). In addition, NGS techniques can be employed to analyse RNA, providing a qualitative and quantitative analysis of the transcriptome, identification of miRNA, and functional analysis of environmental communities. NGS microbial identification is typically based on the analysis of pool of amplicons of a specific phylogenetic marker, such as hypervariable regions of SSU rRNA genes (e.g. 16S rDNA). The exploitation of NGS approaches overcomes older approaches utilized to perform a comprehensive analysis of an

environmental microbial community, such as the whole-genome shotgun sequencing (Petrosino *et al.* 2009; Zhou *et al.* 2015).

The 454-pyrosequencing can be used to study PCR amplicons of phylogenetically informative or functional genes. In such a setting, PCR amplicons contain a sample-specific tag sequence and are modified with an adaptor sequence (barcode). The adaptor is useful to the fragment immobilization on the solid support, while the tag-encoded sequence is used to label the amplicons as belonging to a specific group (sample), allowing for sorting during the analysis.

#### **2.4.6. Evaluation of NGS data and statistics**

The employment of high-throughput technologies requires a meticulous downstream computational analysis of the raw data produced. Some bioinformatics resources are available for the automatized analysis of the data, from the raw nucleotide reads to their taxonomic, or functional, classification. The main resources for metagenomic data analysis are Metagenomics-Rapid Annotation using Subsystems Technology (Meyer *et al.* 2008), Community Cyberinfrastructure for Advanced Microbial Ecology Research and Analysis (Sun *et al.* 2010), Integrated Microbial Genomes and metagenomes (Markowitz *et al.* 2011), EBI metagenomics (EMBL-EBI infrastructure, Hunter *et al.* 2014). Analysis pipelines to characterize amplicon data utilize sequential algorithms for trimming the sequences, denoising the signal, removal of short, low quality sequences and primers (Huse *et al.* 2007; Uhlík *et al.* 2012). The obtained good-quality sequences are further aligned with multisequences alignment programs, such as MUSCLE or NAST (Petrosino *et al.* 2009), and removal of invalid sequences, or those attributable to pyrosequencing errors, are performed. A critical step is the identification and removal of chimeric sequences, whose efficiency depends on the program used, for instance UCHIME or Perseus (Uhlík *et al.* 2012). The selected sequences can be assigned into operational taxonomic units (OTUs), according to the classification performed with Ribosomal Database Project classifier (Cole *et al.* 2014), Greengenes reference database (DeSantis *et al.* 2006), or ARB-SILVA database (Pruesse *et al.* 2007).

The NGS output data set results are very complex and of difficult to interpret. In this case, some statistic tools are a great aid in analysing data with respect to different ecological and temporal variables. Several statistical analysis methods have been adapted from those previously developed for analysing the ecology of higher organisms. Commonly, the analysis is based on constructing data matrices of the sample versus the OTU, and reporting information about the relative abundance or the presence-absence of the data. The majority of the data analysis methods are performed with the statistical software *R*. The *vegan* package can be used to execute the majority of the common

ordination methods. Non-metric multidimensional scaling (NMDS) is a numerical technique suitable for a large variety of data, which relates the major compositional variation of one set of data to the observed environmental variations without assuming particular relationship (Taguchi *et al.* 2005; Holland 2008). On the other hand, suitable constrained ordinations of data are the constrained correspondence analysis (CCA) or the redundancy analysis (RDA) used to analyse linear response of variables (species) along two sets of ecological explanatory variables (Oksanen 2013). Another important function of the vegan package is the multivariate analysis of the variance ANOVA, a linear model analysis to describe variation as the effect of multiple factors (Oksanen 2013). In addition, the package *indicspecies* is utilized to assess the “statistical significance of the relationship between species occurrence/abundance and groups of sites” (De Cáceres *et al.* 2010). Several other packages in *R* as well as other programs can be used for statistical analyses.

The data organization in such graphic interfaces clarifies many aspects of the ecological variables mainly affecting the microbial community structure and metabolic activities and its changes over time.

# **Chapter 3. Aerobic cometabolic bioremediation of CAH-contaminated groundwater in packed bed bioreactors: support of community characterization to the process development and optimization**

## **3.1. Objectives and rationale of the research**

The presented research study was conducted in the framework of the European project EU-FP7 MINOTAURUS (*Microorganisms and enzyme Immobilization: NOvel Techniques and Approach for Upgraded Remediation of Underground-, wastewater and Soil*). This project was aimed to the development of biotechnological processes for the *in situ* remediation of xenobiotic contaminated groundwater, wastewater, or soil relying on the degradation activity of immobilized biocatalysts such as enzymes or microbial cells. The specific objective of the Department of Civil, Chemical, Environmental and Materials Engineering (DICAM) of the University of Bologna was the development of packed bed bioreactors (PBR) inoculated with immobilized and specialized microbial consortia for the on-site bioremediation of groundwater contaminated by chlorinated aliphatic hydrocarbons (CAHs) via aerobic cometabolism (AC).

In order to achieve such an objective, the development of an AC process was articulated in four main stages:

- (i) Selection of the best contaminated groundwater sample and the more suitable growth substrate to enrich a suspended-cell microbial consortium for an effective degradation of CAHs at 30°C;
- (ii) Selection of the most suitable carrier material supporting the immobilization of the microbial consortium selected at (i) and evaluation of the CAH-degradation process both at 30 and 15°C;
- (iii) Establishment of the AC process driven from the immobilized consortium inside continuous-flow 1 L PBR at 30°C; preliminary assessment of the process reliability when a pulsed feeding of oxygen and substrate was adopted;
- (iv) Scale up and optimization of the AC process inside a 31 L PBR pilot plant.

Beyond several advantages resulting from the employment of PBR systems with immobilized-microbial biomass for the on-site bioremediation of pollutant compounds (discussed in the section 2.1.3.2. of this dissertation), a rational procedure for the design and the gradual optimization of the AC process inside a PBR system was developed at the Dept. DICAM.

Some crucial aspects to the overall efficiency and robustness of such a process are a homogeneous growth and activity of the microbial biomass throughout the PBR system. The attainment of these conditions is hindered by working with high concentrations of the growth supporting substrate, which can result in a fast and huge growth of biomass clogging the inlet surroundings and in the early consumption of the substrate, affecting the extension of the process to the remaining parts of the system (Fracari *et al.* 2015). Additional operative aspects require particular attention. For instance, the simultaneous presence of the primary substrate and the chlorinated compounds gives rise to inhibition phenomena of the CAH degradation, since the growth substrate would be preferentially metabolized (Fracari *et al.* 2013a). The proposed solution to circumvent the above mentioned issues was the development and the optimization of an appropriate feeding strategy of the growth substrate, the oxygen and the CAHs, described as *pulsed feeding* by Fracari *et al.* (2012). The principle behind this technique is to supply alternating pulses of substrate and oxygen to the system, as explained in the introductory section 2.1.3. of this dissertation. Such a *pulsed feeding* strategy was adopted during the development of the AC process inside the PBR systems of the stages (iii) and (iv).

The presented study was realized in cooperation with the research unit leaded by Dario Fracari Ph.D. and Professor Davide Pinelli (DICAM). Their research team set up and operated all of the bioreactor systems and carried out the biodegradation kinetic investigation. Thus, an essential description of design, operative conditions and kinetic performances of the microbial communities developed through these processes will be given among this chapter.

With respect to the research personally conducted, it was aimed to determine changes in the structure and function of the complex microbial consortia developed through the steps (i) to (iv) of the work. Dynamic changes in the structure and phylogenetic composition of the microbial consortia along with their functional gene diversity and metabolic potential were mainly investigated. In particular, the study was aimed to infer how such microbial community's features related to specific operative conditions imposed, such as the presence of a certain type of growth substrate and/or groundwater, the presence of immobilization-supporting materials, or, the working temperature. Moreover, the community investigation performed at different sections of the PBR systems (stages iii and iv) was aimed to assess the homogeneity of the system itself in terms of concentration, structure and composition of the microbial biomass. The phylogenetic and functional monitoring of microbial communities was based on PCR-DGGE and/or PCR-cloning approaches.

This pool of information about microbial communities constitute a precious resource for a more conscious modification and optimization of the process operational parameters.

## 3.2. Materials and methods

### 3.2.1. Environmental contaminated matrix, cultivation media and biomass immobilization support materials

All of the complex microbial cultures developed in this study were enriched from native communities of CAH-contaminated groundwater samples and further propagated by utilizing either the same groundwater or a synthetic water solution mimicking the natural groundwater's chemical composition. Variable concentrations of the chlorinated contaminants were always maintained in the culture media, with the double intention of monitoring their degradation and keeping a selective pressure advantageous for CAH-tolerating or degrading microorganisms. The microbial growth, as well as the AC of CAHs, was supported by the presence of different substrates, represented by four aliphatic hydrocarbons, namely methane, propane, butane, pentane, or by phenol. An additional feature of the cultivation strategy was the development of immobilized microbial communities as biofilm on different types of immobilization supporting materials (otherwise referred to as carrier materials). Details of the groundwater samples and the other materials utilized in this study are elucidated in the following paragraphs.

The contaminated environmental site was an aquifer heavily contaminated by trichloroethylene (TCE) and 1,1,2,2-tetrachloroethane (TeCA). Four different groundwater (GW) samples were collected from confined or shallow portions of the aquifer, located in the Northern Italy, and labelled with numbers from 1 to 4. A fifth groundwater solution was prepared by mixing equal volumes of the four aquifer samples (GW-5). The chemical composition of the four types of sampled GW is reported in Table 1.

**Table 3.** Contaminated groundwater samples' composition.

Compounds	Concentration range (mg·L <sup>-1</sup> )
TCE	0.043 – 5.8
TeCA	0.2 – 4.0
Cl <sup>-</sup>	27 - 57
NO <sub>2</sub> <sup>-</sup>	0.1 – 0.8
NO <sub>3</sub> <sup>-</sup>	33 - 53
PO <sub>4</sub> <sup>3-</sup>	1.3 – 2.5
SO <sub>4</sub> <sup>2-</sup>	56 - 274
Suspended solids	54 – 93
pH	7

A synthetic cultivation medium, referred to as synthetic water or synthetic GW, was prepared basing on the chemical composition of the natural site groundwater, as indicated in Table 2. Furthermore, the synthetic GW was always added with vitamin and micronutrient solutions,

respectively prepared as 1000 times and 100 times concentrated stock solutions, according to the receipts showed in Table 3 and Table 4.

**Table 4.** Synthetic water solution composition.

Compounds	Molecular weight $\text{g}\cdot\text{mol}^{-1}$	Concentration mM	Concentration $\text{mg}\cdot\text{L}^{-1}$
$\text{K}_2\text{HPO}_4$	174.22	8.899	1550.4
$\text{NaH}_2\text{PO}_4\cdot\text{H}_2\text{O}$	137.98	5.356	739
$\text{MgSO}_4$	120.37	0.500	60.2
$\text{CaCl}_2$	110.98	0.100	11.1
$(\text{NH}_4)_2\text{SO}_4$	132.14	0.796	105.2
$\text{NaNO}_3$	85	1.612	137
$\text{Na}_2\text{SO}_4$	165	1.515	250
KCl	75	1.213	90.42

**Table 5.** Vitamin stock solution composition (1000X).

Compound	Molecular weight $\text{g}\cdot\text{mol}^{-1}$	Concentration $\text{mg}\cdot\text{L}^{-1}$
Biotin	244.31	2
Folic acid	441.4	2
Pyridoxine HCl	247.14	10
Thiamine HCl	300.81	5
Riboflavin	376.36	5
Nicotinic acid	123.11	5
Pantothenic acid	219.23	5
Vitamin B12	1355.38	0.1
p-aminobenzoic acid	137.14	5
Lipoic acid	206.33	5

**Table 6.** Micronutrient stock solution composition (100X).

Compound	Molecular weight $\text{g}\cdot\text{mol}^{-1}$	Concentration $\text{mg}\cdot\text{L}^{-1}$
Nitrilotriacetic acid	191.14	1500
$\text{MgSO}_4\cdot 7\text{H}_2\text{O}$	120.37	3000
$\text{MnSO}_4\cdot\text{H}_2\text{O}$	169.02	500
NaCl	58.44	1000
$\text{FeSO}_4\cdot 7\text{H}_2\text{O}$	278.05	100
$\text{CoSO}_4\cdot 7\text{H}_2\text{O}$	281.10	180
$\text{CaCl}_2\cdot 2\text{H}_2\text{O}$	147.02	100
$\text{ZnSO}_4\cdot 7\text{H}_2\text{O}$	287.56	180
$\text{CuSO}_4\cdot 5\text{H}_2\text{O}$	249.61	10
$\text{KAl}(\text{SO}_4)_2\cdot 12\text{H}_2\text{O}$	258.21	20
$\text{H}_3\text{BO}_3$	61.83	10
$\text{Na}_2\text{MoO}_4\cdot 2\text{H}_2\text{O}$	143.95	10
$\text{NiCl}_2\cdot 6\text{H}_2\text{O}$	129.60	25
$\text{Na}_2\text{SeO}_3\cdot 5\text{H}_2\text{O}$	262.94	0.3

Butane (99.9%), Propane (99.9%), n-Pentane (99%), or Phenol (99%) purchased from Aldrich (Gillingam, UK) were employed as microbial growth supporting substrates. In addition, the methane gas supplied from the urban network (consisting of Methane 99.5%, Ethane 0.1%, Nitrogen 0.4%) was utilized as methane source.

Stock solutions of TCE and TeCA were prepared as water-saturated solutions inside distinct 119 mL glass vials, filled up till the edge with autoclave-sterilized distilled water and hermetically closed. A volume of 500  $\mu\text{L}$  of pure chlorinated compound (TCE (99.5%) and TeCA (99%) from Aldrich, Gillingam, UK) was added by means of a glass liquid-tight syringe and the attainment of the saturation state was clearly indicated by the formation of a dense bubble of the undissolved excess of chlorinated compound. TCE and TeCA concentrations in the liquid phases were respectively  $1.100 \text{ g}\cdot\text{L}^{-1}$  and  $2.700 \text{ g}\cdot\text{L}^{-1}$ , by virtue of their solubility values in water, at  $20^\circ\text{C}$ . Each stock solution was stored at  $4^\circ\text{C}$ , but brought again at  $20^\circ\text{C}$  before each utilization.

The immobilization of microbial cells was conducted in the presence of four different porous and inert materials: Cerambios<sup>®</sup>, Biomax<sup>®</sup>, Biomech<sup>®</sup> and Biopearl<sup>®</sup>, whose characteristics are reported in Table 5. These materials are easily available on the market since commonly designed for aquarium's water filtration. They were purchased from Zoogiardineria (Casalecchio di Reno, Italy), except Biomax<sup>®</sup> that was provided by Askoll Due (Dueville, Italy).

**Table 7.** Biofilm carrier materials characterization.

	<b>Cerambios<sup>®</sup></b>	<b>Biomax<sup>®</sup></b>	<b>Biomech<sup>®</sup></b>	<b>Biopearl<sup>®</sup></b>
				
<b>Shape</b>	Ceramic empty cylinders	Ceramic cylinder	Ceramic square cuboids	Sintered glass spheres
<b>Diameter/High</b>	15 mm	11 mm	6 mm	8 mm
<b>Length</b>	10 mm	9 mm	14 mm	-
<b>Volume</b>	$0.60 \text{ cm}^3$	$0.70 \text{ cm}^3$	$1.18 \text{ cm}^3$	$2.14 \text{ cm}^3$
<b>Porosity</b>	74 %	60 %	64 %	58 %
<b>Bulk density</b>	$0.659 \text{ g}\cdot\text{mL}^{-1}$	$0.658 \text{ g}\cdot\text{mL}^{-1}$	$0.682 \text{ g}\cdot\text{mL}^{-1}$	$0.950 \text{ g}\cdot\text{mL}^{-1}$

## 3.2.2. Experimental set up

### 3.2.2.1. Batch microcosms

#### 3.2.2.1.1. Set up of batch microcosms

Cultivation of complex microbial communities *in batch* mode was established inside 120 mL glass-serum-bottles sealed with a teflon-lined rubber septum, tightly affixed with a crimped aluminium cap (Figure 12). Such a system is referred to as microcosm.

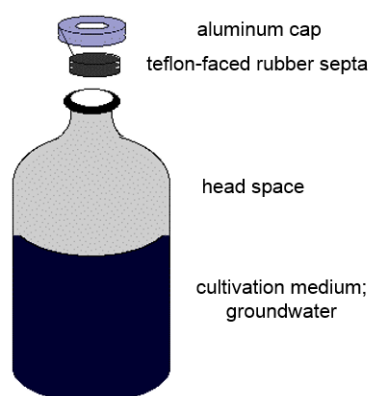


**Figure 12.** Microcosm assembly.

Freely suspended microbial microcosms were prepared with 60 mL of liquid phase (water medium and/or inoculum), while microcosms destined for the growth of immobilized consortia were filled with 60 mL (bulk volume) of carrier material and 50 mL of the liquid medium. The desired volumes of growth substrates, oxygen and CAHs were injected by means of glass gas-tight syringes. Before collecting any sample, the microcosms were shaken at 120 rpm for 15-20 min, at the operative temperature of the process, in order to restore the inner equilibrium of each compound between liquid and gaseous phases.

#### 3.2.2.1.2. Selection of the best growth substrate, microbial consortium and immobilization support material in batch microcosms at 30 and 15°C

The development of an immobilized microbial consortium able to aerobically cometabolize CAHs in the presence of a suitable growth substrate was accomplished following an experimental procedure articulated in two sequential steps: (i) growth substrate and groundwater selection and suspended-cell consortium development; (ii) immobilized community development and biofilm carrier selection, at different temperatures.

During the step (i), the enrichment of CAH-degrading consortia was screened by means of 25 microcosm tests, where each groundwater (GW1 to GW5) (Section 3.2.1), thus its native microbial community, was exposed to the presence of  $2 \text{ mg}\cdot\text{L}^{-1}$  of a candidate primary substrate, represented

by methane (M), propane (PR), butane (B), pentane (PE) or phenol (PH), at 30°C for 60 days. The AC depletion of CAHs was enhanced by addition of oxygen, substrate and CAHs every time that their concentration decreased below 1% of the initial values. Despite this first group of microcosm tests was conducted at a temperature different from the aquifer temperature (15°C) the choice of 30°C stemmed from the possibility of performing a more rapid degradation screening than at 15°C and comparing the results with the literature data. However, once that the best growth substrate promoting the AC degradation of CAHs at 30°C was selected, the best performant microbial consortium was propagated at 10% v/v into new autoclave-sterilized GW of the same type and adapted at 15°C. At the same time, a new group of microcosms was prepared by exposing the GW number 1, 2 and 4 to the presence of the selected growth substrate at 15°C.

The step (ii) was aimed to assess the immobilization of the best performing consortia on different carrier materials and evaluating how the AC degradation of CAHs was affected by the immobilization and the type of carrier. The procedure consisted of culturing freely-suspended consortia in the presence of solid materials enhancing the microbial cells adhesion and biofilm development overtime. Microcosm batch tests were prepared with four types of porous materials, as described in the section 3.2.1., submerged with sterilized GW (or synthetic GW) inoculated at 10% v/v with the best performing suspended consortium enriched at the step (i). As the latter was developed at both 30°C and then 15°C, the immobilization was carried out maintaining the same temperatures of the culture utilized as inoculum. Furthermore, the microbial growth and the AC degradation of CAHs were enhanced by the regular supply of oxygen, CAHs and the growth substrate selected at step (i). Periodically, the liquid phase was removed and replaced with fresh sterile GW (or synthetic GW) in order to ensure oxygen and substrate availability to the immobilized biomass.

The degradation activities of the best performing consortia enriched at 30°C and 15°C during the step (i) and all of the consortia developed during the step (ii) were evaluated by performing standardized kinetic tests consisting of a pulse of only substrate (2.0 mg·L<sup>-1</sup>), followed by a pulse of only TCE (1.0-1.2 mg·L<sup>-1</sup>), by a second substrate pulse (2.0 mg·L<sup>-1</sup>) and by a pulse of only TeCA (1.0-1.2 mg·L<sup>-1</sup>). With respect to the immobilized biomass tests the liquid phase was replaced with fresh medium before the second substrate pulse. The kinetic parameters utilized to describe the behaviour of the microbial consortia were:

- biomass concentration, ( $g_{\text{protein}} \cdot L^{-1}$ );
- initial normalized biodegradation rate ( $r_i$ ) of each compound  $i$  after each pulse, calculated by dividing the biodegradation rate ( $mg_i \cdot L^{-1} \cdot d^{-1}$ ) (limited at the first 4-5 points of the plot of total amount of  $i$  versus time and normalized by the reaction volume, referred to as bulk volume of carrier) by the initial concentration of  $i$  in the liquid phase ( $mg_i \cdot L^{-1}$ ), ( $day^{-1}$ );

- first order constant ( $k_{I,i,15-30}$ ) of net biodegradation of compound  $i$  at 15 or 30°C, obtained by dividing  $r_i$  by the biomass concentrations at the beginning of the pulse ( $L \cdot d^{-1} \cdot g_{\text{protein}}^{-1}$ ).

For each calculated parameter the 95% confidence interval was evaluated on the basis of the uncertainties associated to the experimental measures and to the evaluation of the above mentioned slope, following standard error propagation rules (Frasconi *et al.* 2013b).

### **3.2.2.1.3. Maintenance of the enriched microbial consortia**

Suspended cultures of the selected microbial consortia enriched at 30°C and 15°C were propagated at 10% v/v into bigger batch reactors, represented by 5 L pyrex glass bottles, where the amount of liquid suspension was 1.5 L. According to the initial cultivation medium utilized for the consortia enrichment, the cultures were maintained into GW or into synthetic GW. The cultures were constantly treated with substrate, oxygen, TCE and TeCA and the growth was monitored by spectrophotometric analysis of the optical density at 600 nm and periodic molecular characterization analyses, in order to assess the structural and phylogenetic stability of the suspended communities.

## **3.2.2.2. Process development in 1 L PBR**

### **3.2.2.2.1. Set up of 1 L PBR systems**

The development of the AC process driven by the best selected consortium from the stage (i) and immobilized on the four types of carrier materials was preliminarily evaluated inside 1 L packed bed reactors, PBRs, at 30°C. A comparative study of the process in the presence of the four carrier materials was conducted in a system consisting of four PBRs connected in parallel to a substrates feeding pipeline. As shown in Figure 13, each PBR consisted of a 1 L cylindrical glass column (height 60 cm and inner diameter 4,7 cm) equipped with three sampling doors located at different heights, which allowed the controlled access to the inner part of the system, useful to verify the concentration of the compounds under study. Each column was packed with one type of carrier material and was independently connected to the feeding pipe through stainless steel junctions and tubes, which were fixed at the inlet door of the column by pierced-caps with teflon lined septa. A peristaltic pump was placed through the feeding line that ensured a constant and continuous flow of TCE-contaminated-water to the four PBRs. Upstream the peristaltic pump, a three-ways-electro valve was placed to control the alternate feeding of an oxygen-enriched or a substrate-enriched water solution from two distinct gas-tight 20-L magnetically stirred LDPE (Low Density Poly-Ethylene) bags. The butane-containing LDPE bag was nitrogen-stripped to remove any dissolved oxygen. The TCE was continuously fed together with the groundwater. The water flow inside the PBRs was directed from

the bottom to the upper part and collected in a same pipeline bringing to the drainage system. The PBRs were operated for a period of 100 days at 30°C.

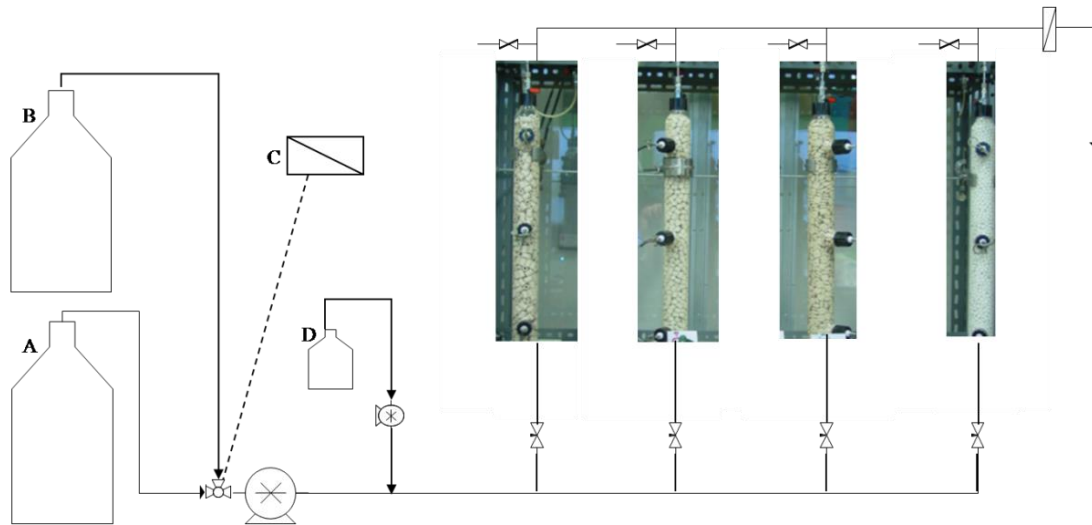


**Figure 13.** Flow sheet of the four columns plant. A: oxygen enriched water tank. B: substrate enriched water tank. C: Control unit. D: TCE saturated water solution.

### 3.2.2.2.2. Operative conditions adopted in 1 L PBRs

Colonization procedure of the 4 PBR plant. In order to enrich a sufficient volume of microbial biomass to inoculate the four PBRs, the selected consortium maintained at 30°C was cultivated in synthetic water inside a 15 L Sartorius fermenter (Figure 14), conducted in *feed batch* mode. During the colonization stage each PBR was operated for two days as a closed loop under recirculation, creating the conditions for a first immobilization of the introduced biomass on the supporting materials and its further development as biofilm.



**Figure 14.** 15 L Sartorius fermenter.

Conduction. Each PBR was operated at 30°C, fed with a synthetic water solution containing a TCE concentration variable in the range 1 – 3 mg·L<sup>-1</sup> and characterized by a hydraulic retention

time (HRT) of 10 hours. Furthermore, growth substrate and oxygen were supplied to the systems by means of a pulsed feeding strategy. An optimized 24 hours pulsation cycle consisted of alternating four substrate pulses with oxygen pulses, and the length of each pulse is indicated in Table 6.

**Table 8.** Pulsed feeding cycle length of substrate and oxygen.

<b>Pulsed Compound</b>	<b>Pulse Length (min)</b>	<b>Concentration (mg L<sup>-1</sup>)</b>
Selected substrate	108	25
Oxygen	252	21

*At the end of the conduction*, each PBR was emptied of the packing materials and the carrier units retrieved from three different sections of each PBR, namely the bottom (close to the inlet), the middle and the upper parts (close to the outlet) of the columns, were utilized either for kinetic evaluation tests or for molecular characterization of the immobilized microbial communities. The kinetic tests were conducted in batch conditions following the same procedure described in section 3.2.2.1.2.

### **3.2.2.3. Scale up of the processes: 31 L pilot plant**

#### **3.2.2.3.1. Set up of a 31 L PBR system**

During the last part of the MINOTAURUS project, a scale up of the AC process was realized inside a pilot plant, where the operative conditions and the pulsed feeding strategy were finally optimized. The pilot plant system consisted of a PBR made of 14 serial glass columns interconnected with steel pipes, a quite inert material to adsorption or release phenomena of substances. Along such steel junctions were distributed several sampling points, represented by valves allowing the access to the system for the collection of liquid volumes of flowing water. Each column of the plant was 1.25 m long with a diameter of 0.05 m and a volume of 2.22 L, thus the total length of the bioreactor amounted to 17.46 m and its total volume was 31.01 L. Furthermore, each column was packed with the selected support material and the whole system was assembled inside a 3.5 m<sup>3</sup> water tank, whose temperature was maintained constant with a controlled thermostatic bath. Throughout the pilot plant conduction period two working temperatures were tested, 30°C and 15°C. Before reaching the drainage system, the effluent water stream was driven through activated carbon filters, in order to remove excess of contaminants and impurities. A schematization of the pilot plant system is represented in the Figure 15, where also the disposition of the substrates tanks along the feeding pipeline is shown.

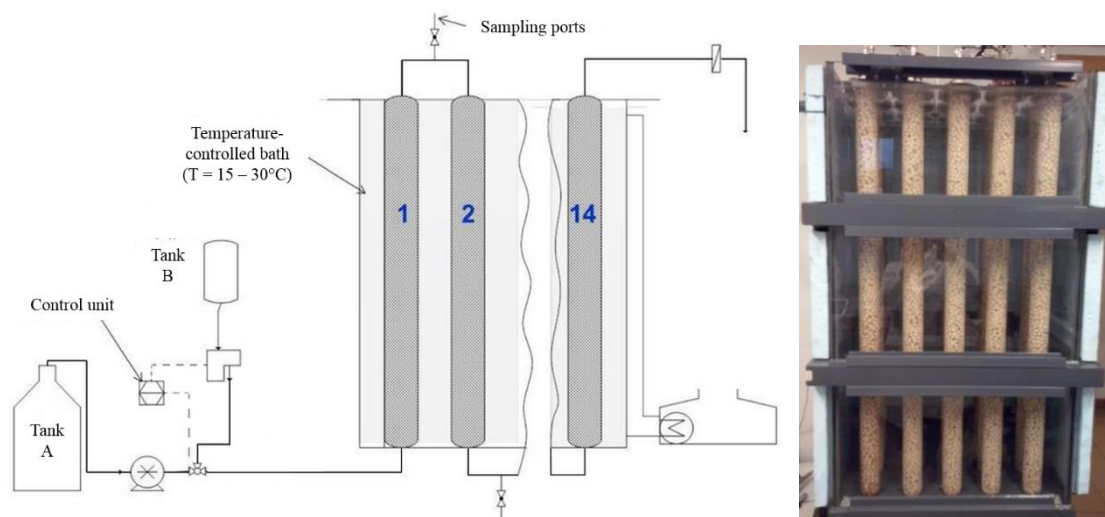


**Figure 15.** 31 L pilot plant system. Tank A: oxygen-saturated groundwater added with TCE and/or TeCA. Tank B: substrate-enriched groundwater.

The selected substrate and the oxygen/TCE/TeCA were provided to the system from two different glass tanks containing 20 L of groundwater (either the synthetic solution or the site-groundwater in a later stage of conduction) initially deprived of oxygen and chlorinated compounds. The groundwater of each tank was then saturated with the respective compound of interest (substrate or oxygen), by fluxing the latter through the liquid phase for several hours. The water tank saturated with oxygen contained also TCE and/or TeCA, which were properly added from the stock saturated solutions (section 3.2.1), in order to keep a desired concentration of contaminant in the tank's liquid phase. The pilot plant was operated for a period of 220 days.

A daily monitoring of the system consisted of collecting water samples from inlet and outlet of each column and measuring the dissolved oxygen, the substrate and the chlorinated solvent concentrations according to the analytical procedures reported in section 3.2.3.1.

### **3.2.2.3.2. Operative conditions adopted in 31 L PBR system**

*Colonization procedure of the 14 columns pilot plant.* The colonization of the system was accomplished utilizing 21 L of the suspended consortium maintained at 30°C, obtained by growth in synthetic GW inside the Sartorius fermenter with the same modalities. A volume of 1.5 L of suspended consortium was introduced into each column inlet to ensure a homogenized colonization procedure inside each column. Then, the connection between all of the columns was restored and the whole reactor was conducted in a recirculated batch mode for two days, in order to allow an efficient adhesion of the microbial cells onto the carrier units. Successively, the pilot plant was conducted in continuous flow, according to a pulsed feeding strategy that was gradually optimized among sequential operational stages as described in the next paragraph.

Conduction. The development of the AC process and a proper pulsed feeding strategy in the PBR plant was a consequence of a comprehensive evaluation of the operational parameters enhancing the establishment of a more effective process. Such an evaluation of the process was carried out by dr. Frascari and Prof. Pinelli, who proposed the gradual change and optimization of the AC process parameters through nine operational phases of the 31 L pilot plant that are following summarized.

During the first 6 phases the system was operated at 30°C and fed with synthetic groundwater. The hydraulic retention time (HRT) was between 4.1 and 4.6 days. These phases were aimed to the optimization of the substrate/oxygen pulsed feeding strategy in the presence of TCE concentrations ranging between 0.3 - 1.2 mg·L<sup>-1</sup> and in the absence of TeCA. While the first four phases were characterized by a simple alternating of substrate and oxygen/TCE pulses of various lengths, a new strategy was introduced with the fifth phase. Over a total cycle length of 4.6 days, the first 2.3 days (referred to as *growth phase*) were characterized by the alternate feeding of 3 substrate pulses of 8 h and 2 oxygen pulses of 16 h, while the remaining 2.3 days (defined as *degradation phase*) were exploited for the TCE biodegradation without any supply of substrate. The sixth phase was aimed to further assess the effectiveness of such a feeding strategy with a pulsation cycle modified by alternating three 8h-substrate pulses with two 23 h-oxygen pulses, followed by 4.1 days of degradation phase. Successively (7<sup>th</sup> phase), the temperature of the system was lowered to 15 °C in order to work closely to the real contaminated site conditions. Here, the cycle length was prolonged to 9 days, with a growth phase characterized by three 8 h-substrate pulses alternated with two 24 h-oxygen pulses and a degradative phase of 6 days. In the last two operational phases (8<sup>th</sup> and 9<sup>th</sup>) the synthetic groundwater supplied to the bioreactor was replaced with real site groundwater. The final optimized feeding cycle was the same as in the 7<sup>th</sup> phase. Only during the 9<sup>th</sup> phase TeCA was added at a concentration of 0.3 mg·L<sup>-1</sup>, in the presence of TCE 0.4 mg·L<sup>-1</sup>. The conduction of the 8<sup>th</sup> and 9<sup>th</sup> phases lasted 18 days.

At the end of the conduction, carrier units collected from the inlet of each column were utilized either for kinetic evaluation tests or for molecular characterization of the immobilized microbial communities. The kinetic tests were conducted in batch conditions following the same procedure described in section 3.2.2.1.2.

### 3.2.3. Analytical techniques

#### 3.2.3.1. Gas chromatography for the measurement of growth substrates, oxygen and chlorinated organic compounds

The gaseous concentrations of chlorinated compounds and substrates were measured by analysing 100  $\mu\text{L}$  of headspace with a Hewlett Packard 6890 GC instrument, equipped with an ECD (Electron Capture Detector) and a FID (Flame Ionization Detector). Details of the gas chromatography method were reported by Frascari *et al.* (2005, 2006a). The actual concentration of each CAH into the cultivation medium was deduced by considering the following equations and the achievement of the equilibrium between the liquid and gas phase:

$$1) C_G = H \cdot C_L$$

$$2) m_T = C_L \cdot V_L + C_G \cdot V_G$$

Where:

$m_T$  = total amount of CE, expressed in mg or  $\mu\text{mol}$

$C_G$  and  $C_L$  = gaseous and liquid concentrations of the CE, expressed in  $\text{mg}\cdot\text{L}^{-1}$  or  $\mu\text{mol}\cdot\text{L}^{-1}$

$V_G$  and  $V_L$  = volumes of the gaseous and liquid phases, in L

H = dimensionless Henry constant, at 30°C or 15 °C.

#### 3.2.3.2. Microbial biomass quantification via protein concentration determination

The microbial biomass concentration, of both freely-suspended-cell cultures and immobilized-cell cultures, was indirectly estimated by measuring the total protein concentration based on the test developed by Lowry *et al.* (1951). Two different protocols were optimized for the sample preparation. In case of suspended microbial consortia, a microbial-cells pellet was obtained from 0.4 mL of cultivation medium and resuspended into 0.5 mL of water solution adjusted with NaOH 0.1 N. Such a suspension was utilized for the test. In order to analyse the concentration of biomass immobilized on carrier materials, few units of carrier (5 for Biomech<sup>®</sup>, 5 for Biomax<sup>®</sup>, 15 for Bioperl<sup>®</sup>, or 4 for Cerambios<sup>®</sup>) were transferred into 15 mL tubes and washed from residual drops of cultivation medium and non-immobilized microbial cells with 7 mL of physiologic solution (0.9% w/v NaCl). The carrier units were then submerged with new physiologic solution and incubated at 30°C for 1 h to allow microbial cells inside the porosity of the carrier-units to diffuse outside. The tubes were then centrifuged at 8,000 rpm for 20 min and the supernatant discharged. Carrier units and cell's pellets were treated with 7 mL of a NaOH 1 N solution for 1.5 h on shaking at 120 rpm, at 30°C. Some 0.5 mL of this suspension were subjected to the reaction test. The dry weight of utilized

carriers was then measured in order to normalize the protein concentration values obtained for gram of carrier. The solutions utilized for the Lowry test execution are following listed:

- solution A:  $\text{Na}_2\text{CO}_3$  2% in NaOH 0.1 N
- solution A2:  $\text{Na}_2\text{CO}_3$  2% in  $\text{dH}_2\text{O}$
- solution B1:  $\text{CuSO}_4 \cdot 5\text{H}_2\text{O}$  1% in  $\text{dH}_2\text{O}$
- solution B2: Na-tartrate ( $\text{C}_4\text{H}_4\text{Na}_2\text{O}_6$ ) 2% in  $\text{dH}_2\text{O}$
- solution C: mixture of solutions A, B1 and B2 with ratio 100:1:1
- solution D: mixture of solutions A2, B1 and B2 with ratio 100:1:1
- solution E: 2X dilution in  $\text{dH}_2\text{O}$  of Folin & Ciocalteu's phenol reagent 2 N (Sigma-Aldrich).

The optimized procedure for the Lowry test consisted of boiling 0.5 mL of sample for 1 min, followed by the addition of 2.5 mL of solution C or D, whether the samples were obtained respectively from suspended or immobilized microbial consortia. After exactly 10 min, each test tube was added with 0.25 mL of solution E, obtaining a final reaction volume of 3.250 mL, in the presence of a final NaOH concentration of about 0.1 N for the suspended-consortia samples, or 0.15 N for the immobilized-consortia samples. Along with each set of sample, standard samples containing concentrations of BSA (bovine serum albumin, Sigma-Aldrich) variable between 0 – 50  $\text{mg} \cdot \text{mL}^{-1}$  were processed in the same way, even utilizing the solutions C or D, according to the type of sample analysed. All of the reaction mixtures were maintained in the dark for 30 min for the complete development of the reaction product. The intensities of the blue tonality assumed by the reaction solutions were quantified with a spectrophotometer UV\_VIS (model Cary 100, Varian Inc.).

### **3.2.4. Molecular analyses of microbial communities**

#### **3.2.4.1. Metagenomic DNA extraction and purification**

Total DNA from suspended complex microbial cultures was extracted from about 0.2 g of cell pellet by using a NucleoSpin<sup>®</sup> Soil kit (MACHEREY-NAGEL GmbH & Co. KG), according to the manufacturer's instructions. A procedure for the isolation of metagenomic DNA from microbial communities immobilized on each type of carrier materials was optimized. Few units of carrier (5 for Biomech<sup>®</sup>, 5 for Biomax<sup>®</sup>, 15 for Biopearl<sup>®</sup>, or 4 in case of Cerambios<sup>®</sup>) were aseptically transferred into sterile 15 ml tubes and washed from residual drops of cultivation medium and non-immobilized microbial cells with 5 mL of physiologic solution (0.9% w/v NaCl). The carrier units were then submerged with 5 mL of a water solution containing EDTA 0.5 M, TRIS 1 M pH 8, Glucose 1 M. Each tube was added with protease K 100 µg/mL, lysozyme 160 µg/mL, mutanolysine 30 µg/mL, and 4 g of autoclaved sand, thus incubated at 37°C in agitation for 30 min, to promote enzymatic and mechanical cellular lysis. A further chemical cellular lysis was enhanced by addition of 1 mL of a SDS 10% solution, vortexed for 10 min at maximum speed, and finally centrifuged for 10 minutes at 10,000 rpm. The supernatant was recovered and incubated at 4°C for 5 min in the presence of 3 mL of NaCl 5M for the proteins precipitation. Metagenomic DNA solution was separated from the protein precipitate, by centrifuging at 8,000 rpm for 5 min, and then transferred into new sterile tube. Here, DNA precipitation/concentration was accomplished adding glycogen 20 µg·mL<sup>-1</sup>, 0.1 volumes of sodium acetate 1 M and 2 volumes of 96% ethanol, the solution was homogenized and incubated overnight at -20 °C, to allow the DNA precipitation. Subsequently, it was centrifuged at 12,000 rpm for 30 min at 4 °C, the supernatant discarded, the DNA-pellet dried in sterile conditions and further suspended into 700 µL of sterile distilled water. Further purification of the isolated DNA was performed with the NucleoSpin<sup>®</sup> Soil kit (MACHEREY-NAGEL GmbH & Co. KG). The quality of the extracted DNA was checked on 1.0-1.2% w/v agarose gel containing the Atlas ClearSight DNA Stain (BIOATLAS) dye, along with a SibEnzyme 100bp+2kb+3kb DNA Ladder (Thermo Scientific, CABRUsas, Italy).

#### **3.2.4.2. PCR-DGGE approach for the microbial community characterization**

##### **3.2.4.2.1. Amplicons preparation and quantification for DGGE**

The characterization of microbial communities, by PCR-DGGE approach, was based on the analyses of hypervariable regions V3-V5 of the community's genes coding for the small subunit 16S rRNA. Amplicons with a final length of 550 bp were prepared by PCR in the presence of a GC-clamped forward primer, GC-357f, and 907 reverse primer (Sass *et al.* 2001). Such a DNA sequences

length could fit through the 7%-polyacrylamide matrix of the DGGE gels, utilized in this study. All PCR reactions were prepared into 50  $\mu$ L mixtures containing 1 $\times$  PCR buffer (Fermentas), MgCl<sub>2</sub> 1.5 mM, each dNTP 0.2 mM, each primer 0.4 mM, 1.0 U of Taq polymerase (Fermentas) and 2  $\mu$ L of template DNA (or its dilution). The standard cycling program was set to 95°C denaturation for 5 min, followed by 30 cycles of 95°C for 30s, 55°C for 30s, 72°C for 45min and a final extension at 72°C for 7min.

The amplicons' quality and correct size were checked by electrophoretic run of 5  $\mu$ L of each PCR product on a 1.0-1.3% agarose gel casted with Atlas ClearSight DNA Stain (BIOATLAS) dye, along with a SibEnzyme 100bp+2kb+3kb DNA Ladder (CABRU sas, Italy), in 1.0X TAE buffer at 130V. The visualization of the amplicons bands was performed with a Bio-Rad (Hercules, CA) Gel Doc imaging system. A more accurate quantification of the PCR products concentration was performed with an Implen NanoPhotometer® instrument (Implen, Germany). The measurement was carried out according to the Implen user`s guide.

#### 3.2.4.2.2. DGGE analysis

DGGE analyses were performed with a DCode System (Bio-Rad Laboratories, Inc. Milan, Italy). Two acrylamide/bis-acrylamide (40% solution; Mix Ratio 29:1; catalogue number A7802; Sigma-Aldrich) stock solutions, with concentration of DNA-denaturing compounds (urea and formamide) equal to 70% and 0% w/v, were periodically prepared as shown in Table 9 and stored at 4°C, to have them readily available for DGGE gel casting.

**Table 9.** Acrylamide/bis-acrylamide stock solutions preparation.

<b>Compound</b>	<b>0% denaturing stock solution (100 ml)</b>	<b>70% denaturing stock solution (100 ml)</b>
Urea	-	29.4 g
Deionized water	80.5 ml	up to 52.5 ml
50X TAE buffer	2.0 ml	2.0 ml
Formamide	-	28.0 ml
40% bis/acrylamide	17.5 ml	17.5 ml

As indicated in the Table 10, volumes of such stock solutions were properly combined in order to prepare a low-density (LD) solution and a high-density (HD) solution, respectively containing the denaturing concentration desired at the top (usually 40-45%) and at the bottom (usually 55-60%) of the DGGE gel.

**Table 10.** Preparation of the LD and HD solutions by mixing volumes of the stock solutions.

Denaturing % concentration of the LD- or HD-solution	Volume from 0% solution	Volume from 70% solution
40%	5.6 ml	7.4 ml
45%	4.6 ml	8.4 ml
55%	2.8 ml	10.2 ml
60%	1.9 ml	11.1 ml

At this point, the acrylamide matrix polymerization was triggered by adding to each solution 88  $\mu$ l of a 10% ammonium persulfate solution (APS for electrophoresis 98% Sigma-Aldrich Co. LLC.) and 8.8  $\mu$ L of TEMED solution (N,N,N',N', tetramethylethylene- diamine for electrophoresis, 98% Sigma-Aldrich Co. LLC.). The HD and LD solutions were rapidly loaded into the 1 mm-thick sandwich space by mean of a semi-automatic mixing system (BioRad) conveying the right ratios of the two solutions into a single Y-fitting tube. At the end of the gel casting, about 1 mL of deionized water was poured on the top of the gradient formed, in order to make its top edge as linear as possible. The denaturing gradient gel was allowed to polymerize for two 2.5 h, then the water layer on the top was removed and the stacking gel casting was done utilizing 6 ml of the 0% denaturant solution added with 44  $\mu$ L of 10% APS and 4.4  $\mu$ L of TEMED. In the stacking gel was inserted a 20 wells comb. After two additional hours, the sandwich was placed into a heated buffer chamber. After that an amount of approximately 400 ng of PCR-amplified DNA was loaded into each well of the stacking layer, the electrophoresis was run at 55V for 16 h at 60 °C.

At the end of the run, the gel was stained in a solution of 1 $\times$ SYBR-Green (Sigma–Aldrich, Milwaukee, WI) in 1 $\times$ TAE for 20 min and its image captured in UV trans illumination with a Gel Doc system equipped with a digital camera (Bio-Rad, Milan, Italy).

The QuantityOne 4.5.2 software (Bio-Rad) was utilized for a comparative analysis of the DGGE profiles in terms of similarity indexes, based on the Dice coefficient, and dendrograms were created basing on the Unweighted Pair Group Arithmetic Average (UPGAMA) clustering algorithm.

The bands visualized along DGGE community profiles were excised from the gel and eluted into 50  $\mu$ L of sterile deionized water by overnight incubation at 4°C. Some 2  $\mu$ L of band-eluted DNA (or its dilution) were used as PCR template in the presence of the primer couple GC357f/907r. The new GC-clamped 550 bp-amplicons were loaded on a second DGGE, exclusively aimed to further purify the retrieved sequences from a background DNA, typically running throughout the DGGE gradient when high amounts of metagenomic DNA are loaded. Usually, the denaturing gradient of the second DGGE is restricted to 45%-55% denaturing concentration range. The two fold DGGE-purified sequences were retrieved in the same way as mentioned above and newly amplified with primers 357f/907r (Sass *et al.* 2001).

The obtained amplicons, representative of a single 16S rDNA sequence, were purified from dNTPs and primer dimers occurring in the PCR mixture with ExoSAP-IT® (Affymetrix, Santa Clara, CA) and proper amounts of samples were prepared and submitted to the BMR Genomics s.r.l. (Padova, Italy) for the sequencing service.

### **3.2.4.3. PCR-cloning approach for the microbial community characterization**

#### **3.2.4.3.1. Amplicons preparation for the cloning reaction**

In the present study, clone libraries were realized to determine either the phylogenetic or the functional-genes composition of investigated communities. When the phylogenetic diversity was investigated, metagenomic libraries were prepared from a pool of amplicons of the full-length 16S rRNA-coding genes from each analysed community. The 16S rDNA sequences were targeted by the primer couple 27f/1525r (Lane 1991), by using the same PCR conditions described in the paragraph 3.2.4.2.1. with the only exception that the elongation step was extended to 1.5 min. After the quantification of the PCR products with nanophotometer, 1 µL of amplicons' solution was destined for cloning.

In some cases, the microbial communities under study were screened for the presence of five types of functional genes, potentially having a crucial role in the processes investigated. Different degenerated primer sets, to target such a functional genes, were selected from the literature and are reported in the Table 11. Thus, each primer set was used to assess the amplification of the targeted functional genes within the analysed communities. The PCR conditions applied were maintained the same as described in the reference papers. Only in the case of *alkB* primers, the PCR reaction was optimized and carried out in the presence of MgCl<sub>2</sub> 2 mM, dNTPs 0.24 mM, primers 1 µM and 1 Unit of Taq Polymerase (Fermentas); while the thermal treatment consisted of an initial denaturing step of 5 min at 95°C, followed by 30 cycles of 30 sec at 95°C, 30 sec at 61°C and 1 min at 72°C, and a final elongation phase of 10 min at 72°C.

**Table 11.** Functional genes screened and primer sets utilized.

Targeted genes	Primer Set	Amplicon size	Reference
Membrane alkane hydroxylase, (alkB)	alkB-1f/alkB-1r	550 bp	Kloos <i>et al.</i> 2006
Soluble di-iron monooxygenase, (SDIMO)	NVC57f, NVC65f, NVC58r, NVC66r	420 - 1100 bp	Coleman <i>et al.</i> 2006
Particulate methane monooxygenase, (pmoA)	A189f/mb661r	500 bp	Bourne <i>et al.</i> 2001
Soluble methane monooxygenase, (mmoX)	mmoX206f/mmoX886r	719 bp	Hutchens <i>et al.</i> 2004
P450 alkane hydroxylase, (P450)	CYP153-f1/CYP153r2	820 bp	Wang <i>et al.</i> 2011

### 3.2.4.3.2. Clone libraries construction and screening

Amplification products volumes, variable between 1  $\mu\text{L}$  and 4  $\mu\text{L}$ , were cloned into pCR@4-TOPO® cloning vector (Invitrogen, Paisley, UK). To increase the efficiency the time of cloning reaction was prolonged to 30 min. The resulting plasmids were utilized to transform chemically competent One Shot® TOP10 *E. coli* cells (Invitrogen, Paisley, UK), following the manufacturer's instructions. Volumes of 20  $\mu\text{L}$  and 50  $\mu\text{L}$  of transformation mixtures were spread on LB media plates containing kanamycin 50  $\mu\text{g}\cdot\text{mL}^{-1}$ . Some 20  $\mu\text{L}$  of S.O.C. medium (provided with the cloning kit) were mixed with 20  $\mu\text{L}$  of the transformation product, to ensure sufficient spreading on the plates. After overnight incubation at 37°C of the LB plates, the obtained colonies were randomly harvested and transferred to 5-7 mL of fresh liquid LB medium, containing kanamycin 50  $\mu\text{g}\cdot\text{mL}^{-1}$ , for an overnight growth at 37°C and 280 rpm. A volume of 1.350 mL from every culture was cryopreserved at -80°C by addition of 0.45 mL of autoclave-sterilized 80% glycerol solution. Plasmids from the grown cultures were recovered according to the alkaline lysis protocol described by Sambrook *et al.* (1989) and their quality was checked by electrophoretic run of 2  $\mu\text{L}$  of plasmid solution on a 1.3% agarose gel.

When 16S rDNA clone libraries were produced, the library screening was performed by means of DGGE. The GC357f/907r primer couple was used to amplify a GC-clamped sequence of 550 bp of the cloned inserts (consisting of the full 16S gene) under the same PCR conditions previously described (Paragraph 3.2.4.2.1.) and a 50 times diluted plasmid DNA was used as template. The amplicons obtained were resolved by DGGE, containing a denaturing gradient of 45-55%, along with a reference lane, represented by the mixture of the same gene portions amplified from the total community, in order to associate the bands visualized for each cloned insert to the corresponding bands of the community profile. Those clones corresponding to unique bands of the total community DGGE profile were selected for the sequencing analysis.

With respect to functional gene libraries, the effectiveness of the ligation and transformation steps was assessed by PCR amplification with the M13f/M13r primer pair provided by the cloning kit (Invitrogen, Paisley, UK), whose priming sites were at the extremities of the insert region. The correct size of the inserts was checked by electrophoretic run of 1.5% agarose gel. Thus, the plasmids containing an insert of the right dimension (depending on the primer set utilized) were selected for the sequencing analysis.

Plasmids corresponding to the selected inserts were newly extracted from the initial transformed-cell cultures (stored as glycerol stocks at -80°C) with a PureLink® Quick Plasmid Miniprep Kit (Invitrogen™) and appropriate amounts were prepared according to the recommended procedures ([www.bmr-genomics.it](http://www.bmr-genomics.it)) for the sequencing analysis. Each plasmid insert was sequenced on both strands by using the T3 primer (5'-ATTAACCCTCACTAAAGGGA-3') or T7 primer (5'-TAATACGACTCACTATAGGG-3'), whose promoter sites were placed at the extremities of the DNA fragments cloned into the pC4®-TOPO® vector. Sequencing reactions and runs were all performed by BMR Genomics s.r.l. (Padova, Italy).

#### **3.2.4.4. Sequencing analysis result evaluations**

Nucleotidic sequences obtained with T3 and T7 primers for both strands of the same insert were evaluated and merged in their overlapping region, obtaining the full sequence of each 16S rRNA or functional gene analysed. In order to remove any primer bias in the sequence data, the primer and vector sequences were removed from each raw sequence file before alignment. Sequence identities were determined by DNA homology searches using the online *Seqmatch* tool of the Ribosomal Database Project (RDP II) (Cole *et al.* 2014), or by entering sequencing data into NCBI BLASTn and BLASTx alignment search tools (Altschul *et al.*, 1997).

### 3.3. Results and discussion

#### 3.3.1. Selection of the best growth substrate and the best microbial consortium under batch conditions at 30°C

The research study conducted to develop an effective bioremediation system for the treatment of CAH-contaminated GW via AC began with the crossed screening of the CAH-degradation activities evolved by five types of groundwater's native microbial communities when exposed to the presence of five types of growth substrates (step (i), described in the section 3.2.2.1.2.). Routinely monitoring analyses of substrate, oxygen and CAH removals inside microcosms, along with specific kinetic evaluations of the processes, were carried out by the research team supervised by dr. Frascari and Prof. Pinelli, Dept. DICAM, University of Bologna.

A preliminary investigation of the microbial community structure of the enriched consortia was performed by means of a PCR-DGGE approach (Figure 16), according to the procedure described in the section 3.2.4.2. Cultures grown in the presence of phenol were not analysed, because the monitoring analyses of substrate, oxygen and CAH removals revealed a very slow activity in these microcosms that were not further considered for the study.

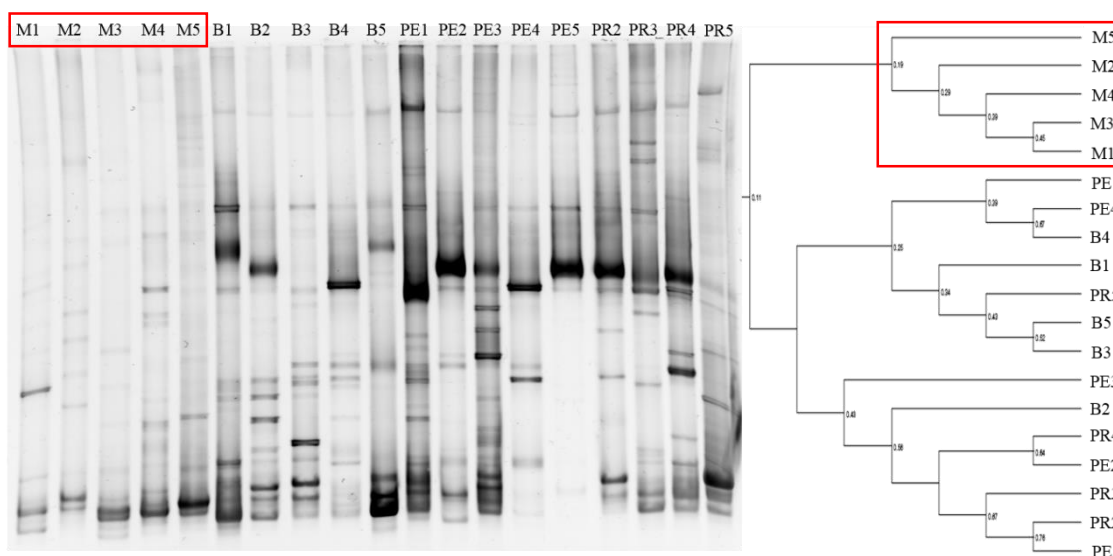


**Figure 16.** DGGE profiling the 20 suspended consortia enriched in the step (i), at 30°C. The clustering analysis was based on the UPGMA algorithm and the dendrogram built with the Quantity One 4.5.2 software (Bio-Rad). Numbers 1-5 indicated the type of GW; M: methane; PE: pentane; PR: propane; B: butane.

DGGE profiles of the twenty analysed communities indicated a wide heterogeneity of the microbial consortia. Similarity indexes between the visualized DGGE profiles were all lower than 54%, except for the consortia B4 and PE4, 67% similar to each other. As showed from the dendrogram, the type of growth substrate was not selective among the investigated groundwater communities, with the only exception of the methane-fed consortia (codes with letter M), which clustered together.

A preliminary evaluation of the biodegradation activity among the microcosms led to individuate eight microbial consortia more performant than the others in terms of AC degradation of TCE and TeCA, namely the microcosms M1, M4, PR2, PR4, B4, B5, PE1, PE4 (letters indicate the substrate and numbers the GW). The selected microcosms did not belong to a specific type of GW, nor a substrate, apparently suggesting a randomized development of the biodegradation activity. A specific biodegradation test was performed to describe the degradation capabilities of the eight consortia by using specific process parameters (section 3.2.2.1.2.). First order biodegradation constants ( $k_{1,i,30}$ ) values obtained from the kinetic evaluation are reported in Table 12.

**Table 12.** First order biodegradation constants ( $k_{1,i,30}$ ) of TCE and TeCA at 30°C for the eight best performing consortia.

Growth substrate	Consortium	$k_{1,TCE,30}$ ( $L \cdot g_{\text{protein}}^{-1} \cdot d^{-1}$ )	$k_{1,TeCA,30}$ ( $L \cdot g_{\text{protein}}^{-1} \cdot d^{-1}$ )
Methane	M1	3.7 ± 0.4	0.72 ± 0.11
	M4	1.2 ± 0.1	0.55 ± 0.06
Propane	PR2	1.3 ± 0.1	1.35 ± 0.15
	PR4	56 ± 6	0.94 ± 0.07
Butane	B4	96 ± 7	0.86 ± 0.07
	B5	42 ± 3	0.73 ± 0.11
Pentane	PE1	0.86 ± 0.08	0.37 ± 0.05
	PE4	0.53 ± 0.04	0.33 ± 0.03

First order constants showed a significantly lower removal of the TeCA in comparison with the TCE, with a  $k_{1,TeCA,30}/k_{1,TCE,30}$  ratio of 0.23 (Frasconi *et al.* 2013b). Further experimental evidences (data not shown) indicated high rates of abiotic conversion of TeCA into TCE; as a consequence, the TeCA biodegradation via AC was not more considered at this stage of the work, while an abiotic pre-treatment for the TeCA conversion into TCE was evaluated (Frasconi *et al.* 2013b). At the same time, kinetic degradation activities of growth substrates were not considered relevant to the selection of a microbial consortium effectively degrading CAHs. Thus, such selection was exclusively based on the TCE degradation activities observed.

Finally, the selected consortium was a butanotrophic community enriched from the GW number 4, referred to as consortium B4, which showed the highest TCE-degradation first order constant ( $96 L \cdot g_{\text{protein}}^{-1} \cdot d^{-1}$ ).

### 3.3.2. Selection of the best immobilization support material and evaluation of the microbial community immobilization under batch conditions at 30 and 15°C

In order to evaluate whether the enrichment/selection stage at 30°C negatively affected the microbial capability of degrading CAHs at the natural site temperature, namely 15°C, the B4 consortium was propagated at 10% v/v in fresh GW n.4 and operated at 15°C. In parallel, a new group of microcosms was prepared by exposing the GW number 1, 2 and 4 to the presence of butane at 15°C. The TCE-degradation activities of such 15°C-cultures were assessed by means of kinetic test (step (i) section 3.2.2.1.) and resulted very similar, with first order constant comprised between 2.8 – 4.3 L·g<sub>protein</sub><sup>-1</sup>·d<sup>-1</sup> (Frasconi *et al.* 2013b). This evidence suggested that a screening of the degradation activity at 30°C was a viable method for the rapid selection of the best performing microbial communities, which could be reversibly re-adapted at their natural temperature (15°C). Thus, the consortium B4 propagated at 15°C was maintained and utilized for further experimental tests.

During the step (ii) of the experimental procedure described in section 3.2.2.1.2., the B4 consortium maintained (details in section 3.2.2.1.3.) at 30 and 15°C (cultures successively referred to as 30°C II and 15°C II, respectively) was propagated into new vials in the presence of four different types of immobilization materials: Biomax (BX), Biomech (BM), Biopearl (BP) and Cerambios (CB). A selective enrichment of the microorganisms able to grow in an immobilized form was favoured by the periodic replacement of the microcosm liquid phases. The immobilized B4 communities were then subjected to kinetic tests, according to the procedure described in the section 3.2.2.1.2.; butane and TCE biodegradation first order constants and initial normalized biodegradation rates are reported in Table 11.

**Table 13.** Butane and TCE first order constants ( $k_i$ ) and initial normalized biodegradation rates ( $r_i$ ), with 95% confidence intervals, relative to the different consortia B4. Each test was performed in three replicates. BX: Biomax. BM: Biomech. BP: Biopearl. CB: Cerambios.  $k_i$  values are expressed in L·d<sup>-1</sup>·g<sub>protein</sub><sup>-1</sup> and  $r_i$  values in day<sup>-1</sup> (Modified from Frasconi *et al.* 2013b).

Cell condition	Compound	$k_{I,30}$	$k_{I,15}$	$r_{i,30}$	$r_{i,15}$
Suspended	Butane	446 ± 13	220 ± 12	81.3 ± 1.35	21.19 ± 1.09
	TCE	96 ± 7	4.3 ± 0.6	17.51 ± 1	0.75 ± 0.11
Immobilized on BX	Butane	1,580 ± 150	315 ± 65	155 ± 12	41 ± 0.2
	TCE	6.2 ± 0.5	4.5 ± 1.1	0.61 ± 0.04	0.59 ± 0.07
Immobilized on BM	Butane	1,782 ± 781	491 ± 204	136 ± 7	12.6 ± 0.3
	TCE	8.2 ± 3.6	13.3 ± 6.1	0.62 ± 0.04	0.34 ± 0.07
Immobilized on BP	Butane	4,750 ± 1,285	234 ± 83	170 ± 8	6.9 ± 0.2
	TCE	10.8 ± 3.1	7.8 ± 3	0.39 ± 0.04	0.23 ± 0.04
Immobilized on CB	Butane	1,768 ± 715	8 ± 5	21 ± 1	0.9 ± 0.4
	TCE	11.5 ± 4.7	1.8 ± 1	0.13 ± 0.01	0.19 ± 0.08

**Table 14.** Concentrations of the microbial biomass immobilized on different support materials, at 30 and 15°C. Each test was performed in three replicates.

<b>Immobilization material</b>	<b>Biomass concentration, 30°C (g<sub>protein</sub>·L<sub>bulk</sub><sup>-1</sup>)</b>	<b>Biomass concentration, 15°C (g<sub>protein</sub>·L<sub>bulk</sub><sup>-1</sup>)</b>
Biomax	0.098 ± 0.015	0.13 ± 0.027
Biomech	0.076 ± 0.033	0.03 ± 0.11
Biopearl	0.036 ± 0.010	0.03 ± 0.010
Cerambios	0.012 ± 0.005	0.10 ± 0.035

As shown in Table 11, the AC process at 30°C was characterized by a general increase of the butane degradation capability of the immobilized biomass, while the TCE first order biodegradation constants were remarkably lower than in the suspended cultures. A different behaviour was observed at 15°C, where the substrate degradation was only slightly increased, but the TCE removal activity was comparable to the suspended cultures. Higher efficiencies of the AC process at 30°C and 15°C were attained in the presence of Biomax and Biomech, rather than other carrier materials. In spite of the fact that the average first order kinetic constants for these materials were comparable, it was observed that the repeatability of the process among the experimental replicates was higher with Biomax, both at 30 and 15°C, rather than with Biomech. Furthermore, the TCE initial biodegradation rates,  $r_i$ , at 15°C for the Biomax immobilized consortium was much higher than in the other immobilized consortia. Considering the biomass concentration per unit of carrier (measured according to the procedure described in section 3.2.3.2.) reported in Table 12, it resulted that Biomax favoured the immobilization of higher amounts of microbial biomass, and the difference with the other carriers was remarkable at 15°C. On the basis of these kinetic evaluations, the Biomax material was selected as the best suitable carrier for the subsequent development of the process inside a PBR system.

Community structure and phylogenetic composition of the suspended and immobilized B4 consortia were determined by PCR-DGGE analysis of the metagenomic 16S rDNA regions targeted by the primer couple 357f/907r (procedure described in section 3.2.4.2.). Initially, changes in the B4 community's composition were evaluated over time, by comparing the suspended consortium B4 enriched at the step (i) (indicated as *B4(I)* in Figure 17) and the same culture maintained for some time at 30°C (*30°C II*, Figure 17), which was later utilized to inoculate the microcosms for the immobilization. Successively, the *30°C II* culture-DGGE profile was compared with the profile obtained from the B4 consortium adapted at 15°C (referred to as culture *15°C II*, Figure 18) in order to evaluate the lower temperature effect on the community structure and composition (Figure 18).

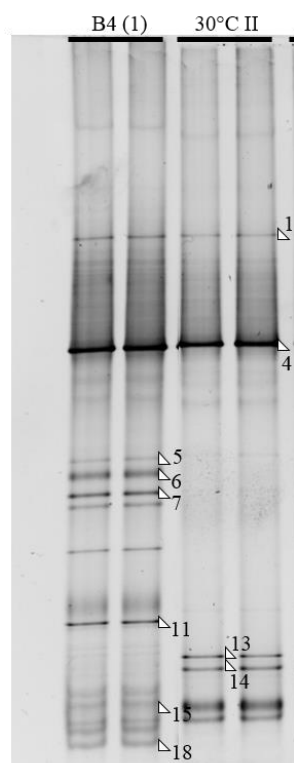


**Figure 17.** DGGE profiles of the initial B4 consortium enriched in the step (i), *B4(I)*, propagated at 30°C in a suspended form, *30°C II*. The sequences phylogenetically identified are indicated by the white triangles and numbers and reported in Table 18 in Appendix. The denaturing gradient range is 40 – 60%.

Percentage index of similarity, based on the Dice coefficient calculation, between the two DGGE profiles *B4(I)* and *30°C II* was 45.3%, an evidence that the microbial community B4 was evolving and the selective enrichment of different phylotypes (band 13 and 14) could be observed after few sub-culturing steps. Nevertheless, some of the main phylotypes maintained their dominance throughout sub-culturing (bands 1, 4). In addition, all of the dominant phylotypes occurring in the profile *B4(I)* were still slightly represented in the culture *30°C II*, indicating that the culture could harbour, but not loose, several microbial phylotypes under the DGGE detection limit. Such phylotypes can potentially become dominant within the community when different cultivation conditions are imposed. For instance, phylotypes represented by the band number 5 and 7 of the culture *B4(I)* were almost non detectable in the culture *30°C II*, while their relative abundance increased again when the consortium B4 was re-adapted at 15°C (*15°C II*, Figure 18). The similarity between the cultures *30°C II* and *15°C II* was equal to 57% (Figure 19), suggesting that the temperature did not strongly affect the community structure of the suspended consortia B4. It was interesting to notice that dominant phylotypes, such as bands 1 and 4, were maintained from the initial consortium *B4(I)*, while other phylotypes (bands 13 and 14) were enriched in parallel cultivation at 30 and 15°C.

The analyses of the sequences (listed in Table 18 - Appendix) associated with the bands among the DGGE profiles of the suspended consortia B4, the most abundant phylotype in terms of relative band intensity was an unclassified bacterium (band 4) affiliated with *Chlorobi*. Several Bacteroidetes were detected (bands 1, 5, 6, 7) and the remaining mostly represented phlotypes belonged to Betaproteobacteria (bands 11, 13, 14), Alphaproteobacteria (band 15) and Actinobacteria (band 18). Interestingly, some microorganisms known to be polycyclic aromatic hydrocarbon-degrading species were identified, such as *Mycobacterium pallens* czh-8 (Hennessee *et al.* 2009) and *Zooglea* sp. (Li *et al.* 2005). A phylotype (band 14) was related (ID 97%) to a strictly anaerobic toluene-degrading microorganism, *Georgfuchsia toluolica* G5G6 (Weelink *et al.* 2009). Another phylotype resulted affiliated with the *Rhodocyclaceae* family and was closely related to the microorganism *Azospira oryzae* (band 11) (99% ID), previously reported to occur as endophyte of rice roots and have a strictly respiratory metabolism with oxygen or nitrate as terminal electron acceptors (Reinhold-Hurek *et al.* 2000). Moreover, microorganisms of the genus *Azospira* (*A. oryzae* and *A. restricta*) were found to be capable of dissimilatory perchlorate ( $\text{ClO}_4^-$ ) reduction (Tan *et al.* 2003; Oosterkamp *et al.* 2011) and were detected or isolated from a wide range of environmental ecosystems, including uncontaminated groundwater sampled from a well located up-gradient from an hazardous waste site in Louisiana, USA (Bae *et al.* 2007).

In the successive phase of molecular investigation, the microbial communities immobilized on the four types of carrier materials, at 30 and 15°C, were analysed at the end of the kinetic tests. The isolation of the metagenomic DNA of the immobilized communities was accomplished according to the procedure described in the section 3.2.4.1., in duplicate. In Figure 18 are compared all the DGGE profiles obtained from the immobilized consortia, along with the two suspended consortia (30°C II and 15°C II) utilized as inocula.

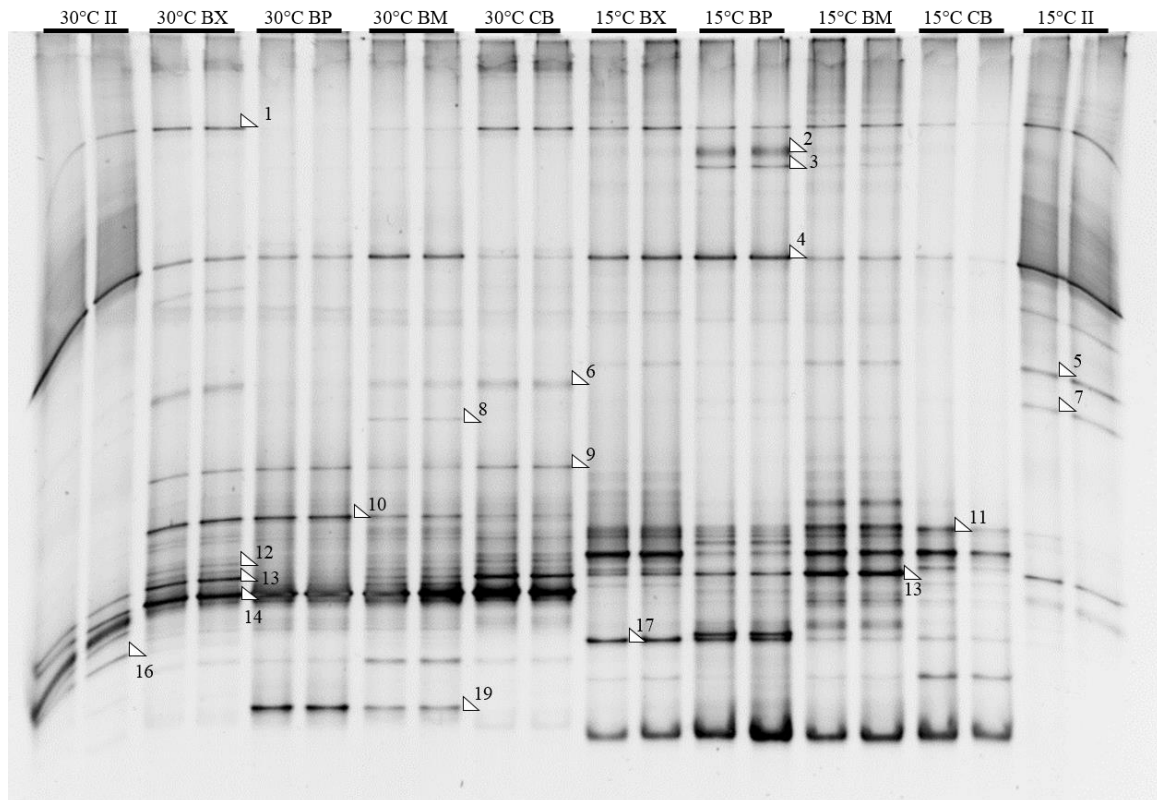


**Figure 18.** Comparison of the suspended and immobilized B4 consortia, at 30 and 15°C, subjected to the kinetic test. *30°C II* : suspended consortium *B4(I)* propagated at 30°C. *15°C II*: suspended consortium inoculated with the original *B4(I)* and grown at 15°C. All of the other lanes represent the *30°C II* or *15°C II* consortia immobilized on Biomax (BX), Biomech (BM), Biopearl (BP) and Cerambios (CM). The sequences phylogenetically identified are indicated by the white triangles and numbers and reported in Table 18 of Appendix.

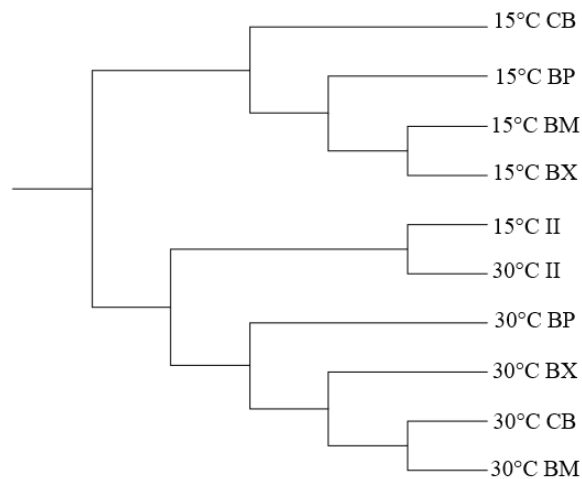


**Figure 19.** Clusterization of the DGGE profiles of the B4 consortia kinetically tested. Dendrogram based on the UPGAMA clustering algorithm, using QuantityOne 4.5.2 software (Bio-Rad).

The immobilized consortia resulted remarkably different from the suspended inocula. Percentage indexes ranging between 17.8% and 42% expressed the low similarity of the suspended culture *30°C II* with the respective immobilized communities; very similar values (between 7.2% and 38.4%) were obtained by comparing the 15°C suspended and immobilized consortia. Hence, the immobilization on porous materials strongly affected the community's structure and composition.

Conversely, as shown in Figure 19, the immobilized consortia clustered together according to their temperature. For instance, the similarity values calculated between the Biomax-immobilized community and those immobilized on Biomech, Biopearl and Cerambios were respectively 73%, 57% and 73.3% at 30°C, or 63.5%, 56.4% and 51.4% at 15°C. Such a results highlighted that different types of porous supporting material (at least those ones tested in this study) did not significantly favour the selective adhesion of certain species over others and the community structure was maintained among consortia immobilized at the same temperature.

Despite the switch of temperature from 30 to 15°C seemed to have only a marginal effect on the suspended consortium B4, as previously discussed, remarkable changes in the immobilized community structures and compositions were observed at different temperatures. The similarity between consortia immobilized on the same type of carrier material at 30°C and at 15°C resulted very low; in particular, such similarity was 36% for Biomax, 27.3% for Biomech, 19.4% for Biopearl, 7.5% for Cerambios. These results evidenced that changes of the operative temperature significantly promoted the prevalence of different phylotypes of the immobilized microbial communities.

The microbial community composition was determined for the bands indicated by white triangles and numbers in Figures 17 and 18 and are reported in Table 18 in Appendix. Several phylotypes occurring in the initial suspended consortium *B4(I)* (Figure 17), and barely or not detected in the cultures propagated at 30 and 15°C, were enriched again among the immobilized communities, at 30 or 15°C (bands 5, 6, 8, 11, 12). Furthermore, while the suspended consortia conducted at 30 and 15°C were mainly represented by microorganisms affiliated with Bacteroidetes and Firmicutes, the dominant phylotypes detected throughout the immobilized consortia belonged to Proteobacteria, with a prevalence of Betaproteobacteria. Among the latter were some new phylotypes, such as the band 8 and 12. The phylotype 8 seemed to be enriched only in the presence of Biomech and was related to *Cupriavidus necator* (100% ID), a microorganism famous for degrading several chloroaromatic compounds (Lykidis *et al.* 2010) and to have relevance in many different environmental processes. The band 12 was detected mainly in cultures at 30°C, although it was not possible to verify its occurrence also at 15°C. However, it related (100% ID) to a microorganism of the genus *Dechloromonas*, previously detected in a TCE-degrading aerobic bioreactor (Tresse *et al.* 2005).

With regard to the attached communities at 30°C, two phylotypes (bands 9-10) belonging to Firmicutes were related to a TCE-degrading *Bacillus* sp. (Dey *et al.* 2009). Other phylotypes prevailing at 30°C were the bands 6, 14 and 19. The band 14 was dominant through the immobilized consortia at 30°C, where its relative abundance was increased in the presence of Biomech and Cerambios. This phylotype related to *Georgfuchsia toluolica* G5G6, a Betaproteobacterium isolated from polluted environments able to grow anaerobically on toluene, ethylbenzene and some other

aromatic compounds, by using nitrate or ferric iron as electron acceptors (Weelink *et al.* 2009). Surprisingly this and other anaerobic species, such as those belonging to the genera *Zooglea* and *Dechloromonas*, were enriched in site of the aerobic treatment.

Concerning the 15°C attached communities, new bands, such as bands 2 and 3, were detected in the presence of Biopearl and Biomech communities. These phylotypes belonged to aerobic Bacteroidetes and band 3 was affiliated with microorganisms of the genus *Sphingobacterium*, which already detected in TeCA-degrading bioreactors (Frasconi *et al.* 2010). Other phylotypes specifically enriched at 15°C were represented by the band no. 5, 11, 17 and the lowest intense band appearing in the 15°C profiles in Figure 18. Band 17 was related to *Acidovorax* spp., which is a metabolically versatile strain, isolated from a broad variety of environmental sites (Choi *et al.* 2010). The bands 5 and 11 related to *Mucillaginibacter* spp. (99% ID) and *Azospira oryzae* (99% ID), respectively, and the latter was enriched exclusively in the immobilized form.

In conclusion, the molecular analysis showed that the biomass immobilization on solid supports determined the enrichment of different complex communities than in the suspended form. Furthermore, the temperature resulted a highly selective factor leading to the specific enrichment of different immobilized consortia at 30 or 15°C, although some ubiquitous phylotypes were detectable throughout the cultures, such as band no. 1, 4 and 13. Considering the molecular results in relation to the biodegradation activities on butane and TCE (Table 13), it was reasonable that the immobilized consortia at 30°C and 15°C behaved differently. Only the latter were able to maintain a TCE biodegradation activity comparable, or even higher, than the respective suspended culture at 15°C. This suggested that the temperature of 15°C was a key factor for the selective maintenance of the metabolic TCE-degrading capabilities, even among those microorganisms with a faster ability to colonize the carrier materials. At the same time, the immobilization at 30°C resulted in a remarkably increase of the butane degradation efficiency, e.g. up to ten times higher in case of Biopearl-consortium, while the TCE degradation was about ten times reduced. Probably, the 30°C temperature was less selective toward the TCE biodegradation and the microbial metabolism was preferentially utilized for the butane consumption. However, the microbial consortia selected at 30°C as well as those selected at 15°C were both characterized by the presence of several aerobic and anaerobic widespread environmental microorganisms with versatile metabolic capabilities and potentially involved in the AC biodegradation of TCE.

### **3.3.3. Process development in 1 L PBR**

The third stage of the study (objective (iii) of the research) was aimed at the evaluation of the reproducibility and repeatability of the AC process at 30°C driven by the selected butanotrophic consortium B4 when immobilized inside four 1 L PBRs packed with the four carrier materials (section 3.2.2.2.1. of materials and methods). At this stage, the process was conducted for a period of 100 days and its reliability was preliminarily evaluated, basing on the identification and further optimization of the operational parameters mainly affecting the process efficiency. With this regard, the process efficiency is strongly enhanced when a uniform growth of highly active microbial biomass occurs throughout the packed bed of the column. For this reason, a pulsed feeding of oxygen and butane was adopted, as described in section 3.2.2.2.2. of materials and methods. An alternating supply of carbon source and oxygen to activate the microbial metabolism would result in a more uniform distribution of the growth substrate through the packed bed, hence a more uniform microbial growth; furthermore, it would minimize the substrate competitive inhibition on CAH cometabolism. Of course, such conditions are attained if proper pulsation cycles (pulse frequency) are imposed to the system and equilibrated substrate or oxygen concentrations are fed per pulse. Thus, the specific objective of the presented study was to investigate whether the pulsed feeding strategy adopted during the conduction of the AC process in 1 L PBRs promoted a homogeneous TCE-degradation activity, growth and phylogenetic composition of the microbial biomass throughout the packed bed.

#### **3.3.3.1. Kinetic aspects of the microbial biomass enriched in 1 L PBRs**

Units of carrier material were retrieved from three different sections of each PBR at the end of conduction. The three sections indicated as lower, middle and upper were respectively representative of the inlet, the middle part and the outlet of each packed column, according to the flow direction. In order to evaluate the uniformity of TCE degradation activity and microbial growth at 30°C in each PBR, the carrier units were subjected to kinetic test, as described in section 3.2.2.1.2. (with the exception that TeCA degradation was not evaluated), while the immobilized biomass concentration was measured according to the procedure described in section 3.2.3.2.

Normalized TCE-biodegradation rates ( $r_i$ ) for the microbial biomass immobilized at the three sections of each PBR are reported in Table 15. The results showed that the TCE-degradation via AC process was achieved inside all of the PBRs; however, a slightly increased degradation occurred in the Biomax-packed PBR (average of  $0.19 \pm 0.06 \text{ d}^{-1}$ ). In addition, comparable TCE-biodegradation rates between the three sections were obtained for each PBR. The biomass growth (Table 16) could be considered uniformly spread along the full length of each PBR, despite a major growth was observed at the inlet of each PBR (lower section).

**Table 15.** Kinetic activity, in terms of TCE normalized biodegradation rate ( $r_i$ ), determined for the immobilized consortia of the lower, middle and upper sections of 1 L PBRs.

PBR	TCE normalized degradation rate ( $\text{day}^{-1}$ )			
	Lower section	Middle section	Upper section	Average
Biomax	$0.24 \pm 0.08$	$0.17 \pm 0.06$	$0.15 \pm 0.03$	$0.19 \pm 0.06$
Biomech	$0.17 \pm 0.05$	$0.15 \pm 0.05$	$0.11 \pm 0.04$	$0.14 \pm 0.04$
Biopearl	$0.12 \pm 0.06$	$0.14 \pm 0.03$	$0.09 \pm 0.06$	$0.14 \pm 0.05$
Cerambios	$0.16 \pm 0.04$	$0.13 \pm 0.07$	$0.14 \pm 0.04$	$0.11 \pm 0.05$

**Table 16.** Concentration of the microbial biomass immobilized per unit of carrier measured at the three sections of each 1 L PBR.

PBR	Biomass concentration ( $\text{mg}_{\text{protein}} \cdot \text{L}_{\text{bulk}}^{-1}$ )		
	Lower section	Middle section	Upper section
Biomax	$0.044 \pm 0.010$	$0.027 \pm 0.010$	$0.028 \pm 0.010$
Biomech	$0.073 \pm 0.023$	$0.043 \pm 0.023$	$0.025 \pm 0.023$
Biopearl	$0.015 \pm 0.002$	$0.004 \pm 0.002$	$0.006 \pm 0.002$
Cerambios	$0.009 \pm 0.003$	$0.002 \pm 0.003$	$0.002 \pm 0.003$

Under the kinetic point of view, the results suggested that the pulsed feeding strategy adopted successfully promoted homogeneous growth and TCE-biodegradation activity of the microbial communities immobilized throughout the length of the packed beds. Thus, this technique could be exploited and optimized for larger scale plants.

Although the selection of the most suitable immobilization material was based on the results from the batch tests, 1 L PBRs were useful to assess the process reliability in the presence of the four materials and to confirm that higher immobilized-biomass concentrations and activities were attainable in continuous-flow in the presence of Biomax, at least at 30 °C.

### 3.3.3.2. Molecular characterization of the enriched microbial communities

The homogeneity of the PBR systems was additionally verified in terms of structure and composition of the communities developed at the three sections of each PBR. Phylogenetic characterization of the communities was accomplished analysing the metagenomic 16S rRNA coding genes, by means of both PCR-DGGE and clone library construction approaches, as described in sections 3.2.4.2. and 3.2.4.3 of materials and methods.

Firstly, the community structure was investigated by PCR-DGGE analysis and the following Figure 9 shows the community band patterns embedded in duplicate on 40-60% denaturing gradient gels.

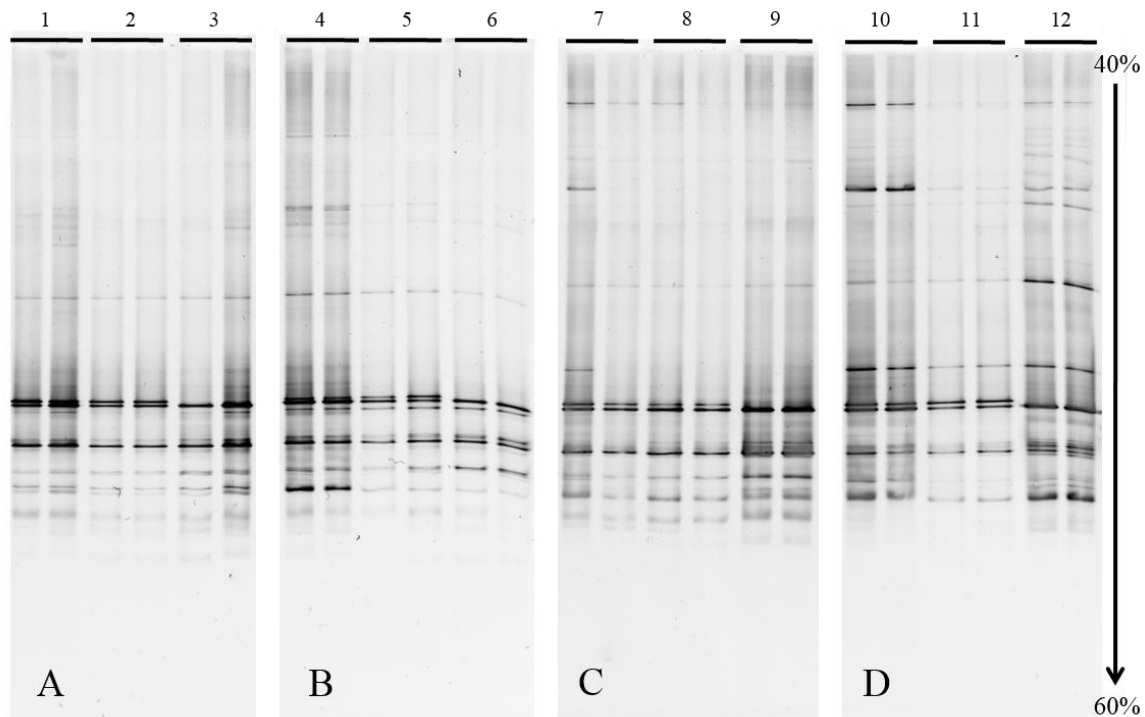


**Figure 20.** DGGE Profiles of microbial communities enriched during the conduction in 1 L PBR. Numbers indicate the attached communities occurring in the lower (lanes 1,4,7,10), medium (lanes 2,5,8,11) and upper (lanes 3,6,9,12) sections of the PBRs packed with Cerambios (gel A), Biomax (gel B), Biomech (gel C) and Biopearl (gel D). Denaturing gradient range: 40% - 60%.

All of the DGGE profiles shown in Figure 20 were compared in terms of percentage similarity indexes, based on the Dice coefficient (section 3.2.4.2.2. materials and methods). The similarity values between immobilized communities of different PBRs considered in pairs were in the range of 70.9 - 78.7% for Biomax and Cerambios, 81.4 - 84.5% for Biomax and Biomech, 50.6 - 72.9% for Biomax and Biopearl, 53.7 - 65% for Biomech and Biopearl, 70 - 71.9% for Biomech and Cerambios and 41.5 - 69.8% by comparing Biopearl and Cerambios. Thus, the analysis revealed a high homogeneity between the consortia developed inside the four PBRs, where the most similar communities were those immobilized on Biomax and Biomech. This indicated that the type of carrier material did not determine a selective adhesion of certain microorganisms over others, as it was already evidenced by the molecular analysis on immobilized communities in batch microcosms.

With respect to the three section of each PBR, the microbial community structure resulted highly conserved throughout the length of each column. The similarity percentages obtained by comparing community profiles from the lower, medium and upper sections ranged between 61.1% - 76.0% on Cerambios, 61.1% - 75.3% on Biomax, 72.9% - 86.6% on Biomech, 62.4% - 67.5% on Biopearl. The highest average value of similarity was obtained inside the Biomech-packed PBR,  $80.83 \pm 7.10$  %, while in the other cases the values were very comparable.

On the basis of these additional evidences concerning the community structure, it was demonstrated that the pulsed feeding of oxygen and butane produced a homogeneous growth and activity of the microbial biomass throughout each PBR column, regardless of the type of packing material.

The next stage of the investigation was aimed to characterize the community phylogenetic diversity and infer which community members could be involved in the TCE mineralization via AC process. To this purpose, clone libraries of the metagenomic pool of 16S rRNA coding genes were constructed according to the procedure described in section 3.2.4.3. Such an approach brought some advantages, such as the opportunity to work with full length 16S rRNA gene and have this sequence available to further analyses (e.g. sequencing or DGGE). Since the PBR communities were very similar to each other, only one metagenomic sample was used as template DNA for the clone library preparation. In particular, it was selected the metagenomic DNA isolated from the microbial community of the lower section of the Biomax PBR (gel B, profile no. 4, Figure 20), because its DGGE profile was characterized by a band pattern representative of most of the bands occurring also in the other community profiles. A total number of 63 clones produced from the library were screened by means of DGGE as specified in section 3.2.4.3.2. of materials and methods. The DGGE denaturing gradient utilized was between 45% and 55%, in order to better resolve and identify as distinct OTUs those amplicons with a similar migration behaviour. All of the cloned fragments under screening were run through DGGE along with two reference samples. One was represented by the total community, the second one consisted of a reference band pattern of six cloned sequences with different migration behaviour (an example is provided in Figure 21).

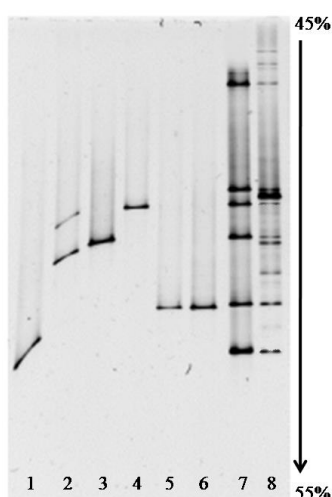


**Figure 21.** DGGE screening of some 16S rRNA gene cloned inserts and their identification as bands of the community profile, within a 45%-55% denaturant gradient. Lanes 1-6: 550 bp DNA portions amplified from some of the cloned inserts. Lane 7: reference band pattern. Lane 8: DGGE profile of the total Biomax community.

The library screening by means of DGGE led to the individuation of 14 different operational taxonomic units (OTUs), whose corresponding plasmid inserts were sequenced on both strands (procedure described in section 3.2.4.3.2.). The sequencing analysis revealed the phylogenetic identity of each OTU (Table 19, Appendix), which was properly assigned to each band of the original total community profile (Figure 22). Despite only 63 library clones were screened, it seemed that the clone library was sampled sufficiently to identify the majority of phylotypes visible among the DGGE profiles. In Figure 23, the cumulative number of unique OTUs is plotted against the cumulative number of screened clones, where an apparent asymptote suggests that the library encompasses almost the full extent of OTU richness in the microbial community.

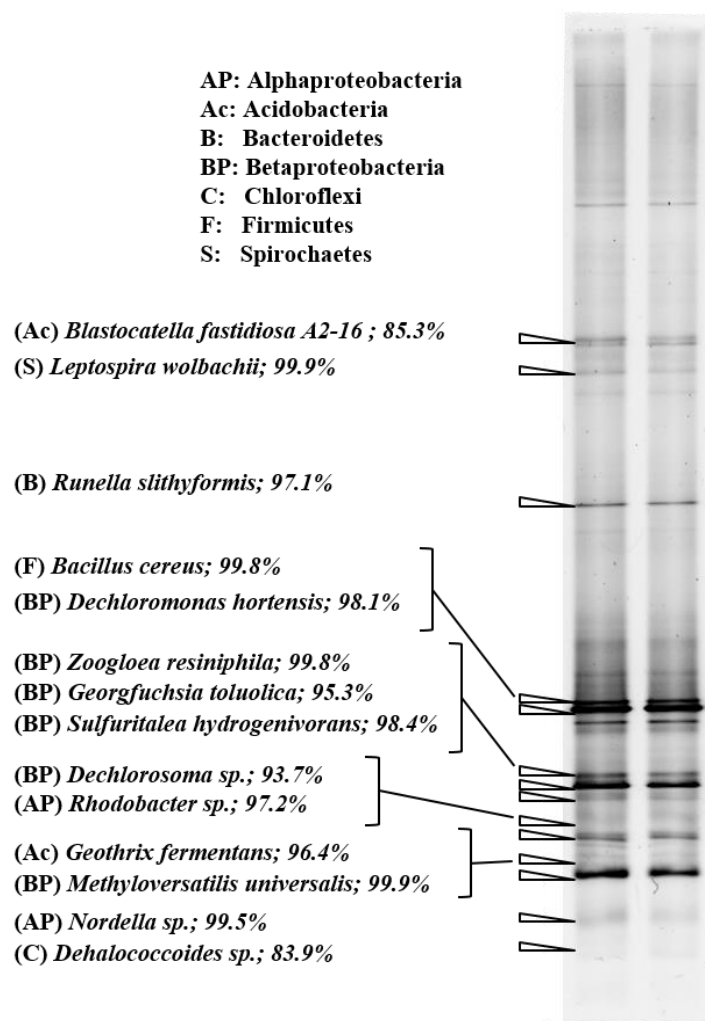


**Figure 22.** Outcome of the association between the sequences analysed from the Biomax attached community and the bands occurring into the DGGE profile.

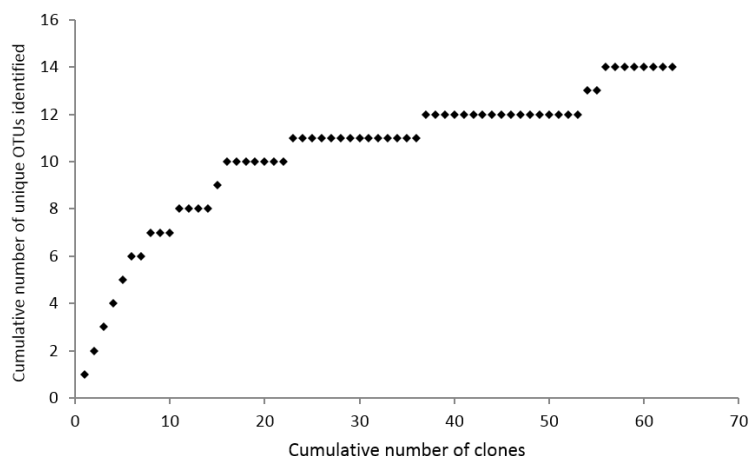


**Figure 23.** Cumulative number of identified OTUs plotted against the cumulative number of screened clones.

Biomax microbial community was characterized by a prevalence of members of Betaproteobacteria and Alphaproteobacteria, similarly to the microbial community immobilized on Biomax during the batch tests in microcosm at 30°C. Moreover, some identified microorganisms were common to both of the communities immobilized on Biomax in microcosm and in PBR at 30°C. Among them there were microbial species belonging to the family of *Rhodocyclaceae* and closely related to *Zooglea resiniphila* and *Georgfuchsia toluolica*, a strictly anaerobic bacterium firstly isolated from polluted aquifer (Weelink *et al.* 2009). Other members of this family were detected only in the PBR immobilized B4 consortium and related to *Methyloversatilis* sp., whose members are ubiquitous in the environment and known to possess metabolic abilities to grow on C<sub>1</sub> compounds and degrade halogenated compounds (Kalyuzhnaya *et al.* 2006), or related to *Sulfuritalea hydrogenovorans*, firstly isolated from a freshwater lake showing high similarity (94.7%) of the 16S rRNA gene sequences with *Georgfuchsia toluolica* G5G6 (T) (Kojima *et al.* 2011). Another phylotype common to the PBR and microcosm's communities was affiliated with microorganisms of the genus *Dechloromonas*. Several studies in the last decade could link strains of the genus *Dechloromonas* to a perchlorate reducing activity occurring under anaerobic conditions (Logan *et al.* 2001).

The occurrence of a high number of anaerobic or facultative anaerobic microbial species suggested the occurrence of anoxic niches, despite the aerobic treatment with oxygen pulses. Probably, this phenomenon concerned the interstitial spaces between carrier units at the inlet of the Biomax packed bed. This would explain the occurrence of strictly anaerobes, for example belonging to the phylum Chloroflexi (OTU 1, Table 19 in Appendix). However, the most of the anaerobic microorganisms detected, was previously described in literature to be involved in catabolism of chlorinated compounds.

Nevertheless, several aerobic microorganisms were detected, mainly affiliated with Firmicutes and Bacteroidetes. In particular, a phylotype related to *Bacillus cereus* (OTU no. 16, Table 19 in

Appendix) was already detected in the B4 communities in batch and represented one of the dominant members of the Biomax-PBR B4 community (Figure 22). Species of the genus *Bacillus* were already reported as responsible for the degradation of TCE (Dey *et al.* 2009) or cDCE (Olaniran *et al.* 2008). The OTU no. 58 was closely related to an aquatic bacterium, *Runella slithyformis*, able to grow at low temperatures as low as 4°C, typical of some groundwater sites, and able to utilize hydrocarbons as carbon source (Copeland *et al.* 2012).

In conclusion, the analysis of the phylogenetic diversity of the microbial community immobilized on Biomax at the inlet (lower part) of the PBR, at 30°C, revealed the occurrence of several microbial species already detected in the microbial community immobilized on Biomax in batch at the same temperature. This was an interesting evidence indicating that the process conditions promoted the enrichment of similar dominant microorganisms of the community, in spite of the fact that the microbial suspended consortium B4 utilized to inoculate the tests was maintained for different periods of time.

### **3.3.3.3. Identification of monooxygenase encoding genes**

An additional molecular investigation of the immobilized microbial community enriched in the Biomax-PBR concerned its functional diversity. In particular, the occurrence of genes coding for the most known oxygenases with a putative role in the degradation of CAHs was assessed.

Such a research of functional genes was carried out by means of PCR reactions in the presence of different primer sets properly selected from the literature in order to amplify possible genes coding for the following classes of enzymes: soluble di-iron monooxygenase (SDIMO), membrane alkane hydroxylase (AlkB), methane monooxygenases (pMOA and sMMO), P450 alkane hydroxylase (CYP153). The literature reference for each set of highly degenerated primers and the amplification conditions are indicated in section 3.2.4.3.1. of materials and methods.

The PCR screening revealed that only by utilizing the *alkB-1f/alkB-1r* primer pair a clear amplification product of the expected size, 550 bp, was observed (Figure 24).

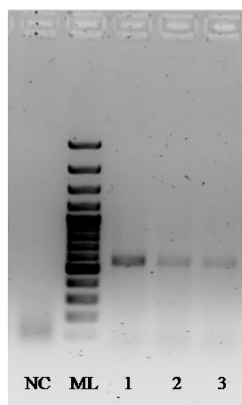


**Figure 24.** alkB amplification products obtained by utilizing three different metagenomic DNA as template: 1) immobilized community at the inlet of Biomax-PBR; 2) community at the middle section of Biomax-PBR; 3) community at the outlet section of Biomax-PBR. NC: negative control.

Subsequently, the amplification product obtained from the microbial community immobilized at the inlet of the PBR packed with Biomax (lane 1, Figure 24) was utilized to prepare a clone library of the community's alkB genes. After the functional library screening, according to the procedure described in section 3.2.4.3.2., a low number of plasmids, only ten, were found to contain the insert. However, inserts of two sizes were detected among the successful clones: a heavier fragment long about 560 bp and a lighter one long about 410 bp. These cloned genes were sequenced.

All of the heavier cloned fragments corresponded to a unique sequence, which resulted 80% similar to a portion of an Ingol Alkane Rubredoxin-dependent monooxygenase (alkB) gene (GU184254.1), by alignment with the NCBI BLASTn tool. Such a sequence was firstly identified from an uncultured bacterium plasmid clone (Schulz *et al.* 2010). A further search in the database by utilizing the NCBI BLASTx tool showed that the same nucleotide sequence was related to an alkane rubredoxin-dependent monooxygenase (ACZ64702.1) (identity of 80%), of an uncultured bacterium (Schulz *et al.* 2010). This sequence was found to be also close to other alkane1 monooxygenase enzymes, occurring in *Runella slithyformis* DSM 19594 (AEI47814.1) (identity 62%), *Fulvivirga imtechensis* (WP\_009581984.1) (identity 74%), or to an alkanal monooxygenase occurring in *Emticicia oligotrophica* (WP\_015028864.1). At the same time, the lighter insert nucleotide sequence was found to have a similarity of 89% with *Mycobacterium rhodesiae* NBB3 (CP003169.1) sequence, coding for an integral membrane protein.

### 3.3.4. Scale up of the process: 31 L pilot plant

The last stage of the study in the framework of the MINOTAURUS project focused on the scale up of the PBR system at a medium-scale pilot plant for the establishment and optimization of the AC process for the treatment of CAH-contaminated groundwater. Naturally, the process development relied on the utilization of the selected butanotrophic consortium B4, the Biomax immobilization material and the adoption of a pulsed feeding strategy to supply oxygen and butane to the system. The 31 L pilot plant was operative for 220 days, under 9 different operational conditions (details of the operational conditions of each phase are specified in section 3.2.2.3.2.) imposed in order to gradually change and/or optimize the main process parameters.

Particular attention was paid to the optimization of the pulsed feeding in terms of frequency, length and concentration of the butane pulses per each feeding cycle. With this regard, it is worth mentioning how the gradual optimization of the pulsed feeding strategy related to changes of the overall TCE biodegradation activity among the different operational phases.

Studies conducted at the laboratories of dr. Frascari and Professor Pinelli during the first four operational phases of the 31 L PBR led to utilize a pulsed feeding cycle characterized by short HRT (4.1 d) and high ratio (15%) of the butane pulse duration over the total cycle length. In these conditions a remarkable improvement of the TCE degradation activity was observed in comparison to the early stages of the process development and the normalized biodegradation rate ( $r_{i,TCE}$ ) was equal to 0.15 days<sup>-1</sup>. However, the highest values of TCE biodegradation rates were attained in the following operational phases (phases 5 – 7), when the pulsed feeding cycle was further optimized in order to minimize phenomena of substrate inhibition on TCE biodegradation. The optimized feeding strategy consisted of a cycle of 9 days characterized by two distinct phases: a growth phase of 3 days, where alternate pulses of butane and oxygen were supplied to the system, and a biodegradation phase of 6 days, where only oxygen and CAHs were fed. Figures 25 and 26 provide an example of the butane, oxygen and CAH concentration profiles along the total length of the 31 L PBR respectively during the growth phase and the biodegradation phase. Such a feeding strategy allowed to obtain normalized TCE biodegradation rates of 0.22 – 0.23 d<sup>-1</sup>, when the process was operated at 30°C. During the last three operative phases (7 – 9), the process temperature was lowered from 30°C to 15°C (7<sup>th</sup> phase) determining a decrease of  $r_{i,TCE}$  to values of about 0.15 d<sup>-1</sup>. Nevertheless, a new increase of the TCE biodegradation activity was attained when the system was fed with the real site groundwater (8<sup>th</sup> phase), reaching values of 0.19 d<sup>-1</sup>.

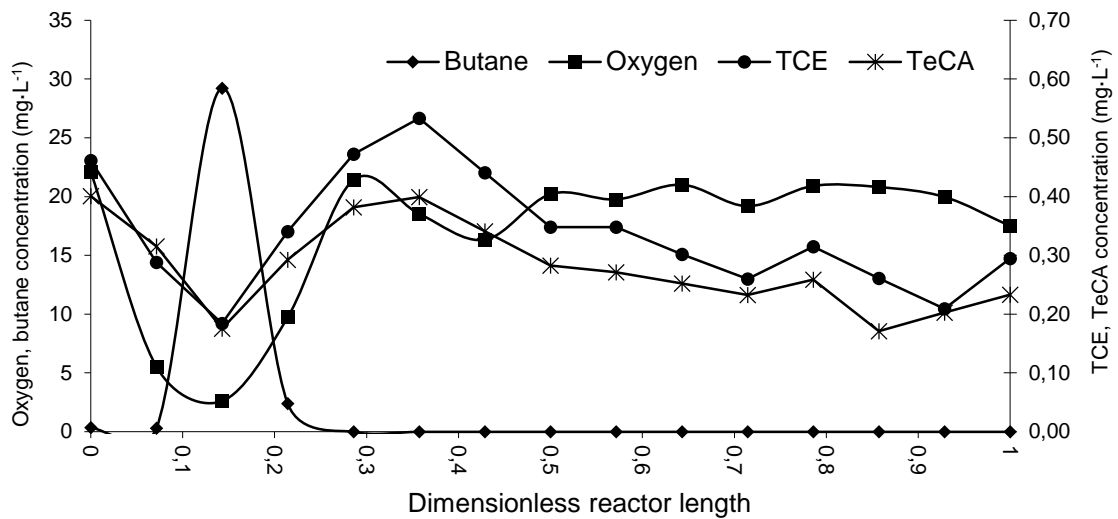


**Figure 25.** Concentration profiles of oxygen, butane and CAHs dissolved in the liquid phase throughout the 31 L PBR length during a typical growth phase. The figure shows the butane pulsation in the absence of oxygen and CAHs, while no degradation activity occurs in the remaining part of the system.

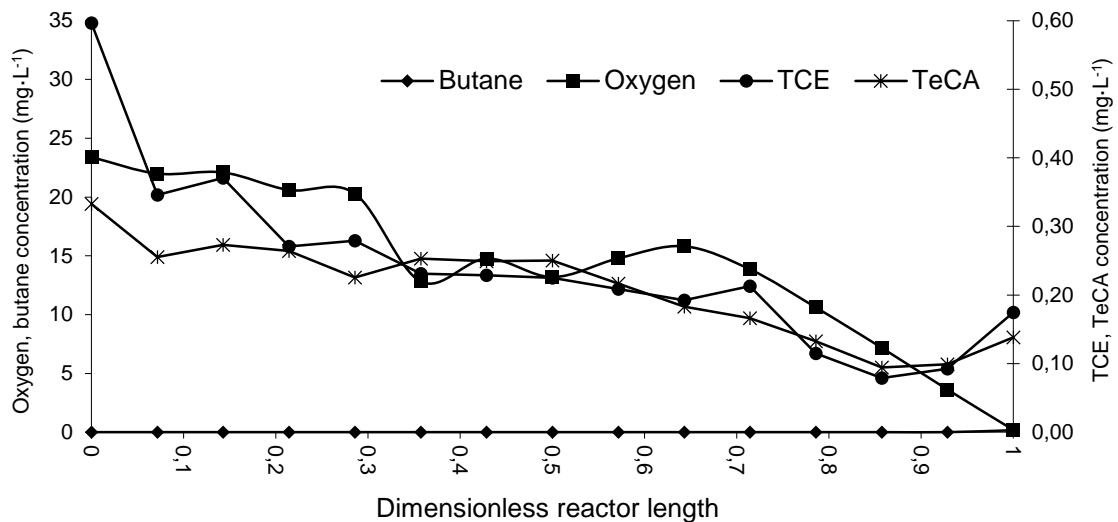


**Figure 26.** Concentration profiles of oxygen, butane and CAHs dissolved in the liquid phase throughout the 31 L PBR length during a typical biodegradation phase. The figure shows that in the absence of butane the oxygen and CAHs are gradually consumed through the 14 PBR columns.

This brief description of the results highlighted that the utilization and optimization of the pulsed feeding technique for the AC process development was crucial for an effective distribution and migration of the substrate pulse throughout the packed bed, with a consequent better distribution of the microbial biomass growth. Furthermore, the TCE biodegradation rate increase indicated an effective minimization of inhibition phenomena, due to the occurrence of bioreactive zones with low substrate concentration. However, the briefly discussed aspects referred to the overall process efficiency through the sequential operational phases. The next paragraphs provide detailed information about the kinetic activity of the microbial biomass enriched at the end of conduction at the inlet of each PBR-column and the microbial community structure and composition at the same 14 inlet sections.

### 3.3.4.1. Kinetic aspects and discussion of the 31 L PBR

At the end of the conduction, the butane and CAH biodegradation activity of the microbial communities enriched at the inlet section of each column of the 31 L pilot plant was assessed by means of standardized kinetic tests, as described in section 3.2.2.3.2. of materials and methods. Since the last operational phase (9<sup>th</sup> phase) of the process was conducted at 15°C, the kinetic test was evaluated at the same temperature. The performances of the microbial biomass were then evaluated in relation to the amount of biomass per gram of carrier at the 14 columns' inlet, determined according to the procedure described in section 3.2.3.2. and the values are reported in the Table 17.

**Table 17.** Microbial biomass concentration at the inlet of each column

Column inlet #	Biomass concentration $\text{mg}_{\text{protein}} \cdot \text{L}_{\text{bulk}}^{-1}$	Column inlet #	Biomass concentration $\text{mg}_{\text{protein}} \cdot \text{L}_{\text{bulk}}^{-1}$
1	0.219	8	0.016
2	0.085	9	0.077
3	0.114	10	0.108
4	0.018	11	0.145
5	0.018	12	0.167
6	0.044	13	0.095
7	0.010	14	0.054

Higher microbial biomass concentrations were measured at the inlet of the first three columns and the last six ones, while lower concentrations, about 5-6 times less, occurred in the central part of the system (columns 4-8).

Histograms of Figures 27 and 28 show the trends of the normalized initial biodegradation rates ( $r_{i,15^\circ\text{C}}$ ) and the first order kinetic constants ( $k_{1,1,15^\circ\text{C}}$ ) for butane and TCE. The evaluation of the former process parameter revealed variable butane degradation rates along the 31 L plant. Higher rates occurred through the inlets of the first five columns (values ranging between 24.8 and 41.6 day<sup>-1</sup>), while values lower than 17.4 d<sup>-1</sup> for all of the other sections, with the exception of inlets 10 and 12 (31.4 and 38.5 d<sup>-1</sup>, respectively). Conversely, the TCE biodegradation process at the 14 inlets was characterized by comparable values of  $r_{i,15^\circ\text{C}}$ , with only a slightly increase of the average value (from  $0.090 \pm 0.013$  to  $0.113 \pm 0.007$ ) at the last six inlets (9 – 14). However, the evaluation of the first order kinetic constants ( $k_{1,1,15^\circ\text{C}}$ ) produced different results (Figure 27 and 28, lower histograms) based on the measure microbial biomass concentration (the description of the process parameters is given in section 3.2.2.1.2.).

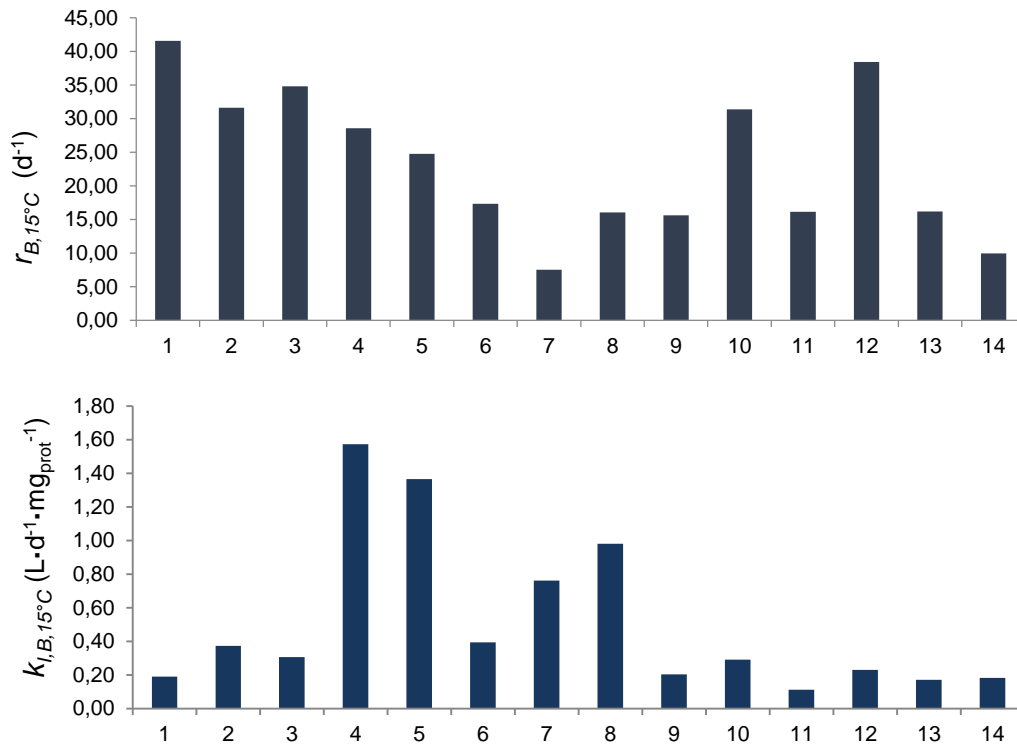


Figure 27. Biodegradation rate ( $r_{B,15^{\circ}C}$ ) and first order constant ( $k_{I,B,15^{\circ}C}$ ) referred to butane at the 14 inlets.

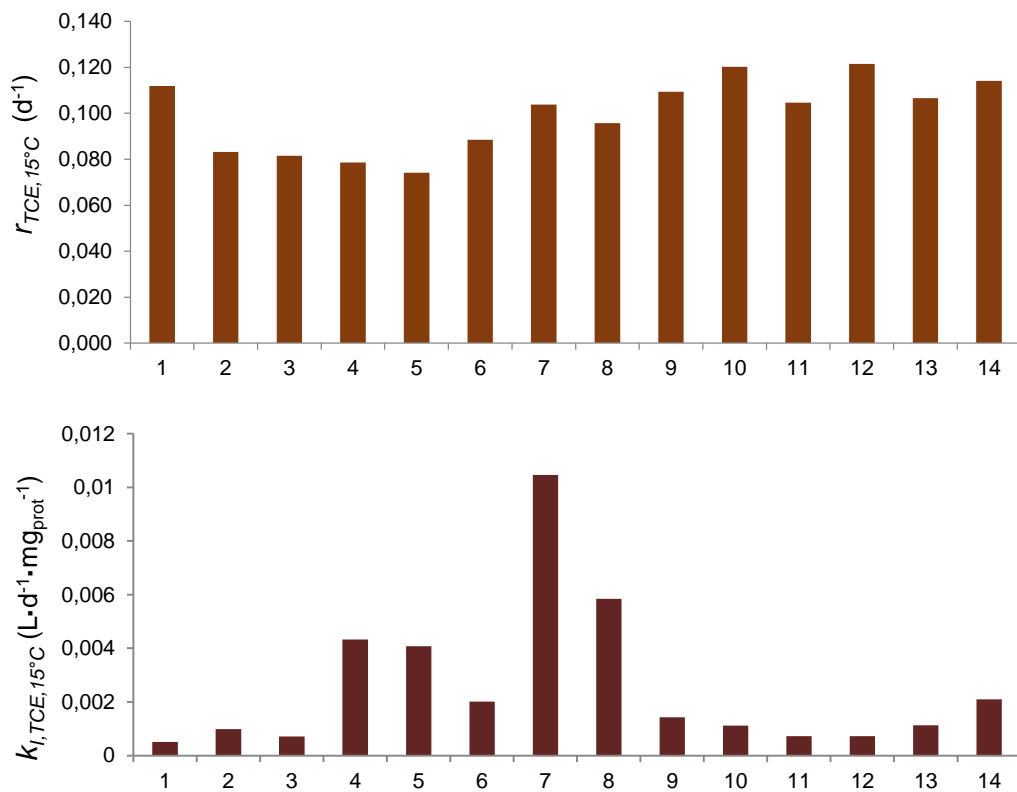


Figure 28. Biodegradation rate ( $r_{TCE,15^{\circ}C}$ ) and first order constant ( $k_{I,TCE,15^{\circ}C}$ ) referred to TCE at the 14 inlets.

Higher first order kinetic constants (ranging from 1.572 to 0.761  $\text{L}\cdot\text{d}^{-1}\cdot\text{mg}_{\text{protein}}^{-1}$ ) were observed for butane in columns 4, 5, 7 and 8, while values lower than 0.400  $\text{L}\cdot\text{d}^{-1}\cdot\text{mg}_{\text{protein}}^{-1}$  were obtained in all the other plant inlets. Similarly, the highest  $k_{I,TCE}$  values were observed in the middle columns of the system, 7 and 8 ( $10.5\cdot 10^{-3}$  and  $5.8\cdot 10^{-3}$   $\text{L}\cdot\text{d}^{-1}\cdot\text{mg}_{\text{protein}}^{-1}$ , respectively), and, to less extent, for the columns 4 and 5 ( $4.3\cdot 10^{-3}$  and  $4.1\cdot 10^{-3}$   $\text{L}\cdot\text{d}^{-1}\cdot\text{mg}_{\text{protein}}^{-1}$ ). The processes at all of the other inlets were characterized by  $k_{I,TCE}$  values between  $0.5\cdot 10^{-3}$  and  $2.1\cdot 10^{-3}$   $\text{L}\cdot\text{d}^{-1}\cdot\text{mg}_{\text{protein}}^{-1}$ .

The observed kinetic behaviour of the microbial biomass could be explained by a different availability of the growth substrate throughout the PBR length, as a consequence of diffusion and dispersion phenomena affecting the substrate pulse distribution and the extension of the bioreactive zone through the packed bed. In the first part of the system, the butane concentration is higher than in the remaining part, but the exposure time of the biomass to such high concentration is lower. Such a conditions might promote the growth of *r*-strategist microorganisms (Andrews *et al.* 1986), i.e., bacteria characterized by a high growth rate but a low substrate utilization efficiency. By moving along the PBR, the concentration of butane progressively decreases, while the exposure time of the microbial biofilm to the butane pulse increases, by virtue of dispersion and diffusion phenomena. In this scenario, the growth of *k*-strategist, i.e., microorganisms growing at lower rate but possessing a high substrate utilization efficiency, might be favoured along the reactor. This could partially explain why the microbial communities developed in the first three columns were characterized by lower first order kinetic constant values than those enriched in the central part of the reactor. With respect to the last six columns, it is reasonable to think that the effect of the pulsed feeding was minimized and process conditions much similar to a typical feeding in continuous mode were established. It is possible that the microbial community developed among this part of the PBR was not subjected to strong and/or cycling perturbations of the fed compounds, but rather exposed to more homogeneous and lower butane and oxygen concentrations over time. In this part of the system, probably, the enrichment of *k*-strategists was enhanced.

In addition, the thickness of the microbial biofilm developed on the carrier's surface could account for the low values of the first order kinetic constant observed when a major concentration of biomass occurred. It is possible that higher concentration of biomass per unit of carrier were due to an increased thickness of the biofilm, where the microbial cell access to the substrate, oxygen and chlorinated compounds was restricted to a superficial biofilm layer. Conversely, thinner biofilms, hence lower measured biomass concentrations, could be entirely involved in the biodegradation process, with performances similar to those of thick biofilms.

### 3.3.4.2. Molecular characterization of the enriched microbial communities

A molecular structure and composition characterization was performed on immobilized microbial communities developed at the inlet sections of the 2<sup>th</sup>, the 6<sup>th</sup> and the 12<sup>th</sup> columns after the PBR plant-colonization phase and from all of the inlet sections at the end of the conduction (after 220 days). In this way, disturbances due to the removal of the packing material during the reactor operation were avoided. For simplicity the inlet section of the column will be called just column. Such a molecular characterization was based on the V3-V5 variable regions of the 16S rRNA coding genes, according to the PCR-DGGE approach described in the section 3.2.4.2. In Figure 29 is shown the amount of metagenomic DNA retrieved from the same amount (weight) of carrier sampled at the 14 inlets at the two sampling times.

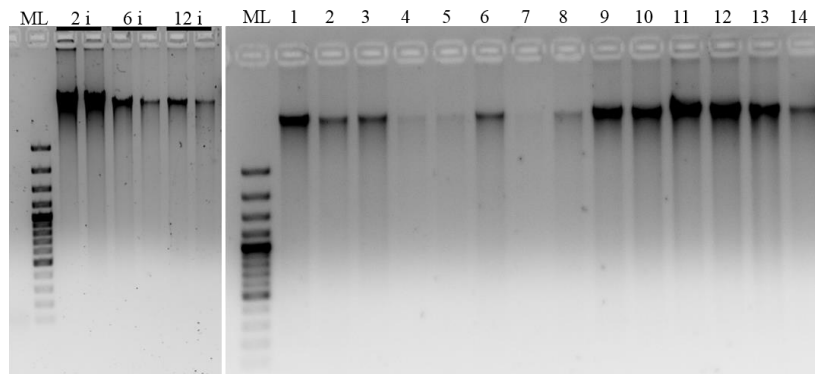


**Figure 29.** 1% Agarose gel of isolated metagenomic DNA samples. ML: 1kb DNA Ladder. 2i, 6i, 12i: intermediate time samples. 1-14: Inlet immobilized microbial community, at the end of conduction.

Remarkably lower amounts of DNA were obtained from the columns 4, 5, 7 and 8, probably confirming the minor extent of the microbial biomass growth in these columns previously observed in terms of protein concentrations.

The DGGE of the analysed microbial communities is represented in Figure 30. The corresponding dendrogram schematization (Figure 31) showed that the suspended consortium B4, utilized to inoculate the system, clustered like an outgroup, stemming from the base of the tree due to its very low similarity (values always lower than 60%) to all of the attached communities. Nevertheless, it seemed that its profile bands, in particular the two main phylotypes corresponding to the band numbers 10 and 13 (Figure 30), were prominently enriched also in the attached communities until the end of the experiment, hinting that they could be two strains crucially involved in the AC process. An additional feature of the dendrogram was that the communities enriched at intermediate times (2i, 6i, 12i) clustered together, with similarity values between 2i-6i and between 6i-12i communities of about 70%, while only a similarity of 50% was obtained for the 2i-12i pair. Such values could indicate that the process conditions imposed at the early operational phases were shaping and gradually homogenising the microbial community structure through the packed bed, but the

similarity between communities enriched inside columns located at the extremities of the system was still low.

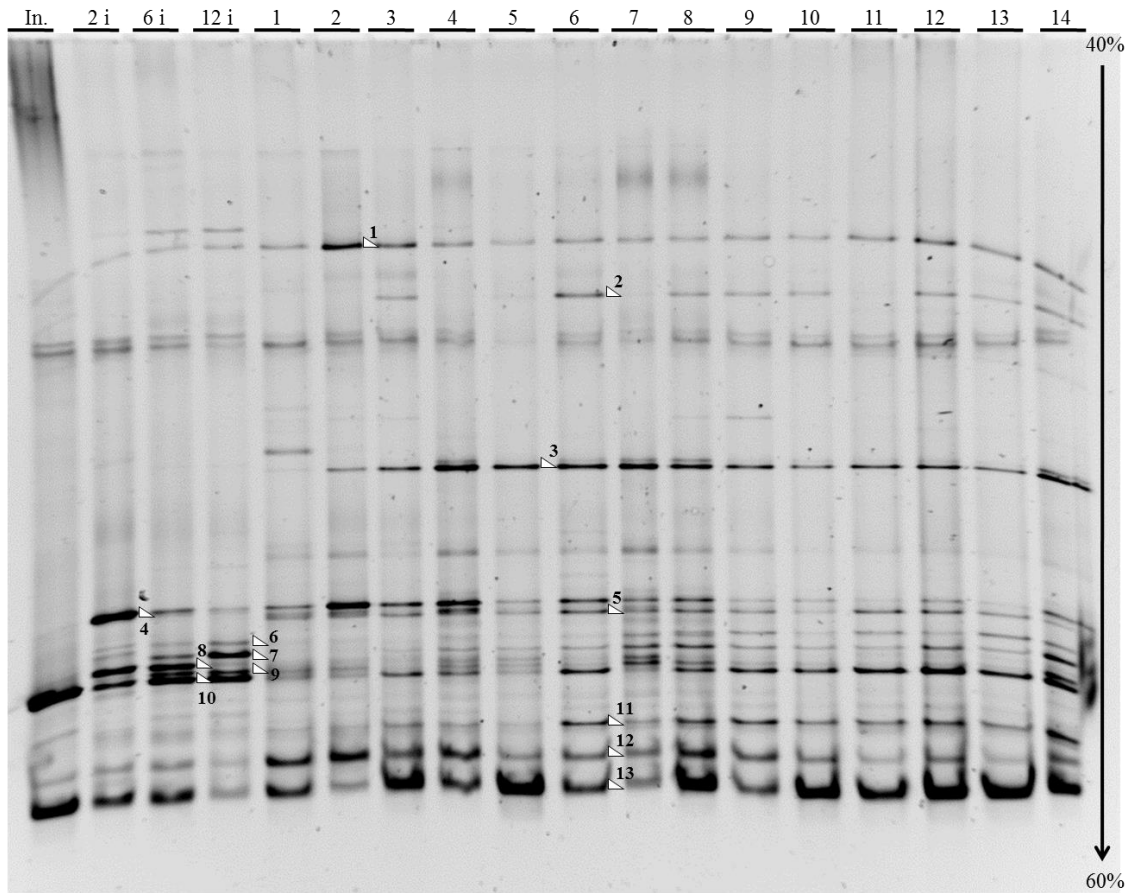


**Figure 30.** DGGE analysis of the 31 L pilot plant. In: suspended B4 consortium utilized to inoculate the bioreactor. 2i, 6i, 12i: intermediate sampling points. 1 to 14: final sampling times. All of the samples were referred to the attached biomass enriched at the inlet sections. Denaturant gradient range: 40% - 60%. Triangles and numbers indicate those bands that were successfully purified sequenced (Table 20 in Appendix).

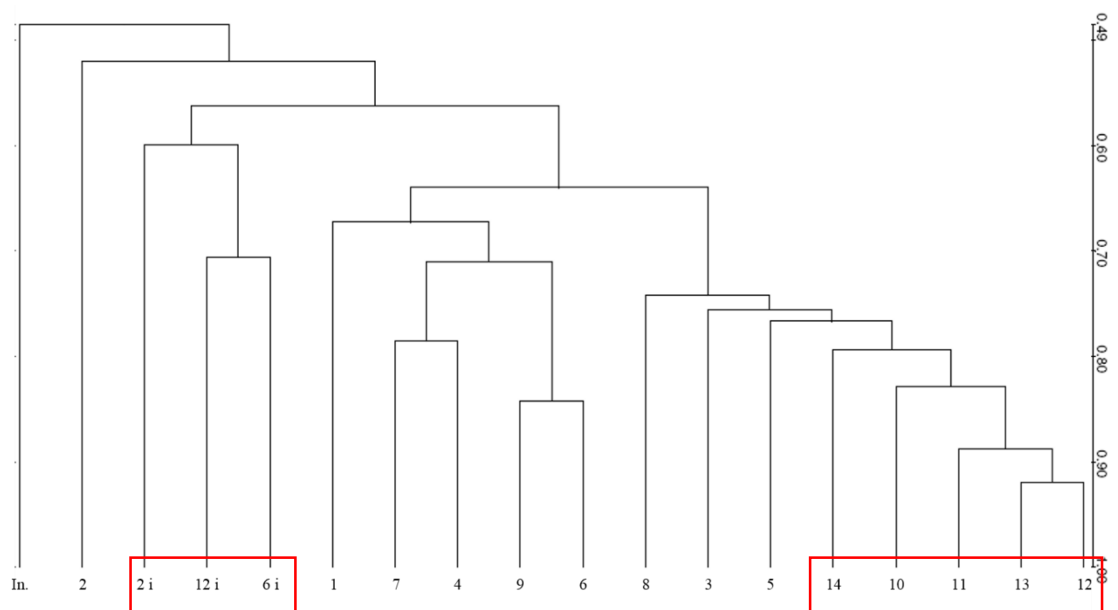


**Figure 31.** Community DGGE profiles dendrogram, based on the UPGAMA clustering algorithm. Red squares indicate similarity index  $\geq 70\%$ .

At the final operational phase of the conduction, the similarity indexes among the communities 1 to 9 were very variable in a range of similarity values ranging from 45% to 80%. For this reason it was not possible to establish a correlation between the sub-clustering groups and their location in the bioreactor system nor in relation to their kinetic performances evaluated for butane and TCE degradation.

Furthermore, the dendrogram showed a progressive clustering of the communities enriched among the columns 10 - 14, whose similarity indexes were comprised between 74% and 92%. It was interesting to notice the higher homogeneity of this portion (columns 10-14) of the 31 L PBR system in terms of molecular structure and composition and kinetic performance of the microbial communities (very comparable first order kinetic constant values). Such a homogeneity could indicate the attainment of a stabilization of the process in the last part of the packed bed. Moreover it could confirm the hypothesis that the communities of this portion of the system were subjected to more uniform and lower butane and oxygen concentrations over time.

In most of the cases, the high variability of similarity indexes between DGGE profiles was mainly determined by strong differences in the band intensities at same levels of the gel, rather than the appearance of new phylotypes. This means that the band patterns obtained among the different DGGE profiles were basically the same, but characterized by very different relative abundances of the occurring bands/phylotypes. Although the evaluation of the DGGE band intensity (relative abundance) is not a reliable way to quantify the abundance of microbial species in the sample, it could be reasonable that such a variability of the phylotypes detected among columns 1 to 7 could indicate the ability of these communities to deal with more frequent changes in the fed oxygen, butane and CAH composition than it happened in the columns 8 to 14. In particular, the dynamic change in the band intensities among columns 1-7 in opposition to the balanced intensification of the occurring phylotypes among the columns 8-14 could support the hypothesis, already proposed in the conclusions of the previous section, that the species enriched in the first portion of the 31 L PBR were characterized by *r*-strategists, while a prevalence of *k*-strategists characterized the second portion.

A further consideration concerns variations in the similarity between microbial communities determined among columns 1-7. In this portion of the plant, the structure of the communities of columns 1-3 was significantly more variable than in the columns 4-7. Such a high variability, despite the long enrichment period, was probably due to stronger changes in the composition of the fed compounds, by virtue of the pulsed feeding strategy. Thus, at the beginning of the PBR the microbial community was cyclically subjected to high concentrated butane pulses and phases of total lack of substrate. Here, the butane pulse was still shaped as a peak, an example is provided in Figure 25, while progressively flattened by dispersion and diffusion phenomena by its shifting through the

packed bed. Once again, such non constant conditions strongly promote the enrichment of r-strategist microorganisms. It was interesting to notice the prominent occurrence of some major phylotypes (4 and 12) only in the communities of the first three inlet sections.

The sequencing analysis results, reported in Table 20 in Appendix, were an aid to elucidate the potential role of the microbial species identified in the AC biodegradation process both at the first and last portions of the 31 L PBR.

Interestingly, the two most ubiquitous bands, 1 and 13, were found to have a 100% correspondence with the microorganism *Rhodococcus aetherivorans* 10bc312, firstly isolated from enrichment cultures of a petrochemical biotreater sludge and able to biodegrade metil-t-butyl etere (MTBE) (Goodfellow *et al.* 2004). The genus *Rhodococcus* encompasses a wide diversity of bacteria possessing different types of mono- and di-oxygenase enzymes, which incredibly broaden the range of organic compounds utilized as substrate (Larkin *et al.* 2005); moreover, the strain 10bc312 was found to be closely related to the *Rhodococcus aetherivorans* BCP1 previously utilized for the aerobic cometabolic degradation of chloroform by utilizing butane as primary growth substrate (Frasconi *et al.* 2006). Such evidences hint that the AC process developed inside the 31L PBR could rely on this strain.

Phylotypes number 4 and 10 were mostly detected among the communities sampled at the early phase of conduction (2i, 6i and 12i). The band 4 was affiliated with Bacteroidetes and shared a 92.4% identity with *Ohtaekwangia koreensis* 3B-2, a strictly aerobic bacterium growing at 30°C as optimum, but also at lower temperatures till 10°C, firstly isolated from marine sand (Yoon *et al.* 2011). This phylotype prevailed also within the first portion (columns 1, 2, 3 and 4) of the plant at the final sampling times; while it was still visible in the profiles 5 to 8. The phylotype 10 was related to an aerobic microorganism of the genus *Acidovorax* (99.8% identity). Microorganisms of *Acidovorax* spp. are widespread in the environment and have been isolated mainly from soil and water habitats (Choi *et al.* 2010). The phylotype 10 appeared to be dominant in the suspended inoculum and through the community profiles obtained for the communities of the columns 6 - 14.

Among the main phylotypes occurring in the first four columns of the system at the final sampling time was the band 12 (along with the already mentioned phylotype 4). This phylotype belonged to the phylum Chloroflexi, whose members were already detected in the previously analysed 1 L PBR communities.

The middle portion of the plant (columns 4 – 7), at the end of the process, was characterized by the intensification of the bands number 3 and 5, respectively related to *Massilia timonae* (99.8% identity) and *Devosia insulae* (100% identity). The latter is an aerobic bacterium belonging to the order *Rhizobiales*. *Devosia* spp. have been previously isolated from diesel-contaminated soil (Ryu *et*

*al.* 2008), or from hexachlorocyclohexane-contaminated site (Kumar *et al.* 2008). The genus *Massilia* encompasses strictly aerobic microbial species affiliated with the family of *Oxalobacteraceae*, and relates to environmental microorganisms such as *Duganella zoogloeoides* and *Telluria mixta* (La Scola *et al.* 1998).

Finally, the phylotypes number 2, 6, 7, 10 and 11 were mainly enriched within the last portion of the 31 L PBR (columns 8 – 14). The former was related to *Owenweeksia hongkongensis* DSM17368, an aerobic orange-pigmented belonging to the phylum of Bacteroidetes (Riedel *et al.* 2012). Among the latter four phylotypes, the number 10, a member of the genus *Acidovorax*, was already detected in the communities 2i, 6i and 12i (Figure 30). In addition, the band no. 7 related to the strictly aerobic microorganism *Comamonas testosteroni*, an environmental widespread and metabolically versatile species, with known abilities to biodegrade several organic pollutants (Ma *et al.* 2009). For instance, some strains express biphenyl dioxygenase enzymes that are involved in catabolic pathway of biphenyl/chlorobiphenyl compounds (Francova *et al.* 2004). Finally, the phylotype 11 resulted closely related (99.7% identity) to the microorganism *Rhizobacter fulvus* Gsoil322, an aerobic Gammaproteobacterium firstly isolated from soil of a ginseng field (Yoon *et al.* 2007).

In conclusion, the evaluation of the microbial species detected in the 31 L pilot plant should take into account some operational factors that introduced a significant variation of the community composition compared to those one of the cultures developed at earlier stages of this study. Firstly, the microbial community enriched through the 14 packed columns was subjected to sequential operational phases characterized by changes in the pulsed feeding technique (gradually optimized) and a switch of the temperature, from 30 to 15°C during the 7<sup>th</sup> phase. A second factor was that the suspended consortium B4 utilized as inoculum of the plant was actually very different from the initial cultures *B4(I)* and *B4-30°C II*, due to gradual changes in its community composition observed during the maintenance at 30°C (procedure details in section 3.2.2.1.3.). However, the utilization of complex microbial communities enriched from environmental sites implicates such a changes in their composition. Furthermore, the B4 consortium was sub-cultured under strictly selective pressure conditions, favouring the survival of microorganisms with the ability to tolerate or aerobically cometabolize CAHs; hence, changes in the microbial consortium composition were considered advantageous.

Despite noticeable differences between the 31 L PBR microbial community and the communities characterized during the previous stages (ii) and (iii) of this study, the occurrence of some phylotypes common to them was observed. In particular, these were microorganisms related to the genera *Zooglea* and *Acidovorax*, or species belonging to the phylum of Chloroflexi.

Differently from what was observed in the previous communities immobilized at 30°C (batch microcosms and 1 L PBR), a prevalence of aerobic microorganisms was detected, suggesting a better distribution and utilization of the oxygen throughout the PBR.

The molecular analysis showed a high homogeneity of the community structure throughout the packed bed of the 31 L pilot plant, but different functional organization of the microbial community were observed within three main portions of the plant: the first three columns, from column 4 to 7, and the last 7 columns (8 – 14). The prevalence of different phylotypes for each of the three portions suggests a correlation between the microorganisms specifically enriched and the biodegradation activity of the same communities tested against butane and TCE (discussed in the previous section). Thus, phylotypes related to the genera *Comamonas*, *Acidovorax* and *Rhizobacter* could play a role as *k*-strategists in the AC process in the columns 8 – 14. On the other hand, microbial species affiliated with the genera *Massilia*, *Devosia*, *Ohtaekwangia*, or belonging to the phylum Chloroflexi would play a role as *r*-strategists at the first portion of the 31 L PBR. In addition, the ubiquitous species *Rhodococcus aetherivorans* was probably one of the main microorganisms responsible for the butane consumption and CAHs mineralization throughout the pilot plant.

### 3.4. Conclusions

The occurrence of a high number of CAH-contaminated aquifers is of public concern due to the highly toxic effects of such pollutants to the human health. Furthermore, their recalcitrant nature and persistence in the shallow portion of aquifers as DNAPLs is the main reason why local authorities require the implementation of hydraulic barriers. In this scenario, the on-site utilization of PBR systems based on the activity of an immobilized microbial biomass for the aerobic cometabolic (AC) treatment of contaminated groundwater represents one of the best bioremediation technologies. Therefore, the objectives of this work was to design, develop and optimize such a process for the groundwater bioremediation. The specific objectives of my investigation were to characterize the phylogenetic and functional diversity of microbial communities developed through the procedural stages of the AC process development and its scale up from tests in batch microcosms to 31 L PBR pilot plant. Four specific objectives were fulfilled:

- (i) *Selection of the best contaminated groundwater sample and the more suitable growth substrate to enrich a suspended-cell microbial consortium for an effective degradation of CAHs at 30°C.*

The molecular characterization of environmental microbial communities from five groundwater samples revealed that their cultivation in the presence of four different

growth substrates did not relate to the selective enrichment of specific microorganisms. Thus, the selection of the most performant microbial consortium relied on the kinetic evaluation of substrate and CAH degradation. A butanotrophic consortium (named B4) was finally selected.

- (ii) *Selection of the most suitable carrier material supporting the immobilization of the microbial consortium selected at (i) and evaluation of the CAH-degradation process both at 30 and 15°C.*

This study revealed that the immobilization on the tested types of immobilization supporting material did not affect structure and composition of the immobilized B4 communities. However it determined different kinetic behaviours with respect to butane and TCE biodegradation, probably explained by the thickness of the microbial biofilm developed on the carrier surfaces. At the same time, it was found that the immobilization of the microbial consortium B4 was strongly affected by the working temperature (30 or 15°C). The microbial communities developed at 30°C were characterized by a prevalence of phylotypes belonging to the classes of Betaproteobacteria and Alphaproteobacteria, mainly represented by the genera *Zooglea* and *Georgfuchsia*, and a minority of Bacteroidetes (*Bacillus* spp.). Conversely, a majority of Bacteroidetes and Firmicutes accounted for the phylogenetic diversity of the immobilized communities at 15°C, such as the genera *Sphingobacterium*, *Sediminibacterium* and *Terrimonas*, but some dominant phylotypes were also affiliated with Betaproteobacteria (*Azospira* spp. and *Acidovorax* spp.). Despite the aerobic treatment of these batch cultures, it was interesting to detect several anaerobes (e.g. belonging to Chloroflexi), with particular occurrence in the 30°C communities.

- (iii) *Establishment of the AC process driven from the immobilized consortium inside continuous-flow 1 L PBR at 30°C; preliminary assessment of the process reliability when a pulsed feeding of oxygen and substrate was adopted.*

During this stage of the study, the molecular characterization of microbial communities gained an additional objective: to verify the community composition homogeneity through long packed beds (60 cm), such as those of the 1 L PBR. The analysis confirmed the uniform microbial growth and composition along the system, in total agreement with the kinetic results indicating uniform biodegradation activity. Here, the microbial communities immobilized at 30°C were characterized by the occurrence of several microbial species already detected in the batch communities, along with some new ones

that resulted to possess the genes encoding for bacterial monooxygenases of the family AlkB, such as *Runella slithyformis*.

(iv) *Scale up and optimization of the AC process inside a 31 L PBR pilot plant.*

In the last stage, the immobilized microbial biomass enriched at the inlet sections of the 31 L pilot plant was evaluated in terms of kinetic degradation activity and phylogenetic diversity. The overall investigation allowed to identify three main portions of the PBR where the microbial community contributed in a different way to the AC biodegradation of CAHs. Different microbial phlotypes were found to prevail within each portion of the system, including microbial species famous for their metabolic versatility and involvement in the bioremediation of several classes of organic contaminants. Among them there were microorganisms of the genera *Rhodococcus*, *Comamonas* and *Acidovorax*.

It is fundamental to highlight that a better understanding of the microorganisms driving environmental relevant processes is crucial for the choice of an effective bioremediation strategy, or the development of cost effective processes. Furthermore, such a knowledge helps to take better-informed decisions in order to consciously modify the process parameters leading to the overall optimization of the bioremediation process.

## Chapter 4. Microbial communities in the bioremediation of PAH-contaminated soil

### 4.1. Objectives and rationale of the research

The presented research was carried out at the laboratories of the Department of Biochemistry and Microbiology, University of Chemistry and Technology, Prague (UCT Prague), under the supervision of Assoc. Prof. Ondřej Uhlík, Ph.D.

The prior objective of the work was to determine the diversity of bacterial populations potentially involved in the bio-degradation of petroleum pollutants, focusing on polycyclic aromatic hydrocarbons (PAHs), within microbial communities occurring in a diesel fuel oil-contaminated soil, previously subjected to different bioremediation treatments. In fact, a previous evaluation of the total diesel range organics (DRO)-biodegradation activity was performed throughout the soil samples utilized in the present work, during a study conducted at the University of Alaska Fairbanks (McFarlin 2010), in cooperation with the Czech research unit led by dr. Uhlík. During this study, a diesel-contaminated soil was vegetated with willow trees (*Salix alaxensis*), with the addition of a fertilizer solution. It was further evaluated the DRO removal driven by the microbial communities enriched over the time in comparison to the non treated contaminated soil. The data outlined that the willow presence strongly enhanced the biodegradation activity of the soil communities at rhizosphere level (McFarlin 2010). In correlation with this previous study, the present investigation was intended to address the question of identifying rhizospheric bacterial populations potentially active in the DRO-mineralization and the soil treatment better inducing such an activity.

To attain this objective a Stable Isotope Probing (SIP) experiment, along with the pyrosequencing analysis of 16S rRNA gene tag-encoded amplicons, was established in order to find out the microbial populations responsible for the degradation of <sup>13</sup>C-labelled-naphthalene in the soil samples obtained from the previous bioremediation treatments. The removal of naphthalene, the simplest of the PAHs, could give insights into the microbial genetic potential to biodegrade even higher molecular weight PAHs, or the ability to co-metabolize other classes of petroleum contaminants (Heitkamp *et al.* 1988). In parallel to the SIP-community analysis, a characterization of the microbial composition of the soil samples not subjected to the SIP was performed, accounting for the microbial diversity due to the rhizoremediation and/or fertilization treatments of the contaminated-soil exploited in the previous study performed in Alaska.

## **4.2. Materials and Methods**

### **4.2.1. SIP-microcosms experimental design**

#### **4.2.1.1. Soil samples**

Soil samples were retrieved from an outdoor pot study for the treatment of a diesel contaminated soil, conducted at the University of Alaska Fairbanks (McFarlin 2010). In the same study, the contaminated soil was subjected to the following 3-months-treatment: (i) non-amended and unfertilized soil, referred as bulk soil (B), (ii) willow (*S. alaxensis*) crushed roots-amended soil (W), (iii) fertilizer only (F), (iv) willow (*S. alaxensis*) crushed roots-amended soil plus fertilizer (WF) (McFarlin 2010). Soil samples were collected according to similar moisture and approximate average MPN values, determined among the experimental replicates in the McFarlin's work, and were sieved, homogenized and further utilized for the SIP experiment discussed in the present study.

#### **4.2.1.2. SIP microcosms setup**

During the stable isotope probing experiment, an amount of 3 g of each type of soil was exposed to about 0.5 mg of  $^{13}\text{C}$ -naphthalene (Sigma-Aldrich, USA) for a period of 3 or 7 days, reproducing each condition in triplicates (indicated as I, II, III). The microcosms were prepared inside 100 mL serum bottles (Sigma-Aldrich, USA) by firstly pipetting 10  $\mu\text{L}$  of a 50  $\text{mg}\cdot\text{mL}^{-1}$   $^{13}\text{C}$ -naphthalene solution in acetone on the inner wall of the vial and waiting for the complete evaporation of the solvent. When only the naphthalene crystals were observable on the glass wall, 3 g of soil were added and moistened with 500  $\mu\text{L}$  water. Afterwards each vial was immediately sealed with crimped silicon septa.

Each triplicate microcosms was destructively harvested after 3 and 7 days (respectively indicated as sampling times T1 and T2), and these samples, along with triplicate samples of each soil-type not exposed to the labelled naphthalene (times T0), were stored at  $-80^{\circ}\text{C}$  until DNA isolation.

### **4.2.2. Experimental workflow to characterize the microbial communities**

#### **4.2.2.1. Metagenomic DNA extraction**

The total (metagenomic) soil DNA of the samples T0, T1 and T2 was isolated with FastDNA Spin Kit for Soil (MP Bio), according to the manufacturer's instructions, and the DNA concentrations were quantified with a NanoPhotometer<sup>®</sup> P-Class (Implen, Germany). All DNA solutions were adjusted to an approximate concentration of 100  $\text{ng}\cdot\mu\text{L}^{-1}$ .

#### 4.2.2.2. Isopycnic Centrifugation and Gradient Fractionation

For each DNA solution a volume of 8  $\mu\text{L}$  ( $\approx 800$  ng DNA) was mixed with about 2 mL of a 1.6  $\text{g}\cdot\text{mL}^{-1}$  dense Cesium Trifluoroacetate (CsTFA) solution (GE Healthcare Life Sciences, Amersham, UK) into a centrifuge cuvette. The cuvettes were sealed and subjected to isopycnic ultracentrifugation at 145,000  $\times g$  for 72 hours, on a Discovery 90 Ultracentrifuge with a TFT-80.2 Fixed-Angle Ultraspeed Centrifuge Rotor (Sorvall, USA). The isopycnic CsTFA gradient formed was fractionated into thirty ( $\sim 33$   $\mu\text{L}$ ) fractions by using a Beckman Fraction Recovery System (Beckman Coulter, USA) and Harvard Pump 11 Plus Single Syringe (Harvard Apparatus, USA) with a flow rate of 200  $\mu\text{L}\cdot\text{min}^{-1}$ . The buoyant density of each gradient-recovered-fraction was inferred by measuring the refractive index of a fractionated blank sample, where 8  $\mu\text{L}$  of water were loaded instead of sample, determined with a Digital Handheld Refractometer (Reichert Analytical Instruments, USA).

The DNA of the gradient-fractions with buoyant densities ranging between 1.46-1.68  $\text{g}\cdot\text{mL}^{-1}$  was retrieved by isopropanol precipitation with glycogen (Uhlík *et al.* 2009).

#### 4.2.2.3. Heavy-DNA containing-region identification by quantitative PCR (qPCR)

The metagenomic DNA distribution among the selected gradient-fractions was quantified by real-time PCR analysis of the 16S rRNA genes conserved regions targeted by the primers 786f (5'-GATTAGATACCCTGGTAG-3') and 939r (5'-CTTGTGCGGGCCCCCGTCAATTC-3') (Baker *et al.* 2003), according to the same qPCR protocol as was previously described by Uhlík *et al.* 2012.

Profiling the variation of the DNA distribution through the increasing buoyant density of the gradient allowed for the determination of those fractions containing  $^{13}\text{C}$ -labeled bacterial DNA for each analysed community DNA. Thus, the heavy DNA retrieved from these fractions was combined for each sample obtaining unique “heavy” fractions to be further analysed.

#### 4.2.2.4. Tag-encoded amplicons preparation for 454 pyrosequencing

The metagenomic DNA isolated from the T0 microbial communities along with the DNA retrieved from the combined heavy fractions for the samples T0, T1 and T2 was analysed by 454 pyrosequencing.

The preparation of PCR products for the 454 pyrosequencing analysis consisted of a modified procedure of that described by Berry *et al.* 2011. Regions V4-V6 of the 16S rRNA genes (numbering according to *E. coli* [J016965] positioning) were amplified with primers 515-530 forward, 5'-GTGCCAGCMGCNGCGG-3' (Dowd *et al.* 2008) and 1068-1052 reverse, 5'-CTGRCGRCCRCCATGCA-3' (Uhlík, unpublished data). The PCR reaction was prepared in a final volume of 15  $\mu\text{L}$  with KAPA HiFi HotStart ReadyMix (KAPA BIOSYSTEMS, Boston, USA),

containing 0.02 U/ $\mu$ L of KAPA HiFi HotStart DNA Polymerase, 2.5 mM MgCl<sub>2</sub> and 0.3 mM of each dNTP, 0.3  $\mu$ M of each primer (Generi Biotech, Czech Republic) and template DNA (1  $\mu$ L). The cycling program was 5 min at 95°C, 35 cycles of 20 s at 98°C, 15 s at 50°C, 15 s at 72°C and a final extension of 5 min at 72°C. Some 5  $\mu$ L of the obtained amplicons were utilized as template for a reconditioning PCR, performed in a final reaction volume of 25  $\mu$ L in the presence of 1  $\mu$ M of each primer and keeping the same concentration of all other reagents as mentioned above. The amplification conditions were maintained as well while decreasing the cycle number to 8-12. The forward and reverse primers utilized for the reconditioning PCR were modified with sequencing adapters (454 Sequencing Application Brief No. 001-2009, Roche), and a further modification of only the forward primer was made by the addition of a barcode sequence (454 Sequencing Technical Bulletin No. 005-2009, Roche), which was different for each sample library. After the pyrosequencing, the presence of such specific barcode sequences allows one to correctly affiliate the reads from a single sequencing run according to the sample library. The obtained PCR products were purified using AMPure XP Beads (Agencourt, Beckman Coulter, USA) and the DNA concentration of purified solutions was measured with Qubit® dsDNA HS (High Sensitivity) Assay Kit (Life Technologies). Proportional amounts of each amplicon were mixed and then unidirectionally sequenced from the forward primer using the GS FLX Titanium chemistry followed by amplicons analysis of signal processing (Roche).

#### **4.2.2.5. Pyrosequencing Data Processing**

Raw pyrosequencing data (\*.sff files) were processed using the mothur software package, version 1.30 (Schloss *et al.* 2009), according to the operating procedure modified by Uhlík *et al.* 2012. In order to track the correctness of the analysis procedure, the analysis pipeline of pyrosequencing data was set based on an artificial mock community as described by Uhlík *et al.* 2012.

During the downstream processing of the data, the OTU occurrence in the heavy-fractions of the SIP-libraries was validated by comparison with their occurrence in the fractions of the Times 0 communities with the same buoyant densities as those of heavy fractions. In particular, the OTU was considered valid when the number of sequences detected in the considered SIP library resulted higher than the mean number of sequences plus standard deviation of the correspondent time 0 – SIP OTU.

Statistical analysis of the data were based on the non-metric multidimensional scaling (NMDS), performed with *vegan 2.0-10* package in *R* (R version 3.1.0 "Spring Dance") and Indicator species analysis performed with *indicspecies 1.7.1* package in *R*, discriminating between most significant environmental variables (treatment, time) in the development of the total microbial

communities of the soil (T0 communities) and their metabolic functionality (SIP-heavy-fractions communities at T1 and T2).

### 4.3. Results and discussion

#### 4.3.1. Evaluation of the heavy-DNA enrichment among SIP-communities

The quantitative PCR analysis of the DNA retrieved from each fraction of the isopycnic CsTFA gradient profiled that the unlabelled metagenomic DNA, represented by the higher peaks in the Figure 32, lay at buoyant density values ranging between 1.55 and 1.57 g·mL<sup>-1</sup> for the bulk soil samples, while it was a bit shifted to values between 1.58 and 1.61 g·mL<sup>-1</sup> in case of willow vegetated soil. For all the SIP-samples (T1 and T2) a secondary peak rose at higher buoyant densities, outlining the enrichment of a heavy carbon into the DNA of naphthalene assimilation populations, not occurring in the T0 (dashed lines, Figure 32).

Considering the robustness of the results obtained among the replicates (experimental and analytical) of each tested condition, it was possible to delineate a trend in the heavy DNA enrichment according to the variables "sampling time" and "soil treatment". In the first case, well distinct heavy-peaks were observable at times T1 for the willow (W) and willow-fertilized (WF) treatments, where the T2-peaks were reduced to be just a shoulder of the light-peak. Such a phenomenon could be explained by cross-feeding contamination events, for instance taking place when microbes not involved in the naphthalene degradation derive heavy-carbon from labelled intermediates released through the metabolism of primary degraders, or simply by the heavy-DNA replacement due to the regular DNA replication when the full amount of the <sup>13</sup>C-naphthalene supplied was already consumed. At the same time, this was not true for the non-vegetated soil, where comparable amounts of heavy DNA were detected at both T1 and T2. This fact could be the evidence of a slower metabolism of the non-vegetated soil microbial communities in the degradation of naphthalene, and more in general of PAHs, supporting the results previously exposed about the DRO-degradation study performed in Alaska (McFarlin 2010).

Higher enrichment of <sup>13</sup>C-DNA occurred in the case of willow and bulk soil in comparison with the fertilized treatments, suggesting that the fertilizer presence slightly delayed the degradation process. Once again, these results seem to be in line with the DRO degradation data previously reported from Kelly M. McFarlin, showing that the fertilizer treatment did not significantly promote the DRO degradation, although it stimulated the microbial growth and produced an increase in the willow plant biomass and delayed the senescence phase of the plant (McFarlin 2010). On the other hand, the comparable enrichment of heavy DNA between the bulk and willow treated soil remains to

be explained. A possible speculation was that the microbial community occurring in the bulk soil could easily degrade naphthalene, harbouring a DRO degrading activity which was promoted by the treatment with the willow crashed roots.

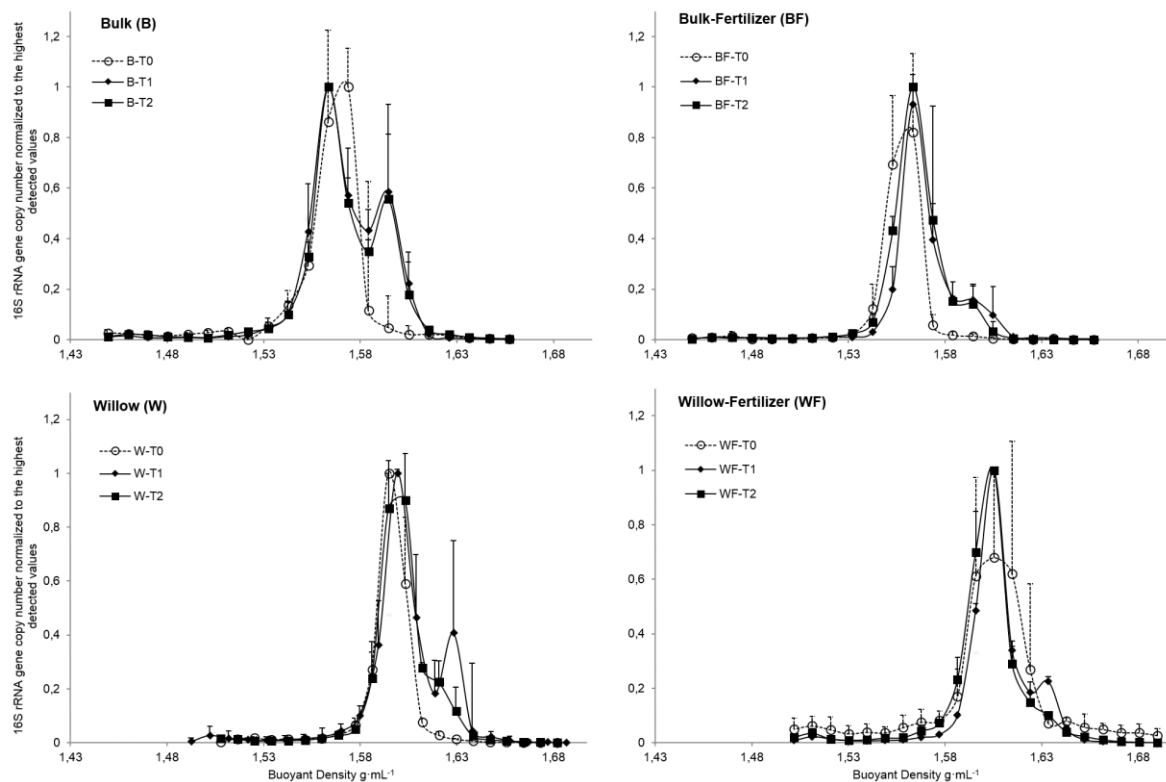


**Figure 32.** qPCR profiles of the DNA distribution along the isopycnic gradients of CsTFA. Each curve represents the average trend of three experimental replicates (I, II, III) for all SIP-tested-conditions, sampled at times T0, T1 and T2; two analytical replicates were run for each qPCR reaction; the standard deviation is presented by the error bars.

### 4.3.2. Investigation of the total community structure

An important task of the work was to characterize the microbial communities initially occurring in the soil samples, obtained from the previous treatments (McFarlin 2010), elucidating the complexity and composition of community structure evolved according to the type of treatment.

The indicator species analysis of the sequencing data, performed at the end of the pipeline analysis procedure, enabled the identification of the indicator OTUs for each library which were identified using Ribosomal Database Project (RDP) *Seqmatch* tool. The resulting data are reported in Appendix, Table 21. The majority of the detected indicator OTUs occurred within the willow treated soil (83.7% of the total OTUs) and the fertilized bulk soil (75.4% of the total OTUs). The 50.3% of the total indicator OTUs were associated to the non treated bulk soil, while only the 25.1% of OTUs accounted for the willow-fertilized treatment. Therefore, the richness of the willow-treated community was significantly represented; at the same time, the soil fertilization did not produced a

much different result, meaning that also this treatment was able to induce a significant enrichment of the main groups of bacteria.

A non-metric multidimensional scaling (NMDS) analysis was performed among the libraries of the total communities analysed in triplicate (Figure 33). The NMDS revealed that the variation among the community compositions could be better explained by the treatment with willow crushed roots over the addition of a fertilizer to the soil.

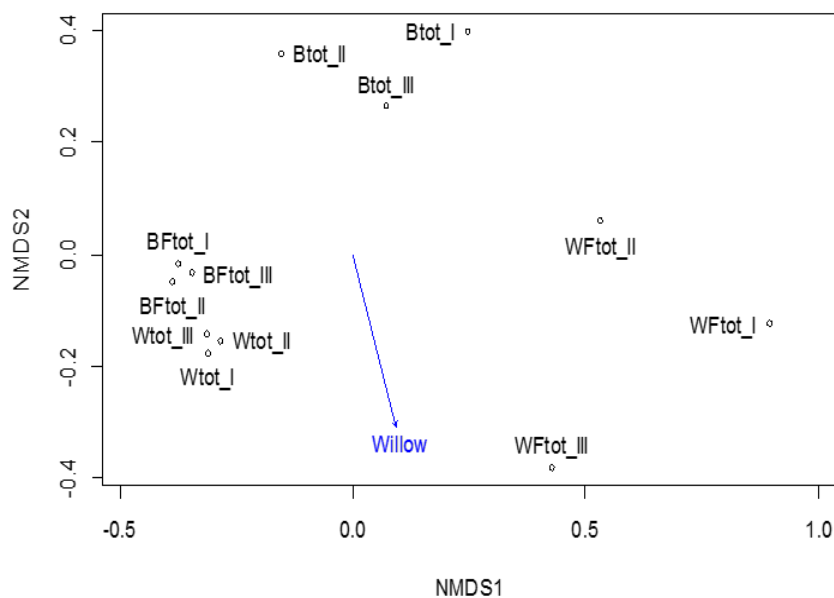


**Figure 33.** Unconstrained ordination (non-metric multidimensional scaling) of the sequence data for total communities. The vector fitting method was used to relate the major compositional variation to observed environmental variation (willow, fertilizer). ANOVA ( $P$  value $<0.5$ ) showed the presence of willow explains the variation, whereas the fertilizer does not.

The phylogenetic analysis of the total communities (Appendix, Table 21) revealed that Proteobacteria, Sphingobacteria, Actinobacteria and Bacteroidetes were the most abundant groups, among all the pyrosequence libraries (Figure 34). Other minor phyla were Planctomycetia, Flavobacteria and Clostridia. This prevalence of Proteobacteria is a common feature within microbial consortia driving aerobic degradation of PAHs (Vinas *et al.* 2005; Singleton *et al.* 2011).

A prominent enrichment of Deltaproteobacteria and Betaproteobacteria was obtained for the bulk fertilized (BF) soil (19.6% and 13.1%, respectively) and the willow-vegetated (W) soil (21.2% and 11.2%, respectively). The most abundant Betaproteobacteria detected among the BF and W libraries were affiliated with the families of *Burkholderiaceae* (genera *Burkholderia*, *Pandorea*), *Comamonadaceae* (genus *Variovorax*), *Rhodocyclaceae* (genera *Georgfuchsia*, *Methyloversatilis*, *Sulfuritalea*). Many members of these phylogenetic groups have been widely described in literature to be involved in the aerobic degradation of 2-3 rings PAHs and co-metabolic degradation of higher-molecular-weight PAHs (Chauhan *et al.* 2008; Habe *et al.* 2014; Jones M.D. 2010). Many others were

not directly associated with PAHs degradation, but were involved in the anaerobic degradation of monoaromatics, such as benzene or toluene, as in the case of *Georgfuchsia* spp. (Weelink *et al.* 2009).

Within the BF and W libraries, Deltaproteobacteria were the predominant group, widely represented by members of the families *Bdellovibrionaceae* (*Bdellovibrio* sp.), *Desulfobacteraceae* (*Desulfovibrio* sp.), *Geobacteraceae* (*Geobacter* sp.), *Myxococcaceae* (*Pyxidicoccus* sp.) and *Phaselicystidaceae* (*Phaselicystis* sp.). Among the detected anaerobic Deltaproteobacteria there was *Geobacter* sp. reported to be a key-microorganism in many bioremediation processes and was isolated from several different environmental polluted sites, including petroleum-contaminated ones (Coates *et al.* 1996). This iron-reducing-strain was found to be also a degrader of aromatic pollutants (Staats *et al.* 2011). Implication of Deltaproteobacteria in PAHs degradation processes has not been often reported, however there are some evidences of sulphate-reducing Deltaproteobacteria involved in the anaerobic mineralization of phenanthrene, enriched from hydrocarbon-contaminated marine sediment (Davidova *et al.* 2007). In this regard, it should be mentioned that several studies assessed the occurrence of anaerobic degradation of PAHs under both denitrifying and sulphate reducing conditions (Zhang *et al.* 2000; Ambrosoli *et al.* 2005). It was interesting to notice the occurrence of some facultative or strictly anaerobic bacteria, despite the aerobic treatment of the contaminated soil. This evidenced the establishment of some anaerobic niches where bacterial guilds were possibly involved in the anaerobic degradation of PAHs.

Furthermore, BF and W libraries (Figure 34) were characterized by a significant presence of *Sphingobacteria* (11.8% and 13.5%, respectively), while the highest enrichment of Alphaproteobacteria (4.6%) was recorded within the BF community. In the latter, members affiliated with *Sphingomonadaceae* (genera *Sphingobium* and *Novosphingobium*) were previously described to degrade 2- and 3-ring PAHs through SIP studies (Jones 2010), and their catabolic pathway for the degradation of higher-molecular-weight PAHs was proposed by other methods (Pinyakong *et al.* 2003).

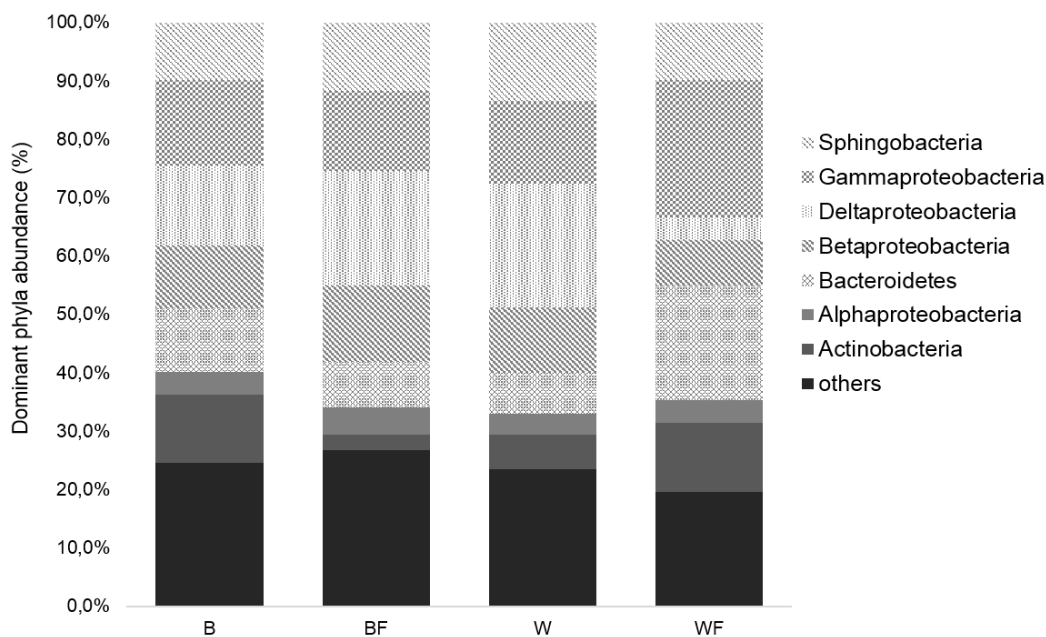


**Figure 34.** Dominant Phyla abundance in the total communities (T0). Percentage values are referred to the total amount of significant OTUs obtained with Indicator species analysis (alpha = 0.05). B: bulk soil; BF: bulk fertilized soil; W: willow-crushed-roots amended soil; WF: willow-crushed-roots plus fertilizer treatment.

Phylogenetic groups mainly enriched within the bulk soil (B) and willow-fertilized soil (WF) were Gammaproteobacteria (14.7% and 23.5%, respectively) and Gram-positive Actinobacteria (11.8% in both cases), such as *Arthrobacter* spp. and *Microbacterium* spp. In addition, the occurrence of species affiliated with Bacteroidetes was particularly high within the willow-fertilized community (19.6%), while a reduction of Deltaproteobacteria was remarkable in the same community.

In conclusion, the analysed communities presented a high microbial diversity, favourable for the development of different degradation pathways of PAHs. At the same time, the composition of the microbial communities seemed to differently evolve according to the soil treatment used. The main taxa of Proteobacteria were similarly enriched within bulk-fertilized (BF) and willow (W) communities, while an increase in Gammaproteobacteria along with Bacteroidetes and Actinobacteria was observed in the willow-fertilized (WF) community. These results suggested a different degree of specialization among the soil communities. The SIP with  $^{13}\text{C}$ -naphthalene, as representative model for all PAHs, was thus exploited to provide additional information about the microbial species involved in the PAH degradation.

#### 4.3.3. Taxonomic identity of naphthalene-degrading communities

As mentioned above, a unique heavy-DNA pool of sequences was compiled for each SIP sample (T1 and T2) and for the T0 communities, utilizing the latter as control to unambiguously validate the occurrence of sequences in the heavy fractions. The pool of heavy-DNA-sequences

corresponding to every single sample-replicate were then amplified using barcoded primers and finally subjected to the pyrosequencing analysis. The pyrosequencing data obtained for the SIP-libraries were statistically evaluated according to the type of treatment (considering each of the three replicate separately) and the sampling time, T1 and T2 (Tables 22 and 23 in Appendix).

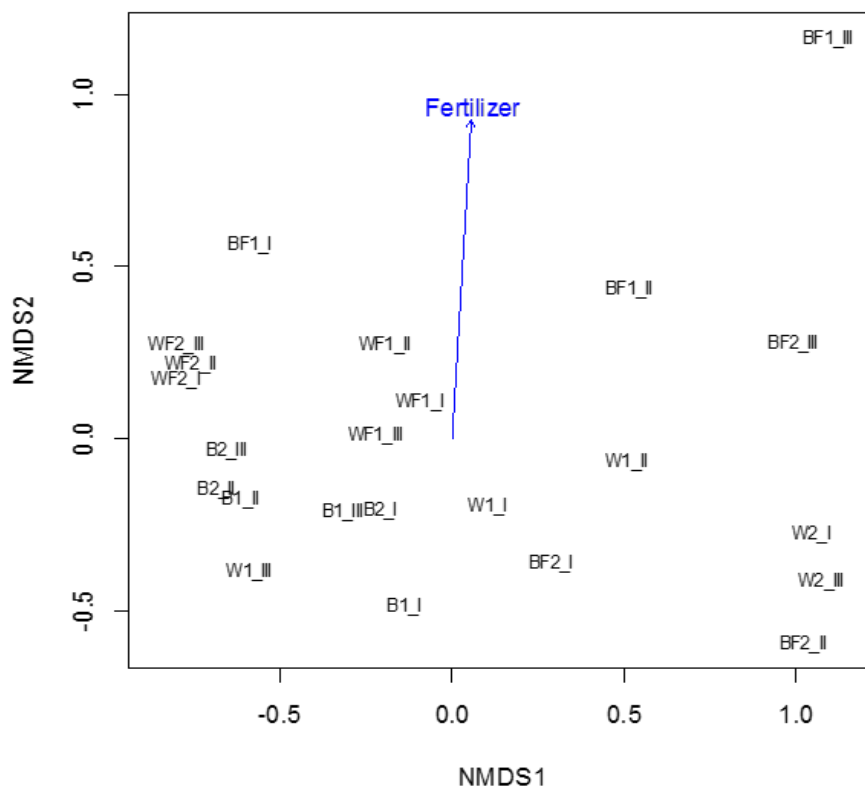


**Figure 35.** Unconstrained ordination (NMDS) of the sequence for SIP data. The vector fitting method was used to relate the major compositional variation to observed environmental variation (willow, fertilizer). ANOVA (P value<0.5).

The NMDS analysis, in Figure 35, showed that the metabolic activity of the SIP communities in the degradation of naphthalene was mainly influenced by the presence of fertilizer, differently to what resulted from analysing the total communities. This difference was probably given by the comparison of the community structure versus metabolic activity. Whereas the former seems to be driven mainly by the plant, the latter by the fertilization.

Betaproteobacteria and Gammaproteobacteria accounted for the majority of sequences detected within the heavy DNA retrieved from all of the soil communities (Table 22 and 23 in Appendix). The mainly occurring genera were represented by *Acidovorax*, *Pseudomonas*, *Hydrogenophaga*, *Polaromonas*, *Herminiimonas* and *Methyloversatilis*. The widespread occurrence of *Pseudomonas* spp. was not surprising, in fact pseudomonads involvement in the degradation of PAHs (Chauhan *et al.* 2008; Jones 2010) and in other petroleum hydrocarbons (Das *et al.* 2011) is well known. In addition, several scientific studies described in detail the naphthalene and salicylic acid catabolic pathways in *Pseudomonas* spp. (Shell 1985; Yen *et al.* 1988; Kurkela *et al.* 1988; Habe

*et al.* 2014). The presence of *Acidovorax* spp., was not surprising either, since it represents an environmental species mainly spread in soil and water habitats (Choi *et al.* 2010) often associated with various types of contamination. Species of *Acidovorax* and *Pseudomonas* have been already identified by mean of SIP with  $^{13}\text{C}$ -labelled naphthalene (Singleton *et al.* 2005; Jones 2010).

Other members of the *Burkholderiales* were affiliated with *Hydrogenophaga* spp. and *Polaromonas* spp., with the latter being mainly detected within the bulk (B) active microbes, while the former was also evidenced in the willow-fertilized (WF) community. As with other members of this family, also *Hydrogenophaga* species have a wide metabolic potential and have been isolated from several environmental polluted matrices, and together with *Acidovorax* spp. were shown to be active PAH degrader during a SIP study with  $^{13}\text{C}$ -phenanthrene (Martin *et al.* 2012). *Polaromonas* spp. detected in this work were related (similarity higher than 97%) to *Polaromonas naphthalenivorans* (AY166684), a strain previously associated with the naphthalene degradation by means of DNA-based SIP investigation (Jeon *et al.* 2003).

Several sequences mainly detected in the willow (W) library were related to known PAH degraders (Table 23 in Appendix). It was the case of the genera *Sphingobium* and *Novosphingobium*. These Alphaproteobacteria were previously described to be associated with the degradation of PAHs, containing from 2 to 5 aromatic rings (Stolz 2009; Jones 2010); their metabolic degradation pathways have also been described (Pinyakong *et al.* 2003). Other Betaproteobacteria detected in the W library were *Achromobacter* spp. and *Herminiimonas* spp., previously associated with the naphthalene and anthracene degradation (Jones 2010). Finally, some Actinobacteria affiliated sequences were more than 99% similar to *Arthrobacter phenanthrenivorans* Sphe3 (AM176541), a phenanthrene degrader isolated from a contaminated soil (Kallimanis *et al.* 2009).

This study showed that the majority of OTUs detected in the  $^{13}\text{C}$ -DNA-enriched sequences was directly or indirectly related to species previously described as key microorganisms in the biodegradation of PAHs. Moreover, their known implication in the degradation of higher-molecular-weight PAHs indicated that the under-study communities could be responsible for the mineralization of a wide pool of diesel organic pollutants.

In this context, it seemed that the fertilization of the diesel-contaminated soil or the treatment with willow plant-biomass produced different effects concerning the total community composition and its metabolically active species. However, analysing the active communities composition, the naphthalene degradation in the willow treated communities seemed mainly driven by the same microbial species active in the fertilized soil. These observations correlate with the results about the DRO removal previously obtained (McFarlin 2010). Here, the major reduction in DRO concentration was measured for the treatment with willow, while a decrease of the degradation activity occurred in

the willow-fertilized soil. It was hypothesized that the reason was based on the delayed senescence of the willow plant, which in turn resulted in a slower root turn over and a minor release of secondary metabolites of the plant, such as salicylic acid, in the rhizosphere (McFarlin 2010). Probably, the same reason could explain a minor differentiation of the willow-fertilizer rhizospheric community from that of the bulk soil.

#### **4.4. Conclusions**

The DNA-based  $^{13}\text{C}$ -naphthalene SIP investigation revealed that soil microbial communities are a precious resource of metabolically active taxa to be exploited for biodegradation of recalcitrant and persistent organic contaminants.

The phytoremediation, and in particular the rhizoremediation, represents an effective strategy for the *in situ* bioremediation of contaminated soil, since it clearly affects the structure of microbial communities. Choosing the best treatment appears crucial for the establishment of the right synergistic plant-microorganism interactions in the rhizosphere, determining a successful bio-stimulation of the desired metabolic/bio-degradative pathways.

In this regard, the knowledge of the microbial communities involved gives the basis to understand, monitor and control the biodegradation of dangerous pollutants in the environment. The presented work provided an example of the remarkable investigation power of the cultivation-independent molecular techniques exploited here.

## **Chapter 5. Production of PHA by sludge communities: community composition and evolution among selective and enriching processes.**

### **5.1. Objectives of the work**

The presented study was aimed to characterize structure, composition and dynamics of PHA-accumulating microbial communities, enriched under strong selective pressure of a feast/famine regime established by means of sequencing batch reactor (SBR) processes.

Such SBR processes were developed by the research team headed by Professor Mauro Majone, at the Department of Chemistry, “Sapienza” University of Rome, in the framework of a research study for the development and optimization of municipal wastewaters treatment processes coupled with the production of polyhydroxyalkanoates (PHA). Details about the conduction mode and the research rationale of the SBR processes (Valentino *et al.* 2014b) have been specified in the introductory section 2.3.4. of this dissertation, while here an insight into the microbial communities driving the PHA-production process is given.

In general, the characterization overtime of microbial communities with high PHA-storage capabilities, along with the investigation of the community’s functional organization stability, provides relevant information about microbial PHA-producers and operative conditions promoting their enrichment. Furthermore, the diversity of microbial populations accumulating PHA determine differences in the molecular weight and other properties of the polymers produced (Valentino *et al.* 2012). In turn, this knowledge can be used to implement further research to optimize process parameters like organic loading rate, hydraulic retention time and, overall, to find out the best feast and famine regime resulting into higher PHA accumulations.

To this purpose, the microbial biomass enriched during five experimental replicates of the SBR process (Runs I to V) has been regularly sampled and analysed by PCR-DGGE approach. Changes of the community’s structure and composition were evaluated over time, in terms of community dynamics, and in relation to the PHA-production performance data. Furthermore, an exhaustive identification of the microbial species associated with the Run (IV)-DGGE-profiles bands was accomplished cloning-DGGE analysis of some of the most representative communities. Based on the specific information obtained, a final objective was to evaluate the general biomass behaviour during the acclimation in the five SBR replicates, fed with a synthetic solution of complex mixture of organic compounds as a feast-famine regime.

## 5.2. Materials and methods

PCR-DGGE analysis of 16S rRNA genes was used to investigate changes of the bacterial community structure during SBR runs. Metagenomic DNA was extracted in duplicate with the UltraClean Soil DNA kit (MoBio Laboratories, Carlsbad, CA, USA) from approximately 250 mg of sludge pellet. PCR amplification of the V3–V5 variable regions was performed with primers GC-357f and 907r as described in section 3.2.4.2. Obtained amplicons were resolved on a 7 % (w/v) polyacrylamide DGGE (acrylamide-N,N'-methylenebisacrylamide, 37:1) containing a denaturing gradient from 40 (top) to 60 % (bottom), prepared as described in section 3.2.4.2.

Similarities between DGGE profiles were calculated using the Dice coefficient with Quantity One 4.5.2 software (Bio- Rad). DGGE patterns were then clustered using the UPGAMA clustering algorithm. Moving windows analysis was performed based on the DGGE profiles as described in Marzorati *et al.* (2008). The analysis provides the percentage change value between consecutive sampling points and the rate of change parameter, which averages the rate of change between consecutive DGGE profiles of the same community over a fixed time interval. Usually, a time interval of approximately 1 week was considered, although shorter time intervals (1–3 days) were also taken into consideration during the start-up (first week) of the shorter SBR runs (Runs I, II and III).

To characterize the composition of selected microbial communities, metagenomic libraries of the 16S rRNA genes were constructed. 16S rRNA genes were PCR amplified from the metagenome with the primer pair 27f/1525r as described in section 3.2.4.3.1. Library screening was performed by DGGE analysis, according to the procedure described in section 3.2.4.3.2. Sequences were aligned to the Ribosomal Database Project (RDP, release 10) sequence database and closest relatives retrieved with the SeqMatch tool.

## 5.3. Results and discussion

A molecular characterization of the microbial community's structure and composition was performed for five SBR processes, conducted as replicates during the study. Their microbial community dynamics were investigated via DGGE analysis, in order to assess the response to the imposed process conditions and the stability of PHA accumulating consortia during enrichment on the substrate synthetic mixture.

Remarkable changes occurred in the structure of the community along all runs, being the Dice similarity indexes between the DGGE profiles at the beginning and the end of the SBR runs in the range 60 % (Run I) – 38 % (Run IV). In order to numerically measure community dynamics from the DGGE profiles, moving window analysis was performed (Figure 36). It is shown that faster changes

occurred during the first days of SBR operation (rate of change of  $37.5 \pm 17.2$ ,  $27.7 \pm 14.8$  and  $11.5 \pm 3.5$  % for Runs I, II and III, respectively), when varying oxygen profiles also indicated that MMC acclimation was in progress. Conversely, very slow community changes occurred after the first week in all runs (rate of change between  $3.1 \pm 0.5$  and  $7.4 \pm 1.3$  %), when more stable process performances (e.g. RBCOD specific removal rate) were established. Such a low level of community dynamics during the steady state of SBR runs indicates that different species might be able to slowly become dominant or exit the bacterial community over a long operation period, without interfering, however, with the overall functionality of the system.

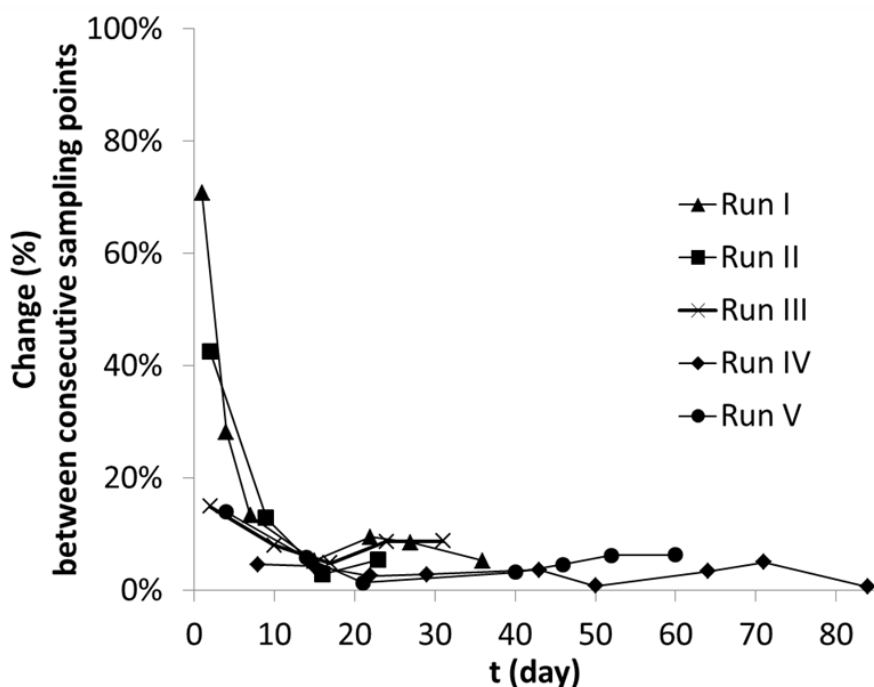


**Figure 36.** Moving window analysis of the DGGE profiles of the microbial community enriched in different runs.

As an example, Figure 37 shows the community DGGE profiles and clustering analysis of the longest SBR run (Run IV). Community profiles of the first 4 weeks of incubation clustered together (cluster I) and separately from those of weeks 6–12 (cluster II). In addition, subclustering of DGGE profiles from consecutive sampling points was observed (sub-clusters Ia, Ib, IIa, IIb), confirming that changes progressively occurred in the community structure. In particular, the phylotypes dominant during the first 4 weeks of steady state operation (bands 2, 3, 7, 9, sub-clusters Ia and Ib) became poorly represented at weeks 6–7 (subcluster IIa). This latter period was instead characterized by the highest relative abundance of phylotypes represented by bands 1, 4, 6, 8 and 12. Finally, during the last period of conduction (weeks 10 and 12, sub-cluster IIb), phylotypes associated with the bands 3 and 7 recovered dominance, while a new phylotype was enriched (band 13).

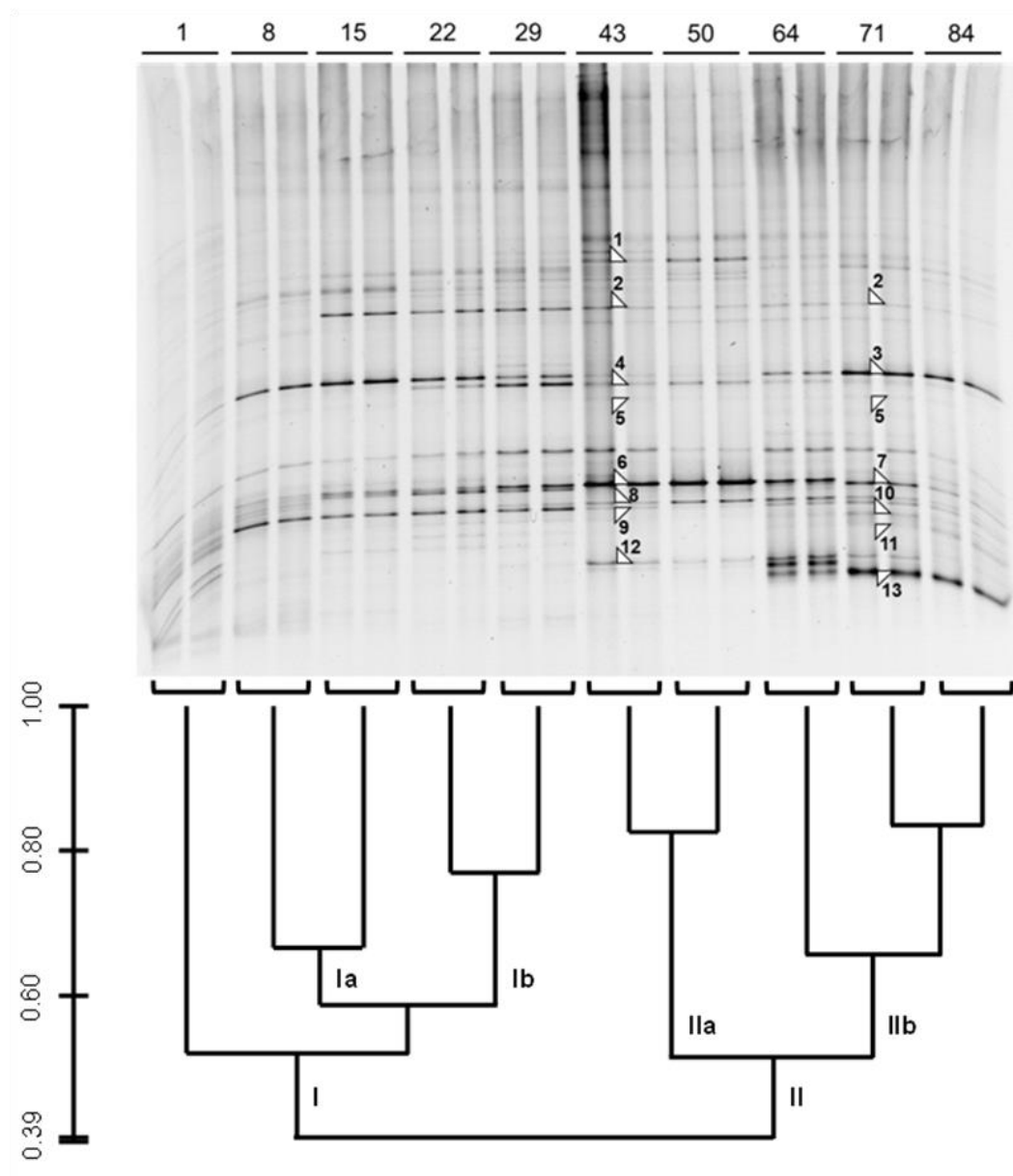


**Figure 37.** DGGE profiles of the microbial community along Run IV (days indicated on top of lanes) and corresponding clustering dendrogram. Arrows and numbers indicate phlotypes (bands) that were identified in clone libraries via DGGE screening and sequenced.

The major phlotypes enriched were identified in clonal libraries of Run IV community (sampling time 43 and 71 days) via DGGE screening and sequencing of clone inserts (Table 24 in Appendix). At least one dominant phlotype per each sub-cluster was previously reported to store PHA. The most representative were *Zoogloea* sp. (band 9, dominant in sub-clusters Ia and Ib) (Huang *et al.* 2012), *Acidovorax* sp. (bands 3 and 7, dominant in sub-clusters Ia, Ib and IIb) (Yee *et al.* 2012), *Hydrogenophaga* sp. (bands 4 and 6, dominant in sub-clusters IIa) (Povolo *et al.* 2013; Choi *et al.* 2003) and *Meganema perideroedes* (band 13, dominant in sub-cluster IIb) (Kragelund *et al.* 2005). Of course, it cannot be excluded that other members of the community may have some PHA storage capability. Interestingly, some of the main phlotypes were dominant in only one sub-cluster,

suggesting a succession of different PHA producers during the long operation period of the SBR. Because of the sharp fluctuations characterizing the PHA production rates throughout the whole Run IV (as discussed in the paper by Valentino *et al.* 2014b), it was inferred that changes in the PHA storage rates were not dependent on changes in the microbial community and its dominant members (that occurred much more slowly).

A similar clustering behaviour, characterized from the gradual and progressive changes of the microbial community structures, was observed for the DGGE profiles of other runs (data not shown). The communities enriched at the end of the shorter SBR Runs I, II and III (i.e. after 23–36 days) showed significant similarity to the community enriched after 15–29 days in Run IV (clusters Ia and Ib). One of the main representative members enriched in such communities was *Zooglea* sp. (band 9). At the same time, microorganisms affiliated with the genera *Zooglea* and *Acidovorax* (band 3) dominated the early phase of the Run V (up to day 21). In addition, the communities analyzed at the end of the Run IV and the Run V similarly enriched members related to *Acidovorax* spp. (bands 3 and 7) (data not shown), while some differences were still evident, for instance the absence of the *M. perideroedes* phylotype at the end of Run V. The appreciable occurrence of similar dominant phylotypes at similar stages of the replicated SBR runs suggested similar trends of succession of PHA-storing populations occurring over time in the different runs.

## 5.4. Conclusions

In conclusion, the microbial community analyses, performed on the five replicates of the SBR processes, revealed high dynamics of the communities' structure and composition during the first week of conduction. This was consistent with the PHA-process data, showing that, on average, the microbial communities needed almost one week of operation in order to achieve a stable response to the imposed process conditions (Valentino *et al.* 2014b). After about one week, the "stable response" of the microbial biomass to the process conditions was in line with the low dynamics observed.

At the same time, the performed molecular analyses indicated that slow, but significant, changes of the community's structure and composition occurred during the overall conduction time, and the prevailing microorganisms were identified as already known PHA-storing microorganisms: *Zooglea* sp., *Acidovorax* sp., *Hydrogenophaga* sp. and *M. perideroedes*. However, changes in the communities' composition were not reflecting changes in the PHA-storage ability, observed as a response of the microbial biomass to the process conditions. In fact, changes in the biomass storage response were much faster than the former mentioned.

A progressive sub-clustering of the community DGGE profiles among successive sampling times indicated a gradual stabilization of the community that occurred for each run; apparently not affecting

the total dynamics and the functionality of the process itself. In addition, the achievement of quite high similarity indexes of the community profiles after the first weeks of conduction, with the enrichment of similar dominant microorganisms, was indicative of the good reproducibility of the process, in spite of the fact that the five replicated SBRs were inoculated with different inocula of sludge, though provided by the same wastewater treatment plant.

## Appendix – Phylogenetic classification of detected microbial phlotypes

**Table 18:** Phylogenetic classification of phlotypes detected within the suspended and immobilized microbial communities of the microcosms.

Band #	Phylum <sup>a)</sup>	Closest relative	%ID <sup>b)</sup>	Closest described	%ID <sup>b)</sup>
1	Bacteroidetes	uncultured <i>Sediminibacterium</i> sp. clone CP3.2.4 [JN697485]	100	<i>Sediminibacterium salmoneum</i> NJ-44 [NR_044197]	97
2	Bacteroidetes	<i>Sphingobacterium</i> sp. P-7; [AM411964]	100	<i>Chitinophaga arvensicola</i> DSM 3695 [AM237311]	92
3	Bacteroidetes	Uncultured bacterium ar2a916 [HM921150]	99	<i>Terrimonas ferrugines</i> DSM 30193 [AM230484]	98
4	Chlorobi	uncultured bacterium C8 [FJ356024]	99		
5	Bacteroidetes	uncultured bacterium clone WW1_a14 [GQ264158]	99	<i>Mucilaginibacter</i> sp.HRB31 [JF778715]	99
6	Bacteroidetes	Uncultured bacterium clone NMA2 [GU183609]	100		
7	Bacteroidetes	<i>Emticicia</i> sp. NL128 [AB636297]	100	<i>Emticicia ginsengisoli</i> strain Gsoil 085 [NR_041373]	99
8	Betaproteobacteria	<i>Cupriavidus necator</i> VKPM B5786 [AJ633674]	100		
9	Firmicutes	<i>Paenibacillus vortex</i> V453 [HQ005270]	99		
10	Firmicutes	<i>Bacillus</i> sp. B3(2008b) [FJ348338]	100	<i>Bacillus cereus</i> MBG26 [JF280126]	99
11	Betaproteobacteria	<i>Azospira oryzae</i> strain 6a3 [NR_024852]	99		
12	Betaproteobacteria	<i>Dechloromonas hortensis</i> MA-1 [NR_042819]	100		
13	Betaproteobacteria	<i>Zoogloea resiniphila</i> DhA-35 [NR_027188]	100		
14	Betaproteobacteria	Uncultured bacterium clone Q7308-HYBA [JN391720]	99	<i>Georgfuchsia toluolica</i> G5G6 [EF219370]	97
15	Alphaproteobacteria	<i>Alphaproteobacterium</i> INAWF007 [AB468975]	100	<i>Pseudolabrys taiwanensis</i> strain CC-BB4 [NR_043515]	97
16	Alphaproteobacteria	uncultured bacterium clone <i>Chlminus</i> _CL-090519_OTU-14 [EU808278]	99		

17	Betaproteobacteria	Uncultured <i>Acidovorax</i> sp. cuticle 2.9; [HQ111169]	99.4
18	Actinobacteria	<i>Mycobacterium pallens</i> czh-8 [NR_043760]	100
19	Acidobacteria	uncultured bacterium clone ly13 [GQ203647]	99

a) Phylogenetic affiliations are based on RDP Seqmatch tool.

b) Similarity reports the percent sequence identity over all pairwise comparable positions.

**Table 19:** Phylogenetic classification of phylotypes detected within the immobilized microbial communities of the 1 L PBR system.

Clone/OTU #	Phylum <sup>a)</sup>	Closest relative	%ID. <sup>b)</sup>	Closest described	%ID. <sup>b)</sup>
1	Chloroflexi	uncultured bacterium K75 [EU862289]	99.2	<i>Dehalococcoides</i> sp. BHI80-15 [AJ431246]	83.9
6	Betaproteobacteria	<i>Dechloromonas</i> sp. JM [AF323489]	99.6	<i>Dechloromonas hortensis</i> MA-1 [AY277621]	98.1
9	Spirochaetes	<i>Leptospira wolbachii</i> CDC [AY631879]	99.9		
12	Acidobacteria	uncultured bacterium CT1C1AA08 [JQ426388]	99.2	<i>Blastocatella fastidiosa</i> A2-16 [JQ309130]	85.3
15	Betaproteobacteria	uncultured bacterium B67 [FJ660535] WW	99.8	<i>Sulfuritalea hydrogenivorans</i> DSM 22779 [AB552842]	98.4
16	Firmicutes	<i>Bacillus cereus</i> BCwr [HE660038]	99.8		
23	Betaproteobacteria	<i>Zoogloea resiniphila</i> DhA-35 [AJ011506]	99.8		
24	Betaproteobacteria	uncultured bacterium MACA-OC25 [GQ500877]	99.1	<i>Georgfuchsia toluolica</i> G5G6 [EF219370]	95.3
32	Alphaproteobacteria	uncultured bacterium RS-A100 [KC541052]	99.0	<i>Rhodobacter</i> sp. EMB 174 [DQ413163]	97.2
33	Betaproteobacteria	uncultured bacterium KIST-JJY046 [EF654714]	99.0	<i>Dechlorosoma</i> sp. SDGM [AF170349]	93.7
35	Alphaproteobacteria	<i>Nordella</i> sp. P-58 [AM411926]	99.5	<i>Nordella oligomobilis</i> OT1 [AB272321]	98.9
40	Acidobacteria	uncultured bacterium pLW-59 [DQ066997]	99.3	<i>Geothrix fermentans</i> H5 [U41563]	96.4
46	Betaproteobacteria	<i>Methyloversatilis universalis</i> EHg5 [AY436796]	99.9		
58	Bacteroidetes	<i>Runella</i> sp. NBRC 15129 [AB680775]	99.7	<i>Runella slithyformis</i> (T)[M62786]	97.1

a) Phylogenetic affiliations are based on RDP Seqmatch tool.

b) Similarity reports the percent sequence identity over all pairwise comparable positions.

**Table 20:** Phylogenetic classification of phylotypes detected within the immobilized microbial communities of the 31 L PBR pilot plant.

Band #	Phylum <sup>a)</sup>	Family <sup>a)</sup>	Closest relative	%ID <sup>b)</sup>	Closest described	%ID <sup>b)</sup>
1	Actinobacteria	<i>Nocardiaceae</i>			<i>Rhodococcus aetherivorans</i> (T); 10bc312 [AF447391]	100
2	Bacteroidetes	<i>Cryomorphaceae</i>	uncultured <i>Bacteroidetes</i> bacterium; JG35+U2A-AG22 [AM114444]	98.6	<i>Owenweeksia hongkongensis</i> DSM 17368 [HQ697914]	89
3	Betaproteobacteria	<i>Oxalobacteraceae</i>			<i>Massilia timonae</i> (T); UR/MT9; [U54470]	99.8
4	Bacteroidetes	-	uncultured bacterium; 82 [FJ623342]	99.5	<i>Ohtaekwangia koreensis</i> (T); 3B-2 [GU117702]	92.4
5	Alphaproteobacteria	<i>Hyphomicrobiaceae</i>			<i>Devosia insulae</i> (T); DS-56; EF012357 [EF012357]	100
6	Betaproteobacteria	<i>Comamonadaceae</i>			<i>Comamonas testosteroni</i> (T); [M11224]	100
7	Betaproteobacteria	<i>Rhodocyclaceae</i>			<i>Sulfuritalea hydrogenivorans</i> (T); DSM 22779; [AB552842]	96.5
8	Betaproteobacteria	<i>Rhodocyclaceae</i>			<i>Zoogloea resiniphila</i> (T); type strain: DhA-35=ATCC 700687; [AJ011506]	96.2
9	Betaproteobacteria	<i>Comamonadaceae</i>			<i>Acidovorax soli</i> (T); BL21; [FJ599672]	99.3
10	Betaproteobacteria	<i>Comamonadaceae</i>			<i>Acidovorax soli</i> (T); BL21; [FJ599672]	99.8
11	Gammaproteobacteria	<i>Pseudomonadaceae</i>			<i>Rhizobacter fulvus</i> (T); Gsoil 322; [AB245356]	99.7
12	Chloroflexi	<i>Anaerolineaceae</i>	uncultured bacterium; FFCH13762; [EU134114]	98.9		
13	Actinobacteria	<i>Nocardiaceae</i>			<i>Rhodococcus aetherivorans</i> (T); 10bc312 [AF447391]	99.8

a) Phylogenetic affiliations are based on RDP Seqmatch tool.

b) Similarity reports the percent sequence identity over all pairwise comparable positions.

**Table 21.** Phylogenetic classification of indicator OTUs detected in the total community libraries.

<b>Taxon (OTU)<sup>a</sup></b>	<b>Closest RDP SeqMatch Type Strain of the OTU representative seq.</b>	<b>Accession No.</b>	<b>Similarity score<sup>b</sup></b>	<b>Habitat</b>	<b>P-value</b>
Acidobacteria Gp1 <b><i>Terriglobus</i></b>	<i>Terriglobus aquaticus</i> 03SUJ4	HQ436501	0.856	BFtot; Wtot	0.083
Acidobacteria Gp3 <b><i>unclassified</i></b>	<i>Bryobacter aggregatus</i> MPL3	AM162405	0.920	BFtot; WFtot; Wtot; Btot	0.072
Acidobacteria Gp4 <b><i>unclassified</i></b>	<i>Blastocatella fastidiosa</i> A2-16	JQ309130	0.937	BFtot; WFtot; Wtot	0.093
Actinobacteria Acidimicrobineae <b><i>Aciditerrimonas</i></b>	<i>Aciditerrimonas ferrireducens</i> IC-180	AB517669	0.94	Btot	0.034
Acidimicrobiaceae <b><i>Ilumatobacter</i></b>	<i>Ilumatobacter fluminis</i> YM22-133	AB360343	0.936	Btot; Wtot	0.032
Cellulomonadaceae <b><i>unclassified</i></b>	<i>Actinotalea fermentans</i> DSM 3133	X79458	0.990	Btot; WFtot; Wtot	0.032
Cryptosporangiaceae <b><i>Cryptosporangium</i></b>	<i>Cryptosporangium minutisporangium</i> IFO 15962T	AB037007	0.944	BFtot; WFtot; Wtot	0.071
Gaiellaceae <b><i>Gaiella</i></b>	<i>Gaiella occulta</i> F2-233	JF423906	0.926	Btot	0.018
Iamiaceae <b><i>Iamia</i></b>	<i>Iamia majanohamensis</i> NBRC 102561	AB360448	0.930	BFtot; Btot; Wtot	0.028
Intrasporangiaceae <b><i>Knoellia</i></b>	<i>Knoellia subterranea</i> HKI 0120	AJ294413	0.996	Btot; WFtot; Wtot	0.082
Microbacteriaceae <b><i>Microbacterium</i></b>	<i>Microbacterium laevaniformans</i> DSM 20140	Y17234	0.996	Btot; WFtot; Wtot	0.021
Micrococcaceae <b><i>Arthrobacter</i></b>	<i>Arthrobacter equi</i> IMMIB L-1606	FN673551	0.996	Btot; WFtot; Wtot	0.021
Nocardioideae <b><i>Nocardioides</i></b>	<i>Nocardioides terrigena</i> DS-17	EF363712	0.973	Btot; WFtot; Wtot	0.055
Streptomycetaceae <b><i>Streptomyces</i></b>	<i>Streptomyces aureocirculatus</i> IFO 13018	CSSP728	0.891	BFtot; Btot; Wtot	0.012
Alphaproteobacteria Caulobacteraceae <b><i>Phenylobacterium</i></b>	<i>Phenylobacterium lituiforme</i> FaiI3	AY534887	0.963	Wtot	0.016
Rhizomicrobium <b><i>Rhizomicrobium</i></b>	<i>Rhizomicrobium palustre</i> A48	AB081581	0.922	Wtot	0.077
Rhodobiaceae <b><i>Parvibaculum</i></b>	<i>Parvibaculum lavamentivorans</i> DS-1	AY387398	0.918	BFtot; Btot; Wtot	0.017

<i>Rhodospirillaceae</i>					
<b><i>Caenispirillum</i></b>	<i>Caenispirillum salinarum</i> AK4	FN995238	0.8	Wtot	0.016
<b><i>Dongia</i></b>	<i>Dongia mobilis</i> LM22	FJ455532	0.953	BFtot	0.021
<b><i>Oceanibaculum</i></b>	<i>Oceanibaculum indicum</i> P24	EU656113	0.896	BFtot; Btot; Wtot	0.096
<b><i>Skermanella</i></b>	<i>Skermanella aerolata</i> 5416T-32	DQ672568	0.875	BFtot; Btot; Wtot	0.069
<i>Sphingomonadaceae</i>					
<b><i>Novosphingobium</i></b>	<i>Novosphingobium lentum</i> MT1	AJ303009	0.965	WFtot	0.017
<b><i>Sphingobium</i></b>	<i>Sphingobium chlorophenicum</i> ATCC 33790	X87161	0.988	BFtot	0.021
<b><i>Sphingopyxis</i></b>	<i>Sphingopyxis panaciterrulae</i> DCY34	EU075217	0.963	BFtot; Btot; WFtot	0.016
Anaerolineae					
<i>Anaerolineaceae</i>					
<b><i>Bellilinea</i></b>	<i>Bellilinea caldifistulae</i> GOMI-1	AB243672	0.818	BFtot	0.021
<b><i>Leptolinea</i></b>	<i>Leptolinea tardivitalis</i> YMTK-2	AB109438	0.908	BFtot; Btot; Wtot	0.048
<b><i>Longilinea</i></b>	<i>Longilinea arvoryzae</i> KOMI-1	AB243673	0.856	BFtot; Wtot	0.009
Armatimonadetes gp5					
<i>Fimbriimonadaceae</i>					
<b><i>Fimbriimonas</i></b>	<i>Fimbriimonas ginsengisoli</i> Gsoil 348	GQ339893	0.906	BFtot; Wtot	0.023
Bacteroidetes					
<b><i>Flexibacter</i></b>	<i>Flexibacter</i> sp. AMV16	FN396961	0.889	BFtot; Wtot	0.009
<b><i>Ohtaekwangia</i></b>	<i>Ohtaekwangia koreensis</i> 3B-2	GU117702	0.998	BFtot; Btot; Wtot; WFtot	0.016
<b><i>Ohtaekwangia</i></b>	<i>Ohtaekwangia kribbensis</i> 10AO	GU117703	0.969	BFtot; Btot; Wtot; Wftot	0.009
Bacteroidia					
<i>Sphingobacteriaceae</i>					
<b><i>Solitalea</i></b>	<i>Solitalea koreensis</i> R2A36-4	EU787448	0.854	Wtot	0.016
Betaproteobacteria					
<i>Alcaligenaceae</i>					
<b><i>Achromobacter</i></b>	<i>Achromobacter xylosoxidans</i> DSM 10346	Y14908	0.996	WFtot	0.017
<i>Burkholderiaceae</i>					
<b><i>Burkholderia</i></b>	<i>Burkholderia multivorans</i> LMG 13010T	Y18703	0.926	BFtot; Btot; Wtot	0.029
<b><i>Burkholderia</i></b>	<i>Burkholderia rhizoxinica</i> HKI 454	AJ938142	0.939	BFtot; Wtot	0.033
<b><i>Burkholderia</i></b>	<i>Burkholderia terrae</i> KMY02	AB201285	0.945	BFtot; Btot; Wtot	0.060
<b><i>Pandoraea</i></b>	<i>Pandoraea oxalativorans</i> TA25	AB469785	0.930	Wtot	0.030
<b><i>Pandoraea</i></b>	<i>Pandoraea pulmonicola</i> LMG 18106	AF139175	0.955	BFtot; Wtot	0.009
<b><i>Pandoraea</i></b>	<i>Pandoraea thiooxydans</i> ATSB16	EF397578	0.926	BFtot; Wtot	0.038
<i>Comamonadaceae</i>					
<b><i>unclassified</i></b>	<i>Variovorax boronicumulans</i> BAM-48	AB300597	0.986	BFtot; Btot; Wtot	0.065
<i>Hydrogenophilaceae</i>					
<b><i>Sulfuricella</i></b>	<i>Sulfuricella denitrificans</i> NBRC 105220	AB506456	0.959	BFtot; Wtot	0.009
<i>Methylophilaceae</i>					
<b><i>Methylophilus</i></b>	<i>Methylophilus methylotrophus</i> NCIMB 10515	AB193724	0.955	BFtot; Btot; Wtot	0.074
<b><i>Methylophilus</i></b>	<i>Methylophilus rhizosphaerae</i> (T)	EU194887	0.949	BFtot	0.021

<i>Neisseriaceae</i>					
<b><i>Aquaspirillum</i></b>	<i>Aquaspirillum arcticum</i> IAM 14963	AB074523	0.975	BFtot; Btot; Wtot	0.086
<i>Nitrosomonadaceae</i>					
<b><i>Nitrospira</i></b>	<i>Nitrospira multiformis</i> ATCC 25196	CP000103	0.992	BFtot; Btot; Wtot; WFtot	0.011
<i>Oxalobacteraceae</i>					
<b><i>Herbaspirillum</i></b>	<i>Herbaspirillum rubrisubalbicans</i> ICMP 5777	AF137508	0.959	Btot	0.018
<i>Rhodocyclaceae</i>					
<b><i>Georgfuchsia</i></b>	<i>Georgfuchsia toluolica</i> G5G6	EF219370	0.953	BFtot; Btot; Wtot	0.065
<b><i>Methyloversatilis</i></b>	<i>Methyloversatilis universalis</i> FAM5	DQ442273	0.994	BFtot; Wtot	0.009
<b><i>Sulfuritalea</i></b>	<i>Sulfuritalea hydrogenivorans</i> DSM 22779	AB552842	0.951	BFtot; Btot; Wtot	0.017
<b><i>Thauera</i></b>	<i>Thauera chlorobenzoica</i> 3CB-1	AF123264	0.924	BFtot	0.021
<i>Caldilineae</i>					
<i>Caldilineaceae</i>					
<b><i>Caldilinea</i></b>	<i>Caldilinea aerophila</i> STL-6-O1	AB067647	0.820	BFtot; WFtot; Wtot	0.072
<i>Clostridia</i>					
<i>Lachnospiraceae</i>					
<b><i>Lachnospiracea</i></b>	<i>Eubacterium uniforme</i> X3C39	GU269550	0.784	BFtot; WFtot; Wtot	0.068
<i>Peptococcaceae</i>					
<b><i>Desulfosporosinus</i></b>	<i>Desulfosporosinus lacus</i> STP12	AJ582757	0.845	BFtot; Wtot	0.009
<i>Cytophagia</i>					
<i>Cytophagaceae</i>					
<b><i>Flexibacter</i></b>	<i>Flexibacter roseolus</i> IFO 16486	AB078062	0.825	BFtot	0.021
<i>Deltaproteobacteria</i>					
<i>Bacteriovoracaceae</i>					
<b><i>Peredibacter</i></b>	<i>Peredibacter starrii</i> A3.12	AF084852	0.965	Btot; WFtot; Wtot	0.042
<i>Bdellovibrionaceae</i>					
<b><i>Bdellovibrio</i></b>	<i>Bdellovibrio bacteriovorus</i> HD 100	AJ292759	0.881	Btot; Wtot	0.016
<i>Desulfobacteraceae</i>					
<b><i>Desulfobotulus</i></b>	<i>Desulfobotulus sapovorans</i> DSM2055	FR733666	0.847	BFtot; Wtot	0.053
<i>Desulfobulbaceae</i>					
<b><i>Desulforhopalus</i></b>	<i>Desulforhopalus singaporensis</i> S'pore T1	AF118453	0.875	BFtot; Btot; Wtot	0.079
<i>Desulfonatronaceae</i>					
<b><i>Desulfonatronum</i></b>	<i>Desulfonatronum thioautotrophicum</i> ASO4-1	FJ469577	0.798	Wtot	0.016
<i>Desulfovibrionaceae</i>					
<b><i>Desulfovibrio</i></b>	<i>Desulfovibrio oceani</i> I.8.1	FJ655907	0.794	BFtot; Wtot	0.009
<i>Desulfuromonadaceae</i>					
<b><i>Pelobacter</i></b>	<i>Pelobacter propionicus</i> DSM 2379	CP000482	0.893	BFtot; Wtot	0.009
<i>Geobacteraceae</i>					
<b><i>Geobacter</i></b>	<i>Geobacter metallireducens</i> GS-15	L07834	0.871	BFtot; Wtot	0.039
<b><i>Geobacter</i></b>	<i>Geobacter bremensis</i> Dfr1	U96917	0.979	Wtot	0.045
<i>Haliangiaceae</i>					

<b>Haliangium</b>	<i>Haliangium ochraceum</i> SMP-2	AB016470	0.901	BFtot; Btot; Wtot	0.017
<b>Haliangium</b>	<i>Haliangium tepidum</i> SMP-10	AB062751	0.903	BFtot; Wtot	0.009
<b>Haliangium</b>	<i>Haliangium ochraceum</i> SMP-2	AB016470	0.911	BFtot; Wtot	0.009
<i>Myxococcaceae</i>					
<b>Corallococcus</b>	<i>Corallococcus macrosporus</i> DSM 14697	AJ811623	0.881	BFtot; Wtot	0.009
<b>Pyxidicoccus</b>	<i>Pyxidicoccus fallax</i> DSM 14698	DQ768123	0.873	BFtot; Wtot	0.009
<b>unclassified</b>	<i>Pyxidicoccus fallax</i> DSM 14698	DQ768123	0.871	BFtot; Wtot	0.053
<i>Nannocystaceae</i>					
<b>Enhygromyxa</b>	<i>Enhygromyxa salina</i> SHK-1	AB097590	0.973	BFtot; Wtot	0.044
<i>Phaselicystidaceae</i>					
<b>Phaselicystis</b>	<i>Phaselicystis flava</i> SBKo001	EU545827	0.928	BFtot; Wtot	0.088
<i>Polyangiaceae</i>					
<b>Byssovorax</b>	<i>Byssovorax cruenta</i> By c2	AJ833647	0.907	BFtot; Btot; Wtot	0.064
<b>Chondromyces</b>	<i>Chondromyces robustus</i> Cm a13	AJ233942	0.910	BFtot; Wtot	0.044
<b>Jahnella</b>	<i>Jahnella thaxteri</i> Pl t4	GU207876	0.967	BFtot; Btot; Wtot	0.017
<b>unclassified</b>	<i>Byssovorax cruenta</i> By c2	AJ833647	0.883	BFtot; Btot; Wtot	0.017
<i>Syntrophaceae</i>					
<b>Desulfomonile</b>	<i>Desulfomonile tiedjei</i> DSM 6799	AM086646	0.862	BFtot; Wtot	0.043
Elusimicrobia					
<i>Elusimicrobiaceae</i>					
<b>Elusimicrobium</b>	<i>Elusimicrobium minutum</i> Pei191	AM490846	0.832	BFtot; Btot; Wtot	0.081
Erysipelotrichia					
<i>Erysipelotrichaceae</i>					
<b>Turicibacter</b>	<i>Turicibacter sanguinis</i> (T)	AF349724	0.727	Wtot	0.016
Fibrobacteria					
<i>Holophagaceae</i>					
<b>Geothrix</b>	<i>Geothrix fermentans</i> H5	U41563	0.819	BFtot; Btot; Wtot	0.015
Fimbriimonadia					
<i>Fimbriimonadaceae</i>					
<b>Fimbriimonas</b>	<i>Fimbriimonas ginsengisoli</i> Gsoil 348	GQ339893	0.89	BFtot; Wtot	0.044
Flavobacteria					
<i>Cryomorphaeae</i>					
<b>Owenweeksia</b>	<i>Owenweeksia hongkongensis</i> UST20020801	AB125062	0.887	BFtot; Btot; Wtot	0.017
<b>Wandonia</b>	<i>Wandonia haliotis</i> Haldis-1	FJ424814	0.865	BFtot	0.021
<i>Flavobacteriaceae</i>					
<b>Elizabethkingia</b>	<i>Elizabethkingia miricola</i> GTC862	AB071953	0.984	Btot; WFtot	0.007
<b>Flavobacterium</b>	<i>Flavobacterium terrigena</i> DS-20	DQ889724	0.984	Btot	0.018
Gammaproteobacteria					
<i>Acidithiobacillaceae</i>					
<b>Acidithiobacillus</b>	<i>Acidithiobacillus caldus</i> DSM 8584	Z29975	0.766	Wtot	0.026
<i>Alteromonadaceae</i>					

<i>Haliea</i>	<i>Haliea salexigens</i> 3X/A02/235	AY576769	0.936	BFtot; Btot; Wtot	0.081
Coxiellaceae					
<i>Aquicella</i>	<i>Aquicella siphonis</i> SGT-108	AY359283	0.953	BFtot; WFtot; Wtot	0.054
<i>Coxiella</i>	<i>Coxiella burnetii</i> ATCC VR-615	HM208383	0.901	Btot	0.018
Ectothiorhodospiraceae					
<i>Ectothiorhodosinus</i>	<i>Ectothiorhodosinus mongolicus</i> M9	AY298904	0.893	WFtot; Wtot; Bftot	0.031
<i>Natronocella</i>	<i>Natronocella acetinitrilica</i> ANL 6-2	EF103128	0.903	WFtot; Wtot; BFtot; Btot	0.017
Legionellaceae					
<i>Legionella</i>	<i>Legionella quinlivanii</i> NTCT 12433	Z49733	0.961	Btot	0.018
Methylococcaceae					
<i>Methylococcus</i>	<i>Methylococcus capsulatus</i> NCIMB 11853	AJ563935	0.883	BFtot; Btot; Wtot	0.017
Pseudomonadaceae					
<i>Rhizobacter</i>	<i>Rhizobacter dauci</i> H6	AB297965	0.971	Wtot	0.016
Sinobacteraceae					
<i>Panacagrimonas</i>	<i>Panacagrimonas perspica</i> Gsoil 142	AB257720	0.916	Wtot	0.016
<i>Steroidobacter</i>	<i>Steroidobacter denitrificans</i> FS	EF605262	0.953	BFtot; Btot; Wtot	0.009
unclassified					
<i>unclassified</i>	<i>Spongiibacter tropicus</i> CL-CB221	EF988653	0.94	BFtot	0.021
Xanthomonadaceae					
<i>Aquimonas</i>	<i>Aquimonas voraii</i> GPTSA 20	AY544768	0.963	BFtot; WFtot; Wtot	0.021
<i>Arenimonas</i>	<i>Arenimonas metalli</i> CF5-1	HQ698842	0.994	BFtot; WFtot; Wtot	0.018
<i>Dokdonella</i>	<i>Dokdonella soli</i> KIS28-6	EU685334	0.971	Wtot	0.031
<i>Dyella</i>	<i>Dyella soli</i> JS12-10	EU604272	0.965	BFtot; WFtot	0.04
<i>Lysobacter</i>	<i>Lysobacter spongiicola</i> KMM 329	AB299978	0.973	Btot; WFtot	0.019
<i>Pseudoxanthomonas</i>	<i>Pseudoxanthomonas mexicana</i> AMX 26B	AF273082	0.998	Wtot	0.016
<i>Silanimonas</i>	<i>Silanimonas lenta</i> 25-4	AY557615	0.840	Btot	0.018
<i>Stenotrophomonas</i>	<i>Stenotrophomonas maltophilia</i> IAM 12423	AB294553	0.998	Btot; WFtot; Wtot	0.088
Gemmatimonadetes					
Gemmatimonadaceae					
<i>Gemmatimonas</i>	<i>Gemmatimonas aurantiaca</i> T-27	AB072735	0.914	BFtot; Btot; Wtot	0.040
Holophagae					
Holophagaceae					
<i>Geothrix</i>	<i>Geothrix fermentans</i> H5	U41563	0.951	BFtot; Btot; Wtot	0.017
<i>Holophaga</i>	<i>Holophaga foetida</i> TMBS4T	X77215	0.861	BFtot; WFtot; Wtot	0.077
Chlamydiae					
Parachlamydiaceae					
<i>Parachlamydia</i>	<i>Parachlamydia acanthamoebae</i> Bn9	Y07556	0.872	BFtot; Btot; Wtot	0.018
<i>Neochlamydia</i>	<i>Neochlamydia hartmannellae</i> A1Hsp	AF177275	0.916	Btot	0.065
Simkaniaceae					
<i>Simkania</i>	<i>Simkania negevensis</i> Z	U68460	0.877	Wtot	0.016
Chthonomonadetes					

<i>Chthonomonadaceae</i>					
<b><i>Chthonomonas</i></b>	<i>Chthonomonas calidirosea</i> T49	AM749780	0.84	BFtot; Wtot	0.047
Ignavibacteria					
<i>Ignavibacteriaceae</i>					
<b><i>Ignavibacterium</i></b>	<i>Ignavibacterium album</i> Mat9-16	AB478415	0.862	BFtot; WFtot; Wtot	0.068
Opitutae					
<i>Opitutaceae</i>					
<b><i>Opitutus</i></b>	<i>Opitutus terrae</i> PB90-1	AJ229235	0.922	BFtot; Btot; Wtot	0.017
Planctomycetia					
<i>Planctomycetaceae</i>					
<b><i>Blastopirellula</i></b>	<i>Blastopirellula marina</i> IFAM 1313	X62912	0.911	BFtot; Btot	0.055
<b><i>Gemmata</i></b>	<i>Gemmata obscuriglobus</i> UQM 2246	X56305	0.900	BFtot; Wtot	0.009
<b><i>Pirellula</i></b>	<i>Pirellula staleyii</i> DSM 6068	CP001848	0.916	BFtot; Wtot	0.034
<b><i>Thermovenabulum</i></b>	<i>Thermovenabulum ferriorganovororum</i> Z-9801	AY033493	0.803	Wtot	0.075
<b><i>Zavarzinella</i></b>	<i>Zavarzinella formosa</i> A10	AM162406	0.907	BFtot	0.062
Spartobacteria					
<b><i>Spartobacteria</i></b>	<i>Chthoniobacter flavus</i> Ellin428	AY388649	0.933	BFtot	0.090
<b><i>Spartobacteria</i></b>	<i>uncultivated soil bacterium clone C019</i>	AF013522	0.897	Btot; WFtot; Wtot	0.082
Sphingobacteriia					
<i>Cytophagaceae</i>					
<b><i>Runella</i></b>	<i>Runella slithyformis</i> ATCC 29530	M62786	0.967	WFtot; Wtot	0.049
<b><i>Solitalea</i></b>	<i>Solitalea koreensis</i> R2A36-4	EU787448	0.858	Bftot; Btot	0.011
<i>Chitinophagaceae</i>					
<b><i>Flavisolibacter</i></b>	<i>Flavisolibacter</i> sp. HY-50R	HM130561	0.942	Btot; Wtot	0.088
<b><i>Hydrotalea</i></b>	<i>Hydrotalea flava</i> CCUG 51397	FN665659	0.889	BFtot; Btot; Wtot	0.017
<b><i>Chitinophaga</i></b>	<i>Chitinophaga japonensis</i> IFO 16041	AB078055	0.882	Wtot	0.054
<b><i>Chitinophaga</i></b>	<i>Chitinophaga ginsengisoli</i> Gsoil 052	AB245374	0.922	BFtot; Wtot	0.038
<b><i>Niastella</i></b>	<i>Niastella yeongjuensis</i> GR20-13	DQ244076	0.988	WFtot; Wtot	0.011
<b><i>Parasegetibacter</i></b>	<i>Parasegetibacter luojiensis</i> RHYL-37	EU877263	0.955	WFtot; Wtot	0.062
<b><i>Sediminibacterium</i></b>	<i>Sediminibacterium ginsengisoli</i> DCY13	EF067860	0.887	BFtot; Wtot	0.087
<b><i>Terrimonas</i></b>	<i>Terrimonas pekingensis</i> QH	JF834159	0.957	BFtot; Btot; Wtot	0.017
<i>Saprospiraceae</i>					
<b><i>Lewinella</i></b>	<i>Lewinella lutea</i> FYK2402M69	AB301494	0.891	BFtot; Wtot	0.009
<b><i>Lewinella</i></b>	<i>Lewinella marina</i> MKG-38	AB301495	0.852	BFtot; Wtot	0.024
		ATCC23147;	0.871	Btot	0.018
<b><i>Lewinella</i></b>	<i>Lewinella nigricans</i>	AF039294			
<b><i>Saprospira</i></b>	<i>Saprospira</i> sp. CNJ640	AY527410	0.932	BFtot	0.064
<i>Sphingobacteriaceae</i>					
<b><i>Arcticibacter</i></b>	<i>Arcticibacter svalbardensis</i> MN12-7	JQ396621	0.965	WFtot; Wtot	0.054
<b><i>Pedobacter</i></b>	<i>Pedobacter oryzae</i> N7	EU109726	0.963	BFtot; Btot; Wtot	0.034
<b><i>Pedobacter</i></b>	<i>Pedobacter glucosidilyticus</i> 1-2	EU585748	0.858	BFtot; Btot; Wtot	0.021

<b><i>Pedobacter</i></b>	<i>Pedobacter bauzanensis</i> BZ42	GQ161990	0.867	Wtot	0.090
<b><i>Pedobacter</i></b>	<i>Pedobacter boryungensis</i> BR-9	HM640986	0.887	BFtot; Btot; Wtot	0.017
<b><i>Solitalea</i></b>	<i>Solitalea koreensis</i> R2A36-4	EU787448	0.912	BFtot; Wtot	0.013
<b><i>Sphingobacterium</i></b>	<i>Sphingobacterium spiritivorum</i> NCTC 11386	EF090267	0.992	WFtot	0.017
Verrucomicrobiae					
<i>Verrucomicrobiaceae</i>					
<b><i>Verrucomicrobium</i></b>	<i>uncultured Verrucomicrobia bacterium</i> VC12	AY211073	0.811	BFtot; Btot; Wtot	0.072
Xanthomonadales					
<i>Xanthomonadaceae</i>					
<b><i>Frateuria</i></b>	<i>Frateuria aurantia</i> IFO3245	AB091194	0.808	BFtot; Wtot	0.044

<sup>a</sup>Phylogenetic affiliations are based on Ribosomal Database Project (RDP) Classifier

<sup>b</sup>Similarity reports the percent sequence identity over all pairwise comparable positions.

**Table 22:** The most abundant OTUs in SIP libraries.

Taxon (OTU) <sup>a</sup>	Closest RDP SeqMatch Type Strain of the OTU representative seq.	GenBank Accession No.	Similarity score <sup>b</sup>	Mean no. of valid reads per treatment									
				B1	B2	BF1	BF2	W1	W2	WF1	WF2		
Alphaproteobacteria													
<i>Caulobacterales</i>													
<b><i>Brevundimonas</i></b>	<i>Brevundimonas vesicularis</i> LMG 2350	AJ227780	0.996	0	0	11	21	10	45	0	0		
Betaproteobacteria													
<i>Rhodocyclales</i>													
<b><i>Georgfuchsia</i></b>	<i>Georgfuchsia toluolica</i> G5G6	EF219370	0.930	35	40	1	0	1	0	1	1		
<i>Burkholderiales</i>													
<b><i>Acidovorax</i></b>	<i>Acidovorax defluvii</i> BSB411	Y18616	0.998	460	555	138	66	458	2	563	242		
<b><i>Hydrogenophaga</i></b>	<i>Hydrogenophaga taeniospiralis</i> ATCC49743	AF078768	0.994	26	37	32	1	8	0	21	228		
<b><i>Polaromonas</i></b>	<i>Polaromonas jejuensis</i> JS12-13	EU030285	0.998	10	12	2	2	11	0	2	2		
<b><i>Achromobacter/Bordetella</i></b>	<i>Achromobacter xylosoxidans</i> DSM 10346	Y14908	0.996	0	0	20	0	16	0	0	0		
<b>unclas. <i>Comamonadaceae</i></b>	<i>Rhodoferax antarcticus</i> ANT.BR	GU233447	0.986	49	64	5	2	7	0	16	27		
<i>Methylophilales</i>													
<b><i>Methylophilus</i></b>	<i>Methylotenera mobilis</i> JLW8	DQ287786	0.994	11	15	6	0	1	0	2	10		
Gammaaproteobacteria													
<i>Pseudomonadales</i>													
<b><i>Pseudomonas</i></b>	<i>Pseudomonas</i> spp.	multiple hits	0.998	1609	1311	68	13	308	49	853	1455		
<b><i>Rhizobacter</i></b>	<i>Rhizobacter fulvus</i> Gsoil 322	AB245356	0.998	19	25	2	0	1	0	0	4		
<b>unclassified</b>	<i>Marinobacter lutaoensis</i> T5054	AF288157	0.940	11	20	0	0	4	0	1	11		
Deltaproteobacteria													
<i>Bdellovibrionales</i>													
<b><i>Bdellovibrio</i></b>	<i>Bdellovibrio bacteriovorus</i> HD 100	AJ292759	0.947	64	130	0	0	1	0	0	1		
Bacteroidetes													
<i>Flavobacteriales</i>													
<b><i>Elizabethkingia</i></b>	<i>Elizabethkingia miricola</i> GTC862	AB071953	0.984	0	0	226	49	0	0	0	0		
Actinobacteria													
<i>Actinomycetales</i>													
<b><i>Arthrobacter</i></b>	<i>Arthrobacter equi</i> IMMIB L-1606	FN673551	0.996	0	6	0	0	3	0	15	45		

<sup>a</sup>Phylogenetic affiliations based on RDP Classifier; <sup>b</sup>Similarity reports the percent sequence identity over all pairwise comparable positions.

**Table 23:** Indicator OTU analysis (P value 0.05) for SIP data grouped by (i) bulk soil/willow, (ii) fertilized/non-fertilized soil, (iii) incubation time points 1 and 2.

<b>Taxon (OTU)<sup>a</sup></b>	<b>Closest RDP SeqMatch Type Strain of the OTU representative seq.</b>	<b>GenBank Accession No.</b>	<b>Similarity score<sup>b</sup></b>	<b>Indicator for treatment</b>	<b>Square root of IndVal</b>
Alphaproteobacteria					
<i>Rhizobiales</i>					
<b><i>Andersenella</i></b>	<i>Andersenella baltica</i> BA141	AM712634	0.925	time 2	0.603
<i>Sphingomonadales</i>					
<b><i>Sphingobium</i></b>	<i>Sphingobium chlorophenicum</i> ATCC	X87161	0.988	willow	0.743
Betaproteobacteria					
<i>Burkholderiales</i>					
<b><i>Hermiimonas</i></b>	<i>Hermiimonas arsenicoxydans</i> ULPAs1	AY728038	0.977	willow	0.739
<b><i>Massilia</i></b>	<i>Massilia aerilata</i> 5516S-11	EF688526	0.986	non-fertilized	0.674
<i>Methylophilales</i>					
<b><i>Methylovorus</i></b>	<i>Methylophilus rhizosphaerae</i> CBMB127	EU194887	0.949	willow	0.603
<i>Rhodocyclales</i>					
<b><i>Methyloversatilis</i></b>	<i>Methyloversatilis universalis</i> FAM5	DQ442273	0.994	fertilized	0.684
Gammaproteobacteria					
<i>Pseudomonadales</i>					
<b><i>Rhizobacter</i></b>	<i>Rhizobacter fulvus</i> Gsoil 322	AB245356	0.998	non-fertilized	0.803
incertae sedis					
<b>unclassified</b>	<i>Thiopfundum hispidum</i> gps61	AB266389	0.930	bulk soil	0.707
Deltaproteobacteria					
<i>Bdellovibrionales</i>					
<b><i>Bdellovibrio</i></b>	<i>Bdellovibrio bacteriovorus</i> HD 100	AJ292759	0.947	non-fertilized	0.796
<b><i>Bdellovibrio</i></b>	<i>Bdellovibrio bacteriovorus</i> HD 100	AJ292759	0.977	time 2	0.667
<i>Myxococcales</i>					
<b><i>Chondromyces</i></b>	<i>Chondromyces robustus</i> Cm a13	AJ233942	0.965	non-fertilized	0.603
Acidobacteria					
Gp4					
<b>unclassified</b>	<i>Blastocatella fastidiosa</i> A2-16	JQ309130	0.929	willow	0.661
Bacteroidetes					
<i>Flavobacteriales</i>					
<b><i>Flavobacterium</i></b>	<i>Flavobacterium</i> spp.			willow	0.749
<b><i>Flavobacterium</i></b>	<i>Flavobacterium weaverense</i> AT1042	AY581114	0.994	time 2	0.603
<i>Sphingobacteriales</i>					

Taxon (OTU) <sup>a</sup>	Closest RDP SeqMatch Type Strain of the OTU representative seq.	GenBank Accession No.	Similarity score <sup>b</sup>	Indicator for treatment	Square root of IndVal
<b>unclas. Saprospiraceae</b>	<i>Lewinella nigricans</i> ATCC23147	AF039294	0.875	time 2	0.642
<b>unclassified</b>	<i>Lewinella nigricans</i> ATCC23147	AF039294	0.876	non-fertilized	0.603
Actinobacteria					
Actinomycetales					
<b>Arthrobacter</b>	<i>Arthrobacter equi</i> IMMIB L-1606	FN673551	0.996	willow	0.818
<b>Marmoricola</b>	<i>Marmoricola aequoreus</i> SST-45	AM295338	0.980	time 2	0.665
Acidimicrobiales					
<b>Aciditerrimonas</b>	<i>Aciditerrimonas ferrireducens</i> IC-180	AB517669	0.936	time 2	0.603
Chlamydiae					
Chlamydiales					
<b>Neochlamydia</b>	<i>Neochlamydia hartmannellae</i> A1Hsp	AF177275	0.908	willow	0.603

<sup>a</sup>Phylogenetic affiliations are based on Ribosomal Database Project (RDP) Classifier.

<sup>b</sup>Similarity reports the percent sequence identity over all pairwise comparable positions.

**Table 24.** Phylogenetic identification of phylotypes corresponding to bands of Run IV DGGE profiles.

<b>Band</b>	<b>Phylogenetic group</b>	<b>Closet match [accession #]</b>	<b>Identity</b>	<b>Close described bacterium [accession #]</b>	<b>Identity</b>
1	Bacteroidetes	uncultured <i>Leadbetterella</i> sp. CG80 [JN541174]	98 %	<i>Leadbetterella byssophila</i> 4M15 [AY854022]	94 %
2	Alphaproteobacteria	uncultured alpha proteobacterium AS_26_BAC [AB473970]	97 %	<i>Microvirga guangxiensis</i> 25B [NR_044563.1]	88 %
3	Betaproteobacteria	uncultured Comamonadaceae bacterium 62 [HQ184358]	100 %	<i>Acidovorax ebreus</i> TPSY [NR_074591.1]	97 %
4	Betaproteobacteria	<i>Hydrogenophaga</i> sp. EMB 75 [DQ413154]	98 %	<i>Hydrogenophaga flava</i> 2 [NR_028718.1]	97 %
5	Alphaproteobacteria	uncultured alpha proteobacterium AS_26_BAC [AB473970]	93 %	<i>Micavibrio aeruginosavorus</i> ARL-1 [NR_074210.1]	89 %
6	Betaproteobacteria	uncultured bacterium Q7169-HYSO [JN391917]	98 %	<i>Hydrogenophaga caeni</i> EMB71 [NR_043769.1 ]	98 %
7	Betaproteobacteria	<i>Acidovorax ebreus</i> TPSY [NR_074591.1]	96 %		
8	Betaproteobacteria	<i>Leptothrix</i> sp. L10 [AB087571]	99 %	<i>Leptothrix discophora</i> SS-1 [NR_025916.1]	98 %
9	Betaproteobacteria	<i>Zoogloea caeni</i> EMB 43 [DQ413148]	99 %		
10	Gammaproteobacteria	uncultured bacterium H2SRC232 [FM213013]	94 %	<i>Pseudoxanthomonas mexicana</i> AMX 26B [NR_025105.1]	92 %
11	Gammaproteobacteria	<i>Thermomonas</i> sp. R039N [KC252868]	92 %	<i>Thermomonas brevis</i> R-13291 [NR_025578.1]	89 %
12	Gammaproteobacteria	<i>Dokdonella</i> sp. RaM5-2 [AM981200]	98 %	<i>Dokdonella immobilis</i> LM 2-5 [NR_108377.1 ]	93 %
13	Alphaproteobacteria	<i>Meganema perideroedes</i> Gr1 [AF180468]	99 %		

<sup>a</sup>Phylogenetic affiliations are based on Ribosomal Database Project (RDP) Classifier

<sup>b</sup>Similarity reports the percent sequence identity over all pairwise comparable positions

## Literature cited

- Albuquerque M.G.E., Eiroa M., Torres C., Nunes B.R., Reis M.A.M.; (2007) Strategies for the development of a side stream process for polyhydroxyalkanoates (PHA) production from sugar cane molasses. *J Biotechnol*, 130: 411-421.
- Anderson J., McCarty P.L.; (1997) Transformation Yields of Chlorinated Ethenes by a Methanotrophic Mixed Culture Expressing Particulate Methane Monooxygenase. *Appl Environ Microbiol*, 63(2): 687-693.
- Andrews J.H., Harris R.F.; (1986) r- and k-selection and microbial ecology. *Adv Microb Ecol*, 9: 99-147.
- Altschul S.F., Madden T.L., Schäffer A.A., Zhang J., Zhang Z., Miller W., Lipman D.J.; (1997) Gapped BLAST and PSI-BLAST: a new generation of protein database search programs. *Nucleic Acids Res*, 25:3389-3402.
- Alvarez-Cohen L., Speitel Jr. G.E.; (2001) Kinetics of aerobic cometabolism of chlorinated solvents. *Biodegradation*, 12: 105-126.
- Amache R., Sukan A., Safari M., Roy I., Keshavarz T.; (2013) Advances In PHAs Production. AIDIC CONFERENCE SERIES (The Italian Association of Chemical Engineering), Vol. 11, doi: 10.3303/ACOS1311002.
- Ambrosoli R., Petruzzelli L., Minati J.L., Marsan F.A.; (2005) Anaerobic PAH degradation in soil by a mixed bacterial consortium under denitrifying conditions. *Chemosphere*, 60: 1231-1236.
- Anzai Y., Kim H., Park J.Y., Wakabayashi H., Oyaizu H.; (2000) Phylogenetic affiliation of the pseudomonads based on 16S rRNA sequence. *Int J Syst Evol Microbiol*, 50: 1563-1589.
- Arp D.J., Yeager C.M., Hyman M.R.; (2001) Molecular and cellular fundamentals of aerobic cometabolism of trichloroethylene. *Biodegradation*, 12:81-103.
- Bae H.S., Rash B.A., Rainey F.A., Nobre M.F., Tiago I., da Costa M.S., Moe W.M.; (2007) Description of *Azospira restricta* sp. nov., a nitrogen-fixing bacterium isolated from groundwater. *Int J Syst Evol Microbiol*, 57: 1521–1526.
- Baker G.C., Smith J.J., Cowan D.A.; (2003) Review and re-analysis of domain specific 16S primers. *J Microbiol Methods*, 55: 541-555.
- Baldwin B.R., Nakatsu C.H., Nies L.; (2003) Detection and enumeration of aromatic oxygenase genes by multiplex and real-time PCR. *Appl Environ Microbiol*, 69: 3350-3358.
- Bale A.S., Barone Jr. S., Scott C.S., Cooper G.S.; (2011) A review of potential neurotoxic mechanisms among three chlorinated organic solvents. *Toxicol Appl Pharm*, 255(1): 113-126.
- Ballschmiter K.; (2003) Pattern and sources of naturally produced organohalogens in the marine environment: biogenic formation of organohalogens. *Chemosphere*, 52(2): 313-324.
- Bamforth S.M., Singleton I.; (2005) Bioremediation of polycyclic aromatic hydrocarbons: current knowledge and future directions. *J Chem Technol Biotechnol*, 80: 723-736.
- Beccari M., Bertin L., Dionisi D., Fava F., Lampis S., Majone M., Valentino F., Vallini G., Villano M.; (2009) Exploiting olive oil mill effluents as a renewable resource for production of biodegradable polymers through a combined anaerobic-aerobic process. *J Chem Technol Biotechnol*, 84: 901-908.
- Behnam F., Vilcinskas A., Wagner M., Stoecker K.; (2012) A Straightforward DOPE (Double Labeling of Oligonucleotide Probes)-FISH (Fluorescence *In Situ* Hybridization) Method for Simultaneous Multicolor Detection of Six Microbial Populations. *Appl Environ Microbiol*, 78(15): 5138-5142.
- Bell T.H., Yergeau E., Martineau C., Juck D., Whyte L.G., Greer C.W.; (2011) Identification of nitrogen-incorporating bacteria in petroleum-contaminated Arctic soils by using <sup>15</sup>N DNA-based stable isotope probing and pyrosequencing. *Appl Environ Microbiol*, 1(77): 4163-4171.
- Bengtsson S., Werker A., Christensson M., Welander T.; (2008) Production of polyhydroxyalkanoates by activated sludge treating a paper mill wastewater. *Bioresour Technol*, 99: 509-516.

- Bento F.M., Camargo F.A.O., Okeke B.C., Frankenberger W.T.; **(2005)** Comparative bioremediation of soils contaminated with diesel oil by natural attenuation, biostimulation and bioaugmentation. *Bioresour Technol*, 96(9): 1049-1055.
- Bernhard A.E., Colbert D., McManus J., Field K.G.; **(2005)** Microbial community dynamics based on 16S rRNA gene profiles in a Pacific Northwest estuary and its tributaries. *FEMS Microbiol Ecol*, 52: 115-128.
- Berry D., Mahfoudh K.M., Wagner M., Loy A.; **(2011)** Barcoded Primers used in Multiplex Amplicon Pyrosequencing Bias Amplification. *Appl Environ Microbiol*, 77(21): 7846-7849.
- Bertin L., Bettini C., Zancaroli G., Fraraccio S., Negroni A., Fava F.; **(2012)** Acclimatation of an anaerobic consortium capable of an effective biomethanization of mechanically-sorted organic fraction of municipal solid waste through a semi-continuous enrichment procedure. *J Chem Technol Biotechnol*, 87(9): 1312-1319.
- Bhatt P., Kumar M.S., Mudliar S., Chakrabarti T.; **(2007)** Biodegradation of chlorinated compounds – A review. *Critical Rev Environ Sci Technol*, 37: 165-198.
- Bhowmik A., Asahino A., Shiraki T., Nakamura K., Takamizawa K.; **(2007)** Dynamic Behaviour of Bacteria in PCE Contaminated Surface During Bioremediation. In: Proceedings of International Symposium on EcoTopia Science, ISETS07.
- Blackert D., Cibrik J., Foster D.; **(2007)** Aerobic soy-based cometabolism of halogenated hydrocarbons in groundwater. In: Proceedings of the Ninth International In Situ and On-Site Bioremediation Symposium. Gavaskar A.R., Silver C.F., (Eds.) Baltimore, Batelle Press, Columbus, vol. 2 pp: 937-945.
- Boschker H.T.S., Nold S.C., Wellsbury P., Bos D., de Graaf W., Pel R., Parkers R.J., Cappenberg T.E.; **(1998)** Direct linking of microbial populations to specific biogeochemical processes by <sup>13</sup>C-labelling of biomarkers. *Nature*, 392: 801-805.
- Bourne D., McDonald I.R., Murrell J.C.; **(2001)** Comparison of *pmoA* PCR Primer Sets as Tools for Investigating Methanotroph Diversity in Three Danish Soils. *Appl Environ Microbiol*, 67(9): 3802-3809.
- Boxall A.; **(2010)** Impacts of emerging contaminants on the environment. In: Ecology of Industrial Pollution, eds. Lesley C. Batty and Kevin B. Hallberg. Published by Cambridge University Press. # British Ecological Society.
- Bradley P.M., Chapelle F.H.; **(1998)** Microbial mineralization of VC and DCE under different terminal electron accepting conditions. *Anaerobe*, 4: 81-87.
- Bradley P.M.; **(2003)** History and ecology of chloroethene biodegradation: a review. *Bioremediation J*, 7: 81-109.
- Bradley P.M., Richmond S., Chapelle F.H.; **(2005)** Chloroethene biodegradation in sediments at 4C. *Appl Environ Microbiol*, 71: 6414-6417.
- Braunegg G., Lefebvre G., Genser K.F.; **(1998)** Polyhydroxyalkanoates, biopolyesters from renewable resources: Physiological and engineering aspects. *J Biotechnol*, 65: 127-161.
- Budde C.F., Riedel S.L., Willis L.B., Rha C., Sinskey A.J.; **(2011)** Production of Poly(3-Hydroxybutyrate-co-3-Hydroxyhexanoate) from Plant Oil by Engineered *Ralstonia eutropha* Strains. *Appl Environ Microbiol*, 77(9): 2847-2854.
- Bugnicourt E., Cinelli P., Lazzeri A., Alvarez V.; **(2014)** Polyhydroxyalkanoate (PHA): Review of synthesis, characteristics, processing and potential applications in packaging. *eXPRESS Polymer Letters*, 8(11): 791-808.
- Bushnell P.J., Shafer T.J., Bale A.S., Boyes W.K., Simmons J.E., Eklund C., Jackson T.L.; **(2005)** Developing an exposure-dose-response model for the acute neurotoxicity of organic solvents: overview and progress on in vitro models and dosimetry. *Environ Toxicol Pharm*, 19(3): 607-614.
- Castilho L.R., Mitchell D.A., Freire D.G.M.; **(2009)** Production of polyhydroxyalkanoates (PHAs) from waste materials and by-products by submerged and solid-state fermentation. *Biores Technol*, 100: 5996-6009.
- Cave M., Falkner K.C., Ray M., Joshi-Barve S., Brock G., Khan R., Bon Homme M., McClain C.J.; **(2010)** Toxicant-associated steatohepatitis in vinyl chloride workers. *Hepatology*, 51(2): 474-481.

- Chang Y.J., Stephen J.R., Richter A.P., Venosa A.D., Bruggemann J., Macnaughton S.J., *et al.*; (2000) Phylogenetic analysis of aerobic freshwater and marine enrichment cultures efficient in hydrocarbon degradation: effect of profiling method. *J Microbiol Methods*, 40: 19-31.
- Chanprateep S.; (2010) Current trends in biodegradable polyhydroxyalkanoates. 110: 621-632.
- Chaudhry Q., Blom-Zandstra M., Gupta S., Joner E.J.; (2005) Utilizing the synergy between plants and rhizosphere microorganisms to enhance breakdown of organic pollutants in the environment. *Environ Sci Pollut Res*, 12: 34-48.
- Chauhan A., Fazlurrahman, Oakeshott J.G., Jain R.K.; (2008) Bacterial metabolism of polycyclic aromatic hydrocarbons: strategies for bioremediation. *Indian J Microbiol*, 48: 95-113.
- Chen S.H., Aitken M.D.; (1999) Salicylate stimulates the degradation of high-molecular weight Polycyclic Aromatic Hydrocarbons by *Pseudomonas saccharophila* P15. *Environ Sci Technol*, 33: 435-439.
- Chen G.Q., Page W.J.; (1997) Production of poly- $\beta$ -hydroxybutyrate by *Azotobacter vinelandii* in a two-stage fermentation process. *Biotechnol Tech*, 11: 347-350.
- Chen G.Q., Zhang G., Park S.J., Lee S.Y.; (2001) Industrial scale production of poly(3-hydroxybutyrate-co-3-hydroxyhexanoate). *Appl Microbiol Biotech*, 57: 50-55.
- Choi J.H., Kim M.S., Roh S.W., Bae J.W.; (2010) *Acidovorax soli* sp. nov., isolated from landfill soil. *Int J Syst Evol Microbiol*, 60: 2715-2718.
- Choi M.H., Lee H.J., Rho J.K., Yoon S.C., Nam J.D., Lim D., Lenz R.W.; (2003) Biosynthesis and local sequence specific degradation of poly(3-hydroxyvalerate-co-4-hydroxybutyrate) in *Hydrogenophaga pseudoflava*. *Biomacromolecules*, 4: 38-45.
- Chow W.H., Dong L.M., Devesa S.S.; (2010) Epidemiology and risk factors for kidney cancer. *Nat Rev Urology*, 7: 245-257.
- Chu K.H., Mahendra S., Song D.L., Conrad M.E., Alvarez-Cohen L.; (2004) Stable Carbon Isotope Fractionation during Aerobic Biodegradation of Chlorinated Ethenes. *Environ Sci Technol*, 38(11): 3126-3130.
- Coates J.D., Phillips E.J.P., Lonergan D.J., Jenter H., Lovley D.R.; (1996) Isolation of *Geobacter* Species from Diverse Sedimentary Environments. *Appl Environ Microbiol*, 62(5): 1531-1536.
- Cole J. R., Wang Q., Fish J.A., Chai B., McGarrell D.M., Sun Y., Brown C.T., Porras-Alfaro A., Kuske C.R., Tiedje J.M.; (2014). Ribosomal Database Project: data and tools for high throughput rRNA analysis. *Nucl. Acids Res.* 41 (Database issue):D633-D642; doi: 10.1093/nar/gkt1244 [PMID: 24288368].
- Cole S.T., *et al.*; (1998) Deciphering the biology of *Mycobacterium tuberculosis* from the complete genome sequence. *Nature*, 396(6707): 190-198.
- Coleman N.V., Mattes T.E., Gossett J.M., Spain J.C.; (2002a) Phylogenetic and kinetic diversity of aerobic vinyl chloride-assimilating bacteria from contaminated sites. *Appl Environ Microbiol*, 68: 6162-6171.
- Coleman N.V., Mattes T.E., Gossett J.M., Spain J.C.; (2002b) Biodegradation of cis-dichloroethylene as the sole carbon source by a beta-Proteobacterium. *Appl Environ Microbiol*, 68: 2726-2730.
- Coleman N.V., Bui N.B., Holmes A.J.; (2006) Soluble di-iron monooxygenase gene diversity in soils, sediments and ethene enrichments. *Environ Microbiol*, 8(7): 1228-1239.
- Collet D.M.; (2004) Willows of Interior Alaska. US Fish and Wildlife Service.
- Cooper W.J., Mehran M., Riusech D.J., Joens J.A.; (1987) Abiotic Transformations of Halogenated Organics. 1. Elimination Reaction of 1,1,2,2-Tetrachloroethane and Formation of 1,1,2-Trichloroethene. *Environ Sci Technol*, 21(11): 1112-1114.
- Copeland A., Zhang X., Misra M., Lapidus A., *et al.*; (2012) Complete genome sequence of the aquatic bacterium *Runella slithyformis* type strain (LSU 4T). *Stand Genomic Sci*, 6: 145-154.
- Dalal J., Sarma P.M., Lavania M., Mandal A.K., Lal B.; (2010) Evaluation of bacterial strains isolated from oil-contaminated soil for production of polyhydroxyalkanoic acids (PHA). *Pedobiologia*, 54(1): 25-30.

- Das N., Chandran P.; (2011) Microbial Degradation of Petroleum Hydrocarbon Contaminants: An Overview. *Biotech Res Int*, doi:10.4061/2011/941810
- Daubaras D., Chakrabarty A.M.; (1992) The environment, microbes and bioremediation: microbial activities modulated by the environment. *Biodegradation*, 3: 125-135.
- Davidova I.A., Gieg L.M., Duncan K.E., Suflita J.M.; (2007) Anaerobic phenanthrene mineralization by a carboxylating sulfate-reducing bacterial enrichment. *ISME J*, 1: 436-442.
- Davies J.I., Evans W.C.; (1964) Oxidative metabolism of naphthalene by soil Pseudomonads: the ring fission mechanism. *Biochem J*, 91: 251-261.
- de Araújo J.C., Schneider R.P.; (2008) DGGE with genomic DNA: suitable for detection of numerically important organisms but not for identification of the most abundant organisms. *Water Research*, 42: 5002-5010.
- De Wildelman S., Diekert G., Van Langerhove H., Verstraete W.; (2003) Stereoselective microbial dehalorespiration with vicinal dichlorinated alkanes. *Appl Environ Microbiol*, 69: 5643-5647.
- De Cáceres M., Legendre P., Moretti M.; (2010) Improving indicator species analysis by combining groups of sites. *Oikos*, 119(10): 1674-1684.
- Delmont T.O., Robe P., Clark I., Simonet P., Vogel T.M.; (2011) Metagenomic comparison of direct and indirect soil DNA extraction approaches. *J Microbiol Methods*, 86(3): 397-400.
- Denaro R., D'Auria G., Di Marco G., Genovese M., Troussellier M., Yakimov M.M., *et al.*; (2005) Assessing terminal restriction fragment length polymorphism suitability for the description of bacterial community structure and dynamics in hydrocarbon-polluted marine environments. *Environ Microbiol*, 7: 78-87.
- Desai C., Madamwar D.; (2007) Extraction of inhibitor-free metagenomic DNA from polluted sediments, compatible with molecular diversity analysis using adsorption and ion-exchange treatments. *Bioresource Technol*, 98: 761-768.
- DeSantis T.Z., Hugenholtz P., Larsen N., Rojas M., Brodie E.L., Keller K., Huber T., Dalevi D., Hu P., Andersen G.L.; (2006) Greengenes, a chimera-checked 16S rRNA Gene database and workbench compatible with ARB. *Appl Environ Microbiol*, 72: 5069-5072.
- Dey K., Roy P.; (2009) Degradation of trichloroethylene by *Bacillus sp.*: isolation strategy, strain characteristics, and cell immobilization. *Curr Microbiol*, 59:256-260.
- Dias J.M.L., Lemos P.C., Serafim L.S., Oliveira C., Eiroa M., Albuquerque M.G.E., Ramos A.M., Oliveira R., Reis M.A.M.; (2006) Recent advances in polyhydroxyalkanoate production by mixed aerobic cultures: From the substrate to the final product. *Macromol Biosci*, 6: 885-906.
- Diaz E.; (2008) Microbial Biodegradation: Genomics and Molecular Biology. Publisher: Caister Academic Press.
- Dionisi D., Majone M., Vallini G., Di Gregorio S., Beccari M.; (2006) Effect of the applied organic load rate on biodegradable polymer production by mixed microbial cultures in a sequencing batch reactor. *Biotechnol Bioeng*, 93: 76-88.
- Dionisi D., majone M., Vallini G., Di Gregorio S., Beccari M.; (2007) Effect of the length of the cycle on biodegradable polymer production and microbial community selection in a sequencing batch reactor. *Biotechnol Progress*, 23: 1064-1073.
- Doronina N.V., Trotsenko Y.A., Tourova T.P., Kuznetsov B.B., Leisinger T.; (2001) *Albibacter methylovorans* gen. nov., sp. nov., a novel aerobic, facultatively autotrophic and methylotrophic bacterium that utilizes dichloromethane. *Int J Syst Evol Microbiol*, 51(3): 1051-1058.
- Dowd S.E., Callaway T.R., Wolcott R.D., Sun Y., McKeehan T., Hegevoort R.G., Edrington T.S.; (2008) Evaluation of the bacterial diversity in the feces of cattle using 16S rDNA bacterial tag-encoded FLX amplicon pyrosequencing (bTEFAP). *BMC Microbiology*, doi:10.1186/1471-2180-8-125.
- Drzyzga O., Gottshal J.C.; (2002) Tetrachloroethene dehalorespiration and growth of *Desulfotobacterium frappieri* TCE1 in strict dependence on the activity of *Desulfovibrio fructosivorans*. *Appl Environ Microbiol*, 68: 642-649.

- Duba A.G., Jackson K.J., Jovanovich M.C., Knapp R.B., Shah N.N., Taylor R.T.; **(1996)** TCE remediation using in situ, resting state bioaugmentation. *Environ Sci Technol*, 30: 1962-1969.
- Duineveld B.M., Kowalchuk G.A., Keijzer A., van Elsas J.D., van Veen J.A.; **(2001)** Analysis of bacterial communities in the rhizosphere of chrysanthemum via denaturing gradient gel electrophoresis of PCR-amplified 16S rRNA as well as DNA fragments coding for 16S rRNA. *Appl Environ Microbiol*, 67: 172-178.
- Dumont M.G., Murrell J.C.; **(2005)** Community-level analysis: key genes of aerobic methane oxidation. *Meth Enzymol*, 397: 413-427.
- Dumont M.G., Pommerenke B., Casper P., Conrad R.; **(2011)** DNA-, rRNA-, and mRNA-based stable isotope probing of aerobic methanotrophs in lake sediment. *Environ Microbiol*, 13(5): 1153-1167.
- Dunn N.W., Gunsalus I.C.; **(1973)** Transmissible plasmid coding early enzymes of naphthalene oxidation in *Pseudomonas putida*. *J Bacteriol*, 114: 974-979.
- Ensign S.A., Hyman M.R., Arp D.J.; **(1992)** Cometabolic degradation of chlorinated alkenes by alkene monooxygenase in a propylene-grown *Xantobacter* strain. *Appl Environ Microbiol*, 58: 3038-3046.
- Entcheva P., Liebl W., Johann A., Hartsch T., Streit W.R.; **(2001)** Direct cloning from enrichment cultures, a reliable strategy for isolation of complete operons and genes from microbial consortia. *Appl Environ Microbiol*, 67: 89-99.
- Escalante A.E., Barbolla L.J., Ramirez-Barahona S., Eguarte L.; **(2014)** The study of biodiversity in the era of massive sequencing. *Revista Mexicana de Biodiversidad*, 85: 1249-1264.
- Farrelly V., Rainey F.A., Stackebrandt E.; **(1995)** Effect of genome size and *rrn* gene copy number on PCR amplification of 16S rRNA genes from a mixture of bacterial species. *Appl Environ Microbiol*, 61: 2798-2801.
- Fedi S., Tremaroli V., Scala D., Perez-Jimenez J.R., Fava F., Young L. *et al.*; **(2005)** T-RFLP analysis of bacterial communities in cyclodextrin-amended bioreactors developed for biodegradation of polychlorinated biphenyls. *Res Microbiol*, 156: 201-210.
- Felsenstein J.; **(1985)** Confidence limits on phylogenies: An approach using the bootstrap. *Evolution*, 39: 783-791.
- Fernandez A.S., Hashsham S.A., Dollhopf S.L., Raskin L., Glagoleva O., Dazzo F.B., *et al.*; **(2000)** Flexible community structure correlates with stable community function in methanogenic bioreactor communities perturbed by glucose. *Appl Environ Microbiol*, 66: 4058-4067.
- Field J.A., Sierra-Alvarez R.; **(2004)** Biodegradability of chlorinated solvents and related chlorinated aliphatic compounds. *Rev Environ Sci Bio/Technol*, 3: 185-254.
- Fischer S.G., Lerman L.S.; **(1983)** DNA fragments differing by single basepair substitutions are separated in denaturing gradient gels: correspondence with melting theory. *Proc Natl Acad Sci USA*, 80: 1579-1583.
- Folsom B.R., Chapman P.J., Pritchard P.H.; **(1990)** Phenol and trichloroethylene degradation by *Pseudomonas cepacia* G4: Kinetics and interactions between substrates. *Appl Environ Microbiol*, 56: 1279-1285.
- Fox B.G., Borneman J.G., Wackett L.P., Lipscomb J.D.; **(1990)** Haloalkene oxidation by the soluble methane monooxygenase from *Methylosinus trichosporium* OB3b: Mechanistic and environmental implications. *Biochem*, 29: 6419-6427.
- Francova K., Mackova M., Macek T., Sylvestre M.; **(2004)** Ability of bacterial biphenyl dioxygenases from *Burkholderia* sp. LB400 and *Comamonas testosteroni* B-356 to catalyze oxygenation of *ortho*-hydroxychlorobiphenyls formed from PCBs by plants. *Environ Pollut*, 127(1): 41-48.
- Frasconi D., Zannoni A., Fedi S., Pii Y., Zannoni D., Pinelli D., Nocentini M.; **(2005)** Aerobic cometabolism of chloroform by butane-grown microorganisms: long-term monitoring of depletion rates and isolation of a high-performing strain. *Biodegradation*, 16: 147-158.
- Frasconi D., Zannoni A., Pinelli D., Nocentini M., Baleani E., Fedi S., Zannoni D., Farneti A., Battistelli A.; **(2006a)** Long-term aerobic cometabolism of a chlorinated solvent mixture by vinyl chloride-, methane- and propane-utilizing biomasses. *J Hazard Mater*, 138:29-39.

- Frascari D., Pinelli D., Nocentini M., Fedi S., Pii Y., Zannoni D.; **(2006b)** Chloroform degradation by butane-grown cells of *Rhodococcus aetherovorans* BCP1. *Appl Microbiol Biotechnol*, 73: 421-428.
- Frascari D., Cappelletti M., Fedi S., Zannoni D., Nocentini M., Pinelli D.; **(2010)** 1,1,2-Tetrachloroethane aerobic cometabolic biodegradation in slurry and soil-free bioreactors: a kinetic study. *Biochem Eng J*, 52:55-64.
- Frascari D., Cappelletti M., Fedi S., Verboschi A., Ciavarelli R., Nocentini M., Pinelli D.; **(2012a)** Application of the growth substrate pulsed feeding technique to a process of chloroform aerobic cometabolism in a continuous-flow sand-filled reactor. *Process Biochem*, 47: 1656-1664.
- Frascari D., Fraraccio S., Nocentini M., Pinelli D.; **(2012b)** Aerobic / anaerobic / aerobic sequenced biodegradation of a mixture of chlorinated ethenes, ethanes and methanes in batch bioreactors. *Bioresource Technol*, 128: 479-486.
- Frascari D., Zanaroli G., Bucchi G., Rosato A., Tavanaie N., Fraraccio S., Pinelli D., Fava. F.; **(2013a)** Trichloroethylene aerobic cometabolism by suspended and immobilized butane-growing microbial consortia: a kinetic study. *Bioresource Technol*, 144: 529-538.
- Frascari D., Bucchi G., Doria F., Rosato A., Tavanaie N., Salviulo R., Ciavarelli R., Pinelli D., Fraraccio S., Zanaroli G., Fava. F.; **(2013b)** Development of an attached-growth process for the on-site bioremediation of an aquifer polluted by chlorinated solvents. *Biodegradation*, 25(3):337-350.
- Frascari D., Zanaroli G., Danko A.S.; **(2015)** In situ aerobic cometabolism of chlorinated solvents: A review. *J Hazard Mater*, 283: 382-399.
- Friedrich M.W.; **(2006)** Stable-isotope probing of DNA: insights into the function of uncultivated microorganisms from isotopically labeled metagenomes. *Curr Opin Biotech*, 17: 59-66.
- Fromin N., Hamelin J., Tarnawski S., Roesti D., Jourdain-Miserez K., Forestier N., Teyssier-Cuvelle S., Gillet F., Aragno M., Rossi P.; **(2002)** Statistical analysis of denaturing gel electrophoresis (DGE) fingerprinting patterns. *Environ Microbiol*, 4: 634-643.
- Fugatami T., Goto M., Furukawa K.; **(2008)** Biochemical and genetic bases of dehalorespiration. *Chem Rec*, 8: 1-12.
- Fuhrman J.A.; **(2012)** Metagenomics and its connection to microbial community organization. *F1000 Biology Reports*, 4:15.
- Fukui T., Abe H., Doi Y.; **(2002)** Engineering of *Ralstonia eutropha* for production of poly(3-hydroxybutyrate-co-3-hydroxyhexanoate) from fructose and solid-state properties of the copolymer. *Biomacromolecules*, 3:618-624.
- Funhoff E.G., *et al.*; **(2006)** CYP153A6, a soluble P450 oxygenase catalyzing terminal-alkane hydroxylation. *J Bacteriol*, 188(14): 5220-5227.
- Gafan G.P., Lucas V.S., Roberts G.J., petrie A., Wilson M., Spratt D.A.; **(2005)** Statistical analyses of complex denaturing gradient gel electrophoresis profiles. *J Clin Microbiol*, 43(8): 3971-3978.
- Gallagher L.G., Vieira V.M., Ozonoff D., Webster T., Aschengrau A.; **(2011)** Risk of breast cancer following exposure to tetrachloroethylene-contaminated drinking water in Cape Cod, Massachusetts: reanalysis of a case-control study using a modified exposure assessment. *Environ Health J*, 10: 47-64.
- Garcia-Moyano A., González-Toril E., Aguilera A., Amils R.; **(2012)** Comparative microbial ecology study of the sediments and the water column of the Rio Tinto, an extreme acidic environment. *FEMS Microbiol Ecol*, 81: 303-314.
- Geissdorfer W., *et al.*; **(1995)** Two genes encoding proteins with similarities to rubredoxin and rubredoxin reductase are required for conversion of dodecane to lauric acid in *Acinetobacter calcoaceticus* ADP1. *Microbiology*, 141(Pt6): 1425-1432.
- Gennaro V., Ceppi M., Crosignani P., Montanaro F.; **(2008)** Reanalysis of updated mortality among vinyl and polivynil chloride workers: confirmation of historical evidence and new findings. *BMC Public Health*, 8: 21.
- Gerngross T.U., Martin D.P.; **(1995)** Enzyme-catalyzed synthesis of poly[(R)-(-)-3-hydroxybutyrate]: formation of macroscopic granules in vitro. *Proc Natl Acad Sci USA*, 92:6279-6283

- Ginzinger D.G.; (2002) Gene quantification using real-time quantitative PCR: an emerging technology hits the mainstream. *Exp Hematol*, 30: 503-512.
- Goodfellow M., Jones A.L., Maldonado A., Salanitro J.; (2004) *Rhodococcus aetherivorans* sp. Nov., A new Species that Contains Methyl t-butyl Ether-Degrading Actinomycetes. *System Appl Microbiol*, 27: 61-65.
- Gossett J.M., Zinder S.H.; (1997) Microbiological Aspects Relevant to Natural Attenuation of Chlorinated Ethenes. In: Proceedings of the Symposium on Natural Attenuation of Chlorinated Organics in Ground Water. EPA/540/R-97/504.
- Grace K., Jahns A.C., Parlane N., Palanisamy R., Rasiah I.A., Atwood J.A., Rehm B.A.; (2009) Bacterial Polyhydroxyalkanoates Granules: Biogenesis, Structure, and Potential Use as Nano-/Micro-Beads in Biotechnological and Biomedical Applications. *Biomacromolecules*, 10(4): 660-669.
- Green J., Dalton H.; (1989) Substrate specificity of soluble methane monooxygenase from *Methylococcus capsolatus* (Bath). *J Biol Chem*, 260: 15795-15801.
- Haas R., Jin B., Zepf F.T.; (2008) Production of Poly(3-hydroxybutyrate) from Waste Potato Starch. *Biosci Biotech Biochem*, 72(1): 253-256.
- Habe H., Omori T.; (2014) Genetics of Polycyclic Aromatic Hydrocarbon Metabolism in Diverse Aerobic Bacteria. *Biosci Biotech Biochem*, 67(2): 225-243.
- Hakemian A.S., Rosenzweig A.C.; (2007) The biochemistry of methane oxidation. *Ann Rev Biochem*, 76: 223-241.
- Hamamura N., Storfa R.T., Semprini L., Arp D.J.; (1999) Diversity in butane monooxygenases among butane-grown bacteria. *Appl Environ Microbiol*, 65: 4586-4593.
- Hamamura N., Yeager C.M., Arp D.J.; (2001) Two distinct monooxygenases for alkane oxidation in *Nocardioides* sp. Strain CF8. *Appl Environ Microbiol*, 67(11): 4992-4998.
- Handelsman J.; (2007) Metagenomics and Microbial Communities. *Encyclopedia of Life Sciences*, doi: 10.1002/9780470015902.a0020367.
- Haritash A.K., Kaushik C.P.; (2009) Biodegradation aspects of Polycyclic Aromatic Hydrocarbons (PAHs): A review. *J Hazard Mater*, 169: 1-15.
- Harker A.R., Kim Y.; (1990) Trichloroethylene degradation by two independent aromatic degrading pathways in *Alcaligenes eutrophus* JMP 134. *Appl Environ Microbiol*, 56: 1179-1181.
- Harper D.B.; (2000) The global chloromethane cycle: Biosynthesis, biodegradation and metabolic role. *Nat. Prod. Rep.*, 17: 337-348.
- Hartmans S., De Bont J.A.; (1992) Aerobic vinyl chloride metabolism in *Mycobacterium aurum* L1. *Appl Environ Microbiol*, 58(4): 1220-1226.
- Hazen T.C., Lombard K.H., Looney B.B., Enzien M.V., Dougherty J.M., Fliermans C.B., Wear J., Eddy-Dilek C.A.; (1994) Summary of in situ bioremediation (methane biostimulation) via horizontal wells at the Savannah river site integrated demonstration project. In: In Situ Remediation: Scientific Basis for Current and Future Technologies. Richland, Washington: Battelle Press, pp: 137-150.
- He J., Ritalahti K.M., Aiello M.R., Löffler F.E.; (2003) Complete detoxification of vinyl chloride by an anaerobic enrichment culture and identification of the reductively dechlorinating population as a *Dehalococcoides* species. *Appl Environ Microb*, 69: 996-1003.
- Heitkamp M.A., Franklin W., Cerniglia C.E.; (1988) Microbial Metabolism of Polycyclic Aromatic Hydrocarbons: Isolation and Characterization of a Pyrene-Degrading Bacterium. *Appl Environ Microbiol*, 54(10): 2549-2555.
- Hennessee C.T., Seo J.S., Alvarez A.M., Li Q.X.; (2009) Polycyclic aromatic hydrocarbon-degrading species isolated from Hawaiian soils: *Mycobacterium crocinum* sp. nov., *Mycobacterium pallens* sp. nov., *Mycobacterium rutilum* sp. nov., *Mycobacterium rufum* sp. nov. and *Mycobacterium aromaticivorans* sp. nov. *Int J Syst Evol Microbiol*, 59: 378-387.
- Hinchee R.E., Miller R.M., Johnson P.C.; (1995) In: In Situ Aeration: Air Sparging, Bioventing, and Related Remediation Processes. Columbus, Ohio, Battelle Press.

- Hoekstra E.J., Verhagen F.J.M., Field J.A., de Leer E.W.B., Brinkman U.A.T.; (1998) Natural production of chloroform by fungi. *Phytochemistry*, 49: 91-97.
- Holland S.M.; (2008) Non-metric multidimensional scaling (MDS). Department of Geology, University of Georgia, Athens, GA 30602-2501.
- Holliger C., Regeard C., Diekert G.; (2003) Dehalogenation by anaerobic bacteria. In: Dehalogenation: Microbial processes and environmental applications. Haggblom M.H. and Bossert ID (Ed), Kluwer Academic Press, Boston, pp 115-117.
- Huang W.E., Ferguson A., Singer A.C., Lawson K., Thompson I.P., Kalin R.M., *et al.*; (2009) Resolving genetic functions within microbial populations: *in situ* analyses using rRNA and mRNA stable isotope probing coupled with single-cell Raman-fluorescence *in situ* hybridization. *Appl Environ Microbiol*, 75: 234-241.
- Huang Y.T., Chen P.L., Semblante G.U., You S.J.; (2012) Detection of polyhydroxyalkanoate-accumulating bacteria from domestic wastewater treatment plant using highly sensitive PCR primers. *J Microbiol Biotechnol*, 22: 1141-1147.
- Hunter S., Corbett M., Denise H., Fraser M., Gonzalez-Beltran A., Hunter C., Jones P., Leinonen R., McAnulla C., Maguire E., Maslen J., Mitchell A., Nuka G., *et al.*; (2014) EBI metagenomics – a new resource for the analysis and archiving of metagenomic data. *Nucleic Acids Res*, 42: D600-D606.
- Huse S.M., Huber J.A., Morrison H.G., Sogin M.L., Welch D.M.; (2007) Accuracy and quality of massively parallel DNA pyrosequencing. *Genome Biol*, 8: R143.
- Hutchens E., Radajewski S., Dumont M.G., McDonald I.R., Murrell J.C.; (2004) Analysis of methanotrophic bacteria in Movile Cave stable isotope probing. *Environ Microbiol*, 6(2): 111-120.
- Hyman M.R., Russell S.A., Ely R.L., Arp D.J.; (1995) Inhibition, inactivation, and recovery of ammonia-oxidizing activity in cometabolism of trichloroethylene by *Nitrosomonas europaea*. *Appl Environ Microbiol*, 61: 1480-1487.
- Ibekwe A.M., Watt P.M., Grieve C.M., Sharma V.K., Lyons S.R.; (2002) Multiplexing fluorogenic real-time PCR for detection and quantification of *Escherichia coli* O157:H7 in dairy wastewater wetlands. *Appl Environ Microbiol*, 68(10): 4853-4862.
- ITRC, Interstate Technology & Regulatory Council, Bioremediation of DNAPLs Team, (2008) *In Situ Bioremediation of Chlorinated Ethene: DNAPL Source Zones*. 50 F Street NW, Suite 350, Washington, DC 20001.
- Jaward F.M., Alegria H.A., Reyes J.G.G., Hoare A.; (2012) Levels of PAHs in the Waters, Sediments, and Shrimps of Estero de Urias, an Estuary in Mexico, and Their Toxicological Effects. *Scientific World J*, doi:10.1100/2012/687034.
- Jeon C.O., Park W., Padmanabhan P., DeRito C., Snape J.R., Madsen E.L.; (2003) Discovery of a bacterium, with distinctive dioxygenase, that is responsible for *in situ* biodegradation in contaminated sediment. *Proc Natl Acad Sci USA*, 100: 13591-13596.
- Joens J.A., Slifker R.A., Cadavid E.M., Martinez R.D., Nickelsen M.G., Cooper W.J.; (1995) Ionic strength and buffer effects in the elimination reaction of 1,1,2,2-Tetrachloroethane. *Water Research*, 29(8): 1924-1928.
- Johnsen A.R., Wick L.Y., Harms H.; (2004) Principles of microbial PAH-degradation in soil. *Environ Pollut*, 133: 71-84.
- Jones Maiysha D'ora; Stable-Isotope Probing-based Investigations of Polycyclic Aromatic Hydrocarbon-Degrading Bacteria in Contaminated Soil. (2010). A dissertation submitted to the faculty of the University of North Carolina at Chapel Hill.
- Jossek R., Reichelt R., Steinbüchel A.; (1998) In vitro biosynthesis of poly(3-hydroxybutyric acid) by using purified poly(hydroxyalkanoic acid) synthase of *Chromatium vinosum*. *Appl Microbiol Biotechnol*, 49: 258-266.
- Joutey N.T., Bahafid W., Sayel H., Ghachtouli N.E.; (2013) Biodegradation: Involved Microorganisms and Genetically Engineered Microorganisms. Chapter 11. <http://dx.doi.org/10.5772/56194>.
- Juhasz A.L., Britz M.L., Stanley G.A.; (1997) Degradation of benzo[a]pyrene, dibenz[a,h]anthracene and coronene by *Burkholderia cepacia*. *Water Sci Tech*, 36: 45-51.

- Juhasz A.L., Naidu R.; (2000) Bioremediation of high molecular weight polycyclic aromatic hydrocarbons: a review of the microbial degradation of benzo[a]pyrene. *Int Biodeter Biodegr*, 45(1-2): 57-88.
- Kahar P., Tsuge T., Taguchi K., Doi Y.; (2004) High yield production of polyhydroxyalkanoates from soybean oil by *Ralstonia eutropha* and its recombinant strain. *Polym Degrad Stabil*, 83(1): 79-86.
- Kallimanis A., Kavakiotis K., Perisynakis A., Sproer C., Pukall R., Drinas C., Koukkou A.I.; (2009) *Arthrobacter phenanthrenivorans* sp. nov., to accommodate the phenanthrene-degrading bacterium *Arthrobacter* sp. strain Sphe3. *Int J Syst Evol Microbiol*, 59: 275-279.
- Kalyuzhnaya M.G., De Marco P., Bowerman S., Pacheco C.C., *et al.*; (2006) *Methyloversatilis universalis* gen. nov., sp. nov., a novel taxon within the Betaproteobacteria represented by three methylotrophic isolates. *Int J Syst Evol Microbiol*, 56: 2517-2522.
- Karen E.G., Huang X.D., Glick B.R., Greenberg B.M.; (2009) Phytoremediation and rhizoremediation of organic soil contaminants: Potential and challenges. *Plant Sci*, 176: 20-30.
- Karlson U., *et al.*; (1993) 2 Independently Regulated Cytochromes-P-450 in a *Rhodococcus-Rhodochrous* Strain That Degrades 2-Ethoxyphenol and 4-Methoxybenzoate. *J Bacteriol*, 175(5): 1467-1474
- Keppler F., Eiden R., Niedan V., Pracht J., Scholer H.F.; (2000) Halocarbons produced by natural oxidation processes during degradation of organic matter. *Nature*, 403: 298-301.
- Keshavarz T., Roy I.; (2010) Polyhydroxyalkanoates: bioplastics with a green agenda. *Curr Opin Microbiol*, 13: 321-326.
- Khanna S., Srivastava A.K.; (2009) On-line Characterization of Physiological State in Poly ( $\beta$ -Hydroxybutyrate) Production by *Wautersia eutropha*. *Appl Biochem Biotechnol*, 157: 237-243.
- Kim Y., Arp D.J., Semprini L.; (2000) Chlorinated solvent cometabolism by butane-grown mixed culture. *J Environ Eng*, 126: 934-942.
- Kloos K.*et al.*; (2006) A new method for the detection of alkane-monoxygenase homologous genes (alkB) in soils based on PCR-hybridization *J Microbiol Methods*, 66: 486-496.
- Kojima H., Fukui M.; (2011) *Sulfuritalea hydrogenivorans* gen. nov., sp. nov., a facultative autotroph isolated from a freshwater lake. *Int J Syst Evol Microbiol*, 61(Pt 7):1651-5.
- Kolvenbach B.A., Helbling D.E., Kohler H.P.E., Corvini P.F.X.; (2014) Emerging chemicals and the evolution of biodegradation capacities and pathways in bacteria. *Curr Opin Biotechnol*, 27: 8-14.
- Konopka A.; (2009) What is microbial community ecology? *The ISME Journal*, 3: 1223-1230.
- Koller M., Salerno A., Muhr A., Reiterer A., Chiellini E., Casella S., Horvat P., BrauneGG G.; (2012) Whey Lactose as a Raw Material for Microbial Production of Biodegradable Polyesters. Licence in: INTECH, <http://dx.doi.org/10.5772/48737>, Chapter 3, pp: 51-92.
- Kotani T., Yamamoto T., Yurimoto H., Sakai Y., Kato N.; (2003) Propane monoxygenase and NAD<sup>+</sup>-dependent secondary alcohol dehydrogenase in propane metabolism by *Gordonia* sp. Strain TY-5. *J Bacteriol*, 185: 7120-7128.
- Kotani T., Kawashima Y., Yurimoto H., Kato N., Sakai Y.; (2006) Gene structure and regulation of alkane monoxygenases in propane-utilizing *Mycobacterium* sp. TY-6 and *Pseudonocardia* sp. TY-7. *J Biosci Bioeng*, 102: 184-192.
- Kotani T., Yurimoto H., Kato N., Sakai Y.; (2007) Novel acetone metabolism in a propane-utilizing bacterium, *Gordonia* sp. Strain TY-5. *J Bacteriol*, 189: 886-893.
- Kowalchuk G.A., Stephen J.R., de Boer W., Prosser J.I., Embley T.M., Woldendorp J.W.; (1997) Analysis of ammonia-oxidizing bacteria of the beta subdivision of the class *Proteobacteria* in coastal sand dunes by denaturing gradient gel electrophoresis and sequencing of PCR-amplified 16S ribosomal DNA fragments. *Appl Environ Microbiol*, 63: 1489-1497.
- Kragelund C., Nielsen J.L., Thomsen T.R., Nielsen P.H.; (2005) Ecophysiology of the filamentous Alphaproteobacterium *Meganema perideroedes* in activated sludge. *FEMS Microbiol Ecol*, 54: 111 - 122.

- Krohn-Molt I., Wemheuer B., Alawi M., Poehlein A., Gullert S., Schmeisser C., Pommerening-Roser A., Grundhoff A., Daniel R., Hanelt D., Streit W.R.; (2013) Metagenome survey of a multispecies and algae-associated biofilm reveals key elements of bacterial-algae interactions in photobioreactors. *Appl Environ Microbiol*, 79 (20): 6196-6206.
- Kuiper I., Lagendijk E.L., Bloemberg G.V., Lugtenberg B.J.J.; (2004) Rhizoremediation: a beneficial plant-microbe interaction. *Mol Plant Microbe Interact*, 17: 6-15.
- Kulpreecha S., Boonruangthavorn A., Meksiriporn B., Thongchul N.; (2009) Inexpensive fed-batch cultivation for high poly(3-hydroxybutyrate) production by a new isolate of *Bacillus megaterium*. *J Biosci Bioeng*, 107: 240-245.
- Kumar M., Verma M., Lal R.; (2008) *Devosia chinhatensis* sp. nov., isolated from a hexachlorocyclohexane (HCH) dump site in India. *Int J Syst Evol Microbiol*, 58(4): 861-865.
- Kurkela S., Lehvaslaiho H., Palva E.T., Teeri T.H.; (1988) Cloning, nucleotide sequence and characterization of genes encoding naphthalene dioxygenase of *Pseudomonas putida* strain NCIB9816. *Gene*, 73: 355-362.
- La Scola B., Birtles R.J., Mallet M.N., Raoult D.; (1998) *Massilia timonae* gen. nov., sp. nov., Isolated from Blood of an Immunocompromised Patient with Cerebellar Lesions. *J Clinical Microbiol*, 36(10): 2847-2852.
- Lalib S., Guo C.H., Williams A., Yauk C.L., White P.A., Halappanavar S.; (2013) Toxicogenomics outcomes predictive of forestomach carcinogenesis following exposure to benzo(a)pyrene: Relevance to human cancer risk. *Toxicol Appl Pharmacol*, 273: 269-280.
- Landa A.S., Sipkema E.M., Weijma J., Beenackers A., Dolging J., Janssen D.B.; (1994) Cometabolic degradation of trichloroethylene by *Pseudomonas cepacia* G4 in a chemostat with toluene as the primary substrate. *Appl Environ Microbiol*, 60: 3368-3374.
- Lane, D.J.; (1991) 16S/23S rRNA sequencing. In: Nucleic Acid Techniques in Bacterial Systematics. Edited by E. Stackebrandt & M. Goodfellow, New York: Wiley, pp. 115–175.
- Larkin M., Kulakov L.A., Allen C.C.R.; (2005) Biodegradation and Rhodococcus – master of catabolic versatility. *Curr Opin Biotechnol*, 16: 282-290.
- Larsson E., Tremaroli V., Lee Y.S., Koren O., Nookaew I., Fricker A., Nielsen J., Ley R.E., Bäckhed F.; (2011) Analysis of gut microbial regulation of host gene expression along the length of the gut and regulation of gut microbial ecology through MyD88. *Gut*, doi:10.1136/gutjnl-2011-301104.
- Le N.B., Coleman N.V.; (2011) Biodegradation of vinyl chloride, cis-dichloroethene and 1,2-dichloroethane in the alkene/alkane-oxidizing Mycobacterium strain NBB4. *Biodegradation*, 22: 1095-1108.
- Leadbetter J.R.; (2003) Cultivation of recalcitrant microbes: cells are alive, well and revealing their secrets in the 21<sup>st</sup> century laboratory. *Curr Opin Microbiol*, 6: 274-281.
- Leahy J.G., Byrne A.M., Olsen R.H.; (1996) Comparison of factors influencing trichloroethylene degradation by toluene-oxidizing bacteria. *Appl Environ Microbiol*, 62: 825-833.
- Leahy J.G., Batchelor P.J., Morcomb S.M.; (2003) Evolution of the soluble diiron monooxygenases. *FEMS Microbiol Rev*, 27: 449-479.
- Lee S.Y.; (1996) Plastic Bacteria? Progress and prospects for polyhydroxyalkanoates production in bacteria. *Trends Biotech*, 14: 431-438.
- Li P., Wang X., Stagnitti F., Li L., Gong Z., Zhang H., Xiong X., Austin C.; (2005) Degradation of phenantrene and pyrene in soil slurry reactors with immobilized bacteria *Zooglea* sp. *Environ Eng Sci*, 22: 390-399.
- Lieberman R.L., Rosenzweig A.C.; (2004) Biological methane oxidation: regulation, biochemistry, and active site structure of particulate methane monooxygenase. *Crit Rev Biochem Mol Biol*, 39(3): 147-164.
- Liu F., Li W., Ridgway D., Gu T.; (1998) production of poly-β-hydroxybutyrate on molasses by recombinant *Escherichia coli*. *Biotechnology Letters*, 20: 345-348.
- Liu H.Y., Hall P.V., Darby J.L., Coats E.R., Green P.G., Thompson D.E., Loge F.J.; (2008) Production of polyhydroxyalkanoates during treatment of tomato cannery wastewater. *Water Environ Res*, 80: 367–372.

- Liu W.T., Marsh T.L., Cheng H., Forney L.J.; **(1997)** Characterization of microbial diversity by determining terminal restriction fragment length polymorphisms of genes encoding 16S rRNA. *Appl Environ Microbiol*, 63: 4516-4522.
- Logan B.E., *et al.*; **(2001)** Kinetics of Perchlorate- and Chlorate-Respiring Bacteria. *JOURNAL Appl Environ Microbiol*, 67(6):2499-2506.
- Lontoh S., Zahn J.A., DiSpirito A.A., Semrau J.D.; **(2000)** Identification of intermediates of in vivo trichloroethylene oxidation by the membrane-associated methane monooxygenase. *FEMS Microbiol Lett*, 186: 109-113.
- Lowry O.H., Rosebrough N.J., Farr A.L., Randall R.J.; **(1951)** Protein measurement with the Folin phenol reagent. *J of Biological Chem*, 265-275.
- Lykidis A., Pérez-Pantoja D., Ledger T., Mavromatis K., Anderson I.J., Ivanova N.N., Hooper S.D., Lapidus A., Lucas S., Gonzalez B., Kyrpides N.C.; **(2010)** The Complete Multipartite Genome Sequence of *Cupriavidus necator* JMP134, a Versatile Pollutant Degradator. *PlosOne*, 5(3): 1-13.
- Lu Y., Conrad R.; **(2005)** In situ stable isotope probing of methanogenic Archaea in the rice rhizosphere. *Science*, 309: 1088-1090.
- Lueders T., Manefield M., Friedrich M.W.; **(2004)** Enhanced sensitivity of DNA- and RNA-based stable isotope probing by fractionation and quantitative analysis of isopycnic centrifugation gradients. *Environ Microbiol*, 6(1): 73-78.
- Ma Y.F., Zhang Y., Zhang J.Y., Chen D.W., Zhu Y., Zheng H., Wang S.Y., Jiang C.Y., Zhao G.P., Liu S.J.; **(2009)** The Complete Genome of *Comamonas testosteroni* Reveals Its Genetic Adaptations to Changing Environments. *Appl Environ Microbiol*, 75(21): 6812-6819.
- Macnaughton S., Stephen J.R., Chang Y.J., Peacock A., Flemming C.A., Leung K.T., *et al.*; **(1999)** Characterization of metal-resistant soil eubacteria by polymerase chain reaction-denaturing gradient gel electrophoresis with isolation of resistant strains. *Can J Microbiol*, 45: 116-24.
- Maier T., *et al.*; **(2001)** Molecular characterization of the 56-kDa CYP153 from *Acinetobacter sp.* EB104. *Biochem Biophys Res Commun*, 286(3): 652-658.
- Malik S., Beer M., Megharaj M., Naidu R.; **(2008)** The use of molecular techniques to characterize the microbial communities in contaminated soil and water. *Environ Int*, 34: 265-276.
- Manefield M., Whiteley A.S., Ostle N., Ineson P., Bailey M.J.; **(2002)** Technical considerations for RNA-based stable isotope probing: an approach to associating microbial diversity with microbial community function. *Rapid Communications in Mass Spectrometry*, 16: 2179-2183.
- Markovitz V.M., Chen I.M., Chu K., Szeto E., Palaniappan K., Grechkin Y., Ratner A., Jacob B., Pati A., Huntemann M., *et al.*; **(2011)** IMG/M: the integrated metagenome data management and comparative analysis system. *Nucleic Acids Res*, 40: D123-D129.
- Marsh S.; **(2007)** Pyrosequencing applications. *Methods Mol Biol*, 373: 15-24.
- Martin F., Torelli S., Le Paslier D., Barbance A., Martin-Laurent F., Bru D., Geremia R., Blake G., Jouanneau Y.; **(2012)** Betaproteobacteria dominance and diversity shifts in the bacterial community of a PAH-contaminated soil exposed to phenanthrene. *Environ Pollut*, 162: 345-353.
- Marzorati M., Wittebolle L., Boon N., Daffonchio D., Verstraete W.; **(2008)** How to get more out of molecular fingerprints: practical tools for microbial ecology. *Environ Microbiol*, 10(6): 1571-1581.
- Maymó-Gatell X., Chien Y., Gossett J.M., Zinder S.H.; **(1997)** Isolation of a Bacterium That Reductively Dechlorinates Tetrachloroethene to Ethene. *Science*, 276(5318): 1568-1571.
- Maymó-Gatell X., Nijenhuis I., Zinder S.H.; **(2001)** Reductive Dechlorination of *cis*-1,2-Dichloroethene and Vinyl Chloride by “*Dehalococcoides ethenogenes*”. *Environ Sci Technol*, 35(3): 516-521.
- Mattes T.E., Alexander A.K., Coleman N.V.; **(2010)** Aerobic biodegradation of the chloroethenes: pathways, enzymes, ecology, and evolution. *FEMS Microbiol Rev*, 1-31.
- McAnulla C., McDonals I.R., Murrell J.C.; **(2001)** Methyl chloride utilizing bacteria are ubiquitous in the natural environment. *FEMS Microbiol Lett*, 201: 151-155.

- McCutcheon S.C., Schnoor J.L.; (2003) Phytoremediation: Transformation and control of contaminants. New Jersey, Wiley & Sons Inc.
- McDonald I.R., Warner K.L., McAnulla C., Woodall C.A., Oremland R.S., Murrell J.C.; (2002) A review of bacterial methyl halide degradation: biochemistry, genetics and molecular ecology. *Environ Microbiol*, 4(4): 193-203.
- McDonald I.R., Radajewski S., Murrell J.C.; (2005) Stable isotope probing of nucleic acids in methanotrophs and methylotrophs: A review. *Organic Geochemistry*, 36: 779-787.
- McFarlin K.M.; (2010) Rhizoremediation of Diesel contaminated soil using *Salix alaxensis*. Master of Science Thesis, University of Alaska Fairbanks.
- Meyer F., Paarmann D., D'Souza M., Olson R., Glass E.M., Kubal M., Paczian T., Rodriguez A., Stevens R., Wilke A., *et al.*; (2008) The metagenomics RAST server – a public resource for the automatic phylogenetic and functional analysis of metagenomes. *BMC Bioinformatics*, 9: 386.
- Middleton S.; (2004) TECHNICAL NOTE Denaturing gradient gel electrophoresis (DGGE) screening of clones prior to sequencing. *Molecular Ecology Notes*, 4: 776– 778.
- Morgan-Sagastume F., Karlsson A., Johansson P., Pratt S., Boon N., Lant P., Werker A.; (2010) Production of polyhydroxyalkanoates in open mixed cultures from a waste sludge stream containing high levels of soluble organics, nitrogen and phosphorous. *Water Res*, 44: 5196-5211.
- Morgulis A., Coulouris G., Raytselis Y., Madden T.L., Agarwala R., Schäffer A.A.; (2008) Database Indexing for Production MegaBLAST Searches. *Bioinformatics*, 24:1757-1764.
- Mueller J.G., Cerniglia C.E., Pritchard P.H.; (1996) Bioremediation of environments contaminated by polycyclic aromatic hydrocarbons. In: Bioremediation: Principles and Applications. Eds by Crawford R and Crawford DL. Cambridge University Press, Idaho, pp 125–194.
- Muyzer G., De Waal E.C., Uitterlinden A.G.; (1993) Profiling of complex microbial populations by denaturing gradient gel electrophoresis analysis of polymerase chain reaction-amplified genes coding for 16S rRNA. *Appl Environ Microbiol*, 59(3): 695-700.
- Muyzer G., Smalla K.; (1998) Application of denaturing gradient gel electrophoresis (DGGE) and temperature gradient gel electrophoresis (TGGE) in microbial ecology. *Antonie van Leeuwenhoek*, 73: 127-141.
- Myers R.M., Fisher S.G., Lerman L.S., Maniatis T.; (1985) Nearly all single base substitutions in DNA fragments joined to a GC-clamp can be detected by denaturing gradient gel electrophoresis. *Nucleic Acids Research*, 13: 3131-3145.
- Neufeld J.D., Vohra J., Dumont M.G., Lueders T., Manefield M., Friedrich M.W., Murrell J.C.; (2007) DNA stable-isotope probing. *Nat Protoc*, 2(4): 860-866.
- Nguyen H.H.T., Elliot S.J., Yip J.H.K., Chan S.I.; (1998) The particulate methane monooxygenase from *Methylococcus capsulatus* (Bath) is a novel copper-containing three-subunit enzyme: Isolation and characterization. *J Biol Chem*, 273: 7957-7966.
- Nichols T.D., Wolf D.C., Rogers H.B., Beyrouthy C.A., Reynolds C.M.; (1997) Rhizosphere microbial populations in contaminated soils. *Water Air Soil Poll*, 95: 165-178.
- Nikel P.I., De Almeida A., Melillo E.C., Galvagno M.A., Pettinari M.J.; (2006) New recombinant *Escherichia coli* strain tailored for the production of poly (3-hydroxybutyrate) from agroindustrial by-products. *Appl Environ Microbiol*, 72: 3949-3954.
- Nübel U., Engelen B., Felske A., Snaird J., Wieshuber A., Amann R.I., Ludwig W., Backhaus H.; (1996) Sequence heterogeneities of genes encoding 16S rRNAs in *Paenibacillus polymyxa* detected by temperature gradient gel electrophoresis. *J Bacteriol*, 178: 5636-5643.
- Nübel U., Garcia-Pichel F., Muyzer G.; (1997) PCR primers to amplify 16S rRNA genes from cyanobacteria. *Appl Environ Microbiol*, 63: 3327-3332.
- Öberg G.; (2003) The biogeochemistry of chlorine in soil. In: The Handbook of Environmental Chemistry. Springer, Berlin, Part P. 3: 43-62.

- Oksanen J.; (2013) Multivariate analysis of ecological communities in R: vegan tutorial.
- Olaniran A.O., Pillay D., Pillay B.; (2008) Aerobic biodegradation of dichloroethenes by indigenous bacteria isolated from contaminated sites in Africa. *Chemosphere* 73:24-29.
- Oldenhuis R., Vink RLJM, Janssen D., Witholt B.; (1989) Degradation of chlorinated aliphatic hydrocarbons by *Methylosinus trichosporium* OB3b expressing soluble methane monooxygenase. *Appl Environ Microbiol*, 55: 2819-2826.
- Oosterkamp M.J., Mehboob F., Schraa G., Plugge C.M., Stams A.J.M.; (2011) Nitrate and (per)chlorate reduction pathways in (per)chlorate-reducing bacteria. *Biochem Soc T*, 39(1): 230-235.
- Pace N.R., Stahl D.A., Olsen G.J., Lane D.J.; (1985) Analyzing natural microbial populations by rRNA sequences. *ASM News*, 51: 4-12.
- Pace N.R., Stahl D.A., Lane D.J., Olsen G.J.; (1986) The analysis of natural microbial populations by ribosomal RNA sequences. *Adv Microb Ecol*, 9: 1-55.
- Pelz O., Chatzinotas A., Andersen N., Bernasconi S.M., Hesse C., Abraham W.R., Zeyer J.; (2001) Use of isotopic and molecular techniques to link toluene degradation in denitrifying aquifer microcosms to specific microbial populations. *Arch Microbiol*, 175: 270-281.
- Petrosino J.F., Highlander S., Luna R.A., Gibbs R.A., Versalovic J.; (2009) Metagenomic Pyrosequencing and Microbial Identification. *Clin Chem*, 55(5): 856-866.
- Phelps T.J., Niedzielski J.J., Schram R.M., Herbes S.E., White D.C.; (1990) Biodegradation of trichloroethylene in continuous-recycle expanded-bed bioreactors. *Appl Environ Microbiol*, 56: 1702-1709.
- Philip S., Keshavarz T., Roy I.; (2007) Polyhydroxyalkanoates: biodegradable polymers with a range of applications. *J Chem Technol Biotechnol*, 82: 233-247.
- Pinyakong O., Habe H., Omori T.; (2003) The unique aromatic catabolic genes in Sphingomonads degrading polycyclic aromatic hydrocarbons (PAHs). *J Gen Appl Microbiol*, 49: 1-19.
- Povolo S., Romanelli M.G., Basaglia M., Ilieva V.I., Corti A., Morelli A., Chiellini E., Casella S.; (2013) Polyhydroxyalkanoate biosynthesis by *Hydrogenophaga pseudoflava* DSM1034 from structurally unrelated carbon sources. *New Biotechnol*, 30: 629–634.
- Pruesse E., Quast C., Knittel K., Fuchs B.M., Ludwig W., Peplies J., Glockner F.O.; (2007) SILVA: a comprehensive online resource for quality checked and aligned ribosomal RNA sequence data compatible with ARB. *Nucleic Acids Res*, 35(7): 7188-7196.
- Qiu X., Reed B.E., Viadero R.C.; (2004) Effects of Flavonoids on <sup>14</sup>C[7,10]-Benzo[a]pyrene Degradation in Root Zone Soil. *Environ Eng Sci*, 21(5): 637-646.
- Radajewski S., Ineson P., Parekh N.R., Murrell J.C.; (2000) Stable-isotope probing as a tool in microbial ecology. *Nature*, 403: 646-649.
- Radajewski S., Webster G., Reay D.S., Morris S.A., Ineson P., Nedwell D.B., Prosser J.I., Murrell J.C.; (2002) Identification of active methyloph populations in an acidic forest soil by stable-isotope probing. *Microbiology*, 148: 2331-2342.
- Radajewski S., McDonald I.R., Murrell J.C.; (2003) Stable-isotope probing of nucleic acids: a window to the function of uncultured microorganisms. *Curr Opin Biotechnol*, 14: 296-302.
- Ramsay B.A., Lomaliza K., Chavarie C., Dube B., Bataille B., Ramsay J.A.; (1990) Production of poly-(β-hydroxybutyric-co-β-hydroxyvaleric) acids. *Appl Environ Microbiol*, 56: 2093–2098.
- Rappe M.S., Giovannoni S.J.; (2003) The uncultured microbial majority. *Annu Rev Microbiol*, 57: 369-394.
- Redmond M.C., Valentine D.L., Sessions A.L.; (2010) Identification of novel methane-, ethane-, and propane-oxidizing bacteria at marine hydrocarbon seeps by stable isotope probing. *Appl Environ Microbiol*, 76(19): 6412-6422.

- Reinhold-Hurek B.; Hurek T.; (2000) Reassessment of the taxonomic structure of the diazotrophic genus *Azoarcus* sensu lato and description of three new genera and new species, *Azovibrio restrictus* gen. nov., sp. nov., *Azospira oryzae* gen. nov., sp. nov. and *Azonexus fungiphilus* gen. nov., sp. nov. *Int J Syst Evol Microbiol*, 50: 649–659.
- Reis M.A.M., Albuquerque M.G.E., Villano M., Majone M.; (2011) Mixed culture processes for polyhydroxyalkanoates production from agro-industrial surplus/wastes as feedstocks. *Compr Biotechnol*, 6: 669-683.
- Rentz J.A., Alvarez P.J.J., Schnoor J.L.; (2004) Repression of *Pseudomonas putida* phenanthrene-degrading activity by plant root extracts and exudates. *Environ Microbiol*, 6(6): 574-583.
- Richardson R.E., Bhupathiraju V.K., Song D.L., Goulet T.A., Alvarez-Cohen L.; (2002) Phylogenetic characterization of microbial communities that reductively dechlorinate TCE based upon a combination of molecular techniques. *Environ Sci Technol*, 36: 2652-2662.
- Riedel T., Held B., Nolan M., Lucas S., Lapidus A., Tice H., *et al.*; (2012) Genome sequence of the orange-pigmented seawater bacterium *Owenweeksia hongkongensis* type strain (UTS20020801<sup>T</sup>). *Stand Genomic Sci*, 7: 120-130.
- Ritalahti K.M., Amos B.K., Sung Y., Wu Q., Koenigsberg S.S., Löffler F.E.; (2006) Quantitative PCR targeting 16S rRNA and reductive dehalogenase genes simultaneously monitors multiple *Dehalococcoides* strains. *Appl Environ Microbiol*, 72: 2765-2774.
- Roberts P.V., Hopkins G.D., Mackay D.M., Semprini L.; (1990) A field evaluation of in situ biodegradation of chlorinated ethenes: Part 1, Methodology and field site characterization. *Ground Water*, 28: 591-604.
- Roh H., Yu C.P., Fuller M.E., Chu K.H.; (2009) Identification of hexahydro-1,3,5-trinitro-1,3,5-triazine-degrading microorganisms via <sup>15</sup>N-stable isotope probing. *Environ Sci Technol*, 43: 2505-2511.
- Rojo F.; (2010) Enzymes for Aerobic Degradation of Alkanes. In: Handbook of Hydrocarbon and Lipid Microbiology, pp. 781-797.
- Ronaghi M., Karamohamed S., Pettersson B., Uhlen M., Nyren P.; (1996) Real-time DNA sequencing using detection of pyrophosphate release. *Anal Biochem*, 242: 84-89.
- Ronaghi M., Elahie E.; (2002) Pyrosequencing for microbial typing. *J Chromatogr B*, 782: 67-72.
- Rondon M.R., Raffel S.J., Goodman R.M., Handelsman J.; (1999) Toward functional genomics in bacteria: Analysis of gene expression in *Escherichia coli* from a bacterial artificial chromosome library of *Bacillus cereus*. *Proc Natl Acad Sci USA*, 96: 6451-6455.
- Rondon M.R., *et al.*; (2000) Cloning the soil metagenome: a strategy for accessing the genetic and functional diversity of uncultured microorganisms. *Appl Environ Microbiol*, 66: 2541-2547.
- Rosenbaum V., Riesner D.; (1987) Temperature-gradient gel electrophoresis. Thermodynamic analysis of nucleic acids and proteins in purified form and in cellular extracts. *Biophys Chemist*, 26: 235-246.
- Rovira A.D., Foster R.C., Martin J.K.; (1976) Origin, nature and nomenclature of the organic materials in the rhizosphere. In: The Root-Soil Interface. Eds. Harley J.L. and Russell, London, Academic Press, pp: 1-4.
- Ryu1 S.H., Chung1 B.S., Le N.T., Jang H.H., Yun P.Y., Park W., Jeon C.O.; (2008) *Devosia geojensis* sp. nov., isolated from diesel-contaminated soil in Korea. *Int J Syst Evol Microbiol*, 58(3): 633-636.
- Saeki H., *et al.*; (1999) Degradation of trichloroethylene by a linear-plasmid-encoded alkene monooxygenase in *Rhodococcus corallines* (*Nocardia corallina*) B-276. *Microbiology*, 145(Pt7): 1721-1730.
- Saharan B.S., Grewal A., Kumar P.; (2014) Biotechnological Production of Polyhydroxyalkanoates: A review on Trends and Latest Developments. *Chinese Journal of Biology*, article ID 802984, <http://dx.doi.org/10.1155/2014/802904>.
- Saitou N., Nei M.; (1987) The neighbor-joining method: A new method for reconstructing phylogenetic trees. *Mol Biol Evolut*, 4:406-425.
- Samanta S.K., Singh O.V., Jain R.K.; (2002) Polycyclic aromatic hydrocarbons: environmental pollution and bioremediation. *Trends Biotechnol*, 20(6): 243-248.

- Sambrook J., Fritsch E.R., Maniatis T.; (1989) Molecular cloning: a laboratory manual. Cold Spring Harbor Laboratory Press, Cold Spring Harbor (NY), 2.
- Sass A.M., Sass H., Coolen M.J., Cypionka H., Overmann J.; (2001) Microbial communities in the chemocline of a hypersaline deep-sea basin (Urania basin, Mediterranean Sea). *Appl Environ Microbiol*, 67: 5392-402.
- Schäfer H., McDonald I.R., Nightingale P.D., Murrell J.C.; (2005) Evidence for the presence of a CmuA methyltransferase pathway in novel marine methyl halide-oxidizing bacteria. *Environ Microbiol*, 7(6): 839-852.
- Scarano L.; (2012) TSCA Workplan Chemical Risk Assessment for Trichloroethylene: Degreaser and Arts/Crafts Uses. EPA- United States Environmental Agency. CASRN: 79-01-6.
- Schattenhofer M., Hubalek V., Wendeberg A.; (2014) Identification of Microorganisms in Hydrocarbon-Contaminated Aquifer Samples by Fluorescence In Situ Hybridization (CARD-FISH). In: Hydrocarbon and Lipid Microbiology Protocols, Springer Protocols Handbooks, McGenity T.J. *et al.* (Ed.), doi:10.1007/8623\_2014\_9.
- Schell M.A.; (1985) Transcriptional control of the *nah* and *sal* hydrocarbon-degradation operons by the *nahR* gene product. *Gene*, 36: 301-309.
- Schulz,S., Perez-de-Mora,A., Engel,M., Munch,J.C. and Schloter,M.; (2010) A comparative study of most probable number (MPN)-PCR vs. Real-time-PCR for the measurement of abundance and assessment of diversity of *alkB* homologous genes in soil. *J. Microbiol. Methods*, 80 (3), 295-298, PUBMED 20079768.
- Schloss P.D., Westcott S.L., Ryabin T., Hall J.R., Hartmann M., *et al.*; (2009) Introducing mothur: Open-source, platform-independent, community-supported software for describing and comparing microbial communities. *App Environ Microbiol*, 75: 7537-7541.
- Schmeisser C., Steele H., Streit W.R.; (2007) Metagenomics, biotechnology with non-culturable microbes. *Appl Microbiol Biotechnol*, 75: 955-962.
- Schmidt K.R., Augenstein T., Heidinger M., Ertl S., Tiehm A.; (2010) Aerobic biodegradation of *cis*-1,2-dichloroethene as sole carbon source: Stable carbon isotope fractionation and growth characteristics. *Chemosphere*, 78(5): 527-532.
- Scoma A., Bertin L., Zanaroli G., Fraraccio S., Fava F.; (2011) A physicochemical-biotechnological approach for an integrated valorization of olive mill wastewater. *Biores Technol*, 102: 10273-10279.
- Scott C.S., Jinot J.; (2011) Trichloroethylene and Cancer: Systematic and Quantitative Review of Epidemiologic Evidence for Identifying Hazards. *Int J Environ Res Public Health*, 8(11): 4238-4272.
- Semprini L.; (1997) Strategies for the aerobic co-metabolism of chlorinated solvents. *Curr Opin Biotechnol*, 8: 296-308.
- Sheffield V.C., Cox D.R., Myers R.M.; (1989) Attachment of a 40-bp G+C rich sequence (GC-clamp) to genomic DNA fragments by polymerase chain reaction results in improved detection of single-base changes. *Proc Natl Acad Sci USA*, 86: 232-236.
- Shennan J.L.; (2006) Utilization of C2-C4 gaseous hydrocarbons and isoprene by microorganisms. *J Chem Technol Biotechnol*, 81(3): 237-256.
- Shigematsu T., Hanada S., Eguchi M., Kamagata Y., Kanagawa T., Kurane R.; (1999) Soluble methane monooxygenase gene cluster from trichloroethylene-degrading *Methylomonas* sp. strains and detection of methanotrophs during in situ bioremediation. *Appl Environ Microbiol*, 65: 5198-5206.
- Siciliano S.D., Germida J.J.; (1998) Mechanisms of phytoremediation: biochemical and ecological interaction between plants and bacteria. *Environ Rev*, 6: 65-79.
- Singh R., Paul D., Jain R.K.; (2006) Biofilms: implications in bioremediation. *Trends Microbiol*, 14: 389-397.
- Singleton D.R., Powell S.N., Sangaiah R., Gold A., Ball L.M., Aitken M.D.; (2005) Stable-isotope probing of bacteria capable of degrading salicylate, naphthalene, or phenanthrene in a bioreactor treating contaminated soil. *Appl Environ Microbiol*, 71: 1202-1209.
- Singleton D.R., Richardson S.D., Aitken M.D.; (2011) Pyrosequence analysis of bacterial communities in aerobic bioreactors treating polycyclic aromatic hydrocarbon-contaminated soil. *Biodegradation*, 22(6): 1061-1073.

- Sluis M.K., Sayavedra-Soto L.A., Arp D.J.; **(2002)** Molecular analysis of the soluble butane monoxygenase from '*Pseudomonas butanovora*'. *Microbiology*, 148: 3617-3629.
- Smidt H., de Vos W.M.; **(2004)** Anaerobic Microbial Dehalogenation. *Ann Rev Microbiol*, 58:43-73.
- Spiegelman D., Whissell G., Greer C.W.; **(2005)** A survey of the methods for the characterization of microbial consortia and communities. *Can J Microbiol*, 51: 355-386.
- Staas M., Braster M., Roling W.F.M.; **(2011)** Molecular diversity and distribution of aromatic hydrocarbon-degrading anaerobes across a landfill leachate plume. *Environ Microbiol*, 13(5): 1216-1227.
- Stanley S.H., Prior D.J., Leak D.J., Dalton H.; **(1983)** Copper stress underlines the fundamental change in intracellular location of methane mono-oxygenase in methane utilizing organisms: studies in batch and continuous cultures. *Biotechnol Lett*, 5: 487-492.
- Stolz A.; **(2009)** Molecular characteristics of xenobiotic-degrading sphingomonads. *Appl Microbiol Biotechnol*, 881: 793-811.
- Sun S., Chen J., Li W., Altintas I., Lin A., Peltier S., Stocks K., Allen E.E., Ellisman M., Grethe J., *et al.*; **(2010)** Community cyberinfrastructure for advanced microbial ecology research and analysis: the CAMERA resource. *Nucleic Acids Res*, 39: 546-551.
- Sung Y., Ritalahti K.M., Sanford R.A., Urbance J.W., Flynn S.J., Tiedje J.M., Löffler F.E.; **(2003)** Characterization of Two Tetrachloroethene-Reducing, Acetate-Oxidizing Anaerobic Bacteria and Their Description as *Desulfuromonas michiganensis* sp. nov. *Appl. Environ. Microbiol.*, 69(5): 2964-2974.
- Susarla S., Medina V.F., McCutcheon S.C.; **(2002)** Phytoremediation: an ecological solution to organic chemical contamination. *Ecol Eng*, 18:647-658.
- Suttinun O., Muller R., Luepromchai E.; **(2009)** Trichloroethylene cometabolic degradation by *Rhodococcus* sp. L4 induced with plant essential oils. *Biodegradation*, 20: 281-291.
- Suyama A., Iwakiri R., Kai K., Tokunaga T., Sera N., Furukawa K.; **(2001)** Isolation and characterization of *Desulfitobacterium* sp. strain Y51 capable of efficient dehalogenation of tetrachloroethene and polychloroethanes. *Biosci Biotechnol Biochem*, 65: 1474-1481.
- Tamura K., Stecher G., Peterson D., Filipowski A., Kumar S.; **(2013)** MEGA6: Molecular Evolutionary Genetics Analysis version 6.0. *Mol Biol Evol*, 30: 2725-2729.
- Tan Z., Reinhold-Hurek B.; **(2003)** *Dechlorosoma suillum* Achenbach *et al.* 2001 is a later subjective synonym of *Azospira oryzae* Reinhold-Hurek and Hurek 2000. *Int J Syst Evol Microbiol*, 53: 1139-1142.
- Tiehm A., Schmidt K.R., Stoll C., Müller A., Lohner S., Heidinger M., Wickert F., Karch U.; **(2007)** Assessment of natural microbial dechlorination. *Italian Journal of Engineering Geology and Environment*, 1: 71-77.
- Tiehm A., Schmidt K.R.; **(2011)** Sequential anaerobic/aerobic biodegradation of chloroethenes – aspects of field application. *Curr Opin Biotechnol*, 22: 415-421.
- Thomas T., Gilbert J., Meyer F.; **(2012)** Metagenomics – a guide from sampling to data analysis. *Microbial Informatics and Experimentation*, 2: 3-12.
- Tresse O., Mounien F., Lévesque M.J., Guiot S.; **(2005)** Comparison of the microbial population dynamics and phylogenetic characterization of a CANOXIS reactor and a UASB reactor degrading trichloroethylene. *J App Microbiol*, 98: 440-449.
- Tsuge T., Saito Y., Kikkawa Y., Hiraishi T., Doi Y.; **(2004)** Biosynthesis and compositional regulation of poly(3-hydroxybutyrate-co-3-hydroxyhexanoate) in recombinant *Ralstonia eutropha* expressing mutated polyhydroxyalkanoate synthase genes. *Macromol Biosci*, 4:238-242.
- Uhlík O., Ječná K., Macková M., Vlček C., Hroudová M., *et al.*; **(2009)** Biphenyl-metabolizing bacteria in the rhizosphere of horseradish and bulk soil contaminated by polychlorinated biphenyls as revealed by stable isotope probing. *Appl Environ Microbiol*, 75: 6471-6477.

- Uhlík O., Wald J., Strejcek M., Musilova L., Ridl J., Hroudová M., Vlček C., Cardenas E., Macková M., Macek T.; (2012) Identification of Bacteria Utilizing Biphenyl, Benzoate, and Naphthalene in Long-Term Contaminated Soil. *PLoS ONE*, 7(7): 1-10.
- Uhlík O., Leewis M.C., Strejcek M., Musilova L., Mackova M., Leigh M.B., Macek T.; (2013) Stable isotope probing in the metagenomics era: A bridge towards improved bioremediation. *Biotechnol Adv*, 31: 154-165.
- US ATSDR, Centers for Disease Control Agency for Toxic Substances and Disease Registry. (1997) "Toxicological Profile for Trichloroethylene (TCE)." <http://www.atsdr.cdc.gov/toxprofiles/tp19.html>.
- US Department of Defence – Environmental Security Technology Certification Program. (2001) Use of Cometary Air Sparging to Remediate Chloroethene-contaminated Groundwater Aquifers. Cost and Performance Report CU-9810. Washington DC.
- US EPA, Environmental Protection Agency. (2010) Toxicological Review of cis-1,2-Dichloroethylene and trans-1,2-Dichloroethylene. [www.epa.gov/iris](http://www.epa.gov/iris)
- Valentino F., Brusca A.A., Beccari M., Nuzzo A., Zanaroli G., Majone M.; (2012) Start up of biological sequencing batch reactor and short-term biomass acclimation for polyhydroxyalkanoates production. *J Chem Technol Biotechnol*, doi: 10.1002/jctb.3824.
- Valentino F., Beccari M., Fraraccio S., Zanaroli G., Majone M.; (2014a) Feed frequency in a Sequencing Batch Reactor strongly affects the production of polyhydroxyalkanoates (PHAs) from volatile fatty acids. *New Biotechnol*, 31: 264-275.
- Valentino F., Morgan-Sagastume F., Fraraccio S., Corsi G., Zanaroli G., Werker A., Majone M.; (2014b) Sludge minimization in municipal wastewater treatment by polyhydroxyalkanoate (PHA) production. *Environ Sci Pollut Res*, doi: 10.1007/s11356-014-3268-y.
- van Beilen J.B., Panke S., Lucchini S., Franchini A.G., Röthlisberger M., Witholt B.; (2001) Analysis of *Pseudomonas putida* alkane degradation gene clusters and flanking insertion sequences: evolution and regulation of the *alk*-genes. *Microbiology*, 147: 1621-1630.
- van Beilen J.B., Smits T.H., Roos F.F., Brunner T., Balada S.B., Rothlisberger M., Witholt B.; (2005) Identification of amino acid position that determines the substrate range of integral membrane alkane hydroxylases. *J Bacteriol*, 187:85-91.
- van Beilen J.B., Funhoff E.G., van Loon A., Just A., Kaysser L., Bouza M., Holtackers R., Rothlisberger M., Li Z., Witholt B.; (2006) Cytochrome P450 alkane hydroxylases of the CYP153 family are common in alkane-degrading eubacteria lacking integral membrane alkane hydroxylases. *Appl Environ Microbiol*, 72: 59-65.
- van Beilen J.B., Funhoff E.G.; (2007) Alkane hydroxylases involved in microbial alkane degradation. *Appl Microbiol Biotechnol*, 74: 13-21.
- Van Wegen R.J., Ling Y., Middelberg A.P.J.; (1998) Industrial Production of Polyhydroxyalkanoates using *Escherichia coli*: An Economic Analysis. *Chem Eng Res Des*, 76(3): 417-426.
- Vannelli T., Logan M., Arciero D.M., Hooper A.B.; (1990) Degradation of halogenated aliphatic compounds by the ammonia-oxidizing bacterium *Nitrosomonas europaea*. *Appl Environ Microbiol*, 56: 1169-1171.
- Venter J.C., Remington K., Heidelberg J.F., *et al.*; (2004) Environmental genome shotgun sequencing of the Sargasso Sea. *Science*, 304: 66-74.
- Verce M.F., Ulrich R.L., Freedman D.L.; (2000) Characterization of an Isolate That Uses Vinyl Chloride as a Growth Substrate under Aerobic Conditions. *Appl Environ Microbiol*, 66(8): 3535-3542.
- Villemur R., Lanthier M., Beaudet R., Lépine F.; (2006) The *Desulfitobacterium* genus. *FEMS Microbiol Rev*, 30(5): 706-733.
- Vinas M., Sabaté J., Guasp C., Lalucat J., Solanas A.M.; (2005) Culture-dependent and -independent approaches establish the complexity of a PAH-degrading microbial consortium. *Can J Microbiol*, 51: 897-909.

- Wackett L.P., Brusseau G.A., Householder S.R., Hanson R.S.; (1989) Survey of microbial oxygenases: Trichloroethylene degradation by propane-oxidizing bacteria. *Appl Environ Microbiol*, 55: 2960-2964.
- Wackett L.P.; (1995) Bacterial co-metabolism of halogenated organic compounds. In: Microbial Transformation and Degradation of Toxic Organic Chemicals. Young L.Y., Cerniglia C. (Ed.): 217-241, John Wiley & Sons, New York.
- Wackett L.P., Hershberger C.D.; (2001) Evolution of catabolic enzymes and pathways. In: Biocatalysts and Biodegradation: Microbial Transformation of Organic Compounds. Washington DC, ASM Press., pp. 115-134.
- Wang F., Lee S.Y.; (1997) Poly(3-Hydroxybutyrate) Production with High Productivity and High Polymer Content by a Fed-Batch Culture of *Alcaligenes latus* under Nitrogen Limitation. *Appl Environ Microbiol*, 63(9): 3703-3706.
- Wang Q., Tappel R.C., Zhu C., Nomura C.T.; (2012) Development of a New Strategy for Production of Medium-Chain-Length Polyhydroxyalkanoates by Recombinant *Escherichia coli* via Inexpensive Non-Fatty Acid Feedstocks. *Appl Environ Microbiol*, 78(2): 519-527.
- Wang X.B., Chi C.Q., Nie Y., Tang Y.Q., Tan Y., Wu G., Wu X.L.; (2011) Degradation of petroleum hydrocarbons (C6-C40) and crude oil by a novel *Dietzia* strain. *Bioresour Technol*, 102: 7755-7761.
- Wani B.A., Khan A., Bodha R.H.; (2011) *Salix*: A viable option for phytoremediation. *African J Environ Sci Technol*, 5(8): 567-571.
- Watkinson R.J., Morgan P.; (1990) Physiology of aliphatic hydrocarbon-degrading microorganisms. *Biodegradation*, 1(2-3): 79-92.
- Weelink SA, van Doesburg W, Saia FT, Rijpstra WI, Röling WF, Smidt H, Stams AJ.; (2009) A strictly anaerobic betaproteobacterium *Georgfuchsia toluolica* gen. nov., sp. nov. degrades aromatic compounds with Fe(III), Mn(IV) or nitrate as an electron acceptor. *FEMS Microbiol Ecol*. Dec 70(3): 575-85.
- Weisel C.P., Jo W.K.; (1996) Ingestion, inhalation, and dermal exposure to chloroform and trichloroethylene from tap water. *Environ Health Persp*, 104(1): 48-51.
- Wellington E.M.H., Berry A., Krsek M.; (2003) Resolving functional diversity in relation to microbial community structure in soil: exploiting genomics and stable isotope probing. *Curr Opin Microbiol*, 6: 295-301.
- Wilsey B.J., Potvin C.; (2000) Biodiversity and ecosystem functioning: importance of species evenness in an old field. *Ecology*, 81: 887-892.
- Winker S., Woese C.R.; (1991) A definition of the domains Archaea, Bacteria and Eucarya in terms of small subunit ribosomal RNA characteristics. *Syst Appl Microbiol*, 14: 305-310.
- Wittebolle L., Boon N., Vanparys B., Heylen K., De Vos P., Vestraete W.; (2005) Failure of the ammonia oxidation process in two pharmaceutical wastewater treatment plants is linked to shifts in the bacterial communities. *J Appl Microbiol*, 99:997-1006.
- Wittebolle L., Marzorati M., Clement L., Balloi A., Daffonchio D., Heylen K., De Vos P., Verstraete W., Boon N.; (2009) Initial community evenness favours functionality under selective stress. In: Nature Letters, Macmillan Publishers Limited, doi:10.1038/nature07840.
- Wo L., Kellogg L., Devol A.H., Tiedje J.M., Zhou J.; (2008) Microarray-Based Characterization of Microbial Community Functional Structure and Heterogeneity in Marine Sediments from the Gulf of Mexico. *Appl Environ Microbiol*, 74(14): 4516-4529.
- Wright E.S., Yilmaz L.S., Corcoran A.M., Ökten H.E., Noguera D.R.; (2014) Automated design of probes for rRNA-targeted Fluorescence *In Situ* Hybridization reveals the advantages of using dual probes for accurate identification. *Appl Environ Microbiol*, 80(16): 5124-5133.
- Xu J.; (2006) Microbial ecology in the age of genomics and metagenomics: concepts, tools, and recent advances. *Mol Ecol*, 15: 1713-1731.
- Yamasaki S., Nomura N., Nakajima T., Uchiyama H.; (2012) Cultivation-independent identification of candidate dehalorespiring bacteria in tetrachloroethylene degradation. *Environ Sci Technol*, 46(14): 7709-7716.

- Yee L.N., Chuah J.A., Chong M.L., Phang L.Y., Raha A.R., Sudesh K., Hassan M.A.; (2012) Molecular characterisation of phaCAB from *Comamonas* sp. EB172 for functional expression in *Escherichia coli* JM109. *Microbiol Res*, 167: 550–557.
- Yen K.M., Serdar C.M.; (1988) Genetics of naphthalene catabolism in Pseudomonads. *CRC Crit. Rev Microbiol*, 15: 247-268.
- Yoon J.H., Kang S.J., Lee S.Y., Lee J.S., Park S.; (2011) *Ohtaekwangia koreensis* gen. nov., sp. nov. and *Ohtaekwangia kribbensis* sp. nov., isolated from marine sand, deep-branching members of the phylum *Bacteroidetes*. *Int J Syst Evol Microbiol*, 61: 1066-1072.
- Yoon M.H., Ten L.N., Im W.T., Lee S.T.; (2007) *Methylibium fulvum* sp. nov., a member of the *Betaproteobacteria* isolated from ginseng field soil, and emended description of the genus *Methylibium*. *Int J Syst Evol Microbiol*, 57: 2062-2066.
- Zhang X., Sullivan E.R., Young L.Y.; (2000) Evidence for aromatic ring reduction in the biodegradation pathway of carboxylated naphthalene by a sulphate-reducing consortium. *Biodegradation*, 11: 117-124.
- Zhang X., Cheng S.P., Zhu C.J., Sun S.L.; (2006) Microbial PAH-Degradation in Soil: Degradation Pathways and Contributing Factors. *Pedosphere*, 16(5): 555-565.
- Zhang Z., Schwartz S., Wagner L., Miller W.; (2000) A greedy algorithm for aligning DNA sequences. *J Comput Biol*, 7(1-2): 203-14.
- Zhang L., Xu Z.; (2008) Assessing bacterial diversity in soil. *J Soil Sediment*, 8: 379-388.
- Zhou J., Thompson D.K.; (2002) Challenges in applying microarrays to environmental studies. *Curr Opin Biotechnol*, 13: 204-207.
- Zhou J., He Z., Yang Y., Deng Y., Tringe S.G., Alvarez-Cohen L.; (2015) High-throughput metagenomic technologies for complex microbial community analysis: open and closed formats. *mBio* 6(1): e02288-14. doi:10.1128/mBio.02288-14.
- Ziemińska A., Ciesielski S., Gnida A., Zabczńska S., Surmacz-Górska J., Miksch K.; (2012) Comparison of ammonia-oxidizing bacterial community structure in membrane-assisted bioreactors using PCR-DGGE and FISH. *J Microbiol Biotechnol*, 22(8): 1035-1043.
- Zogorski J.S., Carter J.C., Iavahnenko T., Lapham W.W., Moran M.J., Rowe B.L., Squillace P.J., Toccalino P.L.; (2006) Volatile Organic Compounds in the Nation's Ground Water and Drinking-Water Supply Wells. U.S. Department of Interior and U.S. Geological Survey, Reston, Virginia.
- Zuckerkindl E., Pauling L.; (1965) Evolutionary divergence and convergence in proteins. Edited in *Evolving Genes and Proteins* by V. Bryson and H.J. Vogel, pp. 97-166. Academic Press, New York.